Mechanistic and Therapeutic Insights of Macrophage MicroRNA in Atherosclerosis

MY-ANH NGUYEN

Thesis submitted to the Faculty of Graduate and Postdoctoral Studies

In partial fulfillment of the requirements

For the degree of

DOCTOR OF PHILOSOPHY

Department of Biochemistry, Microbiology and Immunology

University of Ottawa

Ottawa, Ontario, Canada

Abstract

Macrophages are central players during atherosclerosis. Especially, macrophage cholesterol efflux, which promote the removal of free cholesterol from foam cells, are crucial to prevent lipid accumulation and reverse atherogenesis. microRNAs (miRNAs) are important regulators of various pathways involved in atherosclerosis. During inflammation, macrophages secrete extracellular vesicles (EVs) carrying miRNAs to communicate signals to nearby cells. However, the role of macrophage-derived EVs in atherogenesis is not known. In the first study, we find that EVs derived from cholesterol-loaded macrophages can inhibit macrophage migration *in vitro* and *in vivo*. This effect appears to be mediated by the transfer of several miRNAs, including miR-146a, to recipient macrophages where they repress the expression of specific pro-migratory target genes *Igf2bp1* and *HuR*. Our studies suggest that EV-derived miRNAs secreted from atherogenic macrophages may accelerate the development of atherosclerosis by decreasing cell migration and promoting macrophage entrapment in the vessel wall. Understanding macrophage communication *via* EVs provided the rationale for the design of nanoparticles (NPs) that mimic macrophage EVs to deliver beneficial miRNAs to the atherosclerotic plaque. While cationic lipid/polymer-based NPs have been employed as systemic delivery vehicles of siRNA, none of these have been used to deliver miRNAs to macrophages *in vivo*. In the second study, we developed a chitosan NP platform for effective delivery of miRNAs to alter macrophage function *in vivo*. We showed that our NPs made using a cross-linked chitosan polymer can protect as well as transfer miR-33 to naïve macrophages and regulate the expression of its target gene (*Abca1*) as well as cholesterol efflux *in vitro* and *in vivo.* Finally, almost all miRNAs that have been characterized are efflux-repressing miRNA, thereby accelerating atherosclerosis. miR-223 is one of a few miRNAs whose overexpression can promote cholesterol efflux, modulate the inflammatory response, and thus, be anti-atherogenic. However, its contribution to the pathogenesis of atherosclerosis *in vivo* and the mechanism underlying its effects has not been thoroughly characterized. We herein find that miR-223 is capable of suppressing plaque development *via* modulating cholesterol efflux and inflammatory responses, thus may serve as a potential therapeutic to reduce atherosclerosis. These effects of miR-223 appear to be dependent on the inhibition of its target gene, the transcription factor *Sp3*. Overall, this thesis highlights the importance of both endogenous and extracellular miRNAs in controlling different aspects of atherogenic response.

Acknowledgments

"Đi một ngày đàng, học một sàng khôn" is a famous expression in my mother-tongue language, Vietnamese. It means the more you go, the more you learn. At least, it is absolutely right in my case. Coming to Canada and becoming a graduate student at University of Ottawa Heart Institute have really been the biggest turning point in my life. I have grown a lot, both on a personal and professional level. Eight years are not long time, but not short time either, especially if you have to live far away from your loved ones, if you have to leave all you have known and restart your life from the beginning. Luckily, I have many special people around who give me constant strength, motivation, and encouragement to keep going the way I have chosen. First of all, I know that I always can count on my family. I do not dedicate this achievement for anyone of my family because for me, each of them is meaningful on their own. When everything gets me down, just some simple things such as my grandmother's voice, unlimited chatting with my sisters, funny stories of my brother, or sweet hugs from my aunt are enough to make my day. I can be sure that sometimes nobody in my family can understand what I am doing or what I am talking about, but they are always there for me whenever I need. My life is never complete without them.

Importantly, I want to express my special thanks to Dr. Katey Rayner. Katey is a perfect supervisor who not only knows how to firmly push you forward but also knows how to gently help you realize your valuable abilities and develop them. I can honestly say that I have learnt a lot from her. From the bottom of my heart, I am really grateful to her for her endless patience and guidance. She was always willing to listen to me, even many of my crazy opinions or silly questions, to clear my mind when I was confused, and to bring me back the right way when I got lost. She never gave up on me no matter how many times I made her disappointed.

Besides, I am very grateful to a number of PIs especially for their assistance and guidance that I needed most during this program. I would like to thank Dr. Ruth McPherson and Dr. Derrick Gibbings, who were my TAC member over the years, for giving me critical discussions as well as valuable advices about my projects. I also want to thank Dr. Thomas Lagace, Dr. Mireille Ouimet, Dr. Ross Milne, and Dr. Suresh Gadde who always supported me in a special way. Their constant encouragement usually made me stronger to overcome many difficulties throughout, more hopeful to complete my project, and more determined to pursue my further goals in science.

There will be a mistake if I do not say thanks to many people who I am lucky enough to work with. First of all are my wonderful lab-mates: Michele Geoffrion and Denuja Karunakaran who trained me at the very beginning and always devoted their time as well as effort to assist me whenever I needed; Adil Rasheed, Anne-Claire Duchez, and Benoit Laffont who were always there to teach me anything I did not know, to explain anything I did not understand, and to show me anything I needed to improve; Leah Susser who helped me with the nanoparticle preparation. I cannot remember how many times they helped me get out of my problems, even minor or major. All of them are my best teachers. Also, thanks to every people at the fourth floor of the Heart Institute who was always available for help with chemical, equipment or anything and everything. Thanks all of you for making my graduate student experiences at the Heart Institute more memorable.

To my dearest best friends who always stayed beside me and supported me during this period of my life, I love all of you so much and thank for always being my true friends no matter how freaky I am sometimes.

Finally, thanks to you, my special husband, although you always say that there is no need to say thanks between us and I never can express enough thanks to you.

Contents

List of Abbreviations

ABCA1/G1	ATP-binding cassette transporters A1/G1
ABCB11	ATP binding cassette subfamily B member 11
ADAMTS1	A disintegrin and metalloproteinase with thrombospondin motifs 1
AGO	Argonautes
AKT1	AKT Serine/Threonine Kinase 1
ALDH1A2	Aldehyde dehydrogenase 1 family member A2
ALIX	Apoptosis-linked gene 2-interacting protein X
AMPK	AMP-activated protein kinase
ApoA1	Apolipoprotein A1
ApoE	Apolipoprotein E
ARL7	ADP-ribosylation factor-like 7
ASO	Antisense oligonucleotides
ATP8B1	ATPase phospholipid transporting 8B1
BM	Bone marrow
BMDM	Bone-marrow derived macrophages
BSA	Bovine albumin serum
CAD	Coronary artery disease
CCL2	CC-chemokine ligand 2
CCL5	CC-chemokine ligand 5
CCL19/21	CC-chemokine ligand 19/21
CCR1/5	CC-chemokine receptor 1/5
CCR2	CC-chemokine receptor 2
CCR7	CC-chemokine receptor 7
CDC42	Cell division cycle 42
C. elegans	Caenorhabditis elegans
chNP	Chitosan nanoparticle
CVD	Cardiovascular disease
CXCL8	CXC-chemokine ligand 8
CX_3CL1	CX_3C-chemokine ligand 1
CX_3CR1	CX_3C-chemokine receptor 1

CYP7A1	Cytochrome P450 family 7 subfamily A member 1
DC	Dendritic cell
DEL-1	Developmental endothelial locus-1
DGCR8	DiGeorge syndrome critical region 8
DLS	Dynamic light scattering
EC	Endothelial cell
EGFR	Epidermal growth factor receptor
ER	Endoplasmic reticulum
ERK	Extracellular-signal-regulated kinase
ESCRT	Endosomal sorting complex required for trafficking
EV	Extracellular vesicle
FA	Fatty acid
FBS	Fetal bovine serum
FOXP3	Forkhead box P3
FXR	Farnesoid X receptor
HCC	Hepatocellular carcinoma
HCD	High cholesterol diet
HCV	Hepatitis C virus
HDL	High-density lipoprotein
HMGCS1	3-hydroxy-3-methylglutaryl-CoA synthase 1
hnRNP	Heterogenous nuclear ribonucleoprotein
HuR	Human antigen R or ELAV-like RNA-binding protein 1
ICAM1	Intercellular adhesion molecule 1
IGF2BP1	Insulin-like growth factor 2 mRNA-binding protein 1
IKKα	IκB kinase alpha subunit
ILV	Intraluminal vesicle
iNOS	Inducible nitric oxide synthase
IRAK1/2	Interleukin 1 receptor associated kinase ½
LAMP2B	Lysosome-associated membrane glycoprotein 2b
LD	Lipid droplet
LDL	Low-density lipoprotein

LDLR	Low-density lipoprotein receptor
LFA1	Lymphocyte function-associated antigen 1
LOX1	Lectin-like oxidized low-density lipoprotein receptor 1
LP	Lipoprotein
LPS	Lipopolysaccharide
LSC	Liquid scintillation counter
LXR	Liver X receptor
MAPK	Mitogen-activated protein kinase
M-CSF	Macrophage colony-stimulating factor
MEK	Mitogen-activated protein kinase kinase
miRNA	microRNA
mRNA	messenger RNA
MVB	Multivesicular bodies
NCEH1	Neutral cholesterol ester hydrolase 1
NLRP3	NLR family pyrin domain containing 3
NP	Nanoparticle
NPC1	Neimann-Pick C1
OSBPL6	Oxysterol-binding protein-like 6
PAMPs	Pathogen-associated molecular patterns
PBS	Phosphate-buffered saline
PDK4	Pyruvate dehydrogenase kinase isozyme 4
PEG	Polyethylene glycol
PGC1-α	Peroxisome proliferator-activated receptor γ coactivator 1-α
PKNOX1	PBX/Knotted 1 homeobox 1
PPARγ	Peroxisome proliferator activated receptor γ
P-S	Penicillin-streptomycin
RCT	Reverse cholesterol transport
RHOB	Ras homolog family member B
RISC	RNA-induced silencing complex
ROCK2	Rho-associated coiled-coil containing protein kinase 2
RVG	Rabies virus glycoprotein

SC4MOL	Methylsterol monooxygenase 1
SIAH1	Seven in absentia homolog 1
siRNA	Small interfering RNAs
SLC25A25	Solute carrier family 25
SMC	Smooth muscle cell
SPRED1	Sprouty-related, EVH1 domain-containing protein 1
SR-A1/A2	Scavenger receptor A1/A2
SR-B1	Scavenger receptor B1
SR-PSOX	Scavenger receptor for phosphatidylserine and oxidized LDL
SREBF1/2	Sterol regulatory element binding transcription factor 1/2
TAM	Tumor-associated macrophages
TEM	Transmission electron microscopy
TIM1/4	T-cell immunoglobulin mucin protein 1/4
TLR	Toll-like receptor
TPP	Tripolyphosphate
TRAF6	TNF receptor associated factor 6
TSG101	Tumor susceptibility gene 101
UTR	Untranslated regions
VCAM1	Vascular cell adhesion molecule 1
VLA4	Very late antigen 4
YBX1	Y-box protein 1

List of Figures

List of Tables

1. Introduction

Cardiovascular disease (CVD), which accounts for 31% of all global deaths in 2016 worldwide[1], remains a persistent health burden worldwide. It is well established that atherosclerosis is the major underlying factor leading to fatal cardiovascular complications[2,3]. Atherosclerosis is a chronic inflammatory disease that is driven by the interplay of excess cholesterol accumulation in the vessel wall and a maladaptive immune response. It is characterized by retention of cholesterol-rich lipoproteins (LPs) in susceptible areas of the arterial vasculature, endothelial activation, and macrophage infiltration resulting in plaque formation, narrowing of the arterial lumen and subsequently, leading to the formation of a pro-thrombotic necrotic core. This necrotic core is a hallmark of more advanced, complex plaques and contributes to plaque rupture and intravascular blood clot that underlies myocardial infraction and stroke[4–6]. Traditionally, lipid lowering therapies, such as statins, have been the gold-standard treatment for atherosclerosis, yet a significant burden of atherosclerotic disease still remains even in the setting of low plasma cholesterol[7,8]. In addition, the potential adverse effects in muscle and other tissues of lipid-lowering drugs has reduced the adherence to this therapy across many groups[9]. Thus, not only a better understanding of the mechanisms that govern atherogenesis but also identification of novel therapeutic targets important in the development of atherosclerosis are still needed to improve the diagnosis, prevention and treatment of atherosclerosis and to reduce the global burden of this disease.

Recently, the ENCODE consortium has revealed that around 90% of the eukaryote genome is actively transcribed into non-coding RNA[10], suggesting the potential importance of this neglected genetic information. microRNAs (miRNAs), which are defined as highly conserved small RNA sequences of 20 to 23 nucleotides, are the most popular and well

characterized class of non-coding RNAs. Instead of serving as transcriptional "noise", several lines of evidence have indicated that miRNAs indeed play important roles in modulating atherogenesis, with many miRNAs dysregulated in different disease states and alterations in miRNA expression associated with atherosclerosis progression[11,12]. Therefore, targeting miRNAs as an effective therapeutic strategy for treating atherosclerosis has gained considerable attention.

1.1. Macrophages in atherosclerosis

Although many cell types, including endothelial cells (ECs) and smooth muscle cells (SMCs), contribute to the disease, macrophages are fundamental to atherosclerotic progression due to their capacity to engulf modified lipoproteins and induce a pro-inflammatory state. In addition, macrophages are not only the first inflammatory cells to invade atherosclerotic lesions but also the most abundant component in atherosclerotic plaques (**Figure 1.1**).

Monocyte recruitment: In the early stages of atherosclerosis, the key inflammatory response to lipid accumulation and endothelial activation is recruitment of circulating monocytes into the vascular intima. Circulating monocytes in mice consist of two major subsets, $GR1^{+}Ly6C^{hi}$ and $GR1^{-}Ly6C^{low}$, of which the inflammatory $Ly6C^{hi}$ subset comprises approximately 80% of the monocytes entering progressing atherosclerotic lesions and is proposed to be the source of the pro-inflammatory M1 macrophages that are found in the plaque[13,14]. These monocyte subsets express different chemokine receptors including CC-chemokine receptor 1/5 (CCR1/5), or CX_3C-chemokine receptor 1 (CX_3CR1) that interact with cognate chemokines on activated ECs, which results in the adhesion of leukocyte to the vasculature[15,16]. Monocytes then become firmly adhered to the luminal surface of the endothelium through the interactions of monocyte integrins VLA4 (very late antigen 4) and LFA1 (lymphocyte function-associated

antigen 1) with EC ligands VCAM1 (vascular cell adhesion molecule 1) and ICAM1 (intercellular adhesion molecule 1), respectively. Finally, different chemokine-chemokine receptor pairs such as CCR2 (CC-chemokine receptor 2)-CCL2 (CC-chemokine ligand 2), CX_3CR1-CX_3CL1 (CX_3C-chemokine ligand 1), and CCR5-CCL5 (CC-chemokine ligand 5) are proposed to mediate the transmigration of monocytes across the endothelium into plaques[14]. Inhibition of monocyte entry by blocking different chemokines or their receptors retards atherosclerotic development in mouse models[17,18].

Foam cell formation: In the subendothelial space, the majority of recruited monocytes differentiate into macrophages, a process driven by macrophage colony-stimulating factor (M-CSF) and other factors[19]. Trapped LPs in the artery wall do undergo modification such as lipolysis, proteolysis, aggregation and, more importantly, oxidation, which cause them to be rapidly internalized by macrophages[4,20]. Different mechanisms mediated by enzymes such as 12/15-lipoxygenase[21] and by free radicals including superoxide, hydrogen peroxide and nitric oxide have been shown to promote LP oxidation[22]. Monocyte-derived macrophages take up retained modified LPs *via* numerous scavenger receptors including scavenger receptor A1/A2 (SR-A1/A2), CD36, scavenger receptor B1 (SR-B1), lectin-like oxidized low-density lipoprotein (LDL) receptor 1 (LOX1), and scavenger receptor for phosphatidylserine and oxidized LDL (SR-PSOX), which eventually transform them to cholesterol-laden foam cells[23]. Among these receptors, SR-A1 and CD36 have been shown to mediate the majority of modified LP uptake by macrophages[24]. Additional mechanism such as phagocytosis of aggregated LDL and micropinocytosis of native LDL also contribute to foam cell formation *in vivo*[25,26].

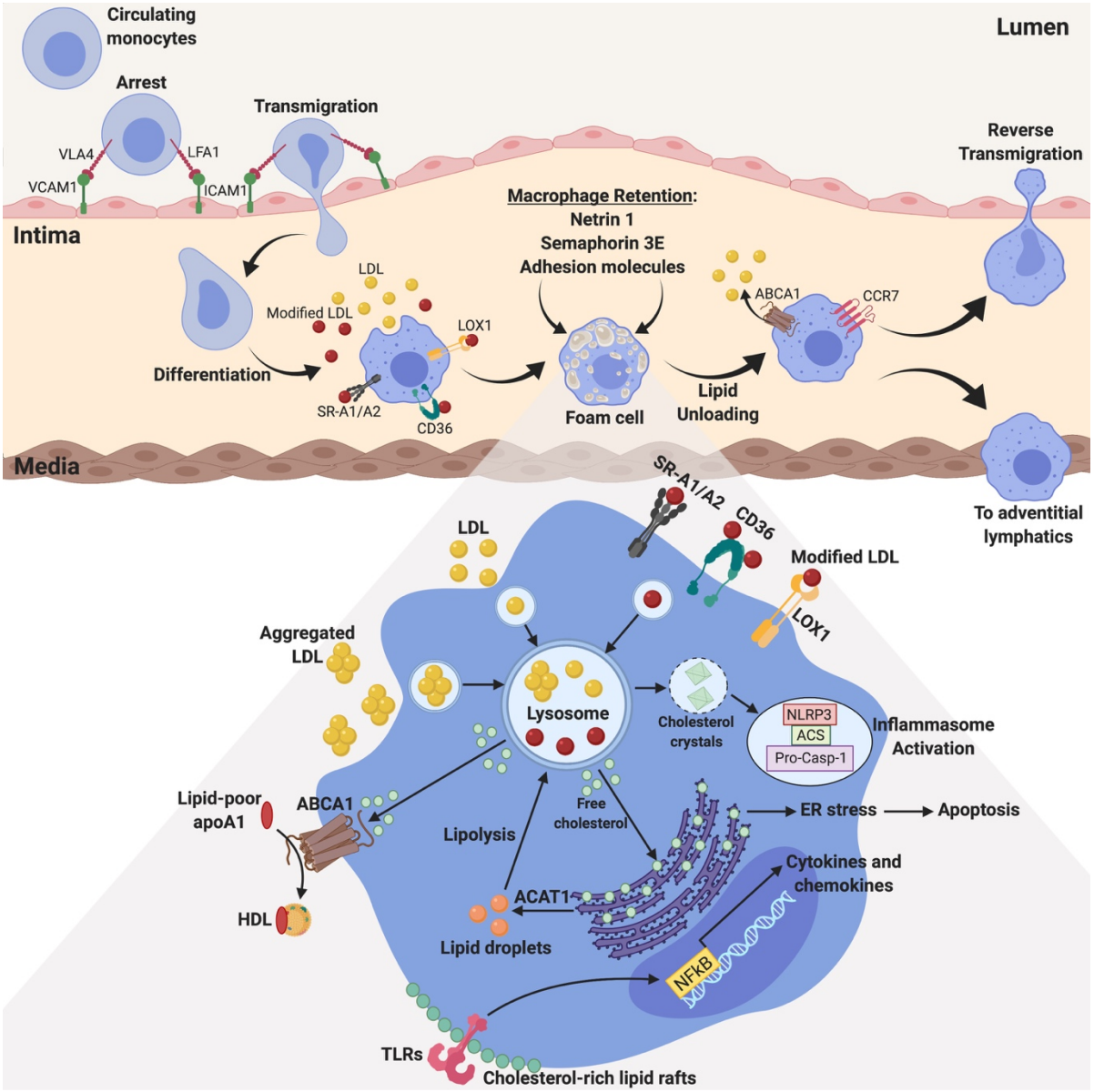

Figure 1.1. Macrophages in the pathogenesis of atherosclerosis. The primary initiating events in atherosclerosis are subendothelial accumulation of cholesterol-rich LPs and endothelial activation, leading to recruitment of circulating monocytes into the vascular intima. In the subendothelial space, recruited monocytes differentiate into macrophages that scavenge retained modified lipoproteins, which transforms them into cholesterol-laden foam cells. The internalized LPs are digested in the lysosome to release free cholesterol that can traffic to the ER or to plasma membrane for cholesterol efflux out of the cells. However, excessive free cholesterol accumulation in macrophage-derived foam cells results in activation of downstream cascades including NLRP3 inflammasome, TLR signaling, and ER stress responses. These inflammatory signals exacerbate not only oxidative stress in the plaques but also the transmigration of additional inflammatory cells including monocytes into the intima. Conversely, lesion regression requires the resolution of inflammation and macrophage emigration out of the plaques through reverse transmigration.

Inflammatory activation of lesional macrophages: How the loading of macrophages with lipoprotein-derived cholesterol affects macrophage function and promotes disease progression has been extensively studied. In foam cells, the internalized LPs and their associated lipids are hydrolyzed in the lysosome, resulting in the release of free cholesterol that can traffic to the endoplasmic reticulum (ER) or to the plasma membrane for cholesterol efflux out of the cells[27,28]. However, excessive cholesterol uptake, leading to excessive free cholesterol accumulation, results in inflammatory activation during disease progression. Macrophages in the lesion may secrete LP-binding proteoglycans, which magnify LP retention in the arterial intima[29]. Moreover, excessive free cholesterol accumulation in macrophage-derived foam cells induces cholesterol crystal formation, lysosomal destabilization, and ultimately, the release of proteases and reactive oxygen species into the cytosol to activate NLRP3 (NLR family pyrin domain containing 3) inflammasome[30]. Enrichment of cell membranes with free cholesterol triggers inflammatory signaling from lipid rafts, particularly Toll-like receptors (TLR) signaling and NF-κB activation, resulting in the secretion of pro-inflammatory mediators (cytokines, chemokines, and reactive oxygen and nitrogen species). These inflammatory signals exacerbate not only oxidative stress in the plaques but also the transmigration of more inflammatory cells including monocytes into the intima, which further aggravate plaque inflammation[31]. Furthermore, free cholesterol accumulation impairs ER function and activates ER stress responses, which if prolonged and combined with other insults, leading to apoptotic cell death and necrotic core formation[32].

Macrophage polarization: Activation of macrophage foam cells through TLR signaling pathways can result in macrophage polarization toward the classically activated M1

phenotype. Different from alternatively activated M2 macrophages that secrete anti-inflammatory cytokines (*i.e.* IL-10 and TGF-β) and mediators of tissue repair (*i.e.* collagen), M1 macrophages produce high levels of pro-inflammatory cytokines (*i.e.* TNFα, IL-6, IL-1β, IL-12)[31,33,34]. Studies of macrophage polarization *in vitro* and in mouse models of atherosclerosis have indicated that increasing macrophage activation toward the M1 phenotype or inhibiting macrophage activation toward M2 can promote plaque inflammation and potentiate atherosclerosis[35–40]. In contrast, driving plaque macrophages to M2-like cells by the administration of IL-13 can attenuate atherosclerosis progression[41]. Furthermore, even though both M1 and M2 macrophages are present in human and mouse atherosclerotic plaques, they localized to distinct areas[42].

Lipid efflux: Conversely, plaque regression involves the removal of free cholesterol and other lipids from macrophage-derived foam cells[31] *via* the ATP-binding cassette transporters A1/G1 (ABCA1/G1), of which ABCG1 promotes cholesterol efflux to mature high-density lipoprotein (HDL) particles while ABCA1 promotes efflux to lipid-poor apolipoprotein A1 (apoA1) that is the building block of HDL[43,44]. The expression of ABCA1 and ABCG1 in macrophages is mainly regulated by liver X receptors (LXRs), which are nuclear receptors activated in response to high intracellular cholesterol levels. Cholesterol efflux from macrophages is the first and potentially the most important step in reverse cholesterol transport (RCT), a pathway by which excess cholesterol from peripheral cells and tissues is transported to the liver for excretion, thus crucial for the prevention of lipid accumulation and atherosclerosis[45]. The significance of macrophage RCT and cholesterol efflux in preventing or reversing atherogenesis has been highlighted by studies where disruption of *Abca1* genes

can induce atherosclerosis[46,47] and in patients where mutated *ABCA1* genes resulted in increased atherosclerosis[48,49].

Autophagy, an evolutionarily conserved process by which cytoplasmic components such as damaged organelles and macromolecules are sequestered in double-membrane vesicles and degraded on fusion with lysosomal compartments, also contributes to macrophage cholesterol efflux. In macrophage foam cells, excess cellular cholesterol is stored as cholesterol ester in cytosolic lipid droplets (LDs)[31]. Aside from lipolysis by neutral cholesterol ester hydrolase 1 (NCEH1), these LDs can be targeted for ABCA1-dependent efflux pathway *via* lipophagy, a special form of selective macroautophagy. During this process, LDs are engulfed by autophagosomes and delivered to the lysosomes for hydrolysis into free and modified cholesterol available for efflux[50,51]. In fact, it has been shown that lipophagy becomes dysfunctional in atherogenesis and deletion of essential autophagy genes can exacerbate plaque formation as well as rupture[52,53], emphasizing the important role of autophagy in the pathological process of atherosclerosis.

Plaque macrophage retention and emigration: Atherosclerosis resolution also involves macrophage emigration out of the plaques through reverse transmigration to the lumen or migration to the adventitial lymphatics[54]. It is known that emigrating macrophages express high levels of CC-chemokine receptor 7 (CCR7), which is the receptor for CC-chemokine ligand 19/21 (CCL19/CCL21) regulating lymph node homing of dendritic cells (DCs), and inhibition of this pathway leads to macrophage retention in the plaque[55]. However, the detailed mechanisms that govern macrophage migration out of the artery wall are still poorly understood. More importantly, this process seems to be impaired during atherosclerosis

progression[56]. Studies have shown that uptake of oxidized LDL by CD36 induces macrophage entrapment in atherosclerotic lesions[57,58]. Furthermore, blocking the oxidized LDL uptake decreases the number of F4/80-positive macrophages in the plaque[59]. Cholesterol-loaded macrophages are known to express retention factors including adhesion molecules, the neuro-immune guidance cues netrin 1 and semaphorin 3E, which shift the cells to a more sessile phenotype and promote macrophage accumulation in the artery wall[60–62].

Given that macrophages play a central role in atherogenesis, it is well known that the quantity as well as the phenotype of these cells influences plaque inflammation and progression. Thus, a better understanding of mechanisms that regulate macrophage burden will provide insights into pathways that may have therapeutic value for the treatment of atherosclerosis.

1.2. miRNA in atherosclerosis

Since their discovery in *Caenorhabditis elegans (C. elegans)*[63], miRNAs have been characterized as important transcriptional modulators that can both fine-tune and dramatically alter cell behavior, with one miRNA repressing multiple target genes simultaneously and one functional gene network can be regulated by a group of miRNAs[64]. In humans, miRNAs are predicted to control the activity of 60% of all protein-coding genes[65,66].

1.2.1. miRNA biogenesis

miRNAs begin as long and primary molecules (pri-miRNAs) that are commonly transcribed by RNA polymerase II from either independent miRNA genes or small parts of protein-coding transcripts. The transcriptional regulation of pri-miRNAs is not fully understood, except that most miRNAs are located in intergenic regions >1 kb away from

annotated/predicted genes and thereby might be transcribed as autonomous transcription units. Several pri-miRNAs, on the other hand, are found in the intronic regions of known genes in the sense or anti-sense orientation, and therefore might be transcriptionally regulated through their host-gene promoters. Furthermore, certain miRNAs are clustered in a single polycistronic transcription unit, indicating that they are coordinately regulated[67,68]. The pri-miRNAs are cleaved in the nucleus by a complex containing the RNase III-type endonuclease Drosha and DiGeorge syndrome critical region 8 (DGCR8) to form smaller precursor miRNA (pre-miRNA) products. Each pre-miRNA possesses a signature motif composing of a short stem in addition to a 2-nucleotide 3' overhang that is recognized by the nuclear export factor Exportin 5, allowing it to be transported to the cytoplasm. Following export into the cytoplasm, these hairpin-shaped pre-miRNAs are further shortened by the ribonuclease III enzyme Dicer to give rise to the mature, double-stranded miRNA molecules. The preferred guide strand is subsequently incorporated into the RNA-induced silencing complex (RISC) by directly binding to the key protein components, the Argonautes (AGO). These complexes localize to miRNA binding sites that are generally present in the 3'-untranslated regions (UTR) of specific messenger RNAs (mRNAs) with perfect and imperfect complementarity, resulting in destabilization and/or translational inhibition of their bound targets. For most cases, complementarity to the "seed" sequence containing nucleotides 2-8 that is located in the 5' region of the miRNA is critical for target recognition. Nevertheless, complementarity to the 3' region of the miRNA also contributes to target selection in some rare circumstances where the mRNA has a weak seed match[69–71].

1.2.2. Macrophage miRNAs in atherosclerosis

miRNAs are important regulators of multiple signaling pathways involved in atherosclerosis. Over the past decade, accumulating evidence have highlighted the role of miRNAs in regulating lipoprotein homeostasis, vascular inflammation, leukocyte recruitment/activation, and vascular smooth muscle function, thus controlling each stage of atherosclerosis from development, progression to disruption[11,12,72]. Here, only miRNAs that have been shown to alter macrophage function, which is the main subject of this thesis, are discussed (**Figure 1.2**).

Cholesterol efflux: As mentioned above, removal of excess cholesterol through activation of cholesterol efflux *via* ABCA1/G1 is critically important for maintain cholesterol homeostasis. One of the most well-known examples of a miRNA that regulates cholesterol efflux is miR-33. In humans and other large mammals, miR-33a and miR-33b are located in intronic regions of two genes encoding key transcriptional regulators of cholesterol, fatty acid (FA) and phospholipid synthesis: *SREBF2* and *SREBF1* (sterol regulatory element binding transcription factor 2 and 1), respectively[73,74]. Rodents and other species have only one copy of miR-33, located in *Srebf2*. In sterol-depleted states, miR-33 down-regulates the expression of ABCA1 and ABCG1 by directly binding to the 3'UTR of these genes[73–77]. This repression of ABCA1 and ABCG1 suppresses cholesterol efflux to apoA1 and nascent HDL to raise intracellular cholesterol levels. In contrast, miR-33 inhibition promotes cholesterol efflux and hence RCT *via* derepressing ABCA1 and ABCG1. In addition to controlling the expression of ABCA1 and ABCG1, miR-33a/b are also involved in the last stage of RCT by regulating factors involved in the synthesis (cytochrome P450 family 7 subfamily A member 1, CYP7A1) and secretion (ATPase phospholipid transporting 8B1, ATP8B1 and ATP binding cassette

subfamily B member 11, ABCB11) of bile acids, which allow removal of cholesterol from the body through the feces[78,79]. Inhibition of miR-33 using anti-sense oligonucleotides or genetic deletion of miR-33 in atherosclerotic mouse models has been shown to significantly increase plasma HDL levels and promote cholesterol removal from the plaque *in vitro* and *in vivo*, resulting in a reduction of lesion size and inflammation[80–82]. This was, in part, owing to enhanced RCT and increased expression of efflux-related genes within plaque macrophages. Not only through its regulation of cholesterol transporters, a recent study by our group has demonstrated that miR-33 also influences macrophage cholesterol efflux *via* directly targeting mitochondrial genes including peroxisome proliferator-activated receptor γ coactivator 1-α (*Pgc1-α*), the master regulator of mitochondrial biogenesis, as well as its target genes *Pdk4* (pyruvate dehydrogenase kinase isozyme 4) and *Slc25a25* (solute carrier family 25)[83]. Efflux of cholesterol from macrophages has been linked to cellular energy status and mitochondrial function because ABCA1, a key factor in mediating cholesterol efflux, requires ATP to function[84]. Loss of mitochondrial function impairs cholesterol efflux to apoA1 and dysregulates cholesterol metabolism in macrophages[83,85]. Indeed, anti-miR-33 treatment significantly boosts mitochondrial respiration and ATP production, leading to increased ABCA1-mediated cholesterol efflux and reduced atherosclerosis[83]. Taken together, these studies emphasize how one miRNA (miR-33) can coordinately regulate cholesterol efflux *via* targeting multiple genes across different functional networks and highlight the potential of anti-miR-33 as a therapeutic to promote macrophage cholesterol efflux and reduce atherosclerosis.

Recent studies reveal another miRNA, miR-144, which can directly target ABCA1 and regulate cholesterol efflux like miR-33[86–88]. Activation of farnesoid X receptor (FXR) and

LXR, two nuclear receptors implicated in cholesterol metabolism, have been shown to increase miR-144 expression, which subsequently reduces ABCA1 expression and dampens cholesterol efflux to apoA1 in mouse macrophages and human hepatocytes. Conversely, delivery of miR-144 antagonists increases ABCA1 expression and plasma HDL-cholesterol both *in vitro* and *in vivo*[86,87]. In *ApoE*$^{-/-}$ (apolipoprotein E) mice fed a high-fat diet, overexpression of miR-144 inhibits cholesterol efflux in macrophage-derived foam cells *via* suppressing ABCA1 expression and impairs RCT, thereby accelerating the progression of atherosclerosis[86,87]. Additionally, miR-144 also enhances inflammatory factors including IL-1β, IL-6 and TNFα in this mouse model[88]. Therefore, these data suggest that miR-144 may serve to temper the actions of LXR-agonists by reducing ABCA1 expression in macrophages, and inhibition of this miRNA feedback loop could serve to enhance the efflux-inducing capabilities of LXR-agonists. Different from miR-144 that is up-regulated by LXR activators, miR-26 expression is repressed by ligand activation of LXR, and inhibition of this miRNA results in enhanced LXR-dependent cholesterol efflux *via* targeting *ABCA1* and *ARL7* (ADP-ribosylation factor-like 7), two of LXR target genes[89].

Other miRNAs including miR-302a[90], miR-758[91], miR-27a/b[92], miR-148a[93,94], miR-128-1, miR-130b, and miR-301b[94]. have also been found to regulate macrophage cholesterol efflux *via* repressing ABCA1 expression. However, except for miR-302a, their potential in modulating macrophage cholesterol efflux capacity and atherosclerosis progression *in vivo* have yet to be examined. In the case of miR-302a, overexpression of this miRNA abolishes cholesterol efflux to apoA1 *in vivo* whereas miR-302a inhibition in an atherosclerosis model results in an increase in hepatic as well as aortic ABCA1 expression, an increase in plasma HDL levels and a reduction in atherosclerotic plaque size[90].

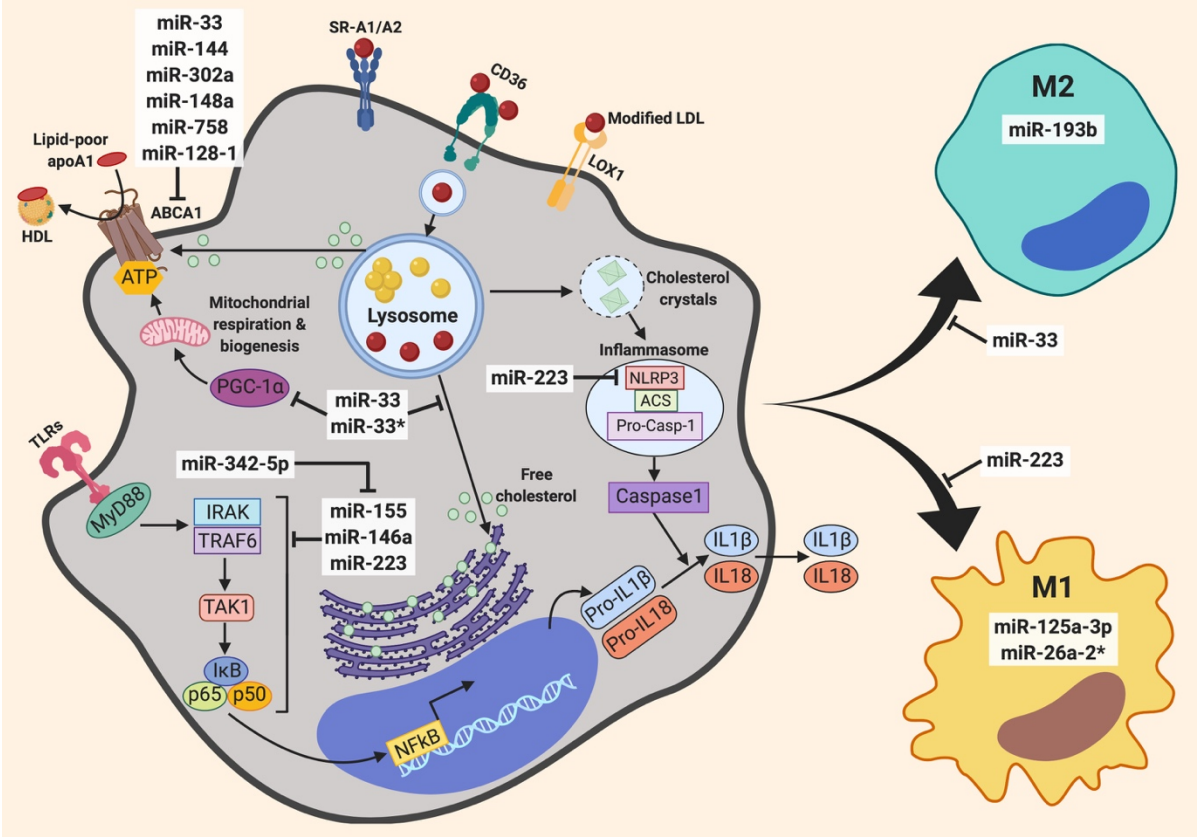

Figure 1.2. miRNA regulation of macrophage function in atherosclerosis. Numerous miRNAs including miR-33, miR-144, miR-302a, miR-148a, miR-758, and miR-128-1 have been found to regulate cholesterol efflux *via* directly targeting ABCA1. In addition to cholesterol transporters, miR-33 targets mitochondrial genes including *Pgc1-α*, *Pdk4*, and *Slc25a25*, thereby controlling mitochondrial respiration as well as biogenesis and in turn, regulating macrophage cholesterol efflux. miR-33, along with miR-33*, also inhibits cholesterol trafficking from the endolysosomal network to the ER and plasma membrane. Similarly, the inflammatory state of macrophage is controlled by multiple miRNAs such as miR-146a, miR-155, miR-342-5p, miR-223 (*via* targeting different components of the NF-κB signaling pathway), and miR-33 (*via* targeting AMPK). miR-223 also directly suppresses NLRP3 expression, thus inhibiting inflammasome activation and IL-1β secretion.

Cholesterol trafficking: Intracellular cholesterol transport is essential for the maintenance of cellular cholesterol homeostasis by delivering cholesterol to the appropriate sites of cholesterol synthesis, esterification, uptake and efflux. In a recent study, Ouimet el al. reported that two miRNA hubs regulating cholesterol homeostasis miR-33 and miR-27b negatively regulated the expression of oxysterol-binding protein-like 6 (OSBPL6), which resulted in aberrant clustering of endosomal reticular network, impaired cholesterol trafficking from the endolysosomal network to the ER for esterification, and promoted the accumulation of free cholesterol in macrophages[95].

The potent regulator of cholesterol efflux miR-33 has also been shown to directly target endolysosomal protein Neimann-Pick C1 (NPC1) expression[74] allowing cholesterol to move from within the lysosomes to the ER and plasma membrane, which further limits cholesterol efflux under sterol-depleted conditions. Notably, miR-33*, which is the passenger strand of miR-33, was also identified as a negative regulator of NPC1[96]. However, further studies are needed to elucidate how miR-33 and miR-33* control cholesterol trafficking *via* targeting NPC1.

Inflammation: Macrophages are the key inflammatory cell type responsible for the propagation of atherosclerosis and other inflammatory disease in the heart. Inflammation involves the coordinated expression of a multitude of genes, including cytokines, chemokines and adhesion molecules. Once again, miRNAs are key to the regulation of the inflammatory response. In macrophages treated with lipopolysaccharide (LPS), a gram-negative stimulus of the NF-κB response, a select group of miRNAs are up- and down-regulated; however, the most commonly up-regulated miRNA in inflammatory macrophages is miR-155[97,98].

Moreover, the observation that miR-155 was significantly increased in atherosclerotic plaques and decreased in the circulation of coronary artery disease (CAD) patients suggested a potential role for this miRNA in the development of atherosclerosis[99]. miR-155 directly repress the expression of BCL6, which is an NF-κB antagonist, and thereby enhances NF-κB activity and pro-inflammatory signals such as CCL2 expression, promoting the recruitment of monocytes to atherosclerotic plaques. In *ApoE*$^{-/-}$ mice, whole-body[100] or leukocyte-specific[99] deletion of miR-155 decreased plaque size and reduced the number of lesional macrophages. However, bone marrow (BM) transplantation from miR-155$^{-/-}$ mice to *Ldlr*$^{-/-}$ (LDL receptor) mice accelerated progression of atherosclerotic plaque and decreased plaque stability, as indicated by increased recruitment of inflammatory cells to the plaque and decreased anti-inflammatory cytokine production by peritoneal macrophages[101]. These opposing observations from miR-155 deficiency on lesion formation in *Ldlr*$^{-/-}$ *versus ApoE*$^{-/-}$ mice could be attributable to the role of miR-155 during different stages of lesion development: *Ldlr*$^{-/-}$ mice generally develop less advanced lesions than *ApoE*$^{-/-}$ mice on a high-cholesterol diet. Despite contradictory results, the accumulating evidence to date indicates that miR-155 is more likely to be pro-inflammatory rather than anti-inflammatory, though definitive evidence of this is still required. Interestingly, miR-342-5p, which is specifically expressed in early atherosclerotic lesions in *ApoE*$^{-/-}$ mice, was recently shown to positively regulate the expression of miR-155. Systemic administration of miR-342-5p inhibitor reduced the progression of atherosclerosis in the aorta of *ApoE*$^{-/-}$ mice by upregulating AKT1 (AKT Serine/Threonine Kinase 1) and suppressing miR-155, which in turn decreases the expression of pro-inflammatory mediators including iNOS (inducible nitric oxide synthase) and IL-6 [102].

Similar to miR-155, the role of miR-146a in atherogenesis is complex. In general, miR-146a functions as a negative feedback in controlling excessive inflammatory cytokine responses. Upon inflammatory cytokines or LPS stimulation, miR-146 expression is induced dependently of NF-κB[103], and up-regulated miR-146 in turn targets components of the NF-κB pathway like IRAK1/IRAK2 (interleukin 1 receptor associated kinase 1/2) and TRAF6 (TNF receptor associated factor 6), thereby suppressing the actions of NF-κB. This decrease in NF-κB activity results in a concomitant decrease in various inflammatory chemokines and cytokines such as CXCL8 (CXC-chemokine ligand 8), CCL5, IL-6 and a protection from inflammatory overactivation[103–105]. Ablation of miR-146a expression in mice resulted in severe immune-related phenotypes including hyper-responsiveness of macrophages to LPS and chronic inflammation in response to endotoxin. Within 6 months, miR-146a$^{-/-}$ mice developed a spontaneous autoimmune disorder that led to death. Opposite effects were observed when miR-146a was specifically overexpressed in monocytes[106]. These observations have classified miR-146a as an anti-inflammatory miRNA, and indeed exogenous delivery of miR-146a mimic to atherosclerosis-prone mice suppresses macrophage NF-κB signaling, thereby attenuating atherosclerosis[107]. However, more recently, the role of macrophage miR-146a in atherosclerosis lesion progression was evaluated directly in *Ldlr*$^{-/-}$ mice receiving BM from wild-type or miR-146a$^{-/-}$ mice. Unexpectedly, lack of miR-146 in BM-derived cells reduces atherogenesis, yet paradoxically enhances inflammatory signaling[108]. Moreover, miR-146a expression is significantly increased in human atherosclerotic plaques[109], suggesting a role of this miRNA in lesion development.

Another miRNA found to control NF-κB signalling pathway is miR-223. miR-223 has been shown to induce the activation of PI3K/AKT signaling, which has recently been

recognized as a negative regulator for TLR4-mediated inflammation, thus suppressing TLR4-NF-κB pathway and leading to a reduction in macrophage foam cell formation, lipid accumulation and pro-inflammatory cytokine production in LPS-activated macrophages[110]. Not only in the canonical pathway, miR-223 has also been considered as a chief component in the noncanonical NF-κB pathway. During monocyte-macrophage differentiation, a significant reduction of miR-223 expression, which was accompanied by a significant increase in IKKα (IκB kinase alpha subunit) protein that was a target of miR-223, induces a shift from the canonical to the noncanonical NF-κB pathway. This aims to prevent macrophage from becoming overactivated while priming them for future NF-κB signaling events[111]. Finally, genome-wide miRNA screens have identified miR-223 as a negative regulator of NLRP3 inflammasome activation. miR-223 directly suppresses NLRP3 expression, thereby abolishing NLRP3 function and IL-1β secretion in primary neutrophils[112,113].

Macrophage polarization: Numerous miRNAs have been found to be differentially expressed in different macrophage subsets, suggesting a role of miRNAs in regulating macrophage polarization. For example, while human macrophages polarized toward the pro-inflammatory M1 phenotype showed enrichment of miR-125a-3p and miR-26a-2*, anti-inflammatory M2 macrophages have increased expression of miR-193b[98].

Also differentially regulated during macrophage polarization, miR-223 directly target PKNOX1 (PBX/Knotted 1 homeobox 1), which exerts a suppressive effect on macrophage pro-inflammatory activation and a stimulatory effect on anti-inflammatory activation. Ablation of miR-223 expression in mice fed a high-fat diet exacerbated the severity of systemic insulin resistance along with an adipose tissue inflammation[114].

In addition to its role in regulating cholesterol metabolism, miR-33 has been shown to instruct macrophage inflammatory polarization by disrupting the balance of aerobic glycolysis and mitochondrial oxidative phosphorylation. *Via* AMP-activated protein kinase (AMPK) targeting, deletion of miR-33 in macrophages promotes fatty acid oxidation, which is reflected by increased mitochondrial oxygen consumption rates and spare respiratory capacity, as well as induces the expression of M2 macrophage markers. Besides, miR-33 inhibition also increased macrophage expression and activity of the retinoic acid-producing enzyme aldehyde dehydrogenase ALDH1A2 although it is not a predicted target of miR-33, equipping these cells with the capacity to promote the differentiation of atheroprotective regulatory T cells. In fact, antagonism of miR-33 in $Ldlr^{-/-}$ fed a Western diet results in accumulation of anti-inflammatory M2 macrophages and $FOXP3^{+}$ (forkhead box P3) regulatory T cells, and reduction of atherosclerosis [83,115].

1.3. Extracellular miRNA in atherosclerosis

In addition to their endogenous physiological role as regulators of gene expression, the complexity of miRNA-mediated pathway control has exploded since the discovery that miRNAs can be released from cells, circulate in a highly stable and cell-free form in various body fluids including serum, plasma, saliva, urine, and importantly, function as paracrine molecules that regulate gene expression in recipient cells[116]. Initially, extracellular miRNAs were simply thought to be a result of passive leakage from broken cells. However, we now understand that secretion of miRNAs is a controlled, active, and specific process. miRNAs can be packaged into extracellular vesicles (EVs), including exosomes and shedding vesicles (or microvesicles), which are membrane-enclosed cell fragments released by almost all cell types under both normal and pathological conditions[117–119]. Additionally, they can be secreted

using a vesicle-free and RNA-binding protein-dependent pathway. In fact, extracellular miRNAs have been found on lipoproteins like HDL and LDL. Moreover, other RNA-binding proteins including AGO2 and nucleophosmin 1 were also found to bind a significant portion of circulating miRNAs in plasma[117,119]. The encapsulation of miRNAs into EVs or their association with lipoproteins as well as RNA-binding proteins protect these small RNAs against ribonuclease-mediated degradation and thereby help them remain stable in the circulation.

EV-encapsulated miRNAs are known to be effective mediators of intercellular communication between different cell types involved in plaque progression[120]. However, the role of EVs, especially specific miRNAs loaded into EVs, in the development of atherosclerosis remains unclear. Therefore, elaborating the function of circulating miRNAs during atherogenesis will certainly improve our understanding of the molecular mechanisms that govern atherosclerotic lesion progression and enable the development of novel therapeutic strategies to treat atherosclerosis.

1.3.1. Structure, biogenesis, and function of EVs

Although most studies attributed the isolated vesicles to exosomes because of their exosome-like protein contents, circulating vesicles detectable *in vitro* and *in vivo* are likely to be mixed populations of both exosomes and microvesicles (Figure 1.3).

Exosomes: Among different lipid-based carriers of extracellular miRNAs, exosomes are specialized membranous vesicles ranging from 30 to more than 100nm in size and are derived from the endosomal compartments called multivesicular bodies (MVBs). In endocytosis, endocytic vesicles form at the plasma membrane and fuse to form early endosomes. These mature and become late endosomes where the membranes of MVBs invaginates inward

forming intraluminal vesicles (ILVs), which are then referred as exosomes. During this process, exosomes are known to encapsulate material from the cell cytoplasm including RNA, cDNA, and protein. Finally, instead of fusing with the lysosome, these MVBs directly fuse with the plasma membrane and release exosomes into the extracellular space, a distinct process that is not shared by other membrane-derived vesicles[121–123]. Exosomes are composed of a hydrophilic core and bilayer-phospholipid shell enriched in tetraspanin family molecules (CD9, CD63, CD81), lipid raft-associated proteins such as flotillin-1, and cell-specific receptors that can bind partnering proteins on recipient cells, allowing a specific interaction of the exosomes with the target cell of interest. Because exosome biogenesis involve the endosomal sorting complex required for transport (ESCRT complex), exosomes also contains components of the ESCRT machinery including ALIX (apoptosis-linked gene 2-interacting protein X) and TSG101 (tumor susceptibility gene 101)[124,125].

Microvesicles: Microvesicles, on the other hand, are larger vesicles (with a diameter of 200nm to 1μm) that are produced by direct budding from the cell plasma membrane as shedding vesicles[126]. Microvesicle formation is proposed to be calcium-dependent and associated with disruption of the cellular cytoskeleton as well as loss of membrane asymmetry. This process is initiated by an increase in intracellular cytosolic calcium that activates calpain and gelsolin, which cleaves tallin/activin and actin-capping proteins respectively, leading to the detachment of membrane protrusions from the cortical actin and remodeling of the cytoskeleton[127]. The next step in microvesicle formation involve the enzymes flippase, floppase, and scramblase that control phospholipid asymmetry[128]. Particularly, the increase in calcium ions also activates floppase and scramblase while inactivates flippase, resulting in the translocation of

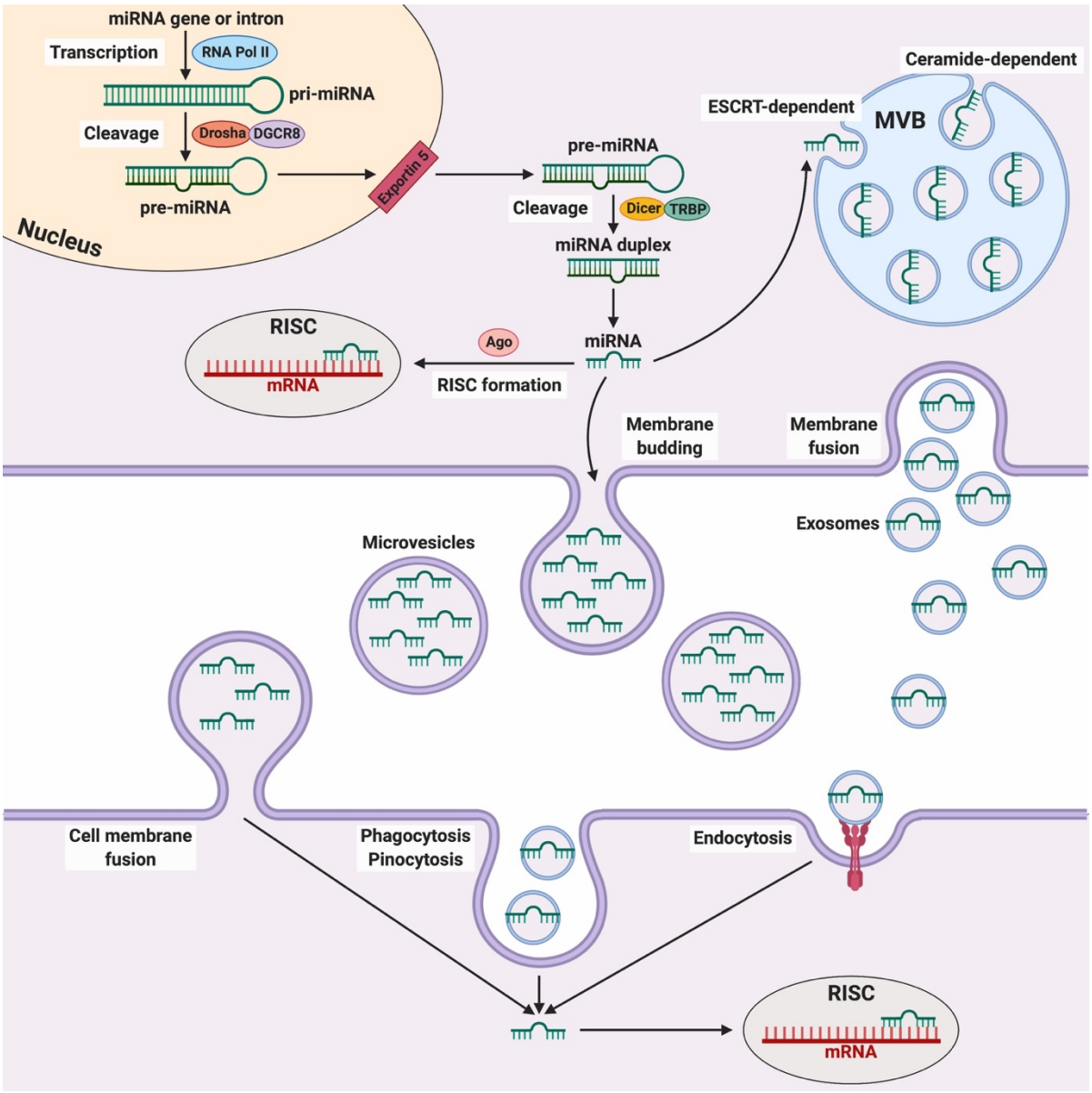

Figure 1.3. Mechanisms regulating extracellular miRNA processing, release, and uptake. miRNAs are transcribed in the nucleus by RNA polymerase II as primary miRNAs, which are then cleaved by Drosha and DGCR8 to form smaller precursor miRNAs. These pre-miRNA molecules are recognized by Exportin 5 for export to the cytoplasm, where they undergo further cleavage by Dicer into mature, double-stranded miRNAs. The preferred guide strand is loaded into the RISC complex and binds to its target mRNA to induce either degradation or translation inhibition of its bound target. In addition, miRNAs can be actively secreted from cells *via* microvesicles formed by plasma membrane budding or exosomes that are released into the extracellular space upon exocytic fusion of MVBs with the plasma membrane. In the circulation, EVs bind to the plasma membrane of a target cell. They either fuse directly with the membrane or first be endocytosed/phagocytosed and then fuse with the delimiting membrane of an endocytic compartment. Both pathways result in the delivery of EV-derived miRNAs to the cytosol of the recipient cell where it can repress specific mRNAs.

phosphatidylserine from the inner leaflet of the cell membrane bilayer to the outer[127]. Even though the mechanisms by which microvesicles are formed are known, much remains to be understood about their definite unique markers. The surface markers of microvesicles are largely dependent on the composition of the membrane of origin; however, whether particular components enriched on microvesicles relative to their originating plasma membrane needs further characterization.

Each cell type appears to secrete a unique assortment of EVs containing a specific set of cargo proteins and RNAs, which allow a precise and regulated signal to be communicated to recipient cells. The nature of the proteins, lipids, and RNAs packaged into an EV is highly dependent on the cell type of origin, the trigger or stimulus for release, and the lipid content of the surrounding membranes. However, the specific mechanisms that define cargo selection and packaging into vesicles remain undetermined. Some evidence suggests that sumoylated heterogenous nuclear ribonucleoproteins (hnRNPs) direct the loading of miRNAs into exosomes through recognition of specific short motifs[129]. MEK-ERK (mitogen-activated protein kinase kinase/extracellular-signal-regulated kinase) signaling downstream of activated KRAS was shown to inhibit sorting of AGO2 and AGO2-dependent miRNA let-7a into tumor cell-derived exosomes[130]. In addition, the RNA-binding protein Y-box protein 1 (YBX1) is required for the sorting of miR-223 in exosomes secreted by HEK293T cells[131]. However, whether these mechanisms are general or cell type- as well as condition-specific awaits further insights.

Additionally, the mechanisms by which EVs are taken up by recipient cells and especially, how RNAs in these vesicles are released and localized to the cytoplasmic or nuclear compartments in which they are functional are not well defined. It has been hypothesized that

EVs can donate their RNAs to recipient cells by endocytosis (clathrin-dependent or -independent), lipid raft-mediated, phagocytosis, macropinocytosis or direct fusion with the plasma membrane[116]. These processes are believed to involve specific ligand-receptor interactions[132]. For examples, exosomes exposing tetraspanin 8 preferentially bind cells expressing Mac1 (CD11b/CD18) and/or CD54, suggesting a role of exosomal tetraspanin complexes in target cell selection[133]. Moreover, developmental endothelial locus-1 (DEL-1), a glycoprotein that is secreted by ECs, has been shown to mediate endothelial uptake of platelet microparticles[134].

1.3.2. Extracellular miRNAs as mediators of CVD

Following the discovery that miRNAs are actively exported from cells, the importance of extracellular miRNA in several diseases including cardiovascular disease has been illustrated by a number of elegant studies showing the uptake and functional consequences in recipient cells (Figure 1.4). One of the earliest studies to show the transfer of miRNAs between different cells was the study of apoptotic bodies. EC-derived apoptotic bodies containing miR-126 conveyed paracrine signals to induce the pro-repair CXCL12/CXCR4 signaling cascade in vascular cells during atherosclerosis[135]. Recently, the same group also reported that the other "arm" of this mature miRNA (*i.e.*, miR-126-5p and not miR-126-3p) inhibits atherosclerosis independently *via* controlling EC proliferation[136], indicating that the guide and passenger strands of a miRNA can have divergent secretory pathways and downstream function. Not only apoptotic bodies, ECs also transfer miR-126 to recipient cells *via* microvesicles. Delivery of miR-126-enriched microvesicles to coronary artery ECs enhances EC migration as well as proliferation *in vitro* and promotes vascular endothelial repair *in vivo via* negatively regulating SPRED1 (sprouty-related, EVH1 domain-containing protein 1)[137]. In addition to miR-126,

EC-derived microvesicles deliver functional miR-222 to recipient cells where miR-222 represses the expression of its target protein Icam1 both intro and *in vivo*, leading to reduced monocyte adhesion[138]. Moreover, it was shown that KLF2-transduced or shear-stress-stimulated ECs released vesicles that are selectively enriched in miR-143/145. Notably, these vesicles were taken up by SMCs where the exogenous miR-143/145 controlled the expression of multiple genes implicated in SMC fate and plasticity, accounting for reduced atherosclerotic lesion formation in the aorta of *ApoE*$^{-/-}$ mice[139]. EVs secreted from KLF2-transduced ECs, on the other hand, have lower expression of inflammation-associated miR-155 compared to EVs from oxidized LDL-induced ECs. Of note, these EVs can suppress monocyte/macrophage pro-inflammatory activation (M1) while promote macrophage activation toward the anti-inflammatory phenotype (M2) *in vitro* and *in vivo*, therefore attenuating atherosclerosis[140]. Also being transported into monocytic cells by endothelial EVs, miR-10a represses monocyte/macrophage activation *via* targeting several components of the NF-κB signaling pathway such as IRAK4[141]. Also derived from ECs, miR146a-enriched exosomes might play a central role in the development of peripartum cardiomyopathy, where the secretion of exosomes containing miR-146a was taken up by cardiomyocytes and resulted in the down-regulation of several genes including *Erbb4*, *Notch1* as well as *Irak1* and reduction of metabolic activity in recipient cells[142]. Furthermore, microvesicles containing secreted monocytic miR-150, which was increased in the plasma of patients with atherosclerosis, was shown to be taken up by neighboring ECs. Interestingly, this miR-150 reduced the expression of its target gene (*c-Myb*), resulting in the enhancement of EC migration both *in vitro* and *in vivo*[143].

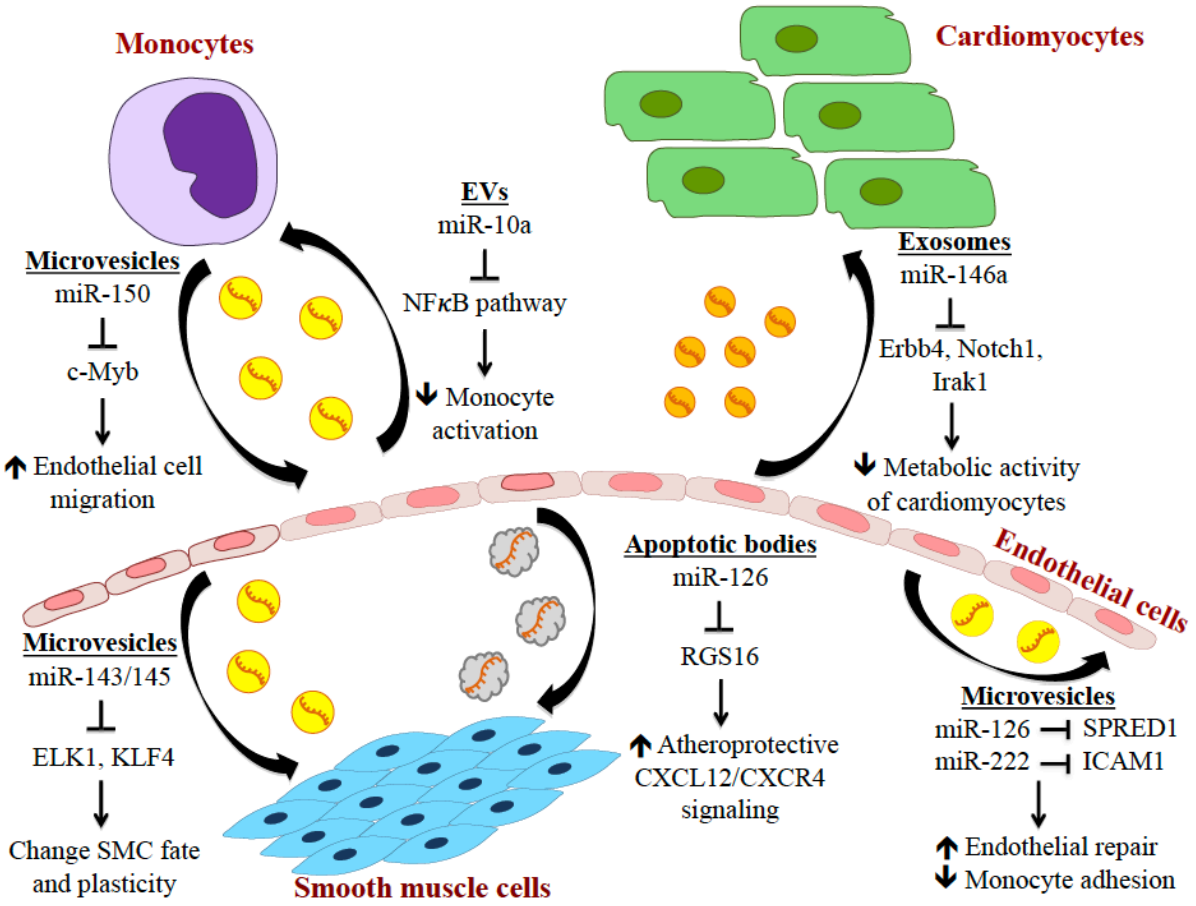

Figure 1.4. Extracellular miRNA mediates intercellular communication in CVD. All cell types involved in CVD are known to secrete miRNAs in EVs to mediate intercellular communication. ECs release EVs that are enriched in either miR-126, miR-222, miR-10a, miR-146a, or miR-143/145, depending on different conditions. These EVs can regulate endothelial cellular functions, monocyte activation, cardiomyocyte metabolism, or SMC phenotypic switching, respectively. EC-derived apoptotic bodies containing miR-126 also convey paracrine signals to induce the pro-repair CXCL12/CXCR4 signaling cascade in SMCs during atherosclerosis. On the other hand, monocytes secrete miR-150 in microvesicles to control EC migration. Images modified from My-Anh Nguyen *et al.* (2014)[144].

1.3.3. Macrophage EVs as extracellular messenger

Macrophages are central players in the development of atherosclerosis. Not only scavenger cells, macrophages also function as immune mediator cells. They utilize extracellular messengers in the form of cytokines, chemokines, and growth factors to communicate inflammatory signals[31,34,145]. EVs has also been shown to serve as another mediator of communication between macrophages and other immune cells during inflammation and infection. Macrophages stimulated with LPS release exosomes containing elevated levels of cytokines and miRNAs that mediate inflammation[146]. Similarly, mycobacteria-infected macrophages secrete exosomes containing pathogen-associated molecular patterns (PAMPs) that can induce cytokine production and recruitment of other immune cells including neutrophils to inflammatory sites, making macrophage-derived exosomes central to the activation of acquired immunity[147]. EVs secreted from mycobacteria-infected macrophages or isolated from the serum of infected mice can also drive inflammatory activation of ECs, resulting in increased expression of genes and proteins (*i.e.* VCAM1, CCL2, CXCL1) known to promote leukocyte recruitment and activation[148]. Additionally, human macrophage-derived exosomes were shown to control endothelial cell migration by inducing the internalization and degradation of integrin β1[149]. It has also been reported that exosomes derived from macrophages showed enrichment of miR-223 and can regulate macrophage differentiation[150]. Furthermore, tumor-associated macrophages (TAMs) were shown to transport miR223-containing exosomes to breast cancer cells, where miR-223 promoted the invasion of recipient cells *via* the MEF2C-β-catenin pathway[151]. Especially, a recent study by Niu *et al.* showed that leukocyte-derived EVs from atherosclerotic patients as well as foam cell-derived EVs can induce ERK and AKT activation in vascular SMCs and thus promote

SMC adhesion and migration[152], highlighting the role of macrophage-derived EVs in the development of atherosclerosis.

1.4. miRNA-based therapeutics in CVD

1.4.1. Current status

Evidence has been accumulating about the crucial role of miRNAs in controlling different aspects of lipid metabolism, inflammation, insulin signaling and other aspects of CVD. Thus, targeting miRNAs as an effective therapeutic strategy for treating CVD has gained considerable attention. For example, global market for miRNA research tools, diagnostics and therapeutics, which reached 756.5 million and 829.8 million dollars in 2015 and 2016 respectively, is currently one of the most valuable markets nowadays. Furthermore, this market is expected to be valued at 1.4 billion dollars in 2021[153].

Different strategies have been currently developed to modulate miRNA effects for therapeutic purposes through two main approaches including inhibition and overexpression. In principle, miRNA inhibitors are used to block the activity of miRNAs that drive disease progression whereas miRNA mimics are delivered to increase the expression of beneficial miRNAs in disease settings. However, the development of miRNA inhibition using oligonucleotides-based methodologies is more advanced than miRNA overexpression through synthetic RNA duplexes[154]. In particular, several methods could be utilized to reduce the expression of endogenous miRNAs including: small-molecule inhibitors that interfere with miRNA expression/processing[155]; miRNA-masking using oligonucleotides complementary to the 3'-UTR of a protein-coding mRNA, leading to the competitive inhibition of the endogenous mRNA:miRNA interaction[156]; miRNA sponges containing multiple miRNA binding sites, which out-compete endogenous mRNA targets[157]; and antisense

oligonucleotides (ASOs) (also known as miRNA antagonists or anti-miRNAs)[154]. All of these approaches are also chemically modified such as changing phosphodiester linkage to phosphorothioate bonds and substituting the 2'-OH group in the ribose ring with 2'-O-methyl, 2'-O-methoxyethyl, or 2'-fluoro groups in order to increase *in vivo* stability and improve pharmacokinetic properties[158,159]. miRNA inhibition through oligonucleotide-based approaches has shown promising results in different experimental animal models of metabolic diseases. For example, therapeutic inhibition of miR-33 was found to significantly increase circulating levels of HDL-cholesterol in mice and non-human primates and protected against atherosclerosis in hyperlipidemia mouse models[73,74,76,160,161]. Despite their great therapeutic potential, the use of oligonucleotides-based approaches in clinical settings is still limited and especially, has not yet reach clinical trials for cardiovascular disorders. Until now, only antisense inhibitors targeting miR-122 have made it through to a phase II clinical trials for the treatment of chronic HCV (hepatitis C virus) infection[162,163]. On the other hand, the chemistry behind miRNA overexpression through mimicry has significantly lagged behind miRNA inhibition owing to substantial challenges in their delivery and design[164]. Although they are now relatively easy to synthesize, double stranded miRNA mimics tend to trigger immune responses against dsRNA while the polyanionic nature of RNA duplexes makes them difficult to pass across the cytoplasmic membrane of cells targeted for therapy. Moreover, miRNA mimics are particularly susceptible to degradation in the circulation, and any chemical modifications to prolong the half-life of these nucleic acids are likely to interfere with their function. The first miRNA mimics entering clinical testing is MRX34[165], a synthetic double stranded RNA oligonucleotide that can replace depleted miR-34 and restore its activity on the p53/Wnt signaling pathway[166].

1.4.2. Future perspectives of miRNA-based therapies

Despite significant achievements in the field, cellular uptake, biodistribution, and toxicity still remain the major limitations for miRNA-targeting therapies. All of these challenges have emphasized the need to develop more comprehensive strategies for miRNA modulation, particularly more efficient delivery systems for miRNA therapeutics, in the context of CVD.

1.4.2.1. Nanoparticles (NPs)

Oligonucleotides including anti-miRs, miRNA mimics and small interfering RNAs (siRNAs) can be linked with nanocarriers not only to improve their resistance to nuclease degradation and intracellular delivery but also to reduce the risks of immune rejection. To date, numerous engineered NP platforms including chitosan-based NPs, polymeric NPs, and liposomes have been developed for wide variety of disease application, some of which have made significant advances towards the clinic[167,168]. However, although these NPs have served as a powerful tool to deliver siRNAs or miRNAs in various cancer models, its application in the cardiovascular filed is still in its infancy and requires further investigation.

Chitosan-based NPs: Chitosan, which is generally produced by deacetylation of chitin from crustacean, is a linear polysaccharide of randomly distributed N-acetyl-D-glucosamine and D-glucosamine units that is protonated in slightly acidic conditions. Due to this cationic nature, which permits an efficient complexation of nucleic acids into NPs, along with natural abundance, low toxicity, and biodegradability, chitosan has been selected as an ideal carrier for siRNAs and miRNAs[169,170]. Chitosan NP (referred to here as chNP)-mediated delivery of the tumor-suppressive miR-34 inhibited tumor growth and preserved bone integrity in a xenograft model representative of established prostate cancer bone metastasis[171].

Liposomes: Similar to chNPs, liposomes, which is one of the first drug delivery vehicles being developed[172], are extensively used in different biomedical applications because of their lack of toxicity and ability to entrap both hydrophobic as well as hydrophilic pharmaceutical agents[173]. For example, Hsu *et al.*[174] in a recent study used liposomes encapsulating the liver-specific miR-122 as a vehicle to restore deregulated gene expression in hepatocellular carcinoma (HCC), suppressing HCC xenograft growth in a mouse model of HCC. Liposomes are vesicle-like structures ranging from 100nm to several micrometers in size, dependent on each type, and comprising an aqueous core and a lipid bilayer shell. Its shell can be formed by one or several concentric lipid bilayers with an aqueous phase between the lipid bilayers[173].

Polymeric NPs: More stable in biological fluids after systemic administration than previously mentioned NPs are polymeric NPs. More importantly, owing to the design flexibility based on functionalization, synthesis methods, and polymer diversity, this kind of NPs have become of interest as potential delivery platforms for wide range of therapeutics from hydrophobic, hydrophilic, to amphiphilic molecules. To date, most of the polymeric NPs reported in the literature are based on poly(lactide), poly(glycolide), poly(ε-caprolactone, poly(lactide-co-glycolide) copolymers, and poly(amino acids)[175]. Polymeric NPs-based nanomedicines are being tested for use in numerous diseases including CVD[176], cancer[177], and diabetes mellitus[178].

NPs-mediated delivery of miRNA therapeutics can provide a unique advantage over other delivery systems, which is tissue-specific targeting. The surface of NPs can be decorated with receptor-targeting ligands, peptides or antibodies capable of recognizing and binding to

cells of interest, facilitating drug accumulation in the desired tissues and organs. For example, to target proangiogenic miR-132, which can induce neovascularization by repressing a negative regulator of Ras RASA1, in ECs, anti-miR-132 was packaged into liposomes bearing $\alpha_V\beta_3$ integrin-targeting cyclic RGD (Arg-Gly-Asp) peptides. Delivery of anti-miR-132 using these NPs did restore the expression of RASA1 in the endothelium, reduce angiogenesis, and decrease tumor burden in a mouse model of human breast carcinoma[179]. Recently, Huang *et al.*[180] showed that by using a cationic polysaccharide that has a significantly high affinity for the mannose receptors on macrophages/DCs to encapsulate let-7b, they can specifically delivered let-7b to macrophages, which reprograms tumor associated macrophages towards M1-like phenotype and inhibits tumor growth in a breast cancer mouse model. These examples provide support for the potential of tissue-specific delivery of miRNA therapeutics without unwanted effects in non-diseased tissues.

1.4.2.2. EVs

Although the field of NPs-based nanomedicines have rapidly advanced during the past few years, issues with low efficacy of delivery, rapid clearance of NPs from the circulation, and poor biocompatibility still cannot be overstated. The only option for completely eliminating the potential of immune response is to use nanocarriers derived from a patient's own body.

The discovery that EVs can transfer miRNAs to regulate gene expression in recipient cells has garnered excitement for the possibility that EVs may serve as novel therapeutic tools for various diseases including CVD[118,181]. Thanks to their non-toxic nature, ability to overcome natural barriers, intrinsic cell targeting properties and stability in the circulation, EVs provides compelling opportunities to harness naturally produced biological carriers for

disease treatment[182]. In this concept, cells can be harvested from a patient and used to produce vesicles *in vitro*, which are then loaded with ncRNA therapeutics of interest for delivery to the patient's diseased tissue. Also similar to NPs, the surface of EVs can be modified with ligands or peptides to improve specific targeting. This concept has been supported by a recent study where cells were engineered to secrete exosomes expressing target cell-compatible ligands on their surface, and these exosomes could be loaded with therapeutic siRNAs[183]. Moreover, the potential use of EVs as drug delivery vehicles have been highlighted by a recent work by Usman *et al.*[184]. This study demonstrated that EVs isolated from human red blood cells can deliver RNA drugs targeting miR-125b, including ASOs, Cas9 mRNA and guide RNAs, leading to efficient miRNA knockdown and gene knockout with CRISPR-Cas9 in leukemia and breast cancer cells both *in vitro* and *in vivo*.

1.5. Summary

Macrophages are central players in the development of atherosclerosis[28]. Especially, macrophage cholesterol efflux and RCT, which promote the removal of free cholesterol and other lipids from foam cells, are crucial to prevent lipid accumulation or reverse atherogenesis[4,28,31]. Thus, targeting macrophage cholesterol efflux could be a promising therapeutic approach to atherosclerosis. miRNAs are important regulators of various pathways involved in atherosclerosis including cholesterol efflux. During inflammation, macrophages secrete EVs carrying RNA, protein and lipids as a form of extracellular communication. In the vessel wall, EV-derived miRNAs can be transferred to naïve vascular cells, where they can alter gene expression, cell function, and ultimately, the progression of atherosclerosis. However, the role of macrophage-derived EVs in atherogenesis is not known. Moreover, while liposomes or polymeric NPs have been employed as systemic delivery vehicles of siRNA in

preclinical models[185–187], none of these platforms have been used to deliver miRNAs to macrophages *in vivo*.

Objectives and Hypotheses:

The objective for the first part of this study was to assess the contribution of EVs secreted from cholesterol-loaded macrophages to atherosclerosis development. We hypothesized that atherogenic macrophages promote pro-inflammatory and pro-atherogenic phenotypes in recipient cells through secretion of EVs containing miRNAs.

In the second part of this study, our objective was to develop chNPs for delivering functional miRNA mimics to macrophages and study the effects of these NPs on RCT *in vivo*.

Our final objective was to investigate the role of BM-derived miR-223 in atherosclerosis development. While numerous miRNAs have been shown to regulate cholesterol efflux, most of them inhibit macrophage cholesterol efflux, thereby accelerating atherosclerosis progression. miR-223 is one of a few miRNAs whose overexpression can promote cholesterol efflux[188], modulate the inflammatory response[110–113], and thus, be anti-atherogenic. We therefore hypothesized that miR-223 can protect against atherosclerosis by acting as a crucial modulator of macrophage cholesterol efflux and inflammation.

1.6. References

1. Naghavi, M. *et al.* Global, regional, and national age-sex specific mortality for 264 causes of death, 1980–2016: a systematic analysis for the Global Burden of Disease Study 2016. *Lancet* **390**, 1151–1210 (2017).
2. Chilton, R. J. Pathophysiology of coronary heart disease: a brief review. *J. Am. Osteopath. Assoc.* **104**, S5-8 (2004).
3. Messier, C., Awad, N. & Gagnon, M. The relationships between atherosclerosis, heart disease, type 2 diabetes and dementia. *Neurol. Res.* **26**, 567–572 (2004).
4. Lusis, A. Atherosclerosis. *Nature* **407**, 233–241 (2000).
5. Tabas, I., García-Cardeña, G. & Owens, G. K. Recent insights into the cellular biology of atherosclerosis. *J. Cell Biol.* **209**, 13–22 (2015).
6. Weber, C. & Noels, H. Atherosclerosis: Current pathogenesis and therapeutic options. *Nat. Med.* **17**, 1410–1422 (2011).

7. Nabel, E. G. & Braunwald, E. A Tale of Coronary Artery Disease and Myocardial Infarction. *N. Engl. J. Med.* **366**, 54–63 (2012).
8. Yang, Q. *et al.* Assessing potential population impact of statin treatment for primary prevention of atherosclerotic cardiovascular diseases in the USA: Population-based modelling study. *BMJ Open* **7**, 1–11 (2017).
9. Golomb, B. A. & Evans, M. A. Statin adverse effects : a review of the literature and evidence for a mitochondrial mechanism. *Am. J. Cardiovasc. Drugs* **8**, 373–418 (2008).
10. Ecker, J. R. *et al.* ENCODE explained. *Nature* **489**, 52–54 (2012).
11. Feinberg, M. W. & Moore, K. J. MicroRNA Regulation of Atherosclerosis. *Circ. Res.* **118**, 703–720 (2016).
12. Lu, Y., Thavarajah, T., Gu, W., Cai, J. & Xu, Q. Impact of miRNA in Atherosclerosis. *Arterioscler. Thromb. Vasc. Biol.* **38**, 159–170 (2018).
13. Swirski, F. K. *et al.* Ly-6Chi monocytes dominate hypercholesterolemia-associated monocytosis and give rise to macrophages in atheromata. *J. Clin. Invest.* **117**, 195–205 (2007).
14. Tacke, F. *et al.* Monocyte subsets differentially employ CCR2, CCR5, and CX3CR1 to accumulate within atherosclerotic plaques. *J. Clin. Invest.* **117**, 185–194 (2007).
15. Ley, K., Laudanna, C., Cybulsky, M. I. & Nourshargh, S. Getting to the site of inflammation: The leukocyte adhesion cascade updated. *Nat. Rev. Immunol.* **7**, 678–689 (2007).
16. Soehnlein, O. *et al.* Distinct functions of chemokine receptor axes in the atherogenic mobilization and recruitment of classical monocytes. *EMBO Mol. Med.* **5**, 471–481 (2013).
17. Mestas, J. & Ley, K. Monocyte-Endothelial Cell Interactions in the Development of Atherosclerosis. *Trends Cardiovasc. Med.* **18**, 228–232 (2008).
18. Combadière, C. *et al.* Combined inhibition of CCL2, CX3CR1, and CCR5 abrogates Ly6Chi and Ly6Clo monocytosis and almost abolishes atherosclerosis in hypercholesterolemic mice. *Circulation* **117**, 1649–1657 (2008).
19. Di Gregoli, K. & Johnson, J. L. Role of colony-stimulating factors in atherosclerosis. *Curr. Opin. Lipidol.* **23**, 412–21 (2012).
20. Steinberg, D. The LDL modification hypothesis of atherogenesis: an update. *J. Lipid Res.* **50 Suppl**, S376–S381 (2009).
21. Cyrus, T. *et al.* Disruption of the 12/15-lipoxygenase gene diminishes atherosclerosis in apo E-deficient mice. *J. Clin. Invest.* **103**, 1597–604 (1999).
22. Miller, Y. I. *et al.* Oxidation-specific epitopes are danger-associated molecular patterns recognized by pattern recognition receptors of innate immunity. *Circ. Res.* **108**, 235–248 (2011).
23. Kzhyshkowska, J., Neyen, C. & Gordon, S. Role of macrophage scavenger receptors in atherosclerosis. *Immunobiology* **217**, 492–502 (2012).
24. Kunjathoor, V. V. *et al.* Scavenger receptors class A-I/II and CD36 are the principal receptors responsible for the uptake of modified low density lipoprotein leading to lipid loading in macrophages. *J. Biol. Chem.* **277**, 49982–49988 (2002).
25. Boyanovsky, B. B., Van Der Westhuyzen, D. R. & Webb, N. R. Group V secretory phospholipase A2-modified low density lipoprotein promotes foam cell formation by a SR-A- and CD36-independent process that involves cellular proteoglycans. *J. Biol. Chem.* **280**, 32746–32752 (2005).

26. Kruth, H. S. *et al.* Macropinocytosis is the endocytic pathway that mediates macrophage foam cell formation with native low density lipoprotein. *J. Biol. Chem.* **280**, 2352–2360 (2005).
27. Maxfield, F. R. & Tabas, I. Role of cholesterol and lipid organization in disease. *Nature* **438**, 612–621 (2005).
28. Moore, K. J. & Tabas, I. Macrophages in the pathogenesis of atherosclerosis. *Cell* **145**, 341–55 (2011).
29. Tabas, I. Macrophage death and defective inflammation resolution in atherosclerosis. *Nat. Rev. Immunol.* **10**, 36–46 (2009).
30. Duewell, P. *et al.* NLRP3 inflammasomes are required for atherogenesis and activated by cholesterol crystals. *Nature* **464**, 1357–1361 (2010).
31. Moore, K. J., Sheedy, F. J. & Fisher, E. a. Macrophages in atherosclerosis: a dynamic balance. *Nat. Rev. Immunol.* **13**, 709–21 (2013).
32. Feng, B. *et al.* The endoplasmic reticulum is the site of cholesterol-induced cytotoxicity in macrophages. *Nat. Cell Biol.* **5**, 781–792 (2003).
33. Murray, P. J. & Wynn, T. A. Protective and pathogenic functions of macrophage subsets. *Nat. Rev. Immunol.* **11**, 723–737 (2011).
34. Chinetti-Gbaguidi, G., Colin, S. & Staels, B. Macrophage subsets in atherosclerosis. *Nat. Rev. Cardiol.* **12**, 10–17 (2015).
35. Buono, C. *et al.* Influence of Interferon-γ on the Extent and Phenotype of Diet-Induced Atherosclerosis in the LDLR-Deficient Mouse. *Arterioscler. Thromb. Vasc. Biol.* **23**, 454–460 (2003).
36. Gupta, S. *et al.* IFN-gamma potentiates atherosclerosis in ApoE knock-out mice. *J. Clin. Invest.* **99**, 2752–2761 (1997).
37. Whitman, S. C., Ravisankar, P., Elam, H. & Daugherty, A. Exogenous interferon-gamma enhances atherosclerosis in apolipoprotein E-/- mice. *Am. J. Pathol.* **157**, 1819–24 (2000).
38. Hanna, R. N. *et al.* NR4A1 (Nur77) Deletion Polarizes Macrophages Toward an Inflammatory Phenotype and Increases Atherosclerosis. *Circ. Res.* **110**, 416–427 (2012).
39. Hamers, A. A. J. *et al.* Bone Marrow–Specific Deficiency of Nuclear Receptor Nur77 Enhances Atherosclerosis. *Circ. Res.* **110**, 428–438 (2012).
40. Liao, X. *et al.* Krüppel-like factor 4 regulates macrophage polarization. *J. Clin. Invest.* **121**, 2736–2749 (2011).
41. Cardilo-Reis, L. *et al.* Interleukin-13 protects from atherosclerosis and modulates plaque composition by skewing the macrophage phenotype. *EMBO Mol. Med.* **4**, 1072–1086 (2012).
42. Chinetti-Gbaguidi, G. *et al.* Human Atherosclerotic Plaque Alternative Macrophages Display Low Cholesterol Handling but High Phagocytosis Because of Distinct Activities of the PPARγ and LXRα Pathways. *Circ. Res.* **108**, 985–995 (2011).
43. Tall, A. R., Yvan-Charvet, L., Terasaka, N., Pagler, T. & Wang, N. HDL, ABC Transporters, and Cholesterol Efflux: Implications for the Treatment of Atherosclerosis. *Cell Metab.* **7**, 365–375 (2008).
44. Yvan-Charvet, L., Wang, N. & Tall, A. R. Role of HDL, ABCA1, and ABCG1 transporters in cholesterol efflux and immune responses. *Arterioscler. Thromb. Vasc. Biol.* **30**, 139–143 (2010).

45. Cuchel, M. & Rader, D. J. Macrophage reverse cholesterol transport: Key to the regression of atherosclerosis? *Circulation* **113**, 2548–2555 (2006).
46. Van Eck, M. *et al.* Leukocyte ABCA1 controls susceptibility to atherosclerosis and macrophage recruitment into tissues. *Proc. Natl. Acad. Sci.* **99**, 6298–6303 (2002).
47. Wang, X. *et al.* Macrophage ABCA1 and ABCG1, but not SR-BI, promote macrophage reverse cholesterol transport in vivo. *J. Clin. Invest.* **117**, 2216–2224 (2007).
48. Brunham, L. R., Singaraja, R. R. & Hayden, M. R. Variations on a Gene: Rare and Common Variants in *ABCA1* and Their Impact on HDL Cholesterol Levels and Atherosclerosis. *Annu. Rev. Nutr.* **26**, 105–129 (2006).
49. Clee, S. M. *et al.* Common genetic variation in {ABCA1} is associated with altered lipoprotein levels and a modified risk for coronary artery disease. *Circulation* **103**, 1198–1205 (2001).
50. Singh, R. *et al.* Autophagy regulates lipid metabolism. *Nature* **458**, 1131–1135 (2009).
51. Ouimet, M. *et al.* Autophagy regulates cholesterol efflux from macrophage foam cells via lysosomal acid lipase. *Cell Metab.* **13**, 655–667 (2011).
52. Liao, X. *et al.* Macrophage autophagy plays a protective role in advanced atherosclerosis. *Cell Metab.* **15**, 545–553 (2012).
53. Razani, B. *et al.* Autophagy links inflammasomes to atherosclerotic progression. *Cell Metab.* **15**, 534–544 (2012).
54. Llodrá, J. *et al.* Emigration of monocyte-derived cells from atherosclerotic lesions characterizes regressive, but not progressive, plaques. *Proc. Natl. Acad. Sci. U. S. A.* **101**, 11779–84 (2004).
55. Trogan, E. *et al.* Laser capture microdissection analysis of gene expression in macrophages from atherosclerotic lesions of apolipoprotein E-deficient mice. *Proc. Natl. Acad. Sci.* **99**, 2234–2239 (2002).
56. Randolph, G. J. Emigration of monocyte-derived cells to lymph nodes during resolution of inflammation and its failure in atherosclerosis. *Curr. Opin. Lipidol.* **19**, 462–468 (2008).
57. Park, Y. M. *et al.* Oxidized LDL/CD36 interaction induces loss of cell polarity and inhibits macrophage locomotion. *Mol. Biol. Cell* **23**, 3057–3068 (2012).
58. Young, M. P., Febbraio, M. & Silverstein, R. L. CD36 modulates migration of mouse and human macrophages in response to oxidized LDL and may contribute to macrophage trapping in the arterial intima. *J. Clin. Invest.* **119**, 136–145 (2009).
59. Zeibig, S. *et al.* Effect of the oxLDL binding protein Fc-CD68 on plaque extension and vulnerability in atherosclerosis. *Circ. Res.* **108**, 695–703 (2011).
60. van Gils, J. M. *et al.* The neuroimmune guidance cue netrin-1 promotes atherosclerosis by inhibiting the emigration of macrophages from plaques. *Nat. Immunol.* **13**, 136–143 (2012).
61. Wanschel, A. *et al.* Neuroimmune guidance cue semaphorin 3E is expressed in atherosclerotic plaques and regulates macrophage retention. *Arterioscler. Thromb. Vasc. Biol.* **33**, 886–893 (2013).
62. Feig, J. E. *et al.* Regression of Atherosclerosis is characterized by broad changes in the plaque macrophage transcriptome. *PLoS One* **7**, (2012).
63. Lee, R. C., Feinbaum, R. L. & Ambros, V. The C. elegans heterochronic gene lin-4 encodes small RNAs with antisense complementarity to lin-14. *Cell* **75**, 843–54 (1993).
64. Lewis, B. P., Shih, I., Jones-Rhoades, M. W., Bartel, D. P. & Burge, C. B. Prediction

of mammalian microRNA targets. *Cell* **115**, 787–98 (2003).
65. Filipowicz, W., Bhattacharyya, S. N. & Sonenberg, N. Mechanisms of post-transcriptional regulation by microRNAs: Are the answers in sight? *Nat. Rev. Genet.* **9**, 102–114 (2008).
66. Friedman, R. C., Farh, K. K. H., Burge, C. B. & Bartel, D. P. Most mammalian mRNAs are conserved targets of microRNAs. *Genome Res.* **19**, 92–105 (2009).
67. Lau, N. C., Lim, L. P., Weinstein, E. G. & Bartel, D. P. An abundant class of tiny RNAs with probable regulatory roles in Caenorhabditis elegans. *Science* **294**, 858–62 (2001).
68. Lagos-Quintana, M., Rauhut, R., Lendeckel, W. & Tuschl, T. Identification of novel genes coding for small expressed RNAs. *Science* **294**, 853–8 (2001).
69. Kim, V. N. MicroRNA biogenesis: coordinated cropping and dicing. *Nat. Rev. Mol. Cell Biol.* **6**, 376–385 (2005).
70. Huntzinger, E. & Izaurralde, E. Gene silencing by microRNAs: contributions of translational repression and mRNA decay. *Nat. Rev. Genet.* **12**, 99–110 (2011).
71. He, L. & Hannon, G. J. MicroRNAs: small RNAs with a big role in gene regulation. *Nat. Rev. Genet.* **5**, 522–531 (2004).
72. Madrigal-Matute, J., Rotllan, N., Aranda, J. F. & Fernández-Hernando, C. MicroRNAs and atherosclerosis. *Curr. Atheroscler. Rep.* **15**, 322 (2013).
73. Najafi-Shoushtari, S. H. *et al.* MicroRNA-33 and the SREBP Host Genes Cooperate to Control Cholesterol Homeostasis. *Science* **328**, 1566–1569 (2010).
74. Rayner, K. J. *et al.* MiR-33 contributes to the regulation of cholesterol homeostasis. *Science* **328**, 1570–3 (2010).
75. Gerin, I. *et al.* Expression of miR-33 from an SREBP2 intron inhibits cholesterol export and fatty acid oxidation. *J. Biol. Chem.* **285**, 33652–33661 (2010).
76. Horie, T. *et al.* MicroRNA-33 encoded by an intron of sterol regulatory element-binding protein 2 (Srebp2) regulates HDL in vivo. *Proc. Natl. Acad. Sci. U. S. A.* **107**, 17321–6 (2010).
77. Marquart, T. J., Allen, R. M., Ory, D. S. & Baldan, A. miR-33 links SREBP-2 induction to repression of sterol transporters. *Proc. Natl. Acad. Sci.* **107**, 12228–12232 (2010).
78. Allen, R. M. *et al.* miR-33 controls the expression of biliary transporters, and mediates statin- and diet-induced hepatotoxicity. *EMBO Mol. Med.* **4**, 882–895 (2012).
79. Li, T., Francl, J. M., Boehme, S. & Chiang, J. Y. L. Regulation of cholesterol and bile acid homeostasis by the cholesterol 7α-hydroxylase/steroid response element-binding protein 2/microRNA-33a axis in mice. *Hepatology* **58**, 1111–1121 (2013).
80. Rayner, K. J. *et al.* Antagonism of miR-33 in mice promotes reverse cholesterol transport and regression of atherosclerosis. *J. Clin. Invest.* **121**, 2921–2931 (2011).
81. Horie, T. *et al.* MicroRNA-33 deficiency reduces the progression of atherosclerotic plaque in ApoE-/- mice. *J. Am. Heart Assoc.* **1**, 1–17 (2012).
82. Rotllan, N., Ramírez, C. M., Aryal, B., Esau, C. C. & Fernández-Hernando, C. Therapeutic silencing of MicroRNA-33 inhibits the progression of atherosclerosis in Ldlr-/- mice - Brief report. *Arterioscler. Thromb. Vasc. Biol.* **33**, 1973–1977 (2013).
83. Karunakaran, D. *et al.* Macrophage Mitochondrial Energy Status Regulates Cholesterol Efflux and Is Enhanced by Anti-miR33 in Atherosclerosis. *Circ. Res.* **117**, 266–278 (2015).
84. Graham, A. Mitochondrial regulation of macrophage cholesterol homeostasis. *Free Radic. Biol. Med.* **89**, 982–992 (2015).

85. Allen, A. M. & Graham, A. Mitochondrial function is involved in regulation of cholesterol efflux to apolipoprotein (apo)A-I from murine RAW 264.7 macrophages. *Lipids Heal. Dis* **11**, 169 (2012).
86. de Aguiar Vallim, T. Q. *et al.* MicroRNA-144 regulates hepatic ATP binding cassette transporter A1 and plasma high-density lipoprotein after activation of the nuclear receptor farnesoid X receptor. *Circ. Res.* **112**, 1602–12 (2013).
87. Ramírez, C. M. *et al.* Control of cholesterol metabolism and plasma high-density lipoprotein levels by microRNA-144. *Circ. Res.* **112**, 1592–601 (2013).
88. Hu, Y.-W. *et al.* An agomir of miR-144-3p accelerates plaque formation through impairing reverse cholesterol transport and promoting pro-inflammatory cytokine production. *PLoS One* **9**, e94997 (2014).
89. Sun, D. *et al.* MiR-26 controls LXR-dependent cholesterol efflux by targeting ABCA1 and ARL7. *FEBS Lett.* **586**, 1472–1479 (2012).
90. Meiler, S., Baumer, Y., Toulmin, E., Seng, K. & Boisvert, W. A. MicroRNA 302a is a novel modulator of cholesterol homeostasis and atherosclerosis. *Arterioscler. Thromb. Vasc. Biol.* **35**, 323–331 (2015).
91. Ramirez, C. M. *et al.* MicroRNA-758 regulates cholesterol efflux through posttranscriptional repression of ATP-binding cassette transporter A1. *Arterioscler. Thromb. Vasc. Biol.* **31**, 2707–2714 (2011).
92. Zhang, M. *et al.* MicroRNA-27a/b regulates cellular cholesterol efflux, influx and esterification/hydrolysis in THP-1 macrophages. *Atherosclerosis* **234**, 54–64 (2014).
93. Goedeke, L. *et al.* MicroRNA-148a regulates LDL receptor and ABCA1 expression to control circulating lipoprotein levels. *Nat. Med.* **21**, 1280–1288 (2015).
94. Wagschal, A. *et al.* Genome-wide identification of microRNAs regulating cholesterol and triglyceride homeostasis. *Nat Med* **21**, 1290–1297 (2015).
95. Ouimet, M. *et al.* MiRNA targeting of oxysterol-binding protein-like 6 regulates cholesterol trafficking and efflux. *Arterioscler. Thromb. Vasc. Biol.* **36**, 942–951 (2016).
96. Goedeke, L. *et al.* A Regulatory Role for MicroRNA 33* in Controlling Lipid Metabolism Gene Expression. *Mol. Cell. Biol.* **33**, 2339–2352 (2013).
97. O'Connell, R. M., Taganov, K. D., Boldin, M. P., Cheng, G. & Baltimore, D. MicroRNA-155 is induced during the macrophage inflammatory response. *Proc. Natl. Acad. Sci.* **104**, 1604–1609 (2007).
98. Graff, J. W., Dickson, A. M., Clay, G., McCaffrey, A. P. & Wilson, M. E. Identifying functional microRNAs in macrophages with polarized phenotypes. *J. Biol. Chem.* **287**, 21816–21825 (2012).
99. Nazari-Jahantigh, M. *et al.* MicroRNA-155 promotes atherosclerosis by repressing Bcl6 in macrophages. *J. Clin. Invest.* **122**, 4190–4202 (2012).
100. Du, F. *et al.* MicroRNA-155 deficiency results in decreased macrophage inflammation and attenuated atherogenesis in apolipoprotein E-deficient mice. *Arterioscler. Thromb. Vasc. Biol.* **34**, 759–767 (2014).
101. Donners, M. M. P. C. *et al.* Hematopoietic miR155 deficiency enhances atherosclerosis and decreases plaque stability in hyperlipidemic mice. *PLoS One* **7**, e35877 (2012).
102. Wei, Y. *et al.* The microRNA-342-5p fosters inflammatory macrophage activation through an Akt1- and microRNA-155-dependent pathway during atherosclerosis. *Circulation* **127**, 1609–19 (2013).

103. Taganov, K. D., Boldin, M. P., Chang, K.-J. & Baltimore, D. NF-kappaB-dependent induction of microRNA miR-146, an inhibitor targeted to signaling proteins of innate immune responses. *Proc. Natl. Acad. Sci. U. S. A.* **103**, 12481–12486 (2006).
104. Chassin, C. *et al.* miR-146a mediates protective innate immune tolerance in the neonate intestine. *Cell Host Microbe* **8**, 358–68 (2010).
105. Perry, M. M. *et al.* Rapid Changes in MicroRNA-146a Expression Negatively Regulate the IL-1β-Induced Inflammatory Response in Human Lung Alveolar Epithelial Cells. *J. Immunol.* **180**, 5689–5698 (2008).
106. Boldin, M. P. *et al.* miR-146a is a significant brake on autoimmunity, myeloproliferation, and cancer in mice. *J. Exp. Med.* **208**, 1189–201 (2011).
107. Li, K., Ching, D., Luk, F. S. & Raffai, R. L. Apolipoprotein e Enhances MicroRNA-146a in Monocytes and Macrophages to Suppress Nuclear Factor-κB-Driven Inflammation and Atherosclerosis. *Circ. Res.* **117**, e1–e11 (2015).
108. Cheng, H. S. *et al.* Paradoxical Suppression of Atherosclerosis in the Absence of microRNA-146a. *Circ. Res.* **121**, 354–367 (2017).
109. Raitoharju, E. *et al.* MiR-21, miR-210, miR-34a, and miR-146a/b are up-regulated in human atherosclerotic plaques in the Tampere Vascular Study. *Atherosclerosis* **219**, 211–217 (2011).
110. Wang, J. *et al.* miR-223 inhibits lipid deposition and inflammation by suppressing toll-like receptor 4 signaling in macrophages. *Int. J. Mol. Sci.* **16**, 24965–24982 (2015).
111. Li, T. *et al.* MicroRNAs modulate the noncanonical transcription factor NF-κB pathway by regulating expression of the kinase IKKα during macrophage differentiation. *Nat. Immunol.* **11**, 799–805 (2010).
112. Haneklaus, M. *et al.* Cutting edge: miR-223 and EBV miR-BART15 regulate the NLRP3 inflammasome and IL-1β production. *J. Immunol.* **189**, 3795–9 (2012).
113. Bauernfeind, F. *et al.* NLRP3 Inflammasome Activity Is Negatively Controlled by miR-223. *J. Immunol.* **189**, 4175–4181 (2012).
114. Zhuang, G. *et al.* A novel regulator of macrophage activation: miR-223 in obesity-associated adipose tissue inflammation. *Circulation* **125**, 2892–903 (2012).
115. Ouimet, M. *et al.* MicroRNA-33–dependent regulation of macrophage metabolism directs immune cell polarization in atherosclerosis. *J. Clin. Invest.* **125**, 4334–4348 (2015).
116. Chen, X., Liang, H., Zhang, J., Zen, K. & Zhang, C.-Y. Secreted microRNAs: a new form of intercellular communication. *Trends Cell Biol.* **22**, 125–32 (2012).
117. Boon, R. a. & Vickers, K. C. Intercellular transport of MicroRNAs. *Arterioscler. Thromb. Vasc. Biol.* **33**, 186–192 (2013).
118. Rayner, K. J. & Hennessy, E. J. Extracellular communication via microRNA: lipid particles have a new message. *J. Lipid Res.* **54**, 1174–81 (2013).
119. Chen, X., Liang, H., Zhang, J., Zen, K. & Zhang, C.-Y. Horizontal transfer of microRNAs: molecular mechanisms and clinical applications. *Protein Cell* **3**, 28–37 (2012).
120. Valadi, H. *et al.* Exosome-mediated transfer of mRNAs and microRNAs is a novel mechanism of genetic exchange between cells. *Nat. Cell Biol.* **9**, 654–659 (2007).
121. Keller, S., Sanderson, M. P., Stoeck, A. & Altevogt, P. Exosomes: from biogenesis and secretion to biological function. *Immunol. Lett.* **107**, 102–8 (2006).
122. Ludwig, A.-K. & Giebel, B. Exosomes: small vesicles participating in intercellular

communication. *Int. J. Biochem. Cell Biol.* **44**, 11–5 (2012).
123. Bobrie, A., Colombo, M., Raposo, G. & Théry, C. Exosome Secretion: Molecular Mechanisms and Roles in Immune Responses. *Traffic* **12**, 1659–1668 (2011).
124. Yellon, D. M. & Davidson, S. M. Exosomes: nanoparticles involved in cardioprotection? *Circ. Res.* **114**, 325–32 (2014).
125. Kowal, J., Tkach, M. & Théry, C. Biogenesis and secretion of exosomes. *Curr. Opin. Cell Biol.* **29**, 116–125 (2014).
126. Muralidharan-Chari, V., Clancy, J. W., Sedgwick, A. & D'Souza-Schorey, C. Microvesicles: mediators of extracellular communication during cancer progression. *J. Cell Sci.* **123**, 1603–1611 (2010).
127. Schara, K. *et al.* Mechanisms for the formation of membranous nanostructures in cell-to-cell communication. *Cell. Mol. Biol. Lett.* **14**, 636–656 (2009).
128. Daleke, D. L. Regulation of transbilayer plasma membrane phospholipid asymmetry. *J. Lipid Res.* **44**, 233–242 (2003).
129. Villarroya-Beltri, C. *et al.* Sumoylated hnRNPA2B1 controls the sorting of miRNAs into exosomes through binding to specific motifs. *Nat. Commun.* **4**, 2980 (2013).
130. McKenzie, A. J. *et al.* KRAS-MEK Signaling Controls Ago2 Sorting into Exosomes. *Cell Rep.* **15**, 978–987 (2016).
131. Shurtleff, M. J., Temoche-Diaz, M. M., Karfilis, K. V., Ri, S. & Schekman, R. Y-box protein 1 is required to sort microRNAs into exosomes in cells and in a cell-free reaction. *Elife* **5**, 040238 (2016).
132. Hulsmans, M. & Holvoet, P. MicroRNA-containing microvesicles regulating inflammation in association with atherosclerotic disease. *Cardiovasc. Res.* **100**, 7–18 (2013).
133. Rana, S., Yue, S., Stadel, D. & Zöller, M. Toward tailored exosomes: The exosomal tetraspanin web contributes to target cell selection. *Int. J. Biochem. Cell Biol.* **44**, 1574–1584 (2012).
134. Dasgupta, S. K., Le, A., Chavakis, T., Rumbaut, R. E. & Thiagarajan, P. Developmental endothelial locus-1 (del-1) mediates clearance of platelet microparticles by the endothelium. *Circulation* **125**, 1664–1672 (2012).
135. Zernecke, A. *et al.* Delivery of MicroRNA-126 by Apoptotic Bodies Induces CXCL12-Dependent Vascular Protection. *Sci. Signal.* **2**, ra81 (2009).
136. Schober, A. *et al.* MicroRNA-126-5p promotes endothelial proliferation and limits atherosclerosis by suppressing Dlk1. *Nat. Med.* **20**, 368–76 (2014).
137. Jansen, F. *et al.* Endothelial microparticle-mediated transfer of microRNA-126 promotes vascular endothelial cell repair via spred1 and is abrogated in glucose-damaged endothelial microparticles. *Circulation* **128**, 2026–2038 (2013).
138. Jansen, F. *et al.* Endothelial microparticles reduce ICAM-1 expression in a microRNA-222-dependent mechanism. *J. Cell. Mol. Med.* **19**, 2202–2214 (2015).
139. Hergenreider, E. *et al.* Atheroprotective communication between endothelial cells and smooth muscle cells through miRNAs. *Nat. Cell Biol.* **14**, 249–56 (2012).
140. He, S. *et al.* Endothelial extracellular vesicles modulate the macrophage phenotype: Potential implications in atherosclerosis. *Scand. J. Immunol.* **87**, 1–16 (2018).
141. Njock, M.-S. *et al.* Endothelial cells suppress monocyte activation through secretion of extracellular vesicles containing antiinflammatory microRNAs. *Blood* **125**, 3202–3212 (2015).

142. Halkein, J. *et al.* MicroRNA-146a is a therapeutic target and biomarker for peripartum cardiomyopathy. *J. Clin. Invest.* **123**, 2143–2154 (2013).
143. Zhang, Y. *et al.* Secreted monocytic miR-150 enhances targeted endothelial cell migration. *Mol. Cell* **39**, 133–44 (2010).
144. Nguyen, M. A., Karunakaran, D. & Rayner, K. J. Unlocking the Door to New Therapies in Cardiovascular Disease: MicroRNAs Hold the Key. *Curr. Cardiol. Rep.* **16**, 1–12 (2014).
145. Cochain, C. & Zernecke, A. Macrophages and immune cells in atherosclerosis: recent advances and novel concepts. *Basic Res. Cardiol.* **110**, 34 (2015).
146. McDonald, M. K. *et al.* Functional significance of macrophage-derived exosomes in inflammation and pain. *Pain* **155**, 1527–1539 (2014).
147. Bhatnagar, S., Shinagawa, K., Castellino, F. J. & Schorey, J. S. Exosomes released from macrophages infected with intracellular pathogens stimulate a proinflammatory response in vitro and in vivo. *Blood* **110**, 3234–44 (2007).
148. Li, L., Cheng, Y., Emrich, S. & Schorey, J. Activation of endothelial cells by extracellular vesicles derived from Mycobacterium tuberculosis infected macrophages or mice. *PLoS One* **13**, 1–19 (2018).
149. Lee, H. D., Kim, Y. H. & Kim, D. S. Exosomes derived from human macrophages suppress endothelial cell migration by controlling integrin trafficking. *Eur. J. Immunol.* **44**, 1156–1169 (2014).
150. Ismail, N. *et al.* Macrophage microvesicles induce macrophage differentiation and miR-223 transfer. *Blood* **121**, 984–995 (2013).
151. Yang, M. *et al.* Microvesicles secreted by macrophages shuttle invasion-potentiating microRNAs into breast cancer cells. *Mol. Cancer* **10**, 117 (2011).
152. Niu, C. *et al.* Macrophage foam cell-derived extracellular vesicles promote vascular smooth muscle cell migration and adhesion. *J. Am. Heart Assoc.* **5**, (2016).
153. Dewan, S. S. MicroRNA Research Tools, Diagnostics and Therapeutics: Global Markets. *BCC Res. Rep. Overv.* 1–11 (2017).
154. van Rooij, E. & Olson, E. N. MicroRNA therapeutics for cardiovascular disease: opportunities and obstacles. *Nat. Rev. Drug Discov.* **11**, 860–72 (2012).
155. Watashi, K., Yeung, M. L., Starost, M. F., Hosmane, R. S. & Jeang, K. T. Identification of small molecules that suppress microRNA function and reverse tumorigenesis. *J. Biol. Chem.* **285**, 24707–24716 (2010).
156. Wang, Z. The principles of MiRNA-masking antisense oligonucleotides technology. *Methods Mol. Biol.* **676**, 43–9 (2011).
157. Ebert, M. S. & Sharp, P. A. MicroRNA sponges: Progress and possibilities. *Rna* **16**, 2043–2050 (2010).
158. Davis, S., Lollo, B., Freier, S. & Esau, C. Improved targeting of miRNA with antisense oligonucleotides. *Nucleic Acids Res.* **34**, 2294–2304 (2006).
159. Gandellini, P., Profumo, V., Folini, M. & Zaffaroni, N. MicroRNAs as new therapeutic targets and tools in cancer. *Expert Opin. Ther. Targets* **15**, 265–79 (2011).
160. Rayner, K. J. *et al.* Inhibition of miR-33a/b in non-human primates raises plasma HDL and lowers VLDL triglycerides. *Nature* **478**, 404–7 (2011).
161. Rottiers, V. *et al.* Pharmacological inhibition of a microRNA family in nonhuman primates by a seed-targeting 8-mer antimiR. *Sci. Transl. Med.* **5**, (2013).
162. Janssen, H. L. A. *et al.* Treatment of HCV Infection by Targeting MicroRNA. *N. Engl.*

J. Med. **368**, 1685–1694 (2013).
163. Gebert, L. F. R. *et al.* Miravirsen (SPC3649) can inhibit the biogenesis of miR-122. *Nucleic Acids Res.* **42**, 609–621 (2014).
164. Condorelli, G., Latronico, M. V. G. & Cavarretta, E. microRNAs in cardiovascular diseases: current knowledge and the road ahead. *J. Am. Coll. Cardiol.* **63**, 2177–87 (2014).
165. Bader, A. G. MiR-34 - a microRNA replacement therapy is headed to the clinic. *Front. Genet.* **3**, 1–9 (2012).
166. Liu, C. *et al.* The microRNA miR-34a inhibits prostate cancer stem cells and metastasis by directly repressing CD44. *Nat. Med.* **17**, 211 (2011).
167. Kamaly, N., Xiao, Z., Valencia, P. M., Radovic-Moreno, A. F. & Farokhzad, O. C. Targeted polymeric therapeutic nanoparticles: Design, development and clinical translation. *Chem. Soc. Rev.* **41**, 2971–3010 (2012).
168. Gadde, S. & Rayner, K. J. Nanomedicine meets microRNA current advances in RNA-based nanotherapies for atherosclerosis. *Arterioscler. Thromb. Vasc. Biol.* **36**, e73–e79 (2016).
169. Mao, S., Sun, W. & Kissel, T. Chitosan-based formulations for delivery of DNA and siRNA. *Adv. Drug Deliv. Rev.* **62**, 12–27 (2010).
170. Garcia-Fuentes, M. & Alonso, M. J. Chitosan-based drug nanocarriers: Where do we stand? *J. Control. Release* **161**, 496–504 (2012).
171. Gaur, S. *et al.* Chitosan nanoparticle-mediated delivery of miRNA-34a decreases prostate tumor growth in the bone and its expression induces non-canonical autophagy. *Oncotarget* **6**, 29161–29177 (2015).
172. Bangham, A. D. Liposomes: the Babraham connection. *Chem. Phys. Lipids* **64**, 275–285 (1993).
173. Torchilin, V. P. Recent advances with liposomes as pharmaceutical carriers. *Nat. Rev. Drug Discov.* **4**, 145–160 (2005).
174. Hsu, S. hao *et al.* Cationic lipid nanoparticles for therapeutic delivery of siRNA and miRNA to murine liver tumor. *Nanomedicine Nanotechnology, Biol. Med.* **9**, 1169–1180 (2013).
175. Banik, B. L., Fattahi, P. & Brown, J. L. Polymeric nanoparticles: the future of nanomedicine. *Wiley Interdiscip. Rev. Nanomed. Nanobiotechnol.* **8**, 271–99 (2016).
176. Wang, Y. J. *et al.* The use of polymer-based nanoparticles and nanostructured materials in treatment and diagnosis of cardiovascular diseases: Recent advances and emerging designs. *Prog. Polym. Sci.* **57**, 153–178 (2016).
177. Prabhu, R. H., Patravale, V. B. & Joshi, M. D. Polymeric nanoparticles for targeted treatment in oncology: Current insights. *Int. J. Nanomedicine* **10**, 1001–1018 (2015).
178. Veiseh, O., Tang, B. C., Whitehead, K. A., Anderson, D. G. & Langer, R. Managing diabetes with nanomedicine: Challenges and opportunities. *Nat. Rev. Drug Discov.* **14**, 45–57 (2014).
179. Anand, S. *et al.* MicroRNA-132-mediated loss of p120RasGAP activates the endothelium to facilitate pathological angiogenesis. *Nat. Med.* **16**, 909–914 (2010).
180. Huang, Z. *et al.* Targeted delivery of let-7b to reprogramme tumor-associated macrophages and tumor infiltrating dendritic cells for tumor rejection. *Biomaterials* **90**, 72–84 (2016).
181. Chen, X., Liang, H., Zhang, J., Zen, K. & Zhang, C. Y. Secreted microRNAs: A new

form of intercellular communication. *Trends Cell Biol.* **22**, 125–132 (2012).
182. Armstrong, J. P. K. & Stevens, M. M. Strategic design of extracellular vesicle drug delivery systems. *Adv. Drug Deliv. Rev.* **130**, 12–16 (2018).
183. Alvarez-Erviti, L. *et al.* Delivery of siRNA to the mouse brain by systemic injection of targeted exosomes. *Nat. Biotechnol.* **29**, 341–5 (2011).
184. Usman, W. M. *et al.* Efficient RNA drug delivery using red blood cell extracellular vesicles. *Nat. Commun.* **9**, (2018).
185. Dahlman, J. E. *et al.* In vivo endothelial siRNA delivery using polymeric nanoparticles with low molecular weight. *Nat. Nanotechnol.* **9**, 648–655 (2014).
186. Yin, H. *et al.* Non-viral vectors for gene-based therapy. *Nat. Rev. Genet.* **15**, 541–55 (2014).
187. Khan, O. F. *et al.* Endothelial siRNA delivery in nonhuman primates using ionizable low–molecular weight polymeric nanoparticles. *Sci. Adv.* **4**, 1–11 (2018).
188. Vickers, K. C. *et al.* MicroRNA-223 coordinates cholesterol homeostasis. *Proc. Natl. Acad. Sci.* **111**, 14518–14523 (2014).

2. Extracellular Vesicles Secreted by Atherogenic Macrophages Transfer MicroRNA to Inhibit Cell Migration

Authors: My-Anh Nguyen, Denuja Karunakaran, Michele Geoffrion, Henry S. Cheng, Kristofferson Tandoc, Ljubica Perisic Matic, Ulf Hedin, Lars Maegdefessel, Jason E. Fish, Katey J. Rayner

Arteriosclerosis, Thrombosis, and Vascular Biology

Published: 2018 Jan;38(1):49-63. Epub 2017 Sep 7.

2.1. Author contributions

The experiments were planned by Katey J. Rayner and me. As the first author, I performed the majority of the experiments required for this study. Denuja Karunakaran, Michele Geoffrion and Kristofferson Tandoc helped me perform the *in vitro* RNA and protein analyses. Henry S. Cheng analyzed the aortic expression of *Igf2bp1* and *HuR* in *Ldlr*$^{-/-}$ mice transplanted with wild-type BM or miR-146a$^{-/-}$ BM. Ljubica Perisic Matic, Ulf Hedin, and Lars Maegdefessel analyzed the expression of miR-146a in human atherosclerosis samples from the Biobank of Karolinska Endarterectomy (BiKE). Jason E. Fish provided miR-146a$^{-/-}$ mice. I wrote the preliminary draft of the manuscript and together, Katey J. Rayner and I edited the manuscript until the paper was accepted to be published.

2.2. Abstract

Objective: During inflammation, macrophages secrete vesicles carrying RNA, protein and lipids as a form of extracellular communication. In the vessel wall, EVs have been shown to

be transferred between vascular cells during atherosclerosis; however, the role of macrophage-derived EVs in atherogenesis is not known. Here, we hypothesize that atherogenic macrophages secrete miRNAs in EVs to mediate cell-cell communication and promote pro-inflammatory and pro-atherogenic phenotypes in recipient cells.

Approach and Results: We isolated EVs from mouse and human macrophages treated with an atherogenic stimulus (oxidized LDL) and characterized the EV miRNA expression profile. We confirmed the enrichment of miR-146a, miR-128, miR-185, miR-365 and miR-503 in atherogenic EVs compared to controls and demonstrate that these EVs are taken up and transfer exogenous miRNA to naive recipient macrophages. Bioinformatic pathway analysis suggests that atherogenic EV miRNAs are predicted to target genes involved in cell migration and adhesion pathways, and indeed delivery of EVs to naive macrophages reduced macrophage migration both *in vitro* and *in vivo*. Inhibition of miR-146a, the most enriched miRNA in atherogenic EVs, reduced the inhibitory effect of EVs on macrophage migratory capacity. EV-mediated delivery of miR-146a repressed the expression of target genes *Igf2bp1* (insulin-like growth factor 2 mRNA-binding protein 1) and *HuR* (human antigen R or ELAV-like RNA-binding protein 1) in recipient cells, and knockdown of IGF2BP1 and HUR using siRNA greatly reduced macrophage migration, highlighting the importance of these EV-miRNA targets in regulating macrophage motility.

Conclusion: EV-derived miRNAs from atherogenic macrophages, in particular miR-146a, may accelerate the development of atherosclerosis by decreasing cell migration and promoting macrophage entrapment in the vessel wall.

2.3. Introduction

Cell-to-cell communication facilitates the functional coordination of different cell types within a tissue and is a hallmark of multicellular organisms. In addition to cell junctions, adhesion contacts and soluble messengers, cells communicate *via* the release and transfer of EVs, which have recently emerged as multifaceted regulators of intercellular communication[1–5]. Depending on their size and mechanism of generation, EVs can be classified as exosomes, microvesicles or apoptotic bodies. Exosomes are membrane vesicles ranging from 30 to 150nm in size that are generated by inward budding of the limiting membrane of MVBs. MVBs release exosomes into the extracellular environment by directly fusing with the plasma membrane[6,7]. Microvesicles, on the other hand, are larger vesicles (with a diameter of 200nm to 1μm) that are produced by direct budding from the cell plasma membrane as shedding vesicles[8,9]. Secreted EVs can be taken up by target cells through endocytosis, phagocytosis or direct fusion with the plasma membrane, leading to the delivery of EV proteins and RNAs to modulate specific cellular signaling pathways in recipient cells[10].

Like other cell types, macrophages utilize EVs to communicate inflammatory signals. During infection, macrophages secrete exosomes containing PAMPs that promote cytokine production and recruitment of other immune cells to inflammatory sites[11]. Moreover, there is increasing evidence that inflammatory macrophages transfer miRNAs packaged into EVs which alter gene expression in recipient cells[12]. Macrophage-derived microvesicles are enriched in miR-223 and are thought to regulate macrophage differentiation[13]. Although being extensively characterized in infectious inflammation, the role of macrophage-derived EVs, especially the unique EV loading of miRNAs in sterile inflammatory diseases, has not been well studied.

Atherosclerosis is a lipid-driven chronic inflammatory disease where excess cholesterol accumulation in the vessel wall drives a non-resolving immune response[14]. Although many cell types contribute to the disease, macrophages are fundamental to atherosclerotic progression and are one of the most abundant components in atherosclerotic plaques. In the early stages of atherosclerosis, the key inflammatory response to lipid accumulation and endothelial activation is recruitment of circulating monocytes into the vascular intima. Recruited monocytes differentiate into macrophages that scavenge retained modified lipoproteins, transforming into cholesterol-laden foam cells[15,16]. Excessive free cholesterol accumulation in macrophage-derived foam cells results in activation of downstream cascades including NLRP3 inflammasome, TLR signaling, and ER stress responses. These inflammatory signals exacerbate not only oxidative stress in the plaques but also the transmigration of additional inflammatory cells including monocytes into the intima[16–18]. Lesion regression requires the resolution of inflammation and macrophage emigration out of the plaques through reverse transmigration. However, during atherosclerosis progression, the expression of retention factors renders the macrophage immobile and prevent their emigration out of the artery wall[19–21]. A better understanding of mechanisms that regulate macrophage motility during atherosclerosis will provide insights into pathways that may have therapeutic value.

It is known that secreted factors such as guidance cues and chemotactic proteins are crucial for controlling monocyte recruitment and macrophage emigration, but whether or not macrophage-derived EVs also play a key role in modulating macrophage migration is unknown. We hypothesized that macrophages can promote pro-inflammatory and pro-atherogenic phenotypes in recipient cells through secretion of EVs containing miRNAs. In the

current study, we find that EVs derived from cholesterol-loaded macrophages can inhibit macrophage migration *in vitro* and *in vivo*. This effect appears to be mediated by the transfer of several miRNAs, including miR-146a, to recipient macrophages where they repress the expression of specific pro-migratory target genes *Igf2bp1* and *HuR*. Our studies suggest that EV-derived miRNAs secreted from atherogenic macrophages may accelerate the development of atherosclerosis lesions by decreasing cell migration and promoting macrophage entrapment in the vessel wall.

2.4. Materials and methods

2.4.1. Reagents

Hi-TBAR oxidized human LDL (BT-910X) and human LDL (BT-903) was purchased from Alfa Aesar (Thermo Fisher Scientific Inc.). GW4869 and Hoechst 33342 were obtained from Sigma Aldrich. Lipofetamine RNAiMAX, Lipofectamine 2000 and Vybrant DiO Cell-labeling Solution were purchased from Thermo Fisher Scientific Inc.

2.4.2. Mice

C57BL6 wild-type and *ApoE*$^{-/-}$ were purchased from Jackson Laboratories. miR-146a$^{-/-}$ mice (on a C57BL6 background) were kindly provided by Dr. Jason Fish, Toronto General Research Institute, Canada.

2.4.3. Cell culture

Peritoneal macrophages were isolated by peritoneal lavage with 3 x 5ml sterile PBS (phosphate-buffered saline) from wild-type mice that had intraperitoneal injection of 3% thioglycollate 4 days prior. Cells were maintained in DMEM (Gibco-Life Technologies) supplemented with 10% (v/v) FBS (fetal bovine serum) and 1% (v/v) penicillin-streptomycin

(P-S). BM derived macrophages (BMDMs) were harvested from femurs of wild-type mice and differentiated into macrophages using DMEM supplemented with 10% (v/v) FBS, 20% (v/v) L929 conditioned media and 1% (v/v) P-S for 7 days. RAW 264.7 macrophages were cultured in DMEM supplemented with 10% (v/v) FBS, 1% (v/v) P-S, and 1mM sodium pyruvate. THP-1 cells were maintained in RPMI 1640 media supplemented with 10% (v/v) FBS, 1% (v/v) P-S, 1mM sodium pyruvate, 40nM β-mercaptoethanol and 2g/L glucose. Prior to treatment, THP-1 cells were then differentiated with 100nM phorbol-12-mysristate acetate (PMA) for 72 hours.

2.4.4. Isolation and characterization of EVs

Macrophages were incubated in the presence or absence of 50 μg/ml of oxidized LDL in DMEM supplemented with 2% exosome-depleted FBS (System Biosciences) for 24 hours. Culture medium was collected and macrophage-derived EVs were isolated using ExoQuick-TC Exosome Precipitation Solution (System Biosciences) according to the manufacturer's instructions. In some experiments, EVs were isolated using differential ultracentrifugation. Culture medium was precleared by centrifugation at 300x*g* for 10 minutes, then 3,000x*g* for 20 minutes to eliminate cells and cellular debris. The supernatant was ultracentrifuged at 120,000x*g* for 180 minutes at 4°C, followed by washing of the EV pellet with PBS at 120,000x*g* for 180 minutes at 4°C (L8-70M Ultracentrifuge, Beckman Coulter). In other experiments, microvesicles were also isolated by ultracentrifuging at 16,000x*g* for 180 minutes at 4°C, followed by washing of the pellet with phosphate-buffered saline (PBS) at 16,000x*g* for 180 minutes at 4°C. The EV pellets were either resuspended in PBS for visualization on the NanoSight LM10 (Malvern Instruments, UK)[22] as well as on the Zetaview (Particle Metrix GmbH, Germany) (Nanoparticle Tracking Analyzer) or in ice-cold RIPA

protein lysis buffer containing protease inhibitor cocktail (Roche) for immunoblot analysis of Calnexin (Santa Cruz Biotechnology), TSG101 (Abcam) and CD9 (Abcam). Protein amount of EVs was quantified using Micro BCA Protein Assay Kit (Thermo Fisher Scientific Inc.).

2.4.5. miRNA expression profiling

Total RNA was extracted from EVs using miRNeasy Micro kit (QIAGEN) according to the manufacturer's protocol. RNA integrity and concentration were verified by Bioanalyzer RNA 6000 Pico chip (Agilent Technologies Inc.). Profiling of miRNA expression in EVs secreted from control/oxidized LDL-treated macrophages was measured using QuantiMir kit (System Biosciences) as per the manufacturer's protocol and the Affymetrix miRNA 3.0 microarray (performed at The Centre for Applied Genomics (TCAG) Microarray Facility, Sick Kids Hospital, Canada). Candidate miRNAs were confirmed by quantitative real-time PCR (qRT-PCR) using miScript II Reverse Transcription kit, miScript Primer Assays and Quantitect SYBR Green (QIAGEN), in which the expression of candidate miRNAs was normalized to an external spike-in RNA *cel*-miR-39 (QIAGEN).

2.4.6. Cell transfection with miRNA inhibitors, miRNA mimics and siRNAs

Macrophages were transfected with control anti-miR or anti-miR146a (miRIDIAN microRNA Hairpin Inhibitor – GE Dharmacon), control mimic or miR-146a mimic (miRIDIAN microRNA mimic) at a concentration of 100nM using Lipofectamine RNAiMAx as previously described[23–25]. Briefly, transfection of macrophages was performed in OPTIMEM media overnight. The next day, same volume of DMEM containing 20% (v/v) FBS was added and transfected cells were harvested 48 hours or 72 hours after transfection. Similarly, macrophages were transfected with 50nM negative (non-silencing) control siRNA, *Igf2bp1* siRNA, or *HuR* siRNA (FlexiTube siRNA – QIAGEN) for 72 hours.

2.4.7. Isolation and tracking of labeled EVs

Macrophages were stained with Vybrant DiO (green) and cultured in the presence or absence of 50 μg/ml of oxidized LDL. Labeled EVs were isolated using ExoQuick-TC Solution as described above and applied to naïve macrophages, which were grown in exosome-depleted medium (DMEM supplemented with 10% exosome-depleted FBS) using Lab-Tek Chambered Coverglass System (Thermo Fisher Scientific Inc.). Uptake of labeled EVs was visualized by the confocal microscope Fluoview FV1000 Version 2.1 (Olympus) using a 488nm laser. In the experiments where GW4869 was used, macrophages were stained with Vybrant DiO and were then treated with GW4869 (10μM) to inhibit exosome generation for 24 hours. Culture medium was collected and directly applied to naïve macrophages. Uptake of labeled vesicles was visualized by the confocal microscope Fluoview FV1000 Version 2.1 using the 488nm laser.

2.4.8. Co-culture experiments

Transwell Permeable Support systems (Corning) for 6-well plates with a 0.4μM pore-size filter were used as per the manufacturer's instructions. Vybrant DiO-labeled macrophages, *cel*-miR-54 transfected macrophages, miR-146a transfected macrophages, or wild-type macrophages were seeded into 6-well plates and recipient macrophages (naïve wild-type macrophages or miR-146a$^{-/-}$ macrophages) were seeded into the well inserts. Before starting the co-culture, transfected cells were washed extensively with PBS. All co-culture experiments were done in the presence or absence of 50 μg/ml of oxidized LDL. In the case of labeled macrophages, the well inserts were fixed with 3.7% formaldehyde in PBS and stained with Hoechst 33342 to visualize the nucleus. The membranes were separated from the

well inserts, mounted with the fluorescent medium (Dako) and visualized under the confocal microscope Fluoview FV1000 Version 2.1.

2.4.9. Bioinformatic analysis

miRSystem (http://mirsystem.cgm.ntu.edu.tw/) was used to predict the potential target genes and the pathways regulated by the top candidate miRNAs. By combining seven well-known miRNA target gene prediction programs (DIANA, miRanda, miRBridge, PicTar, PITA, rna22, and TargetScan) and two validated databases (TarBase and miRecords), potential gene targets of miRNAs are predicted based on the consistency across independent algorithms and observed/expected ratios. Lastly, five functional pathway databases (KEGG, Biocarta, PID, Reactome, and Gene Ontology) are included to characterize the enriched pathways of these target genes through bootstrap approaches[26]. In our analysis, a gene is considered a predicted target of a miRNA using at least 3 prediction algorithms.

2.4.10. Migration assays

Macrophages (BMDMs and RAW 264.7 macrophages) were treated with or without 50 μg/ml of oxidized LDL and EVs were isolated using ExoQuick-TC solution as described above. EVs were applied to naïve macrophages in exosome-depleted medium and the cells were allowed to uptake for 48 hours. The migration of macrophages to CCL2 (150 ng/ml) (R&D Systems) was monitored by the xCELLigence Real-Time Cell Analyzer System (ACEA Biosciences), which monitored chemotaxis every 5 minutes for 24 hours.

2.4.11. *In vivo* studies of macrophage emigration from the peritoneum

Mice (n=4/group) were injected intraperitoneally with 3% thioglycollate to trigger a sterile peritonitis. After 4 days, peritoneal macrophages were labeled by injection of 1μm Fluoresbrite green fluorescent plain microspheres (Polysciences) and subsequently, the mice

were pre-treated with RAW 264.7 macrophage-derived EVs (100μg) or PBS for 24 hours. The next day, the mice were injected with an inflammatory stimulus (400ng LPS) to induce efflux of macrophages from the peritoneum to the draining lymph nodes. Following LPS injection (3 hours), the peritoneal cells were collected by peritoneal lavage and counted. The percentage of macrophages in the lavage was quantified by flow cytometry using the pre-conjugated antibody PE/Cy7 anti-mouse F4/80 (BioLegend).

2.4.12. 3' UTR luciferase reporter assays

HEK293T cells were transfected with 0.8ng of a luciferase construct that includes the potential miR-146a binding site in the 3' UTR of *IGF2BP1* (GeneCopoeia), and 50nM of control or miR-146a mimics using Lipofectamine 2000. After 24 hours, cell lysates were collected, and luciferase activity was determined using the Dual Luciferase Reporter Assay System (Promega). Firefly luciferase activity was normalized to Renilla luciferase activity for transfection efficiency.

2.4.13. Gene expression analysis

Total RNA was isolated using Trizol (Invitrogen) and reverse transcribed using iScript Reverse Transcription Supermix for qRT-PCR (Bio-Rad). qRT-PCR was performed using the SsoAdvanced Universal SYBR Green Supermix (Bio-Rad) and gene expression was normalized to HPRT and 18S. The primers used are: *Igf2bp1* (Forward: 5' AGGACGAGGCTAGGAATAAGC 3'; Reverse: 5' GCCTTCGATCCAAGCCAGTA 3'), *HuR* (Forward: 5' CGGCAACCTCAACGAGAGT 3'; Reverse: 5' GTAGCCGGATTTGACCAAGAA 3')

2.4.14. Western blot analysis

Cells were washed in ice-cold PBS and lysed in ice-cold RIPA buffer supplemented with

protease inhibitor cocktail (Roche). Proteins (50μg) were subjected to 4-20% SDS-PAGE and transferred to PVDF membranes (Bio-Rad) for immunoblot analysis[23,27]. PVDF membranes were blocked with 5% (w/v) milk in TBST and incubated overnight with antibodies against IGF2BP1 (Santa Cruz Biotechnology), HUR (Santa Cruz Biotechnology), HSP90 (Santa Cruz Biotechnology), GAPDH (Millipore). Goat anti-mouse or anti-rabbit IRDye® secondary antibodies were used for detection on a LI-COR Odyssey infrared imaging system (LI-COR Biosciences).

2.4.15. Mouse and human atherosclerotic lesion analysis

ApoE$^{-/-}$ mice were fed either a regular chow or high-fat (0.2% cholesterol, Harlan Teklad) diet (n=5 per group). After 6-week diet, mice were anesthetized and perfused with RNase-free PBS. The aortic arch was excised from the heart, and lesion areas were separated from non-lesion areas using a dissection microscope. Tissue segments were homogenized in QIAzol lysis reagent (QIAGEN) using microbeads along with the Bullet Blender. Total RNA was reversed transcribed using miScript II Reverse Transcription kit and miR-146a expression was quantified by qRT-PCR as described above.

For BM transplant models, 10-week-old *Ldlr*$^{-/-}$ mice subjected to whole-body irradiation (10 Gys) was injected with BM donor cells (1 x 10^6 cells) *via* tail vein injection. These mice were then placed on a high-cholesterol diet (1.25% cholesterol, Research Diets Inc.) for 12 weeks. Total RNA was extracted from the aortic arch and RNA isolation as well as qRT-PCR was performed as describe above.

Human atherosclerotic plaques were collected by the Biobank of Karolinska Endarterectomy (BiKE) at Department of Molecular Medicine and Surgery, Karolinska Institute, as previously described[24,28,29]. miR-146a levels were analyzed by Taqman

MicroRNA assays (Life Technologies) on n=14 atherosclerotic plaque samples and n=6 control arteries. Statistical analyses were done with the GraphPad Prism 6 software and a p-value <0.05 was considered significant.

2.4.16. Statistics

Data shown is either mean ± SD of at least 3 independent experiments or a single representative experiment that were performed in triplicate. Comparison between control and treatment was made using Student's t-test ($p \leq 0.05$) or comparison between groups by one-way ANOVA ($p \leq 0.05$) using Prism GraphPad.

2.5. Results

2.5.1. Characterization of macrophage-derived EVs and EV-derived RNA

In order to characterize EVs from atherogenic macrophages, we isolated EVs from primary mouse macrophages treated with or without oxidized LDL. Nanoparticle tracking analysis showed that isolated EVs from both control and oxidized LDL-treated macrophages ranged in size from 40 to 300nm with a mean particle size of 111 and 125nm, respectively, which is the typical size range of exosomes or small microvesicles[8] (**Figure 2.1A**). Quantification of the size of EVs across multiple experiments revealed that there was a small but significant increase in the size of EVs secreted from oxidized LDL-loaded macrophages (**Figure 2.1B**). To further confirm the purity of macrophage-derived EVs, Western Blot analysis was performed and showed that EV samples isolated from control and oxidized LDL-treated macrophages were positive for CD9 and TSG101, well-known exosomal markers[6], and were negative for Calnexin, an integral ER membrane protein that was used as a marker for cell contamination (**Figure 2.1C**). We then characterized total RNA recovered from

macrophage-derived EVs using Bioanalyzer analysis and found that total EV-derived RNA mainly contained small RNAs and did not contain the prominent peaks of 18S and 28S rRNA (**Figure 2.1D).** Bioanalyzer analysis was also used to analyze total RNA isolated from oxidized LDL-containing media alone (incubated in cell-free wells) which revealed that there was little or no RNA in oxidized LDL **(Supplemental Figure 2.1A**). In addition, we examined the secretion of EVs from atherogenic macrophages using transmission electron microscopy (TEM). Results showed that some vesicles were visible as intraluminal vesicles located inside MVBs, which is typical for exosomes (**Figure 2.1E**). A different type of vesicle was also observed and characterized as clusters of endomembrane vesicles enclosed by the plasma membrane (**Figure 2.1F**). These MVB-like structures are similar to the vesicles released by smooth muscle cells implicated in vascular calcification[30]. Together, these data indicate that primary mouse macrophages secrete EVs that share many characteristics with exosomes including size, marker expression and ultrastructural secretion patterns.

2.5.2. Differential miRNA expression profile in EVs secreted from cholesterol-loaded macrophages

To characterize the EV-derived miRNA signature of atherogenic macrophages, we performed miRNA arrays on atherogenic EVs compared to control EVs and confirmed *via* qRT-PCR that EVs secreted from cholesterol-loaded macrophages were enriched in miR-146a, miR-128, miR-185, miR-365, and miR-503 (**Figure 2.2A**). We also examined the expression of these miRNAs in atherogenic EVs isolated from other macrophages, including mouse primary BMDMs, RAW 264.7, and human THP-1 monocyte-derived macrophages. As expected, the signature of EV-derived miRNAs showed similar patterns of expression in different types of macrophages (**Figure 2.2B** and **Supplemental Figure 2.1B-C**). Because of

the observation that EV-derived miRNA profiles can be slightly affected by the vesicle isolation method[31,32], we also isolated EVs from control and cholesterol-loaded macrophages using ultracentrifugation and confirmed the increased expression of top 5 miRNAs in atherogenic EVs (**Supplemental Figure 2.1D**). miRNAs are believed to be selectively packaged into EVs and do not necessarily reflect miRNA profiles observed in the parental cells[33]. To determine whether the changes of miRNA expression that occurred in EVs also occurred in the cell of origin, we examined the expression of top candidate miRNAs in the corresponding intracellular RNA samples. Although highly up-regulated in EVs secreted from atherogenic macrophages, the cellular expression levels of miR-146a, miR-128, miR-185, miR-365, and miR-503 in atherogenic macrophages did not significantly change compared to controls (**Figure 2.2C** and **2.2D**). We also confirmed that these candidate miRNAs are enriched only in exosomes or small microvesicles secreted from oxidized LDL-loaded macrophages, not in larger microvesicles isolated from oxidized LDL-loaded cells nor EVs from LDL-treated macrophages (**Supplemental Figure 2.1E-F**). Time course analysis of miRNA expression showed that upregulation of candidate miRNAs in atherogenic EVs occurred early, after 6 hours of oxidized LDL treatment, with peak expression at 24 hours and persisted until 48-hour post-treatment (**Figure 2.2E**). Together, these data indicated that macrophages loaded with oxidized LDL secrete EVs enriched in miR-146a, miR-128, miR-185, miR-365, and miR-503.

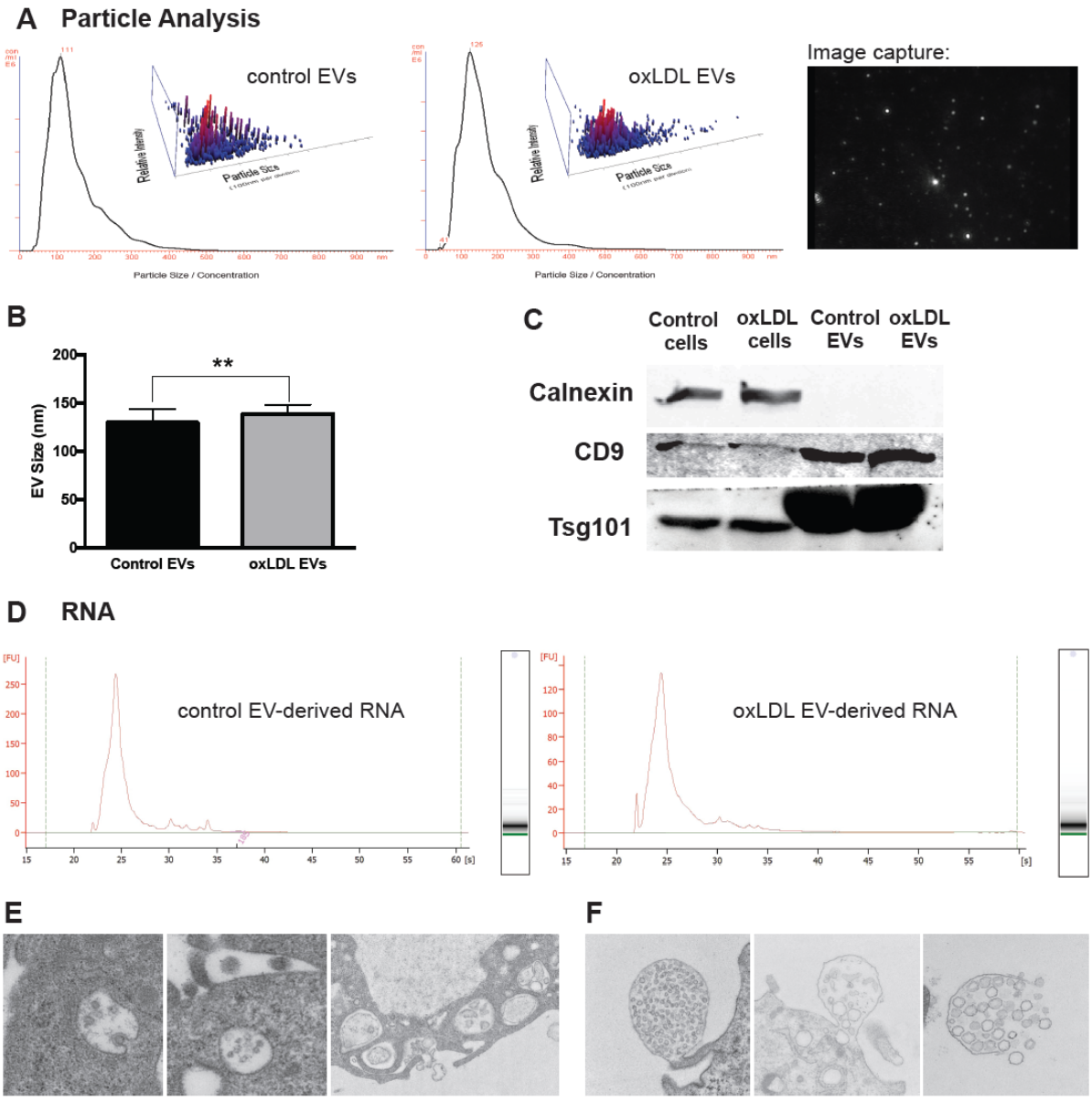

Figure 2.1. Characterization of macrophage-derived EVs and EV-derived RNA. EVs secreted from control and oxidized LDL-loaded (50 µg/ml for 24h) peritoneal macrophages were purified using ExoQuick-TC solution. **(A)** EVs were visualized on NanoSight LM10. **(B)** Mean size of EVs secreted from control and oxidized LDL-loaded macrophages. Analysis from duplicates from n=3 experiments **$p<0.01$. **(C)** EVs were subjected to immunoblot analysis of Calnexin, TSG101 and CD9 in non-reducing conditions. **(D)** Total RNA was extracted from EVs and was analyzed using Bioanalyzer RNA 6000 Pico chip. **(E)** Electron microscope images of multivesicular bodies where the membrane invaginates inward to form intraluminal vesicles referred as exosomes. **(F)** Electron microscope images of a different type of EVs secreted from oxidized LDL-loaded macrophages.

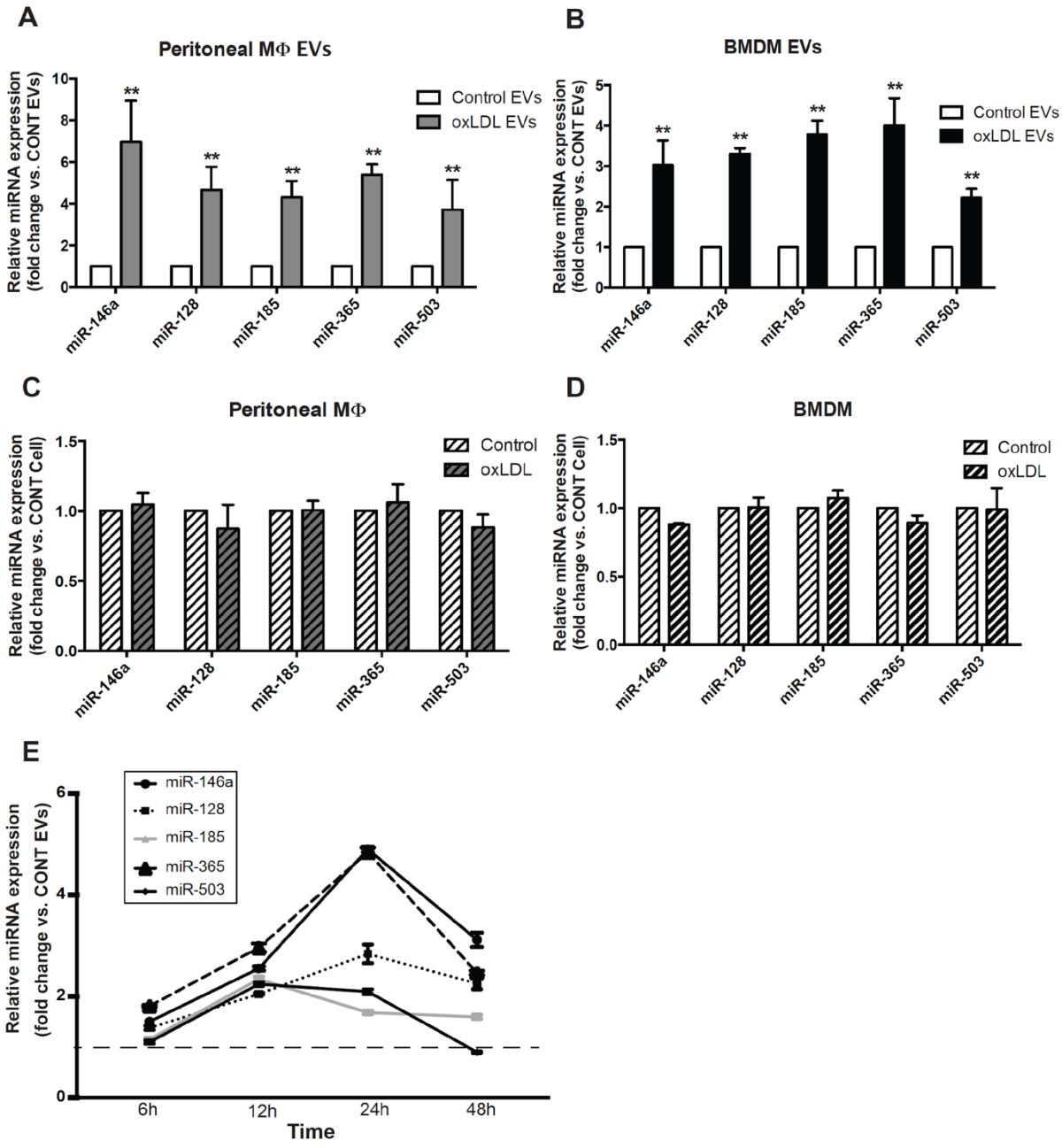

Figure 2.2. Differential miRNA expression profile in EVs secreted from oxidized LDL-loaded macrophages. **(A)** miRNA expression in EVs isolated from oxidized LDL-treated peritoneal macrophages (same experimental conditions as Figure 1). **(B)** miRNA expression in EVs isolated from oxidized LDL-treated BMDMs. (**C**) and (**D**) miRNA expression in corresponding cellular RNA samples. (**E**) Time course profile of miRNA expression in peritoneal macrophage-derived EVs. Graphs represent the means ± SD from n=3 independent experiments, **p<0.01.

2.5.3. EVs from atherogenic macrophages are taken up by naïve macrophages and transfer miRNA

In order for EV-derived miRNAs to exert paracrine effects, EVs need to be taken up and contents delivered to recipient cells. Following the identification of the most highly dysregulated miRNAs in atherogenic EVs, we proceeded to test whether control and atherogenic EVs could be taken up by naïve macrophages. We established a co-culture system where fluorescently-labeled macrophages were cultured together with naïve (unlabeled) macrophages, separated by a 0.4μm transwell filter to avoid direct cell contact or transfer of larger vesicles. Confocal microscopy analysis showed that naïve cells co-cultured with membrane labeled macrophages took up the label, indicating transfer of small (less than 0.4μm) membranous vesicles between these cells (**Figure 2.3A**). We next isolated labeled macrophage-derived EVs from control and oxidized LDL-treated cells and applied them directly to naïve macrophages. As expected, we observed a rapid uptake of fluorescently-labeled EVs from both control and atherogenic EVs into naïve cells (**Figure 2.3B**). Notably, when we inhibited exosome generation using GW4869[34], the levels of fluorescent signals in naïve cells significantly decreased as compared to control (**Figure 2.3C-D**).

To determine if macrophage-derived EVs can transfer miRNAs to naïve macrophages, we once again employed a co-culture system of macrophages transfected with *cel*-miR-54 (naturally present only in *C. elegans*) with naïve macrophages separated by a 0.4μm filter. The expression levels of *cel*-miR-54 in naïve macrophages were analyzed after 24-hour and 48-hour co-culture and demonstrated that *cel*-miR-54 is transferred to naïve macrophages (**Figure 2.3E**). Overall, this shows that EVs secreted by donor macrophages can be taken up and

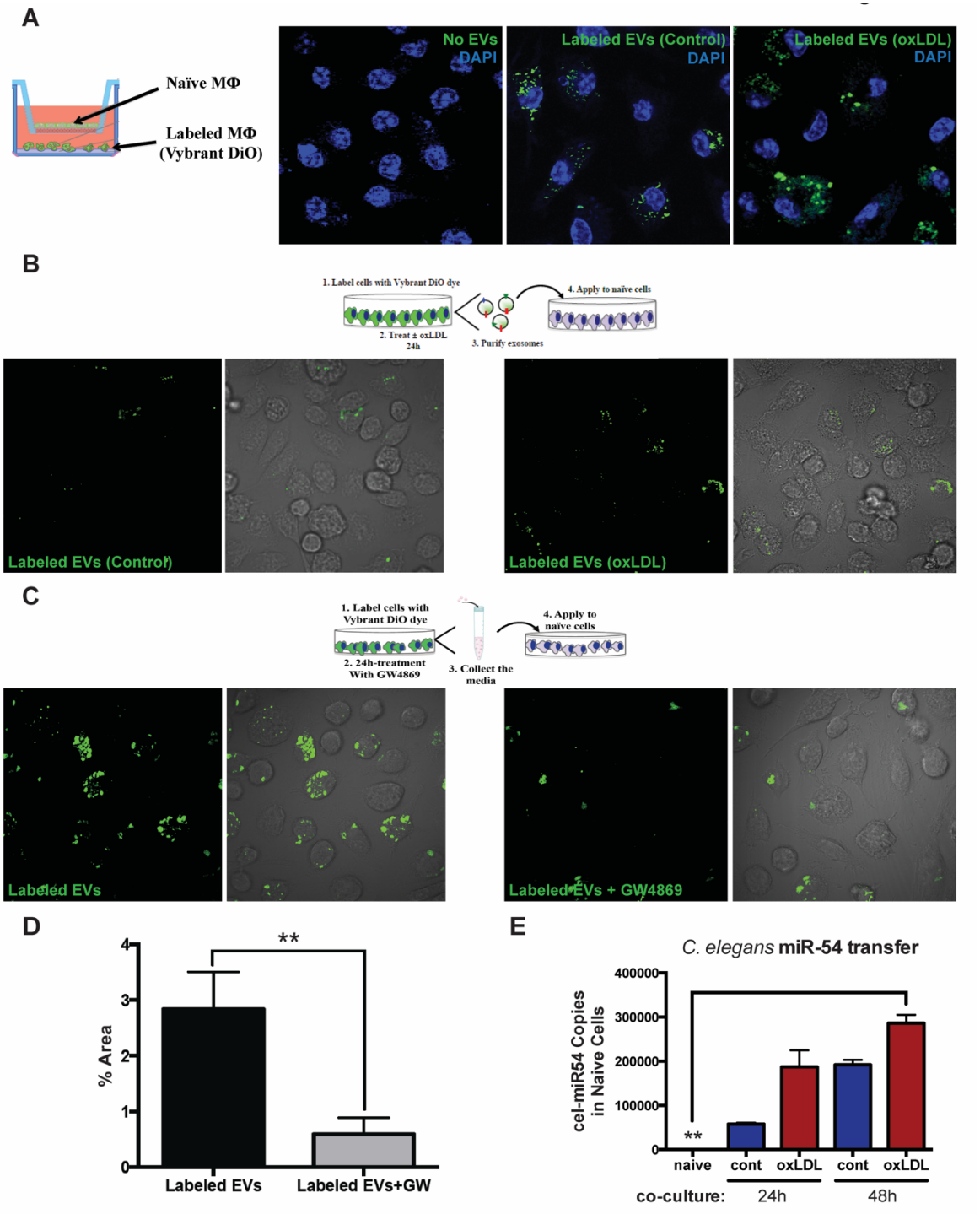
A
Naïve MΦ
Labeled MΦ
(Vybrant DiO)
No EVs
DAPI
Labeled EVs (Control)
DAPI
Labeled EVs (oxLDL)
DAPI
B
1. Label cells with Vybrant DiO dye
2. Treat ± oxLDL
24h
3. Purify exosomes
4. Apply to naïve cells
Labeled EVs (Control)
Labeled EVs (oxLDL)
C
1. Label cells with
Vybrant DiO dye
2. 24h-treatment
With GW4869
3. Collect the
media
4. Apply to
naïve cells
Labeled EVs
Labeled EVs + GW4869
D
% Area
**
Labeled EVs
Labeled EVs+GW
E
C. elegans miR-54 transfer
cel-miR54 Copies
in Naive Cells
400000
300000
200000
100000
0
**
naive
cont
oxLDL
cont
oxLDL
co-culture:
24h
48h

Figure 2.3. EVs from atherogenic macrophages are taken up and deliver exogenous miRNAs to naïve macrophages. **(A-C)** Peritoneal macrophages (donor cells) were stained with Vybrant DiO cell labeling solution, and visualization of EV uptake was performed using confocal microscopy. (**A**) Labeled macrophages were co-cultured with naïve macrophages in the absence/presence of oxidized LDL (50 μg/ml) for 24h. (**B**) Labeled macrophages were treated without/with oxidized LDL (50 μg/ml) for 24h. EVs were then purified using ExoQuick-TC solution and applied to naïve macrophages. (**C**) Labeled macrophages were pre-treated with GW4869 (10μM) for 24h. Culture media was collected and applied to naïve macrophages. **(D)** The area of fluorescent signal from (C) was quantified using Image J software using 5 fields for each condition. Graph represents the mean ± SD from n=3 independent experiments. Images are representative of experiments done in triplicate (n=3). **(E)** Macrophages (donor cells, BMDMs) were transfected with *C.elegans* miR-54 mimics and then co-cultured with naïve macrophages in the absence/presence of oxidized LDL (50 μg/ml) for 48h. Total RNA was isolated from naïve macrophages and cel-miR-54 levels were measured by qRT-PCR. The experiment was performed in triplicate (n=3), **p <0.01.

transfer their miRNA contents to recipient macrophages and these EVs are likely derived from the exosomal pathway.

2.5.4. Atherogenic EVs inhibit macrophage migration *in vitro*

To determine the potential pathways regulated by the signature of EV-derived miRNA, we performed bioinformatic analysis on the most dysregulated miRNAs in atherogenic EVs (including up- and down-regulated miRNAs) using miRSystem[26]. The rationale for this approach is that although the magnitude of gene repression exerted by a single miRNA is relatively small, distinct miRNAs can simultaneously target many genes in a given pathway and collectively alter cell function. Pathway analysis demonstrated that EV-derived miRNAs secreted from atherogenic macrophages putatively target cell migration pathways, with at least 7 out of 10 dysregulated miRNAs predicted to target genes that control leukocyte transendothelial migration, cell adhesion molecules, regulation of actin cytoskeleton and axon guidance (**Table 2.1**); many of which have been shown to play a role in atherosclerosis[35–37].

Because of the importance of macrophage migration during all stages of atherosclerosis[15,16], we investigated whether or not EVs secreted from atherogenic macrophages can indeed control migration in recipient cells. We treated naïve macrophages with EVs either from control or oxidized LDL-treated cells for 48 hours and measured their migration towards CCL2 – a chemokine known to promote macrophage migration[20,21]. Treatment of naïve macrophages with EVs derived from atherogenic macrophages inhibited the migration of naïve cells towards CCL2 to a greater extent than EVs from control macrophages (80% decrease in migration relative to control, $p \leq 0.01$) (**Figure 2.4A-B**). Similar results were observed when we examined the effects of atherogenic EVs on the migration ability of RAW 264.7 macrophages (**Supplemental Figure 2.2A-B**). To confirm that the

inhibitory effect on macrophage migration is specific for EVs, we again inhibited exosome generation using GW4869 and showed that blockade of exosome generation partially relieved the effect of EVs on macrophage migration (**Supplemental Figure 2.2C**). Thus, EVs isolated from atherogenic macrophages can be transferred to naïve macrophages and inhibit their migration *in vitro*.

2.5.5. Macrophage-derived EVs reduce macrophage emigration *in vivo*

During atherosclerosis regression, plaque macrophages emigrate from the lesion *via* nearby lymphatics upon cholesterol lowering and removal *via* efflux pathways[38]. This is similar to mechanisms used by inflammatory macrophages as they rapidly emigrate from the inflamed peritoneum to the draining lymph nodes during resolving peritonitis[39]. Therefore, we used a well-characterized peritonitis model to test the effect of EVs on macrophage emigration *in vivo*. Mice were first injected with thioglycollate to trigger macrophage accumulation in the peritoneal cavity, after which LPS was delivered to induce the rapid efflux of macrophages from the peritoneum. As previously observed[40], injection of LPS reduced the number of macrophages in the peritoneum by 60% compared to control PBS-injected mice. In contrast, mice pretreated with macrophage-derived EVs prior to LPS stimulation had equivalent macrophages remaining in the peritoneum as PBS treated mice, indicating that macrophage emigration out of the peritoneal cavity was not efficient (**Figure 2.4C**). Taken together, these data indicate that macrophage-derived EVs can inhibit macrophage migration both *in vitro* and *in vivo*.

Table 2.1. Bioinformatic pathway analysis of the most significantly up-regulated miRNAs from atherogenic EVs. miRSystem (http://mirsystem.cgm.ntu.edu.tw/) was used and listed here are the most enriched pathways, including how many miRNAs (out of 10) are predicted to target the pathway. A gene is considered as a potential target of a miRNA using at least 3 prediction algorithms.

Pathways Predicted to be targeted by dysregulated miRNAs	Predicted pathways	Target Genes of Interest	# miRNAs targeting pathway (/10)
	Leukocyte Transendothelial Migration	PI3 kinase receptor 1, RhoA, ROCK1, ROCK2, PECAM, Cadherin 5, Cdc42, Protein kinase C-β	7
	Cell Adhesion Molecules	PTEN, PI3 kinase R1, Cell adhesion molecule 1 (CADM1), Cadherin 5, VEGFA, Collagen 1α2, Collagen 4α6, CD34	6
	Regulation of Actin Cytoskeleton	Fibronectin, FGF1, FGFR1, FGF12, Actinin alpha 1 (ACTN1), Actinin α4 (ACTN4), Integrin α3	7
	Axon Guidance	DCC, UNC5C, Eph receptor A7 (EPHA7), Netrin G1, Semaphorin 3A, Semaphorin 6A, Eph receptor B2 (EPHB2), Eph receptor B1, ROBO1	7
	Chemokine Signaling Pathway	CX3CL1, CXCL12, CXCL2, CXCR4, LYN, STAT5B, ELMO1	7

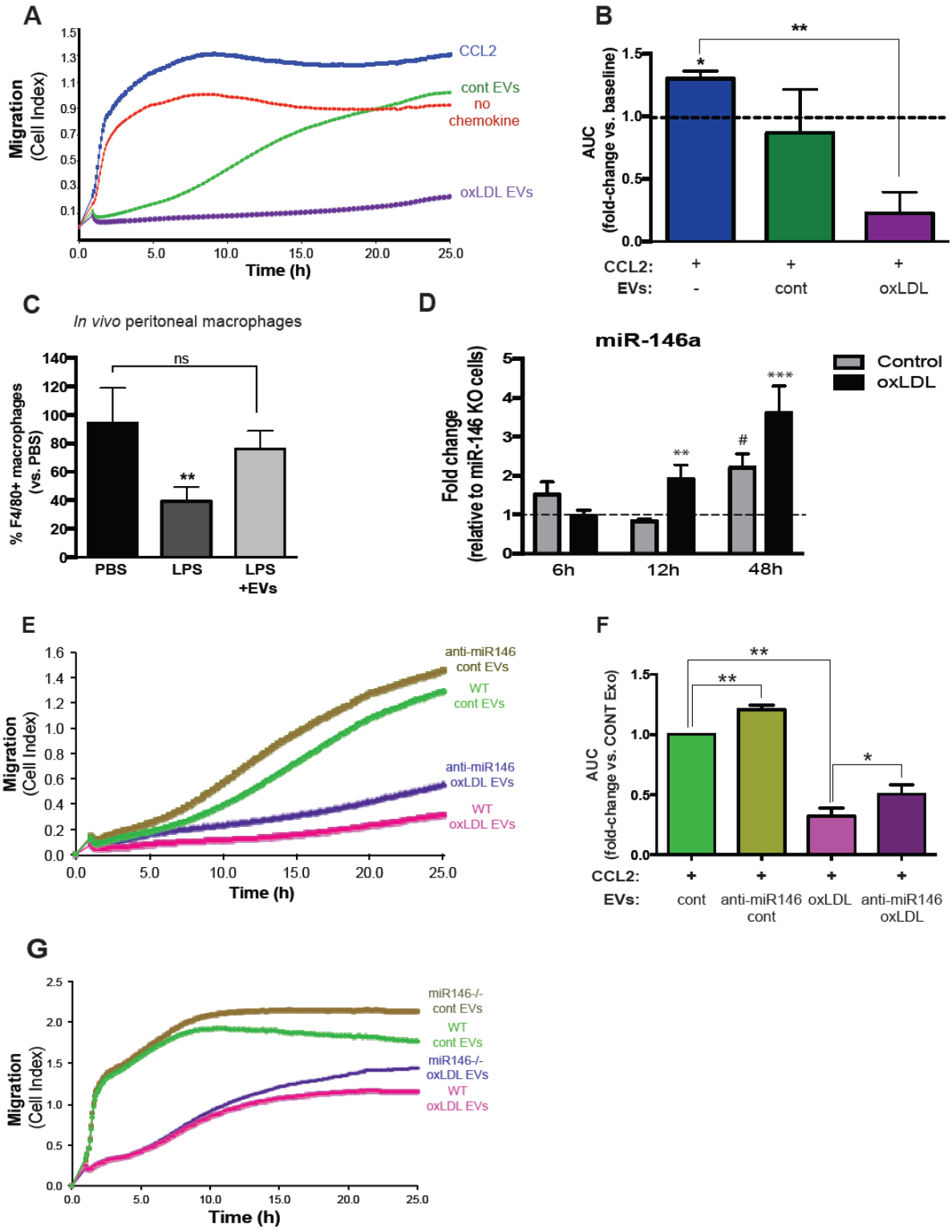
A
Migration (Cell Index)
Time (h)
CCL2
cont EVs no chemokine
oxLDL EVs
B
AUC (fold-change vs. baseline)
CCL2:
EVs:
cont
oxLDL
C
In vivo peritoneal macrophages
% F4/80+ macrophages (vs. PBS)
ns
PBS
LPS
LPS +EVs
D
miR-146a
Fold change (relative to miR-146 KO cells)
Control
oxLDL
6h
12h
48h
E
Migration (Cell Index)
Time (h)
anti-miR146 cont EVs
WT cont EVs
anti-miR146 oxLDL EVs
WT oxLDL EVs
F
AUC (fold-change vs. CONT Exo)
CCL2:
EVs:
cont
anti-miR146 cont
oxLDL
anti-miR146 oxLDL
G
Migration (Cell Index)
Time (h)
miR146-/- cont EVs
WT cont EVs
miR146-/- oxLDL EVs
WT oxLDL EVs

Figure 2.4. EVs secreted from atherogenic macrophages inhibit macrophage migration and is partly mediated by miR-146a. **(A-B)** BMDMs were cultured without/with oxidized LDL (50 μg/ml) for 24h and EVs were purified using ExoQuick-TC solution. Isolated EVs were applied to naïve macrophages for 48h. The migration of naïve macrophages towards CCL2 (150 ng/ml) was measured using xCELLigence System. Area under the curve (AUC) was measured for each condition and is shown as mean ± SD of n=3 experiments of quadruplicates, **p<0.01. **(C)** *In vivo migration assay*: C57BL6 mice (n=4/group) were injected intraperitoneally (I.P.) with thioglycollate and 4 days later peritoneal macrophages were labeled using 1μm Fluoresbrite microspheres. Mice were pre-treated with EVs (100μg, from RAW macrophages, injected I.P.) or PBS for 24h before treatment with LPS. Three hours following LPS injection, peritoneal cells were collected and the percentage of macrophages in the lavage was quantified by flow cytometry, **p<0.01. **(D)** Transfer of miR-146a from wild-type macrophages to miR-146a$^{-/-}$ macrophages. Wild-type macrophages (donor cells, BMDMs) were co-cultured with miR-146a$^{-/-}$ macrophages (recipient cells) in the absence/presence of oxidized LDL (50 μg/ml). Total RNA was isolated from recipient macrophages and miR-146a levels were measured by qRT-PCR. Graphs represent the means ± SD from pooled BMDM of n=5 mice performed in triplicate. **p<0.01, ***p<0.001 vs control and background; # p<0.001 vs background. **(E-F)** EVs isolated from BMDMs transfected with control anti-miR or anti-miR146a were applied to naïve BMDMs and migration was measured using xCELLigence System as described above. Graphs represent the means ± SD from n=3 independent experiments, *p<0.05 **p<0.01. **(G)** Control/Atherogenic EVs were isolated from wild-type or miR-146a$^{-/-}$ BMDMs and applied to naïve macrophages and migration was examined using xCELLigence System as described above. Shown here is the representative experiment done in triplicate (n=3).

2.5.6. Role of miR-146a in macrophage migration

As miR-146a was among the most significantly altered miRNA in atherogenic EVs, we postulated that miR-146a might partially mediate the effects exerted by these EVs. Using a co-culture system, we find that endogenous miR-146a from wild-type macrophages could be transferred to miR-146$^{-/-}$ naive cells, and this process was accelerated with oxidized LDL (**Figure 2.4D**). To test the role of EV miR-146a in macrophage migration, we knocked down miR-146a using anti-miR oligonucleotides and then isolated normal and atherogenic EVs from these cells. Macrophage-derived EVs deficient in miR-146a showed an increased macrophage migration index compared to EVs from control anti-miR macrophages. This increase in migration in the absence of miR-146a was observed regardless of whether the EVs were isolated from control or atherogenic conditions (**Figure 2.4E-F**). Additionally, we isolated EVs from miR-146a$^{-/-}$ macrophages and examined the effects of these EVs on macrophage migration. Naïve macrophages treated with control or atherogenic EVs from miR-146a$^{-/-}$ macrophages exhibited increased migration to CCL2 compared to EVs from wild-type mice (**Figure 2.4G**). Therefore, miR-146a delivered *via* EVs dampens macrophage migration towards a chemokine stimulus, which is relieved by inhibition of miR-146a.

2.5.7. EV-derived miR-146a may inhibit macrophage migration *via* targeting IGF2BP1 and HuR

We next sought to understand the mechanisms underlying the inhibitory effects of EV-derived miR-146a on macrophage migration. Based on bioinformatics analysis, a number of potential genes predicted to be targeted by miR-146a are also implicated in cell migration pathways, including *Igf2bp1* and *HuR*. Both IGF2BP1 and HUR are RNA binding proteins that modulate the expression of β-actin and have well-characterized roles in promoting cell

migration[41,42]. Over-expression of miR-146a suppressed and inhibition of miR-146a elevated the expression of IGF2BP1 at both the mRNA and protein level (**Figure 2.5A-B**). Luciferase reporter constructs containing the 3'UTR *IGF2BP1* showed that miR-146a directly represses the UTR activity of *IGF2BP1* (**Figure 2.5C**), confirming that it is a direct target of miR-146a. To test whether EV-derived miR-146a targets recipient cell *Igf2bp1*, we co-cultured miR-146a enriched macrophages with naïve macrophages and demonstrated that miR-146a was transferred to naïve cells where the expression levels of *Igf2bp1* were concomitantly decreased (**Figure 2.5D**). To examine the function of IGF2BP1 in regulating macrophage migration, we measured the migration of macrophages in which IGF2BP1 was knocked down by short interfering RNA (siRNA). Inhibition of IGF2BP1 reduced macrophage migration towards CCL2 (**Figure 2.5E-F)** confirming its role as a modulator of migration in immune cells.

In agreement with the previous study that identified *HuR* as a direct gene target of miR-146a[43], qRT-PCR and Western blot analysis of macrophages showed that levels of HUR mRNA and protein increased or decreased when miR-146a were knocked down or over-expressed, respectively (**Figure 2.6A-B**). Similar to what was observed with *Igf2bp1*, transfer of miR-146a from transfected macrophages to naïve macrophages increased the levels of miR-146a and reduced the expression levels of *HuR* in recipient cells (**Figure 2.6C**). Knock down of HUR using siRNA also reduced migration of macrophages towards CCL2 (**Figure 2.6D-E**). Together these data confirm that IGF2BP1 and HUR functionally promote macrophage migration, and both IGF2BP1 and HUR are targets of EV-derived miR-146a, which may contribute to the reduced chemotaxis in EV-treated cells.

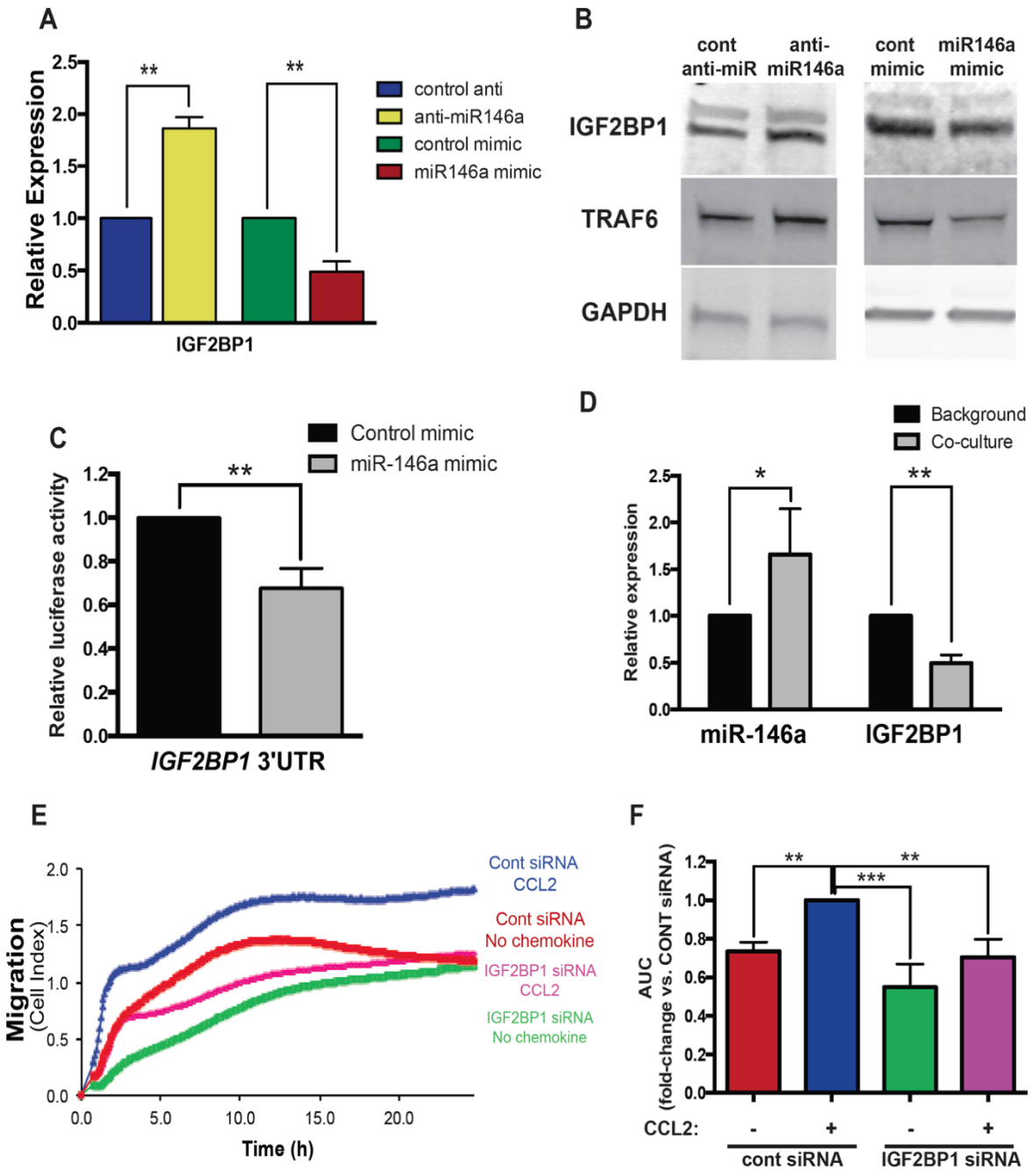
A
Relative Expression
2.5
2.0
1.5
1.0
0.5
0.0
**
**
control anti
anti-miR146a
control mimic
miR146a mimic
IGF2BP1
B
cont anti-miR
anti-miR146a
cont mimic
miR146a mimic
IGF2BP1
TRAF6
GAPDH
C
Control mimic
miR-146a mimic
Relative luciferase activity
1.2
1.0
0.8
0.6
0.4
0.2
0.0
**
IGF2BP1 3'UTR
D
Background
Co-culture
Relative expression
2.5
2.0
1.5
1.0
0.5
0.0
*
**
miR-146a
IGF2BP1
E
Migration
(Cell Index)
2.0
1.5
1.0
0.5
0.0
0.0
5.0
10.0
15.0
20.0
Time (h)
Cont siRNA
CCL2
Cont siRNA
No chemokine
IGF2BP1 siRNA
CCL2
IGF2BP1 siRNA
No chemokine
F
AUC
(fold-change vs. CONT siRNA)
1.2
1.0
0.8
0.6
0.4
0.2
0.0
**
**
***
CCL2:
-
+
-
+
cont siRNA
IGF2BP1 siRNA

Figure 2.5. IGF2BP1 is a target of EV-derived miR-146a. **(A-B)** IGF2BP1 mRNA (**A**) and protein (**B**) expression in BMDMs transfected with control anti-miR/anti-miR146a and control mimic/miR-146a mimic. TRAF6, a validated target of miR-146a, was used as a control for transfection efficiency. **(C)** Reporter 3'UTR assay for the human *IGF2BP1* UTR. Graph depicts luciferase activity relative to control miR after 24h, **p<0.01. **(D)** Co-culture of miR-146a enriched macrophages and naïve macrophages resulted in an increased expression of miR-146a and a decreased expression of *Igf2bp1* in naïve cells in the absence/presence of oxidized LDL for 72h. **(E-F)** Knockdown of IGF2BP1 using siRNA reduces macrophage migration. BMDMs were transfected with control or *Igf2bp1* siRNA for 72h. The migration of transfected cells towards CCL2 (150 ng/ml) was measured using the xCELLigence System. All graphs in this figure represent the means ± SD from n=3 independent experiments, *p<0.05 **p<0.01. Western blot is representative of a single experiment done in triplicate (n=3).

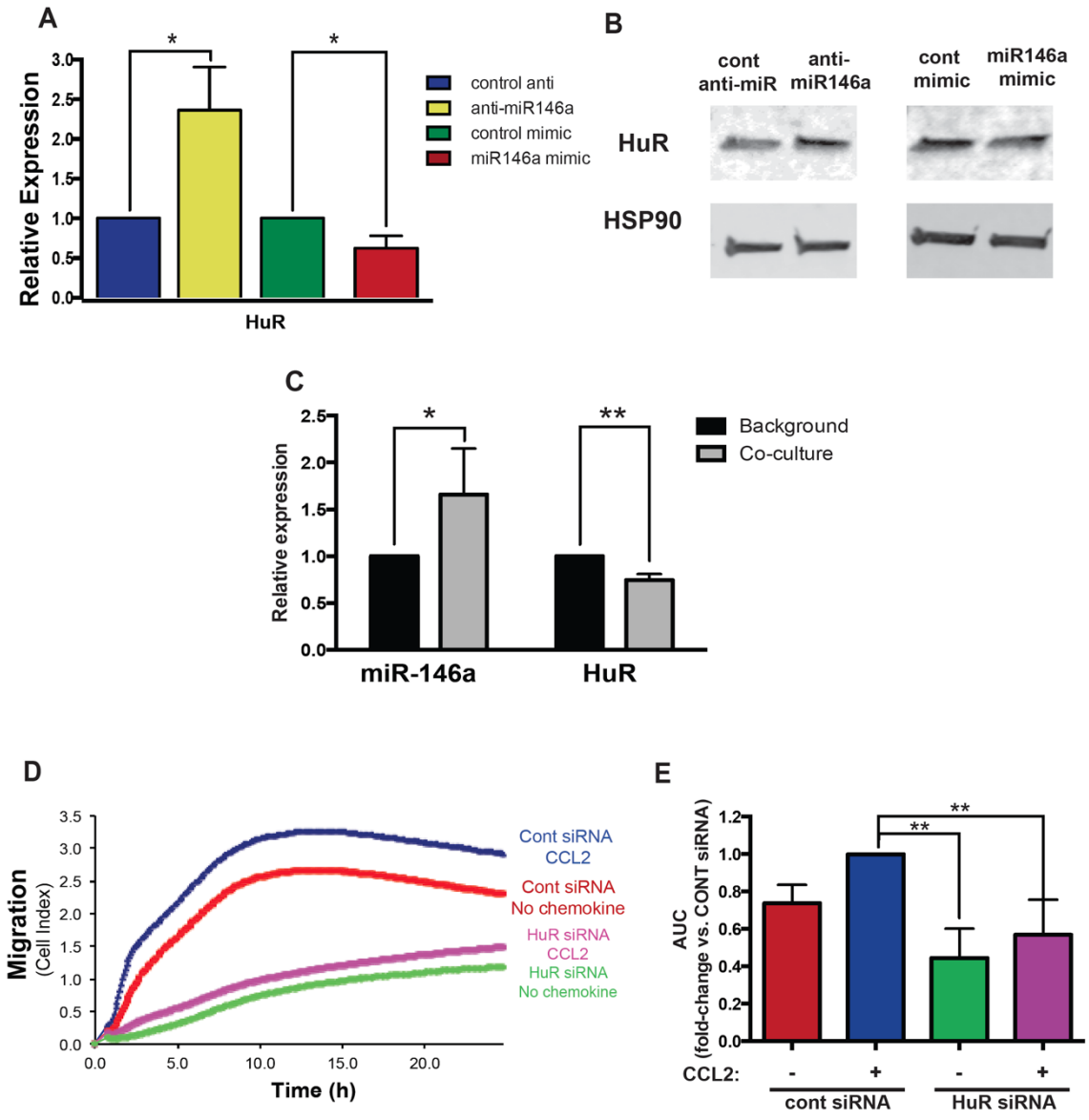

Figure 2.6. HuR is a target of EV-derived miR-146a. **(A-B)** HUR mRNA (**A**) and protein (**B**) expression in BMDMs transfected with control anti-miR/anti-miR146a and control mimic/miR-146a mimic. **(C)** Co-culture of miR-146a transfected macrophages in the absence/presence of oxidized LDL for 72hs with naïve macrophages resulted in an increased expression of miR-146a and a decreased expression of *HuR* in naïve cells. **(D-E)** Knockdown of HUR using siRNA reduces macrophage migration. BMDMs were transfected with control or *HuR* siRNA for 72h. The migration of transfected cells towards CCL2 (150 ng/ml) was measured using the xCELLigence System. All graphs in this figure represent the means ± SD from n=3 independent experiments, *p<0.05, **p <0.01. Western blot is representative of a single experiment done in triplicate (n=3).

2.5.8. miR-146a is elevated in atherosclerotic plaques and its targets IGF2BP1 and HuR are de-repressed in lesions from miR-146$^{-/-}$ mice

Because a dysregulation of miR-146a might alter macrophages in the vessel wall during atherogenesis, we examined miR-146a expression in lesions from *ApoE*$^{-/-}$ mice fed a chow or high-cholesterol diet. There was a significant upregulation in the expression of miR-146a in atherosclerotic lesions from *ApoE*$^{-/-}$ fed a high-cholesterol diet compared to mice fed a chow diet (**Figure 2.7A**). To extend these findings to humans, we analyzed miRNA expression in carotid plaques from patients with atherosclerosis, which revealed a significant increase of miR-146a expression compared to disease-free control arteries (**Figure 2.7B**). Because we find that miR-146a in EVs dampens macrophage migration, high levels of plaque miR-146a may adversely impact the ability of macrophages to emigrate from the plaque, and contribute to lesion development. To understand how miR-146a targets may be regulated in the atherosclerotic plaque, we examined the aortic expression of *Igf2bp1* and *HuR* in lethally irradiated *Ldlr*$^{-/-}$ mice transplanted with wild-type or miR146a$^{-/-}$ BM and fed a high cholesterol diet for 12 weeks. We found that *Igf2bp1* and *HuR* expression was increased in lesions from *Ldlr*$^{-/-}$ mice receiving miR146a$^{-/-}$ BM compared to mice receiving wild-type BM transplant (**Figure 2.7C-D**). Together, these data suggest that atherosclerotic lesions contain high levels of miR-146a compared to normal arteries, and, in the absence of miR-146, target genes *Igf2bp1* and *HuR* are upregulated and may play a role in lesion development.

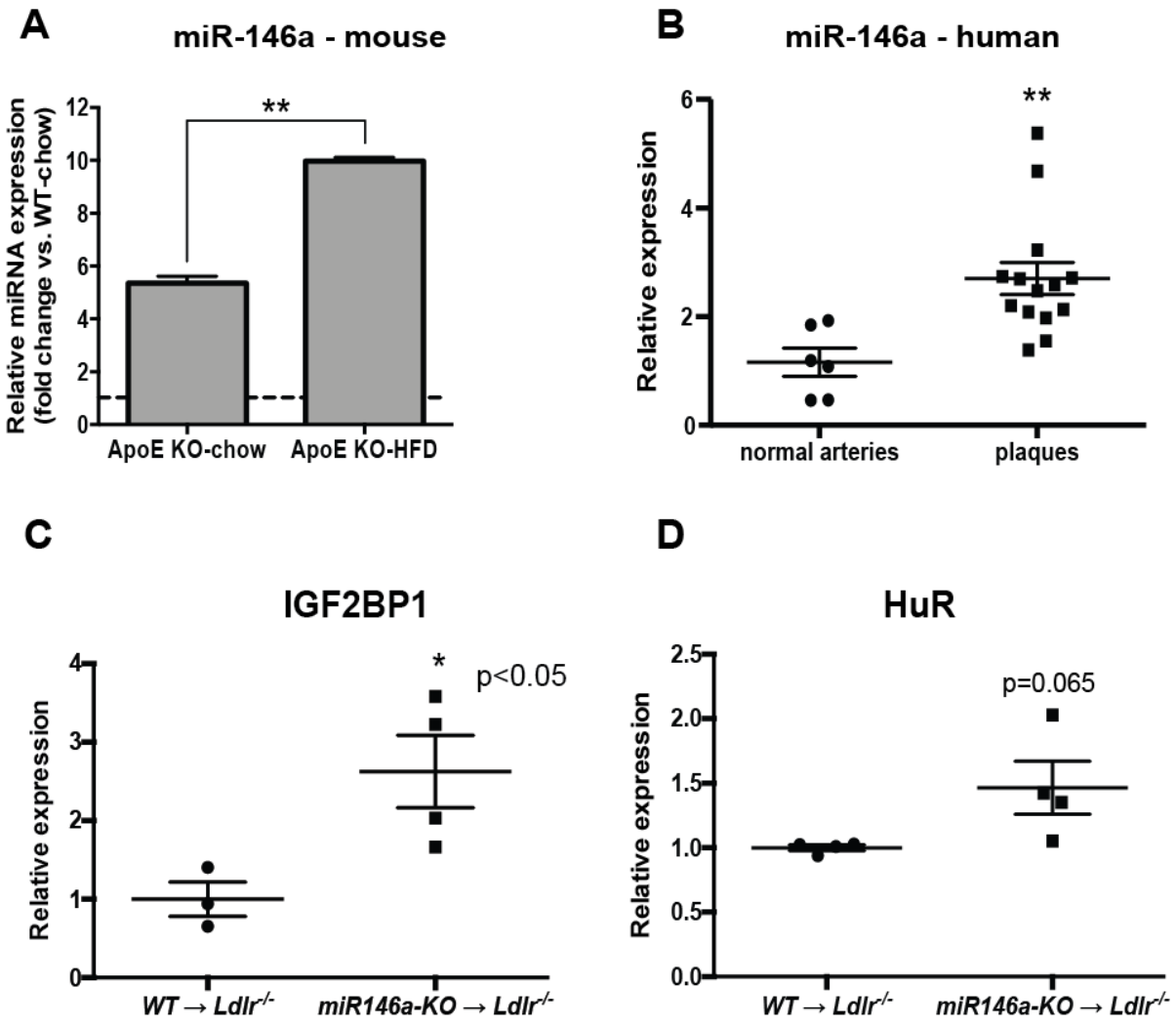

Figure 2.7. The expression of miR-146a and its targets, Igf2bp1 and HuR, in atherosclerosis. **(A)** Aortic expression of miR-146a in *ApoE*$^{-/-}$ mice fed a chow or high-cholesterol (0.2%) diet for 6 weeks. Graphs represent the means ± SD from pooled cDNA of n=5 mice per group, **p<0.01. **(B)** Human miR-146a expression in non-diseased arteries (normal) or carotids from humans with atherosclerosis (plaques) from the Biobank of Karolinska Endarterectomy (BiKE). **(C-D)** Aortic expression of *Igf2bp1* (**C**) and *HuR* (**D**) in *Ldlr*$^{-/-}$ mice transplanted with wild-type BM or miR146a$^{-/-}$ BM. These mice were fed a high-cholesterol (1.25%) diet for 12 weeks. Graphs represent means ± SEM from n=4 mice per group.

2.6. Discussion

miRNAs are important modulators of multiple signaling pathways involved in atherosclerosis[44]. The complexity of miRNA-mediated pathway control has expanded since the discovery that miRNAs can be released and function as paracrine molecules to regulate gene expression in recipient cells[10]. miRNAs are packaged into EVs by a broad range of cell types, and different cell types involved in atherosclerosis progression are known to secrete miRNA-containing EVs[45,46]. In this study, we demonstrate that atherogenic macrophages secrete EVs containing a specific set of miRNAs, which can be taken up by naïve macrophages and mediate the transfer of miRNAs to naïve cells. Functionally, we show that EVs derived from macrophages can inhibit the migration of naïve cells *in vitro* and *in vivo*. The effect of EVs on macrophage migration is partially attributable to the transfer of miR-146a to naïve cells where it represses the expression of specific target genes *Igf2bp1* and *HuR*. Our study is the first to explore communication between macrophages in an atherogenic scenario and suggest that miRNAs may act as paracrine modulators in the development of atherosclerosis.

EVs are primarily classified based on their size and mechanism of secretion. In atherosclerosis, exosomes, microvesicles and apoptotic bodies can mediate signals between cells in the plaque[46]. Although vascular ECs, SMCs and platelets have been shown to bi-directionally shuttle miRNA between cells *via* exosomes and apoptotic bodies[47–49], the current study is the first to show that lipid-laden macrophages can functionally alter pro-atherogenic phenotypes in recipient macrophages by directly transferring miRNAs *via* EVs. Although we cannot entirely exclude the role of microvesicles and/or apoptotic bodies in this macrophage-to-macrophage communication, our results using inhibitors, co-culture and nanoparticle tracking analysis suggests that EVs used in our study are likely exosomes.

Accumulation of lipid-laden macrophages in the artery wall, which results from the imbalance of macrophage recruitment to plaque and macrophage emigration from plaque to regional lymph nodes, contributes to the inflammatory propagation of atherosclerosis and plaque instability[16,38]. Thus, macrophage migration is central to the development of atherosclerosis. Our study shows that EVs secreted from macrophages can block macrophage migration towards a chemokine stimulus (CCL2), which along with its receptor, CCR2, can promote myeloid trafficking to the lymph nodes during inflammation[50,51]. Our findings parallel the observation that oxidized LDL induces the migratory arrest of macrophages *in vitro* which involves focal adhesion kinase and reorganization of the actin cytoskeleton[40,52]. We find that EV-derived miR-146a represses the expression of several genes implicated in cell migration pathways including *HuR* and *Igf2bp1*. The RNA-binding protein HUR is a validated target of miR-146a[43], and in several cancer cell lines, HUR promotes cell migration by stabilizing β-actin and Snail mRNAs[41,53]. Here, we confirm that EV-derived miR-146a decreases *HuR* in macrophages. Knockdown of HUR using RNA interference reduces migration towards CCL2 stimulus, confirming a role of this protein in modulating macrophage migration. We also identify the RNA-binding protein IGF2BP1 as a novel target of both endogenous and EV-derived miR-146a. IGF2BP1 is a potent oncogenic factor that regulates the migration and invasiveness of tumor cells by interfering with the translation of MAPK4 (mitogen-activated protein kinase 4) and β-actin[42,54]. Supporting the role of IGF2BP1 in regulating macrophage migration, IGF2BP1 knockdown strongly reduced macrophage migration, and we noted the lower expression of *Igf2bp1* in cholesterol-loaded macrophages which have impaired chemotaxis (data not shown). Thus, foam cells may promote migration arrest in other macrophages *via* the secretion of EVs containing miR-146a, which along with

other factors, may inhibit macrophage migration *via* downregulation of RNA-binding proteins IGF2BP1 and HUR.

To confirm our *in vitro* findings, we used a model of thioglycollate-elicited peritonitis to study macrophage emigration *in vivo*[20,40,55]. We show that macrophage-derived EVs reduce macrophage migration to lymph nodes in response to LPS, confirming a role of macrophage-derived EVs in regulating macrophage emigration out of inflamed tissues and into the lymph nodes. Interestingly, EVs from mycobacteria-infected macrophages has also been shown to induce cell migration *in vitro* and *in vivo*[56,57], suggesting that EVs from atherogenic macrophages may target similar pathways but exert opposing effects. Our *in vivo* and *in vitro* data suggest that EVs secreted from atherogenic macrophages decrease macrophage migration and may promote macrophage entrapment in the vessel wall, which would accelerate the development of atherosclerosis. However, we cannot exclude the possibility that atherogenic EVs may dampen inflammatory cell migration into the arterial intima. Blocking monocyte recruitment, which is crucial for both plaque progression and regression, may be advantageous or disadvantageous in atherosclerosis depending on the timing of inhibition[58]. Therefore, whether EVs from atherogenic macrophages have beneficial effects on the development of atherosclerosis still needs further investigation.

EVs isolated from oxidized LDL-loaded macrophages showed enrichment of several miRNAs including miR-146a, miR-128, miR-185, miR-365, and miR-503. Notably, oxidized LDL did not induce changes in the intracellular levels of these miRNAs in donor cells. Previous studies also demonstrated that the expression of RNAs in secreted vesicles does not reflect the intracellular content of RNAs, and selective packaging of miRNAs into vesicles may be crucial for the specificity of the biological functions of secreted miRNAs[59,60]. The

results from our study indicate that oxidized LDL stimulation of macrophages induces the selective enrichment of miRNAs into exosome-like EVs, and this is not simply a result of packaging of abundant miRNAs into microvesicles or the passive release of miRNAs that is commonly observed during cell death. Moreover, individual cell types appear to secrete a unique assortment of EVs containing a specific set of cargo proteins and RNAs, which allow a precise and regulated signal to be communicated to recipient cells. In our case, several specific miRNAs including miR-146a, miR-128, miR-185, miR-365 and miR-503 were up-regulated in EVs isolated from cholesterol-loaded macrophages. In contrast, EVs derived from LPS-stimulated macrophages showed enrichment of different signature of miRNAs including miR-21, miR-126, miR-146a/b, miR-212, miR-222[12]. The mechanisms that define cargo selection and packaging into vesicles remain poorly understood. Some evidence suggests that sumoylated hnRNPs direct the loading of miRNAs into exosomes through recognition of specific short motifs[61]. MEK-ERK signaling downstream of activated KRAS was shown to inhibit sorting of AGO2 and AGO2-dependent miRNA let-7a into tumor cell-derived exosomes[62]. In addition, the RNA-binding protein YBX1 is required for the sorting of miR-223 in exosomes secreted by HEK293T cells[63]. Collectively these studies strongly support the notion that small RNAs are selectively packed into EVs and that different cells may use diverse RNA sorting mechanisms. Additionally, in our study we could only partially inhibit EV generation by treating with GW4869, likely because GW4869 inhibits only one pathway of exosome secretion, namely neutral sphingomyelinase, and only reduces EV secretion by 40-50%. Whether macrophages secrete EVs *via* the ESCRT/Rab machinery from MVBs, and how these mechanisms are unique in certain cell types awaits further insights. And finally, there is the possibility that LDL can co-precipitate in the EV preparations from our oxidized

LDL-treated cells, resulting in some carryover of oxidized LDL into naïve cells. However, when cells are treated with 50μg/ml as in our study, the majority of oxidized LDL is taken up by macrophages after 5h[64]. Thus, in cells treated with EVs from oxidized LDL-treated BMDMs, there is likely only a minor contribution of contaminating oxidized LDL.

Many of the atherogenic EV-enriched miRNAs found in our study have been shown to play a role in inflammatory and lipid homeostasis pathways. For example, miR-128 acts as a key post-transcriptional regulator controlling networks of lipid and energy metabolism genes such as *Ldlr*, *Abca1*, sirtuin 1, and insulin receptor substrate 1[65]. Interestingly, miR-146a inhibits NF-κB and MAPK signaling *via* targeting TRAF6, IRAK1/2 and HUR, which limits inflammatory responses in a diverse range of cells[43,66–68]. miR-146a also decreases lipid uptake and cytokine release in oxidized LDL-activated macrophages through repressing the expression of TLR4[69]. These observations have classified miR-146a as an anti-inflammatory miRNA, and indeed exogenous delivery of miR-146a to atherosclerosis-prone mice resulted in the accumulation of miR-146a in macrophages and a reduction in plaque size after 6 weeks of treatment[68]. However, more recently, macrophage miR-146a in atherosclerosis lesion progression was evaluated directly in *Ldlr*$^{-/-}$ mice receiving BM from wild-type or miR-146a$^{-/-}$ mice. After 12 weeks, miR-146$^{-/-}$ BM recipients had significantly less aortic lesion development compared to wild-type recipients[70]. Importantly, we now show that in these same mice, both *Igf2bp1* and *HuR* expression is elevated, in agreement with these genes serving as miR-146a targets. These two studies suggest that macrophage- and endothelial-cell miR-146a play different roles during atherogenesis. We and others find that miR-146a is significantly up-regulated in atherosclerotic plaques[71] as well as in the circulation of coronary artery disease patients and is associated with an increased risk of atherosclerosis[72]. In the atherosclerotic

milieu, the reduction in macrophage migration would promote the retention of macrophages and plaque progression, suggesting EV-derived miR-146a may be pro-atherogenic. Collectively these results suggest a potential pro-atherogenic role for miR-146a in the plaque. Given that endogenous miR-146a levels *in vitro* remain at steady state whereas EV levels increase upon oxidized LDL treatment, the mechanisms that govern miR-146a targeting are likely dependent on cell of origin and stimulation. Moreover, the individual contributions of the other miRNAs enriched in atherogenic EVs were not tested in this study, therefore we can only conclude that the reduction in macrophage migration observed in EV-treated cells is partially impacted by the enrichment of miR-146a, but may be influenced by other EV-derived miRNAs.

In conclusion, our study provides evidence that macrophages under pro-atherogenic conditions secrete EVs containing a specific signature of miRNAs, which can be transferred to nearby macrophages and functionally alter recipient cell function. As shown in the model in **Figure 2.8**, our study has characterized a new intercellular communication during atherogenesis, in which atherogenic macrophages secrete EVs and deliver miRNAs to naïve macrophages where EV-derived miRNAs repress the expression of specific target genes implicated in migration pathways, leading to decreased macrophage migration and potential entrapment in the atherosclerotic plaque.

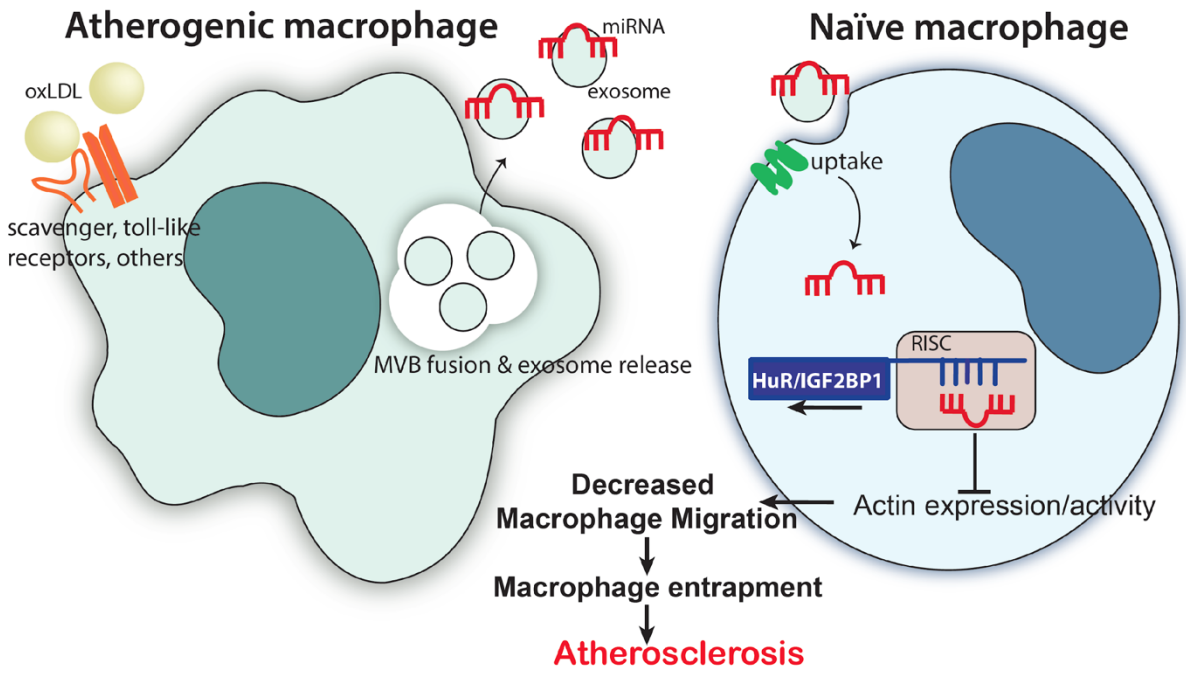

Figure 2.8. Model of macrophage-to-macrophage communication during atherogenesis. Atherogenic macrophages secrete EVs containing specific miRNAs including miR-146a. These EVs mediate the transfer of miRNAs to naïve macrophages where EV-derived miRNAs repress the expression of target genes involved in migration pathways such as *Igf2bp1* and *HuR*, leading to decreased macrophage migration and potential entrapment in the atherosclerotic plaque.

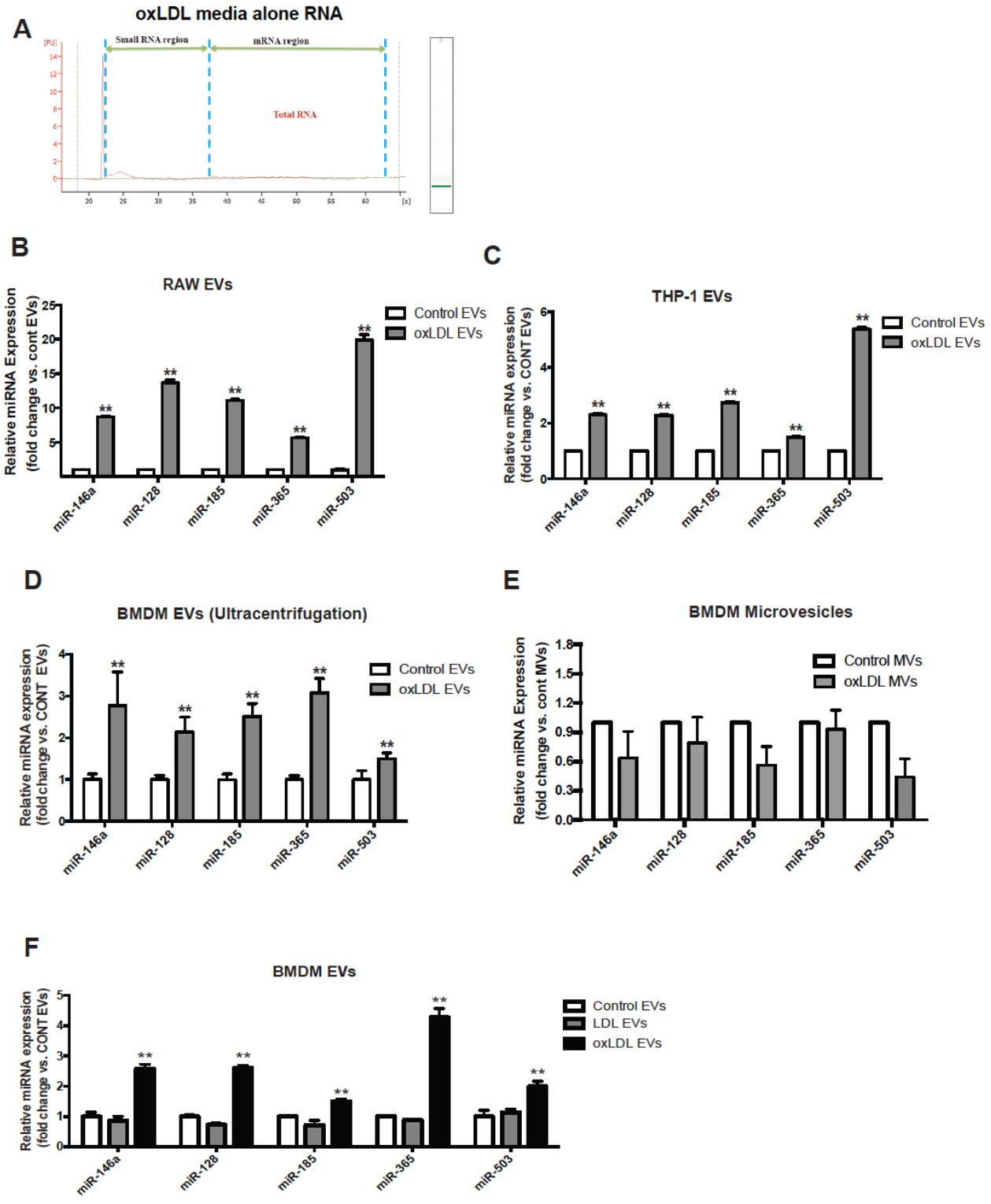
A
oxLDL media alone RNA
Small RNA region
mRNA region
Total RNA
B
RAW EVs
Relative miRNA Expression (fold change vs. cont EVs)
Control EVs
oxLDL EVs
miR-146a
miR-128
miR-185
miR-365
miR-503
C
THP-1 EVs
Relative miRNA expression (fold change vs. CONT EVs)
Control EVs
oxLDL EVs
D
BMDM EVs (Ultracentrifugation)
Relative miRNA expression (foldchange vs. CONT EVs)
Control EVs
oxLDL EVs
E
BMDM Microvesicles
Relative miRNA Expression (fold change vs. cont MVs)
Control MVs
oxLDL MVs
F
BMDM EVs
Relative miRNA expression (fold change vs. CONT EVs)
Control EVs
LDL EVs
oxLDL EVs

Supplemental Figure 2.1. qPCR confirmation of potential EV-derived miRNAs. **(A)** Total RNA was extracted from oxidized LDL-containing media (50 μg/ml) incubated in cell-free wells and was analyzed using Bioanalyzer RNA 6000 Pico chip. **(B-C)** miRNA expression in atherogenic EVs secreted from (**B**) RAW 264.7 macrophages and (**C**) human monocyte-derived cells THP-1. EVs secreted from control and oxidized LDL-loaded macrophages (50 μg/ml) were purified using ExoQuick-TC solution. The expression levels of different candidate miRNAs were analyzed by qPCR. Shown here is the representative experiment done in duplicate (n=2), **p<0.01. **(D)** EVs secreted from control and oxidized LDL-loaded BMDMs (50 μg/ml) were purified using ultracentrifugation. Shown here is the representative experiment done in duplicate (n=2), **p<0.01. **(E)** Microvesicles secreted from control and oxidized LDL-loaded BMDMs (50 μg/ml) were purified using ultracentrifugation. Shown here is the representative experiment done in triplicate (n=3). **(F)** miRNA expression in EVs secreted from control (untreated) BMDMs, LDL-treated BMDMs (50 μg/ml) and oxidized LDL-loaded BMDMs (50 μg/ml). Shown here is the representative experiment done in triplicate (n=3), **p<0.01.

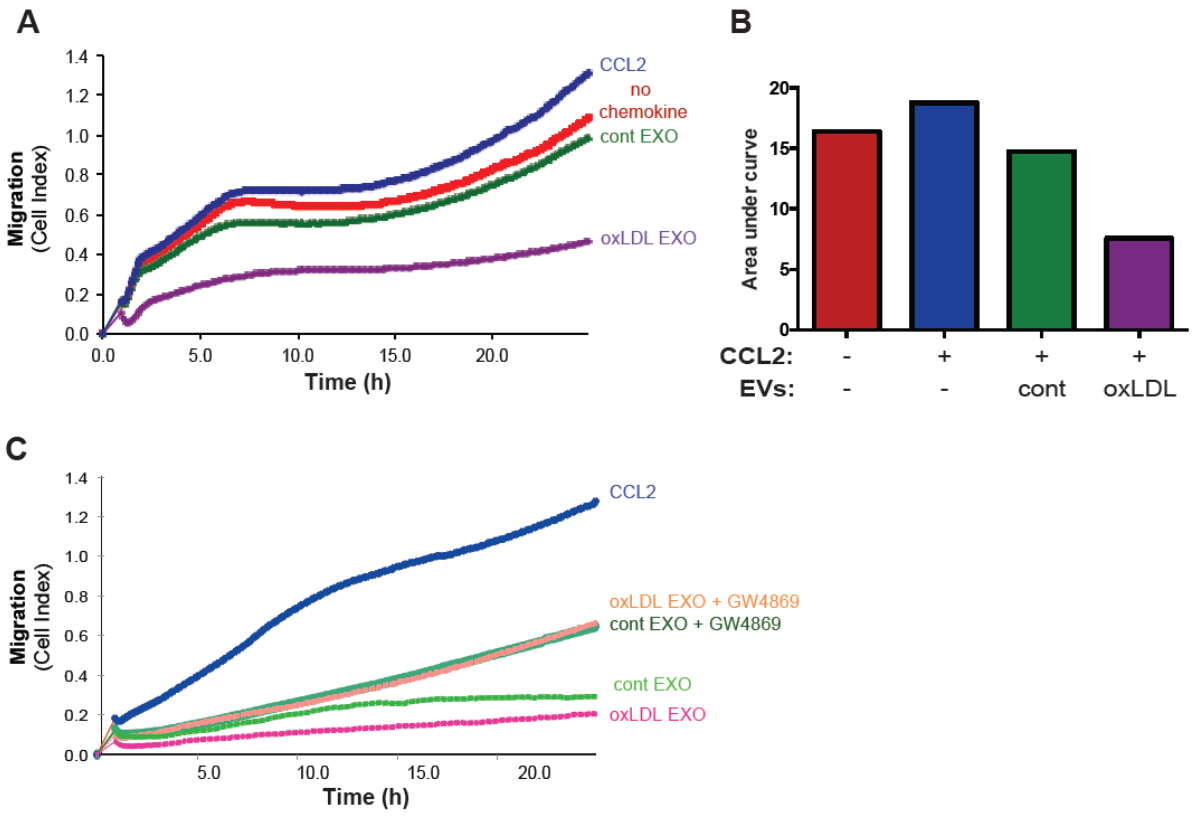

Supplemental Figure 2.2. Confirmation of the inhibitory effect of atherogenic EVs on macrophage migration. **(A-B)** EVs isolated from oxidized LDL-treated macrophages also inhibit RAW migration. RAW 264.7 macrophages were cultured without/with oxidized LDL (50 µg/ml) for 24h and EVs were purified using ExoQuick-TC solution. Isolated EVs were applied to naïve macrophages for 48h. The migration of naïve macrophages towards CCL2 (150 ng/ml) was measured using xCELLigence System. Shown here is the representative experiment done in duplicate (n=2). **(C)** Blockade of exosome generation with GW4869 (15µM) relieved the inhibitory effect of EVs on BMDM migration. Shown here is the representative experiment done in triplicate (n=3).

2.7. Acknowledgements

We thank Dr. Arkadiy Reunov for his expertise with the electron microscopy.

2.8. Significance of this manuscript

While there has been a significant progress in the understanding of how lipids and inflammatory cells initiate lesion development, less is known about how macrophages become entrapped in the atherosclerotic plaque. Our study shows that macrophages loaded with cholesterol secrete extracellular vesicles and deliver microRNA to neighboring macrophages. These pro-atherogenic extracellular vesicles exert an inhibitory effect on migration in recipient cells, which may contribute to the chemotactic arrest seen in plaque progression. miR-146a secreted from macrophages may surprisingly act as a pro- rather than anti-atherogenic factor. Combined with the observation that miR-146a is paradoxically increased in human and mouse atherosclerotic lesions, our data suggests that extracellular vesicles secreted from lipid-loaded macrophages may contribute directly to the pro-atherogenic phenotype of foam cells and may partially act through miR-146a.

2.9. References

1. Kjenseth, A., Fykerud, T., Rivedal, E. & Leithe, E. Regulation of gap junction intercellular communication by the ubiquitin system. *Cell. Signal.* **22**, 1267–1273 (2010).
2. Denef, C. Paracrinicity: The story of 30 years of cellular pituitary crosstalk. *J. Neuroendocrinol.* **20**, 1–70 (2008).
3. Singer, S. J. Intercellular communication and cell-cell adhesion. *Science* **255**, 1671–7 (1992).
4. Majka, M. *et al.* Numerous growth factors, cytokines, and chemokines are secreted by human CD34(+) cells, myeloblasts, erythroblasts, and megakaryoblasts and regulate normal hematopoiesis in an autocrine/paracrine manner. *Blood* **97**, 3075–85 (2001).
5. Ratajczak, J., Wysoczynski, M., Hayek, F., Janowska-Wieczorek, A. & Ratajczak, M.

Z. Membrane-derived microvesicles: important and underappreciated mediators of cell-to-cell communication. *Leukemia* **20**, 1487–95 (2006).
6. Keller, S., Sanderson, M. P., Stoeck, A. & Altevogt, P. Exosomes: from biogenesis and secretion to biological function. *Immunol. Lett.* **107**, 102–8 (2006).
7. Bobrie, A., Colombo, M., Raposo, G. & Théry, C. Exosome Secretion: Molecular Mechanisms and Roles in Immune Responses. *Traffic* **12**, 1659–1668 (2011).
8. Camussi, G., Deregibus, M. C., Bruno, S., Cantaluppi, V. & Biancone, L. Exosomes/microvesicles as a mechanism of cell-to-cell communication. *Kidney Int.* **78**, 838–48 (2010).
9. Lee, Y., El Andaloussi, S. & Wood, M. J. a. Exosomes and microvesicles: extracellular vesicles for genetic information transfer and gene therapy. *Hum. Mol. Genet.* **21**, R125-34 (2012).
10. Chen, X., Liang, H., Zhang, J., Zen, K. & Zhang, C. Y. Secreted microRNAs: A new form of intercellular communication. *Trends Cell Biol.* **22**, 125–132 (2012).
11. Bhatnagar, S., Shinagawa, K., Castellino, F. J. & Schorey, J. S. Exosomes released from macrophages infected with intracellular pathogens stimulate a proinflammatory response in vitro and in vivo. *Blood* **110**, 3234–44 (2007).
12. McDonald, M. K. *et al.* Functional significance of macrophage-derived exosomes in inflammation and pain. *Pain* **155**, 1527–1539 (2014).
13. Ismail, N. *et al.* Macrophage microvesicles induce macrophage differentiation and miR-223 transfer. *Blood* **121**, 984–995 (2013).
14. Lusis, A. Atherosclerosis. *Nature* **407**, 233–241 (2000).
15. Moore, K. J. & Tabas, I. Macrophages in the pathogenesis of atherosclerosis. *Cell* **145**, 341–55 (2011).
16. Moore, K. J., Sheedy, F. J. & Fisher, E. a. Macrophages in atherosclerosis: a dynamic balance. *Nat. Rev. Immunol.* **13**, 709–21 (2013).
17. Feng, B. *et al.* The endoplasmic reticulum is the site of cholesterol-induced cytotoxicity in macrophages. *Nat. Cell Biol.* **5**, 781–792 (2003).
18. Duewell, P. *et al.* NLRP3 inflammasomes are required for atherogenesis and activated by cholesterol crystals. *Nature* **464**, 1357–1361 (2010).
19. Randolph, G. J. Emigration of monocyte-derived cells to lymph nodes during resolution of inflammation and its failure in atherosclerosis. *Curr. Opin. Lipidol.* **19**, 462–468 (2008).
20. van Gils, J. M. *et al.* The neuroimmune guidance cue netrin-1 promotes atherosclerosis by inhibiting the emigration of macrophages from plaques. *Nat. Immunol.* **13**, 136–143 (2012).
21. Wanschel, A. *et al.* Neuroimmune guidance cue semaphorin 3E is expressed in atherosclerotic plaques and regulates macrophage retention. *Arterioscler. Thromb. Vasc. Biol.* **33**, 886–893 (2013).
22. Dragovic, R. a. *et al.* Sizing and phenotyping of cellular vesicles using Nanoparticle Tracking Analysis. *Nanomedicine* **7**, 780–8 (2011).
23. Rayner, K. J. *et al.* MiR-33 contributes to the regulation of cholesterol homeostasis. *Science* **328**, 1570–3 (2010).
24. Karunakaran, D. *et al.* Macrophage Mitochondrial Energy Status Regulates Cholesterol Efflux and Is Enhanced by Anti-miR33 in Atherosclerosis. *Circ. Res.* **117**, 266–278

(2015).
25. Karunakaran, D. *et al.* Therapeutic Inhibition of miR-33 Promotes Fatty Acid Oxidation but Does Not Ameliorate Metabolic Dysfunction in Diet-Induced Obesity. *Arterioscler. Thromb. Vasc. Biol.* **35**, 2536–2543 (2015).
26. Lu, T.-P. *et al.* miRSystem: an integrated system for characterizing enriched functions and pathways of microRNA targets. *PLoS One* **7**, e42390 (2012).
27. Rayner, K. J. *et al.* Antagonism of miR-33 in mice promotes reverse cholesterol transport and regression of atherosclerosis. *J. Clin. Invest.* **121**, 2921–2931 (2011).
28. Razuvaev, A. *et al.* Correlations between clinical variables and gene-expression profiles in carotid plaque instability. *Eur. J. Vasc. Endovasc. Surg.* **42**, 722–730 (2011).
29. Perisic, L. *et al.* Profiling of atherosclerotic lesions by gene and tissue microarrays reveals pcsk6 as a novel protease in unstable carotid atherosclerosis. *Arterioscler. Thromb. Vasc. Biol.* **33**, 2432–2443 (2013).
30. Krohn, J. B., Hutcheson, J. D., Martínez-Martínez, E. & Aikawa, E. Extracellular vesicles in cardiovascular calcification: Expanding current paradigms. *J. Physiol.* **594**, 2895–2903 (2016).
31. Alvarez, M. L., Khosroheidari, M., Kanchi Ravi, R. & DiStefano, J. K. Comparison of protein, microRNA, and mRNA yields using different methods of urinary exosome isolation for the discovery of kidney disease biomarkers. *Kidney Int.* **82**, 1024–1032 (2012).
32. Rekker, K. *et al.* Comparison of serum exosome isolation methods for microRNA profiling. *Clin. Biochem.* **47**, 135–138 (2014).
33. Hu, G., Drescher, K. M. & Chen, X.-M. Exosomal miRNAs: Biological Properties and Therapeutic Potential. *Front. Genet.* **3**, 1–9 (2012).
34. Kosaka, N. *et al.* Secretory mechanisms and intercellular transfer of microRNAs in living cells. *J. Biol. Chem.* **285**, 17442–52 (2010).
35. Harry, B. L. *et al.* Endothelial cell PECAM-1 promotes atherosclerotic lesions in areas of disturbed flow in ApoE-deficient mice. *Arterioscler. Thromb. Vasc. Biol.* **28**, 2003–2008 (2008).
36. Tsoyi, K. *et al.* PTEN differentially regulates expressions of ICAM-1 and VCAM-1 through PI3K/Akt/GSK-3β/GATA-6 signaling pathways in TNF-α-activated human endothelial cells. *Atherosclerosis* **213**, 115–21 (2010).
37. Van Gils, J. M. *et al.* Endothelial expression of guidance cues in vessel wall homeostasis dysregulation under proatherosclerotic conditions. *Arterioscler. Thromb. Vasc. Biol.* **33**, 911–919 (2013).
38. Llodrá, J. *et al.* Emigration of monocyte-derived cells from atherosclerotic lesions characterizes regressive, but not progressive, plaques. *Proc. Natl. Acad. Sci. U. S. A.* **101**, 11779–84 (2004).
39. Bellingan, G. J., Caldwell, H., Howie, S. E., Dransfield, I. & Haslett, C. In vivo fate of the inflammatory macrophage during the resolution of inflammation: inflammatory macrophages do not die locally, but emigrate to the draining lymph nodes. *J. Immunol.* **157**, 2577–2585 (1996).
40. Young, M. P., Febbraio, M. & Silverstein, R. L. CD36 modulates migration of mouse and human macrophages in response to oxidized LDL and may contribute to macrophage trapping in the arterial intima. *J. Clin. Invest.* **119**, 136–145 (2009).

41. Dormoy-Raclet, V. *et al.* The RNA-binding protein HuR promotes cell migration and cell invasion by stabilizing the beta-actin mRNA in a U-rich-element-dependent manner. *Mol. Cell. Biol.* **27**, 5365–5380 (2007).
42. Stöhr, N. & Hüttelmaier, S. IGF2BP1: A post-transcriptional 'driver' of tumor cell migration. *Cell Adhes. Migr.* **6**, 312–318 (2012).
43. Cheng, H. S. *et al.* MicroRNA-146 represses endothelial activation by inhibiting pro-inflammatory pathways. *EMBO Mol. Med.* **5**, 949–966 (2013).
44. Feinberg, M. W. & Moore, K. J. MicroRNA Regulation of Atherosclerosis. *Circ. Res.* **118**, 703–720 (2016).
45. Hulsmans, M. & Holvoet, P. MicroRNA-containing microvesicles regulating inflammation in association with atherosclerotic disease. *Cardiovasc. Res.* **100**, 7–18 (2013).
46. Chistiakov, D. a., Orekhov, A. N. & Bobryshev, Y. V. Extracellular vesicles and atherosclerotic disease. *Cell. Mol. Life Sci.* **72**, 2697–2708 (2015).
47. Zernecke, A. *et al.* Delivery of MicroRNA-126 by Apoptotic Bodies Induces CXCL12-Dependent Vascular Protection. *Sci. Signal.* **2**, ra81 (2009).
48. Hergenreider, E. *et al.* Atheroprotective communication between endothelial cells and smooth muscle cells through miRNAs. *Nat. Cell Biol.* **14**, 249–56 (2012).
49. Ramakrishnan, D. P., Hajj-Ali, R. A., Chen, Y. & Silverstein, R. L. Extracellular vesicles activate a CD36-dependent signaling pathway to inhibit microvascular endothelial cell migration and tube formation. *Arterioscler. Thromb. Vasc. Biol.* **36**, 534–544 (2016).
50. Sato, N. *et al.* CC chemokine receptor (CCR)2 is required for langerhans cell migration and localization of T helper cell type 1 (Th1)-inducing dendritic cells. Absence of CCR2 shifts the Leishmania major-resistant phenotype to a susceptible state dominated by Th2 cytokin. *J. Exp. Med.* **192**, 205–18 (2000).
51. Jimenez, F. *et al.* CCR2 plays a critical role in dendritic cell maturation: possible role of CCL2 and NF-kappa B. *J. Immunol.* **184**, 5571–81 (2010).
52. Chen, Y. *et al.* Oxidized LDL-bound CD36 recruits an Na^+/K^+-ATPase-Lyn complex in macrophages that promotes atherosclerosis. *Sci. Signal.* **8**, ra91 (2015).
53. Dong, R. *et al.* Stabilization of Snail by HuR in the process of hydrogen peroxide induced cell migration. *Biochem. Biophys. Res. Commun.* **356**, 318–21 (2007).
54. Stöhr, N. *et al.* IGF2BP1 promotes cell migration by regulating MK5 and PTEN signaling. *Genes Dev.* **26**, 176–189 (2012).
55. Cao, C., Lawrence, D. A., Strickland, D. K. & Zhang, L. A specific role of integrin Mac-1 in accelerated macrophage efflux to the lymphatics. *Blood* **106**, 3234–41 (2005).
56. Singh, P. P., Smith, V. L., Karakousis, P. C. & Schorey, J. S. Exosomes Isolated from Mycobacteria-Infected Mice or Cultured Macrophages Can Recruit and Activate Immune Cells In Vitro and In Vivo. *J. Immunol.* **189**, 777–785 (2012).
57. Walters, S. B. *et al.* Microparticles from Mycobacteria-Infected Macrophages Promote Inflammation and Cellular Migration. *J. Immunol.* **190**, 669–677 (2012).
58. Nathan, C. & Ding, A. Nonresolving Inflammation. *Cell* **140**, 871–882 (2010).
59. Valadi, H. *et al.* Exosome-mediated transfer of mRNAs and microRNAs is a novel mechanism of genetic exchange between cells. *Nat. Cell Biol.* **9**, 654–659 (2007).
60. Zhang, Y. *et al.* Secreted monocytic miR-150 enhances targeted endothelial cell

migration. *Mol. Cell* **39**, 133–44 (2010).
61. Villarroya-Beltri, C. *et al.* Sumoylated hnRNPA2B1 controls the sorting of miRNAs into exosomes through binding to specific motifs. *Nat. Commun.* **4**, 2980 (2013).
62. McKenzie, A. J. *et al.* KRAS-MEK Signaling Controls Ago2 Sorting into Exosomes. *Cell Rep.* **15**, 978–987 (2016).
63. Shurtleff, M. J., Temoche-Diaz, M. M., Karfilis, K. V., Ri, S. & Schekman, R. Y-box protein 1 is required to sort microRNAs into exosomes in cells and in a cell-free reaction. *Elife* **5**, 040238 (2016).
64. Lougheed, M. *et al.* High affinity saturable uptake of oxidized low density lipoprotein by macrophages from mice lacking the scavenger receptor class A type I/II. *J. Biol. Chem.* **272**, 12938–12944 (1997).
65. Wagschal, A. *et al.* Genome-wide identification of microRNAs regulating cholesterol and triglyceride homeostasis. *Nat Med* **21**, 1290–1297 (2015).
66. Taganov, K. D., Boldin, M. P., Chang, K.-J. & Baltimore, D. NF-kappaB-dependent induction of microRNA miR-146, an inhibitor targeted to signaling proteins of innate immune responses. *Proc. Natl. Acad. Sci. U. S. A.* **103**, 12481–12486 (2006).
67. Saba, R., Sorensen, D. L. & Booth, S. A. MicroRNA-146a: A dominant, negative regulator of the innate immune response. *Front. Immunol.* **5**, 1–11 (2014).
68. Li, K., Ching, D., Luk, F. S. & Raffai, R. L. Apolipoprotein E enhances microRNA-146a in monocytes and macrophages to suppress nuclear factor-κB-driven inflammation and atherosclerosis. *Circ. Res.* **117**, e1–e11 (2015).
69. Yang, K. *et al.* MiR-146a inhibits oxidized low-density lipoprotein-induced lipid accumulation and inflammatory response via targeting toll-like receptor 4. *FEBS Lett.* **585**, 854–860 (2011).
70. Cheng, H. S. *et al.* Paradoxical Suppression of Atherosclerosis in the Absence of microRNA-146a. *Circ. Res.* **121**, 354–367 (2017).
71. Raitoharju, E. *et al.* MiR-21, miR-210, miR-34a, and miR-146a/b are up-regulated in human atherosclerotic plaques in the Tampere Vascular Study. *Atherosclerosis* **219**, 211–217 (2011).
72. Xiong, X.-D. *et al.* A common variant in pre-miR-146 is associated with coronary artery disease risk and its mature miRNA expression. *Mutat. Res.* **761**, 15–20 (2014).

3. Delivery of MicroRNAs by Chitosan Nanoparticles to Functionally Alter Macrophage Cholesterol Efflux *In Vitro* and *In Vivo*

Authors: My-Anh Nguyen, Hailey Wyatt, Leah Susser, Michelle Geoffrion, Adil Rasheed, Anne-Claire Duchez, Mary Lynn Cottee, Esther Afolayan, Eliya Farah, Zaina Kahiel, Marceline Côté, Suresh Gadde, Katey J. Rayner

ACS Nano

Published: 2019 Jun;13(6):6491-6505. Epub 2019 Jun 12.

3.1. Author contributions

The experiments were planned by Katey J. Rayner, Suresh Gadde and me. As the first author, I performed the majority of the experiments required for this study. Hailey Wyatt and Michele Geoffrion helped me perform the *in vitro* RNA and protein analyses. Leah Susser helped me prepare the NP samples. Esther Afolayan, Eliya Farah, and Zaina Kahiel helped me characterize the NP samples. Adil Rasheed, Anne-Claire Duchez, and Mary Lynn Cottee helped me perform the RCT assays. Marceline Côté provided critical input into interpretation of experiments. I wrote the preliminary draft of the manuscript and together, Katey J. Rayner, Suresh Gadde and I edited the manuscript until the paper was accepted to be published.

3.2. Abstract

The prevention and treatment of CVD has largely focused on lowering circulating LDL-cholesterol, yet a significant burden of atherosclerotic disease remains even when LDL is low. Recently, miRNAs have emerged as exciting therapeutic targets for cardiovascular

disease. miRNAs are small noncoding RNAs that post-transcriptionally regulate gene expression by degradation or translational inhibition of target mRNAs. A number of miRNAs have been found to modulate all stages of atherosclerosis, particularly those that promote the efflux of excess cholesterol from lipid laden macrophages in the vessel wall to the liver. However, one of the major challenges of miRNA-based therapy is to achieve tissue-specific, efficient and safe delivery of miRNAs *in vivo*. We sought to develop chNPs that can deliver functional miRNA mimics to macrophages and to determine if these NPs can alter cholesterol efflux and reverse cholesterol transport *in vivo*. We developed chNPs with a size range of 150-200nm *via* ionic gelation method using tripolyphosphate (TPP) as a crosslinker. In this method, negatively charged miRNAs were encapsulated in the NPs by ionic interactions with polymeric components. We then optimized the efficiency of intracellular delivery of different formulations of chitosan/TPP/miRNA to mouse macrophages. Using a well-defined miRNA with roles in macrophage cholesterol metabolism, we tested whether chNPs could deliver functional miRNAs to macrophages. We find chNPs can transfer exogenous miR-33 to naïve macrophages and reduce the expression of *Abca1*, a potent miR-33 target gene, both *in vitro* and *in vivo,* confirming that miRNAs delivered *via* NPs can escape the endosomal system and function in the RISC complex. Because miR-33 and ABCA1 play a key role in regulating the efflux of cholesterol from macrophages, we also confirmed that macrophages treated with miR-33-loaded chNPs exhibited reduced cholesterol efflux to apoA1, further confirming functional delivery of the miRNA. *In vivo*, mice treated with miR33-chNPs showed decreased RCT to the plasma, liver, and feces. In contrast, when efflux-promoting miRNAs were delivered *via* chNPs, ABCA1 expression and cholesterol efflux into the RCT pathway was improved. Over all, miRNAs can be efficiently delivered to macrophages *via* NPs where they

can function to regulate ABCA1 expression and cholesterol efflux, suggesting that these miRNA NPs can be used *in vivo* to target atherosclerotic lesions.

3.3. Introduction

CVD remains the leading cause of morbidity and mortality in westernized countries. Lowering cholesterol levels, particularly plasma LDL-cholesterol, has been the focus of the prevention and treatment of CVD and its sequelae for the past 3 decades[1]. While statins, which inhibit cholesterol synthesis, are the most effective drugs to treat CVD, their potential adverse effects in muscle and other tissues reduce the adherence to statin therapy across many groups[2]. In addition, a significant burden of CVD still remains even with low LDL-cholesterol[3]. Thus, there remains an urgent need to develop other strategies that can be used individually or in combination with current statin therapies to treat heart disease and to improve human health.

With atherosclerosis being the major underlying factor leading to cardiovascular complications[4,5], there is a growing interest in finding ways to reverse lipid buildup in the plaques. Atherosclerosis is characterized by retention of cholesterol-rich lipoproteins in susceptible areas of the arterial vasculature, endothelial activation, and macrophage infiltration resulting in plaque formation. In contrast, plaque regression involves the removal of free cholesterol and other lipids from macrophage-derived foam cells[6–8] *via* the ABCA1/ABCG1[9,10]. Cholesterol efflux from macrophages is the first and potentially the most important step in RCT, a pathway by which excess cholesterol from peripheral cells and tissues is transported to the liver for excretion, thus crucial for the prevention of lipid accumulation and atherosclerosis[11]. The significance of macrophage RCT and cholesterol efflux in preventing or reversing atherogenesis has been highlighted by studies where disruption of

Abca1 genes can induce atherosclerosis[12,13] and in patients where mutated *ABCA1* genes resulted in increased atherosclerosis[14,15]. The absence of ABCA1 can also activate the inflammasome-dependent activation of IL-1β and IL-18, which is independent of circulating HDL-cholesterol levels[16]. Therefore, targeting macrophage cholesterol efflux and ABCA1 could be of great therapeutic value even if the protective effects of raising HDL-cholesterol are less certain.

Since the realization of that the human genome is comprised largely of transcribed but non-coding genetic elements, the study of non-coding RNAs has burgeoned. The most well characterized class of non-coding RNA are miRNAs, which are defined as highly conserved small RNA sequences of 20 to 23 nucleotides that interact with target sites present in the 3'-UTR of specific mRNAs. This 3'UTR pairing results in the destabilization and/or translational inhibition of their bound targets[17]. miRNAs represent an important class of transcriptional modulators for both fine-tuning and dramatically altering cell behavior, and it is believed that miRNAs control the activity of 60% of all protein-coding genes in humans[18,19]. Multiple miRNAs are involved in the progression of atherosclerosis and numerous miRNAs have been found to regulate cholesterol efflux *via* directly targeting ABCA1. For example, overexpression of miR-33[20,21], miR-144[22,23], miR-148a [24,25], and miR-302a[26] reduces ABCA1 expression and abolishes cholesterol efflux to apoA1. Conversely, inhibition of these miRNAs using ASOs promotes cholesterol efflux and RCT through de-repression of the *Abca1* gene. Thus, miRNA-based therapeutic approaches for treating atherosclerosis has gained considerable attention.

Different strategies have been developed to modulate miRNA function for therapeutic purposes through by miRNA inhibition or overexpression *in vivo*. In principle, miRNA

inhibitors are used to block the activity of miRNAs that drive disease progression whereas miRNA mimics are delivered to increase the expression of beneficial miRNAs in disease settings. However, the development of miRNA overexpression through synthetic RNA duplexes has significantly lagged behind miRNA inhibition owing to substantial challenges in their design and delivery[27]. Although they are now relatively easy to synthesize, double stranded miRNA mimics tend to trigger immune responses against dsRNA while the polyanionic nature of RNA duplexes makes them difficult to pass through the cytoplasmic membrane of cells targeted for therapy. Moreover, miRNA mimics are particularly susceptible to degradation in the circulation, and any chemical modifications to prolong the half-life of these nucleic acids are likely to interfere with their function. All of these challenges have emphasized the need to develop more efficient delivery systems for miRNA therapeutics, particularly in the context of cardiovascular disease.

In recent years, nanotechnology-based RNAi therapeutic platforms have shown great promise for various disease applications. While cationic lipid/polymer-based NPs have been explored for systemic delivery of siRNA in preclinical models[28–30], none of these platforms have been used to deliver miRNAs to macrophages *in vivo*. In this study, we developed chNPs for delivering functional miRNA mimics to macrophages and studied the effect of these NPs on RCT *in vivo*. We find that our chNPs made using a cross-linked chitosan polysaccharide polymer can protect as well as transfer exogenous miR-33 to naïve macrophages and alter the expression of its target gene, *Abca1*, both *in vitro* and *in vivo.* Additionally, we confirmed that macrophages treated with chNPs containing miR-33 exhibited reduced cholesterol efflux to apoA1 and mice treated with these NPs also showed a decrease in RCT. In contrast, treatment with NPs containing efflux-promoting miRNAs miR-206 and miR-223 enhanced ABCA1

expression and the RCT pathway. Thus, our studies indicated that miRNAs can be efficiently delivered to macrophages *via* chNPs where they can function to regulate ABCA1 expression and cholesterol efflux, suggesting that these miRNA NPs can be used *in vivo* to target atherosclerotic lesions.

3.4. Materials and methods

3.4.1. Reagents

Low molecular weight chitosan (50-190kDa) with a 75-85% degree of deacetylation and TPP, FITC, EDC, and NHS were obtained from Sigma-Aldrich. $mPEG_{2K}$-COOH (polyethylene glycol), and $mPEG_{5K}$-COOH were purchased from Laysan Bio Inc. Acetylated human LDL (BT-906) and human apoA1 (BT-927) were purchased from Alfa Aesar (Thermo Fisher Scientific Inc.). Control mimic, miR-33 mimic, and Dy547-labeled cel-miR-67 (miRIDIAN microRNA mimic) were obtained from Dharmacon (Horizon Discovery Group). Lipofectamine RNAiMAX and RNase A (DNase and protease-free) were purchased from Thermo Fisher Scientific Inc.

3.4.2. Mice

C57BL6 wild-type mice were purchased from Charles River Laboratories.

3.4.3. Cell culture

Peritoneal macrophages were isolated by peritoneal lavage with 3 x 5ml sterile PBS from wild-type mice that had intraperitoneal injection of 3% thioglycollate 4 days prior. Cells were maintained in DMEM (Gibco-Life Technologies) supplemented with 10% (v/v) FBS and 1% (v/v) P-S. BMDMs were harvested from femurs of wild-type mice and differentiated into

macrophages using DMEM supplemented with 10% (v/v) FBS, 20% (v/v) L929 conditioned media and 1% (v/v) P-S for 7 days.

3.4.4. Synthesis and characterization of PEGylated chitosan

PEGylation of chitosan polymer was carried *via* ester coupling reaction[31]. First, 200 mg of either PEG_{2K} or PEG_{5K} was dissolved in 0.5 ml of anhydrous DMF and added EDC (5 equ) followed by NHS (7 equ) and stirred at room temperature for 2 hours. Chitosan was dissolved in 1% (v/v) acetic acid and pH was adjusted to 5.8-6.3 using 1N NaOH. NHS activated PEG was then added stepwise to the chitosan solution and stirred at room temperature for 48h. After the reaction, crude product is transferred into dialysis tube (10K MWCO) and dialysed against dd H_2O for 48h remove unreacted PEG and the reaction side products. After the dialysis sample was collected and freeze-dried to obtain solid chitosan-PEG conjugates. Chitosan-PEG conjugates were characterized by ^{1}H NMR spectroscopy using 1:1 CD_3COOD:D_2O. ^{1}HNMR δ in ppm: chitosan monosaccharide peaks: 4.1-4.2, 3.55-3.75, 3.35, 3.1-3.2; PEG peaks 3.6-3.8.

3.4.5. Preparation of chNPs containing miRNA mimics

miRNA mimic-loaded chNPs were prepared *via* the ionic gelation method as previously described[32] with some modifications. To avoid RNase contamination, all the solutions were made in RNase-free water and filtered through 0.45 μm syringe filters. Chitosan-PEG_{2K} and chitosan-PEG_{5K} solutions (2 mg/ml) was prepared by dissolving PEGylated chitosan in 0.2M sodium acetate buffer (pH = 4.5). The pH value of this solution was then adjusted to 5.8 using 10M NaOH solution. TPP solution (1 mg/ml) was prepared by dissolving TPP in RNase-free water. The negatively charged components including microRNA mimics and TPP were added to the positively charged component such as PEGylated chitosan (chitosan-PEG_{2K} or chitosan-

PEG_{5K}). The mixture was then vortexed for 30 seconds and incubated at room temperature for 45 minutes with vigorous shaking. chNPs were collected using Amicon Ultra-0.5ml centrifugal filters with 10 kDa-molecular weight cut-off (Millipore).

3.4.6. Characterization of chNPs containing miRNA mimics

miR-chNPs hydrodynamic size and surface charge measurements were performed using dynamic light scattering (DLS). Briefly, miR-chNPs were diluted 10-20 times in H_2O or 1% PBS and transferred into cuvettes, and measured size and zeta potentials using Malvern zetasizer (Particle Metrix GmbH, Germany). TEM samples were prepared by depositing 10ul of freshly prepared chNPs on carbon-coated copper grids (300 mesh). The excess solution was blotted, and the dried grids imaged using FEI Tecnai G2 Spirit Twin electron microscope. To quantify encapsulated miRNA mimic, standard curve was prepared using Dy547-labeled miRNA mimics based on the dye fluorescence intensity (525/575), and encapsulation efficiency was calculated based on literature procedure[33]. The release kinetics of miRNA mimics from miR-chNPs were measured using Dy547-labeled miRNA mimics and cel-miR-54. chNPs containing Dy574-labeled miRNA mimics or cel-miR-54 were prepared as described above. In the case of Dy547-miR-chNPs, chNPs were incubated in PBS and at each indicated time point, Dy574-miR-chNPs were pelleted down by spinning at 13,300 xg for 15-20 minutes. Supernatant was collected and the concentration of Dy547-miRNA mimic in the supernatants were identified by measuring the dye fluorescence intensity (525/575). In the case of miR54-chNPs, chNPs were applied to naïve macrophages and cells were collected at each indicated time point for miR-54 expression analysis.

3.4.7. Tracking of FITC-labeled chNPs containing Dy547-labeled miRNA mimics

Chitosan-FITC conjugate was synthesized by reacting 25 mg of low molecular weight chitosan in 15 ml of 0.1M acetic acid, and 1mg of FITC in ethanol at room temperature (in the dark) for 24h. After reaction, crude product was dialyzed against ddH_2O for 48h, and samples were freeze-dried to obtain FITC-chitosan conjugates.

FITC-labeled chNPs containing Dy547-labeled miRNA mimics were prepared as described above and applied to naïve macrophages, which were plated in Lab-Tek Chambered Coverglass System (Thermo Fisher Scientific Inc.). Uptake of labeled EVs was visualized by the confocal microscope Zeiss LSM 880 Airyscan Elyra PS.1 (Zeiss) using a 488nm laser and a 561nm laser.

3.4.8. Cell transfection with miRNA mimics

Macrophages were transfected with control mimic or miR-33 mimic (miRIDIAN microRNA mimic) at a concentration of 100nM using Lipofectamine RNAiMAx as previously described[20,34,35]. Briefly, transfection of macrophages was performed in OPTIMEM media overnight. The next day, same volume of DMEM containing 20% (v/v) FBS was added and transfected cells were harvested 72 hours after transfection.

3.4.9. Cell viability assays

Cell death was determined by measuring LDH release into the medium as previously described[36]. Briefly, macrophages were treated with chNPs containing miRNA mimics for 24, 48, and 72 hours, and the medium collected at the indicated time points was at 12,000x*g* for 5 minutes at room temperature to pellet cell debris. The amount of LDH in the medium was measured in a kinetic assay by adding PBS containing 0.02% NADH (reduced form of NAD^+) and 0.03% sodium pyruvate and measuring absorbance at 340 nm for 10 min at 1-min

intervals. The slope of the curve provides a measure of cell death, which was expressed as fold change relative to control.

3.4.10. Serum protection assay

chNPs containing 1.5μg of cel-miR-54 was incubated with mouse serum at a final concentration of 10%, 20%, 35% or 50% for 30 minutes at 37^{o}C. Unprotected cel-miR-54 acted as a control and was treated in the same manner. Serum pre-treated miR54-chNPs and naked cel-miR-54 were then applied to naïve macrophages and cells were collected 24 hours after treatment for miR-54 expression analysis. Dispersion stability of miR-chNPs were also examined by incubating miR-chNPs in H_2O, DMEM supplemented with 5% FBS, or DMEM supplemented with 10% FBS. The size of miR-chNPs were measured pre- and 2h post-incubation using Malvern zetasizer (Particle Metrix GmbH, Germany).

3.4.11. Cholesterol efflux

Peritoneal macrophages were treated with chNPs containing control mimic or miR-33 mimic ($5.6x10^9$ particles containing 3.5μg of miRNA mimics) for 48 hours and subsequently, were loaded with 37.5 μg/ml acetylated LDL and labeled with 1 μCi/ml [^{3}H] cholesterol (Perkin Elmer) for 24 hours. The next day, cells were washed extensively with PBS and equilibrated in 2% fatty acid-free BSA (bovine albumin serum) in DMEM media for 4 hours before being treated with 50 μg/ml apoA1 (Alfa Aesar) for 6 hours or 24 hours. Medium and cellular [^{3}H] were counted using liquid scintillation counting and expressed as a percentage of total cellular [^{3}H] cholesterol content.

3.4.12. *In vivo* RCT assays

Peritoneal macrophages were isolated and maintained in DMEM supplemented with 10% (v/v) FBS as described above. For the first RCT assay, macrophages treated with chNPs

containing control mimic, miR-33, miR-223, or miR-206 mimic ($1.4x10^{10}$ particles containing 8.75μg of miRNA mimics) for 48 hours were loaded with 37.5 μg/ml acetylated LDL and labeled with 5 μCi/ml [^{3}H] cholesterol for 24 hours as described previously[13,21]. The next day, cells were washed twice, harvested and resuspended in ice-cold DMEM, of which 2-3 $x10^6$ cells were then injected subcutaneously into individually housed wild-type mice (n=5/group). Prior to injection, the level of ^{3}H-labeled tracer in a cell aliquot was counted using liquid scintillation counter (LSC) to measure baseline radioactivity. Blood was obtained by saphenous vein puncture at 6 and 24 hours after injection and by cardiac puncture after 48 hours at sacrifice. Plasma ^{3}H-labeled tracer was determined using the LSC immediately at each time point. Feces were collected for 24 and 48 hours after injection and homogenized in 50% ethanol overnight, after which an aliquot was used to count fecal total ^{3}H-labeled sterols. At sacrifice, liver samples were collected, and a portion of the liver was homogenized in PBS, which was then assayed using the LSC to determine the level of ^{3}H-labeled tracer in the liver. Hepatic lipids were also extracted in hexane/isopropanol (3:2 v/v) as previously described[21]. The lipids were dried and resuspended in liquid scintillation fluid for radioactivity counting. RCT to liver, feces, and plasma was calculated as a percentage of total radioactivity injected at baseline. The second RCT assay was performed similarly to the first one, except that individually housed wild-type mice (n=5/group) were injected subcutaneously with acetylated LDL-loaded/[^{3}H]cholesterol-labeled peritoneal macrophages and chNPs containing either control or miR-33 mimics simultaneously ($2.24x10^{10}$ particles containing 14μg of miRNA mimics).

3.4.13. miRNA and gene expression analysis

For miRNA expression analysis, total RNA was isolated using Trizol (Invitrogen) and

the expression levels of miRNAs of interest was measured by qRT-PCR using miScript II Reverse Transcription kit, miScript Primer Assays and Quantitect SYBR Green (QIAGEN), in which the expression of candidate miRNAs was normalized to RNA, U6 small nuclear 6, pseudogene (QIAGEN). For gene expression analysis, total RNA was isolated using Trizol and reverse transcribed using iScript Reverse Transcription Supermix for qRT-PCR (Bio-Rad). qRT-PCR was performed using the SsoAdvanced Universal SYBR Green Supermix (Bio-Rad) and gene expression was normalized to HPRT and 18S. The primers used are: *Abca1* (Forward: 5' GCTTGTTGGCCTCAGTTAAGG 3'; Reverse: 5' GTAGCTCAGGCGTACAGAGAT 3').

3.4.14. Western blot analysis

Cells were washed in ice-cold PBS and lysed in ice-cold RIPA buffer supplemented with protease inhibitor cocktail (Roche). Proteins (50µg) were subjected to 4-20% SDS-PAGE and transferred to PVDF membranes (Bio-Rad) for immunoblot analysis[35]. PVDF membranes were blocked with 5% (w/v) milk in TBST and incubated overnight with antibodies against ABCA1 (Novus Biologicals) and HSP90 (Santa Cruz Biotechnology). Goat anti-mouse or anti-rabbit IRDye® secondary antibodies were used for detection on a LI-COR Odyssey infrared imaging system (LI-COR Biosciences).

3.4.15. Statistics

Data shown is either mean ± SD of at least 3 independent experiments or a single representative experiment that was performed in triplicate. Comparison between control and treatment was made using Student's t-test ($p \leq 0.05$) or comparison between groups by one-way ANOVA ($p \leq 0.05$) using Prism GraphPad, as indicated in the Figure legends.

3.5. Results

3.5.1. Development and characterization of chNPs containing miRNA

For efficient delivery of miRNA mimics, we developed a chitosan polymer-based NP platform. Chitosan polymers are biodegradable, biocompatible, and have a positively charged back bone, which is ideal for complexing negatively charged nucleotides *via* ionic interactions. To improve water solubility as well as to extend circulation half-life, chitosan was modified at amine groups by two different molecular weight PEG chains (molecular weight of PEG unit = 2000 or 5000). We conjugated free amine groups on the chitosan polymers with carboxylic acid end groups of PEG_{2K} or PEG_{5k} *via* ester coupling reaction[31]. PEG conjugation was confirmed by ^{1}HNMR spectroscopy, which showed a typical PEG peak around 3.7 and chitosan monomer chemical shifts around ~4.1, and 3.1 ppm[37,38]. Covalently attached PEG molecules form a shell-like structure to not only prevent the aggregation but also to improve the stability of particles[39,40]. The preparation of the chNPs was done *via* the ionic gelation method[32] using appropriate ratios of chitosan, TPP and miRNA mimics (**Figure 3.1A**). The principle of this method relies on the ionic interaction between the cationic charges of primary amine groups of the chitosan with the anionic charges of the miRNA mimics where TPP is used to stabilize the miRNA mimic-chitosan and chitosan-chitosan interactions *via* crosslinking between the phosphate groups of TPP and the amine groups of chitosan polymer. Upon synthesis and purification, miR-chNPs were characterized by DLS for the hydrodynamic size and the surface zeta potential. The resultant NPs showed a narrow size distribution with hydrodynamic size ranged approximately from 150nm to 200 nm (**Figure 3.1B**) and a surface charge of 2-6 mV (**Figure 3.1C**). In addition, they demonstrated a uniform and compact

spherical morphology with lower size ranges due lack solvent layer as determined by TEM (**Figure 3.1D**).

We next tested the encapsulation efficacy of different NP formulations for systemic miRNA delivery of varying chitosan/TPP/miRNA mimic weight ratios. The miRNA mimic loading capacity of PEGylated chitosan-TPP NPs was calculated as the ratio of the amount of Dy547-labeled miRNA mimics (*C. elegans* miR-67) encapsulated in the NPs to the initial quantity of miRNA mimics. Results showed that NPs formed at a chitosan-PEG_{5K}/TPP/miRNA mimic ratio of 30:4:1 yielded highest encapsulation efficiency, with 60% of miRNA mimics were complexed into the NPs; therefore, this formulation was used for further *in vitro* and *in vivo* experiments.

3.5.2. Cytotoxicity, cellular uptake and intracellular delivery efficiency of miR-chNPs

To test the biocompatibility of chNPs, we first assessed the effects of miR-chNPs on the viability of primary mouse macrophages after 24-hour, 48-hour and 72-hour treatment. As shown in **Figure 3.1E**, miR-chNPs did not cause any severe toxicity to peritoneal macrophages in comparison to cells treated with empty chNPs or untreated cells even after 72-hour treatment (1.2 ± 0.09-fold induction of cell death relative to untreated cells, p=ns). We also examined if miR-chNPs are toxic to other types of macrophages including BMDMs and indicated that chNPs did not exhibit any toxicity in BMDMs, as expected (data not shown). Together, these results suggest that miR-chNPs are non-toxic and can maintain the cell viability *in vitro*.

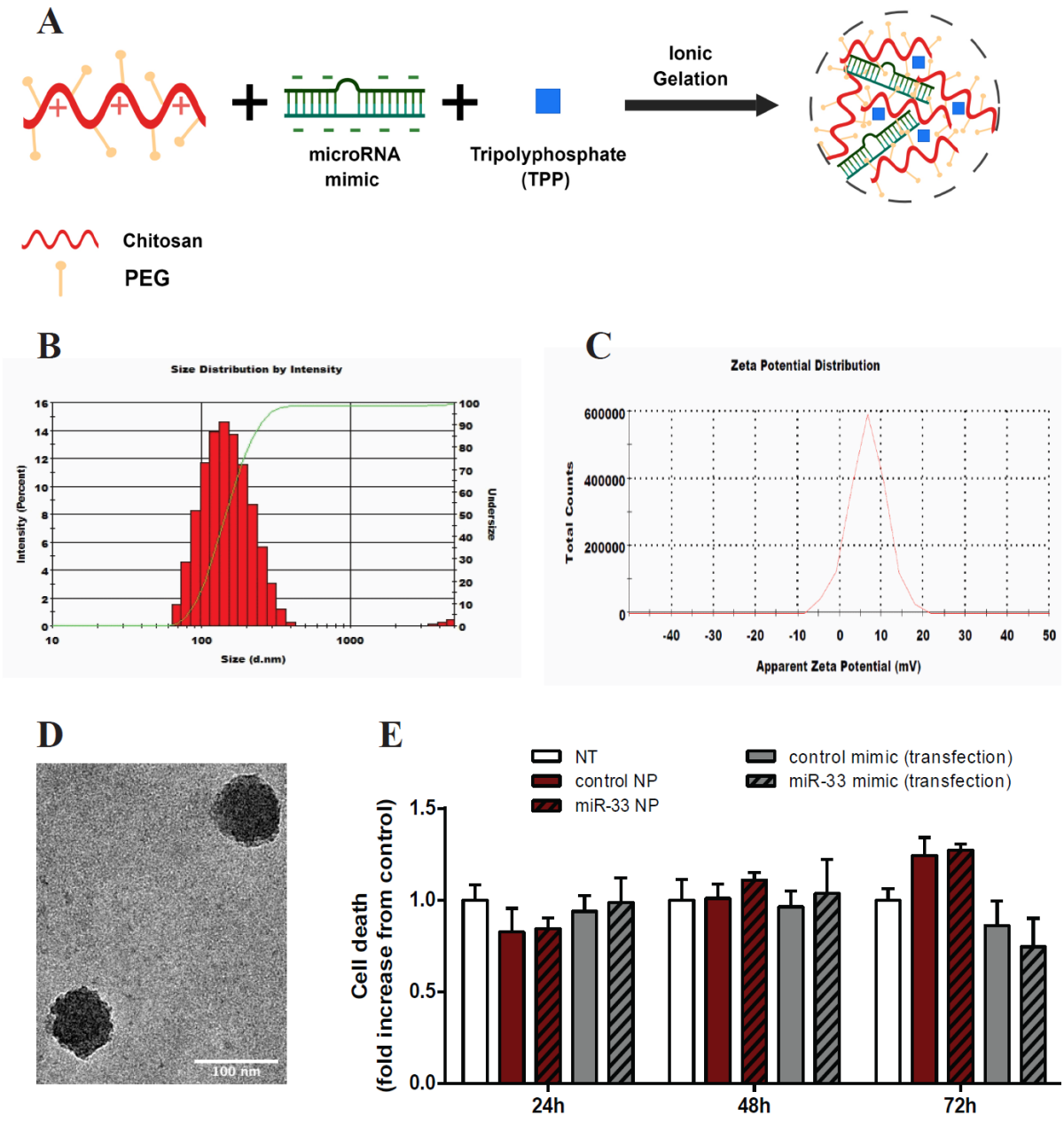

Figure 3.1. Characterization of chNPs containing miRNA mimics. (**A**) Schematic illustration of miRNA mimic-loaded chNPs prepared using the inonic gelation method. (**B-C**) The size of miRNA mimic-loaded chNPs post-synthesis (**B**) was measured using dynamic light scattering, and their surface Zeta potential were also obtained using Malvern Zetasizer (**C**). (**D**) Electron microscope images of chNPs containing miRNA mimics showing a uniform and contact spherical morphology. Scale bar represents 100 nm. (**E**) Effects of chNPs containing miRNA mimic on the viability of peritoneal macrophages. Shown here is the representative experiment done in triplicate (n=3).

Intracellular delivery of nucleic acids such as miRNA mimics remains one of the major limitations for several engineered NP platforms[41]. Following the optimization of NP formulation, we proceeded to test whether or not chNPs could be taken up by naïve macrophages and these NPs could transfer miRNA mimics to recipient cells. We produced FITC labeled miR-chNPs loaded with Dy547-labeled miRNA mimics and applied them to naïve macrophages. Uptake of labeled NPs and labeled miRNA mimics was visualized using live-cell imaging, and showed a rapid uptake of both FITC-labeled NPs and Dy547-labeled miRNA mimics into the cytosol of naïve macrophages within 8-hour treatment (**Figure 3.2A**). The levels of fluorescent signal in naïve cells reached their peak at 24-hour treatment before starting to decrease at 48-hour and 72-hour treatment (**Supplemental Figure 3.1A-B**). The release kinetics of miRNA mimics from NPs was measured to further investigate the miRNA delivery characteristics of the chNPs. Dy547-labeled miRNA showed an initial burst of release from chNPs into PBS with approximately 20% miRNAs released during the first two hours, followed by a slow release up to 48 hours (**Figure 3.2B**). This was confirmed by measuring delivery of *Cel*-miR-54 (naturally present only in *C. elegans*) over time (**Figure 3.2C**). These data for miRNA release are similar to what has been observed for siRNA[42]. To confirm that chNPs can protect and deliver exogenous miRNAs to macrophages, we again employed miR-chNPs containing cel-miR-54. miR54-chNPs were pretreated with serum at different final concentrations varying from 10% to 50% and then applied to naïve macrophages. Free (non-chNP bound) miR-54 was used as a positive control for serum nuclease activity. There was no significant difference in miR-54 transfer capacity of chNPs after pre-treatment with serum (**Figure 3.2D**), suggesting that miRNA molecules contained in the NP membrane are protected from serum nuclease activity. This is in contrast to free cel-miR-54, whose delivery was

significantly decreased after treatment with 10% serum and became nearly undetectable after treatment with 50% serum. Furthermore, there was no significant difference in size of miR-chNPs between various dispersion media (H_2O, 5% FBS, or DMEM supplemented with 10% FBS) (**Supplemental Figure 3.1C**), again confirming the stability of miR-chNPs in different physiological conditions. Taken together, these data demonstrate that chNPs can be taken up by macrophages and transfer miRNA mimics to recipient cells *in vitro* and protect the miRNA cargo from extracellular nuclease degradation.

3.5.3. chNPs can transfer exogenous miR-33 to naïve macrophages and regulate the expression of its target gene both *in vitro* and *in vivo*

NPs can be taken up by target cells *via* endocytosis, thus resulting in sequestration of the NP cargo in the endocytic vesicles. Because of being separated from the cytosol by the endosomal limiting membrane, these cargos cannot exert their intended function in the recipient cells[43,44]. In addition, maturation of endosomes to late endosomes is coupled with a decrease in intravesicular pH and fusion with lysosomes, potentially resulting in destruction of the functional nanomaterials by degradative lysosomal enzymes[45]. Therefore, in order for the cargo packaged and delivered by NPs to preserve their function, NPs need to escape from the endosomes and release their cargos into the cytosol in a timely manner. This has made endosomal escape a bottleneck in achieving successful delivery of NPs. We therefore sought to determine if miRNAs delivered *via* chNPs can be released from the endosomal system and function in the RISC complex by examining changes of target gene expression in response to NP treatment. In this experiment, we treated naïve macrophages with chNPs containing control mimic or miR-33 mimic (cont-miR-chNP or miR33-chNP) and measured the expression level of *Abca1*, a bona fide target gene of miR-33[20,46,47], in naïve cells. As a positive

control, we also compared miR-chNPs to traditional miRNA transfection reagents in their ability of transferring miR-33 mimic to macrophages. Following 72-hour exposure to miR33-chNP, we again confirmed that our NPs acted as carriers to transfer miR-33 to naïve macrophages (**Figure 3.3A**). Treatment of macrophages with miR33-chNP but not cont-miR-chNP reduced the expression of ABCA1 at both the mRNA and protein level (**Figure 3.3B-C**). ABCA1 plays a key role in stimulating the efflux of cholesterol from macrophages, thereby reducing foam cell formation and the development of atherosclerosis[9,10]. We therefore tested the effects of these NPs on macrophage cholesterol efflux and confirmed that macrophages treated with miR33-chNPs exhibited reduced cholesterol efflux to apoA1 at 6h (5.3 ± 0.3% for cont-miR-chNP *versus* 3.8 ± 0.3% for miR33-chNP; $P \leq 0.01$) and 24 hours (17.9 ± 1.0% for cont-miR-chNP *versus* 12.7 ± 0.5% for miR33-chNP; $P \leq 0.01$) (**Figure 3.3D**).

We next examined the effect of miR33-chNP on macrophage expression of ABCA1 following delivery *in vivo*. C57BL6 mice were injected intraperitoneally with thioglycollate to trigger macrophage accumulation in the peritoneal cavity[48]. Three days after thioglycollate injection, cont-miR-chNP or miR33-chNP were delivered to the peritoneum and macrophages were collected by lavage two days later. The miR-33 delivery was confirmed in peritoneal macrophages (**Figure 3.4A**) and miR33-chNPs reduced ABCA1 expression at both the mRNA and protein level, indicating the chNPs could deliver miR-33 mimics that retained functional capability to repress target gene expression *in vivo* (**Figure 3.4B-C**). Thus, miR-33 mimic can be efficiently delivered to macrophages *via* chNPs where they can function to regulate ABCA1 expression and cholesterol efflux *in vitro* and *in vivo*.

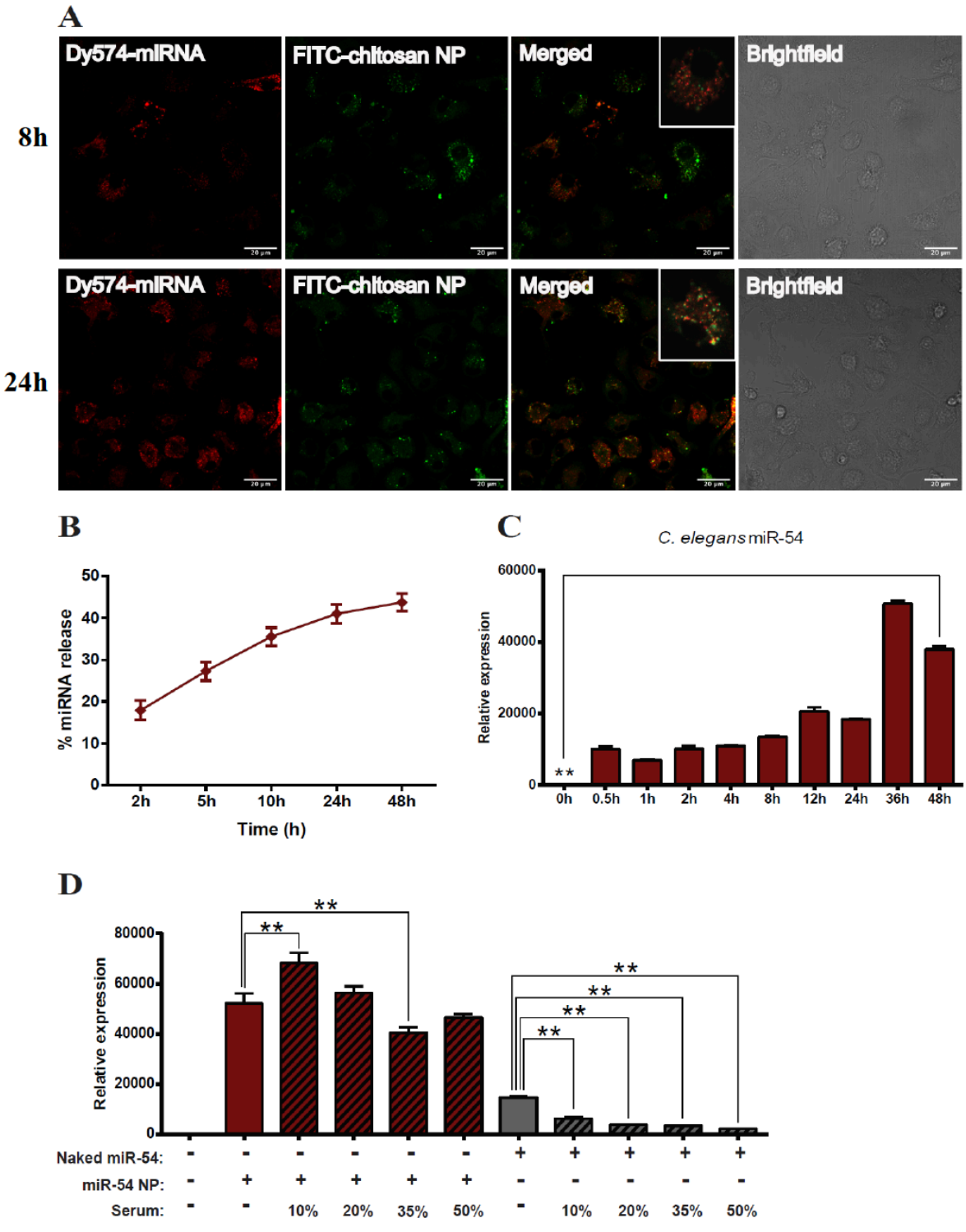
A
8h
24h
Dy574-miRNA
FITC-chitosan NP
Merged
Brightfield
B
% miRNA release
Time (h)
2h
5h
10h
24h
48h
C
C. elegans miR-54
Relative expression
0h
0.5h
1h
2h
4h
8h
12h
24h
36h
48h
D
Relative expression
Naked miR-54:
miR-54 NP:
Serum:
10%
20%
35%
50%

Figure 3.2. chNPs containing miRNA mimics are taken up and deliver exogenous miRNAs to naïve macrophages. (**A**) FITC-labeled chNPs containing Dy547-labeled miRNA mimics were prepared and applied to peritoneal macrophages. Uptake of labeled NPs and miRNA mimics was visualized using confocal microscopy. Scale bar represents 20 μm. (**B**) The release kinetics of Dy547-labeled miRNA mimics from chNPs. (**C**) Time-course delivery of cel-miR-54 by chNPs to naïve macrophages. (**D**) Peritoneal macrophages were incubated with cel-miR-54-loaded chNPs untreated or pretreated with serum at the final concentration of 10%, 20%, 35% or 50% for 30min at 37ºC. Naked miR-54 was used as a positive control for serum nuclease activity. After 24h treatment, total RNA was isolated and cel-miR-54 levels were measured by qPCR. Shown here is the representative experiment done in triplicate (n=3), **p <0.01 by One-way ANOVA.

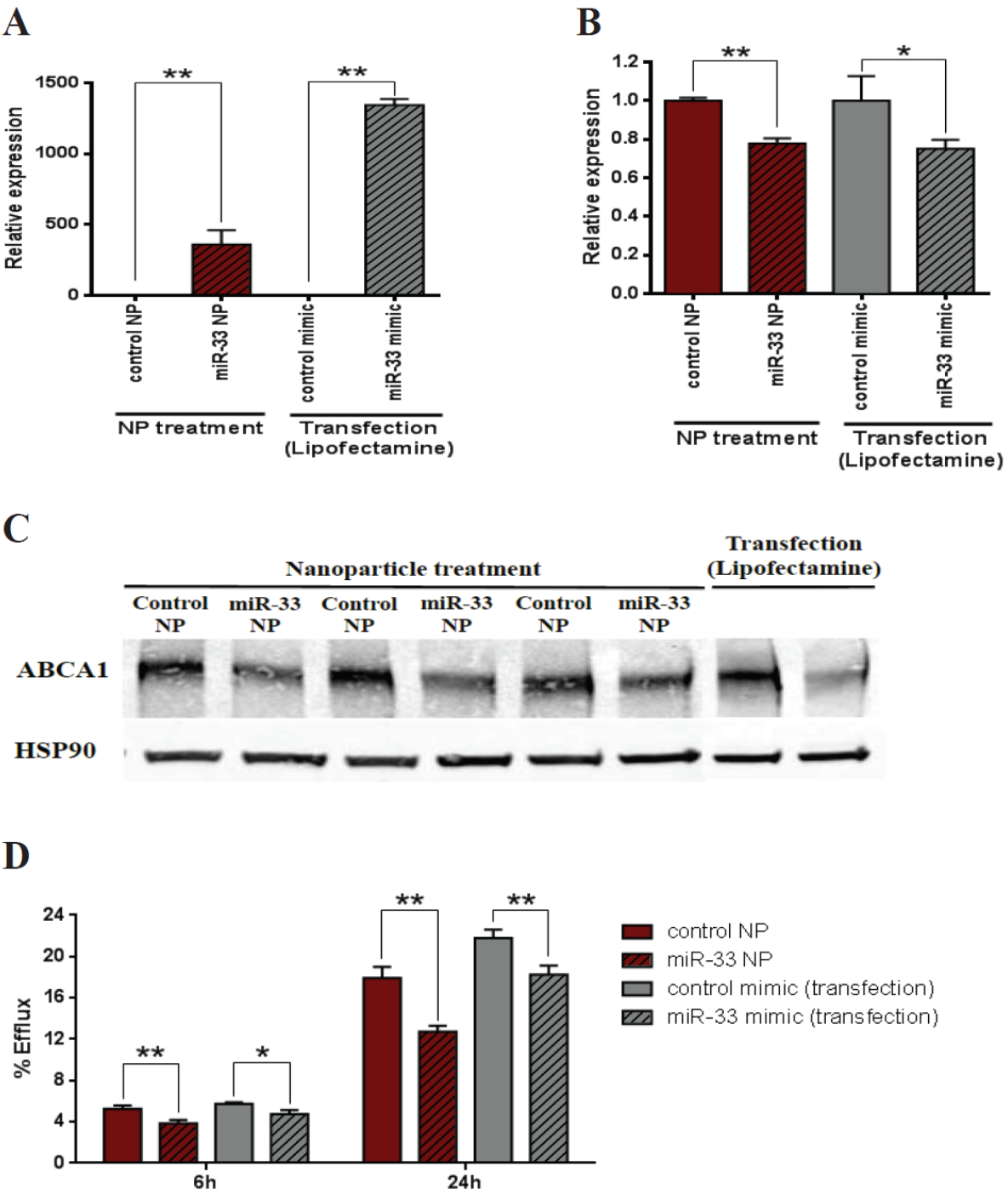
A
Relative expression
1500
1000
500
0
**
**
control NP
miR-33 NP
control mimic
miR-33 mimic
NP treatment
Transfection (Lipofectamine)
B
Relative expression
1.2
1.0
0.8
0.6
0.4
0.2
0.0
**
*
control NP
miR-33 NP
control mimic
miR-33 mimic
NP treatment
Transfection (Lipofectamine)
C
Nanoparticle treatment
Transfection (Lipofectamine)
Control NP
miR-33 NP
Control NP
miR-33 NP
Control NP
miR-33 NP
ABCA1
HSP90
D
% Efflux
24
20
16
12
8
4
0
**
*
**
**
6h
24h
control NP
miR-33 NP
control mimic (transfection)
miR-33 mimic (transfection)

Figure 3.3. miR-33 mimic can be delivered to macrophages via chNPs where they can function to regulate ABCA1 expression and cholesterol efflux in vitro. Peritoneal macrophages were treated with chNPs containing control mimic or miR-33 mimic for 72h. Cells transfected with miR-33 mimic by Lipofectamine RNAiMax were used as a positive control for the efficiency of miRNA mimics. (**A**) miR-33 expression in macrophages treated with control mimic-loaded/miR-33-loaded NPs or transfected with control mimic/miR-33 mimic. (**B-C**) Treatment of macrophages with chNPs containing miR-33 mimic reduced the expression of ABCA1, a validated target of miR-33, at the mRNA (B) and protein (C) level. (**D**) Macrophages treated with miR-33 containing chNPs exhibited reduced cholesterol efflux to apoA1. Following NP treatment, macrophages were cholesterol-loaded for 24h, and cholesterol efflux to apoA1 (50 μg/ml) was measured for 6h and 24h. % efflux is shown as a proportion of total radiolabeled cholesterol in the cell. Graphs represent the experiments performed in triplicate (n=3), *$p<0.05$ **$p<0.01$ by One-Way ANOVA. Western blot is representative of a single experiment done in triplicate (n=3).

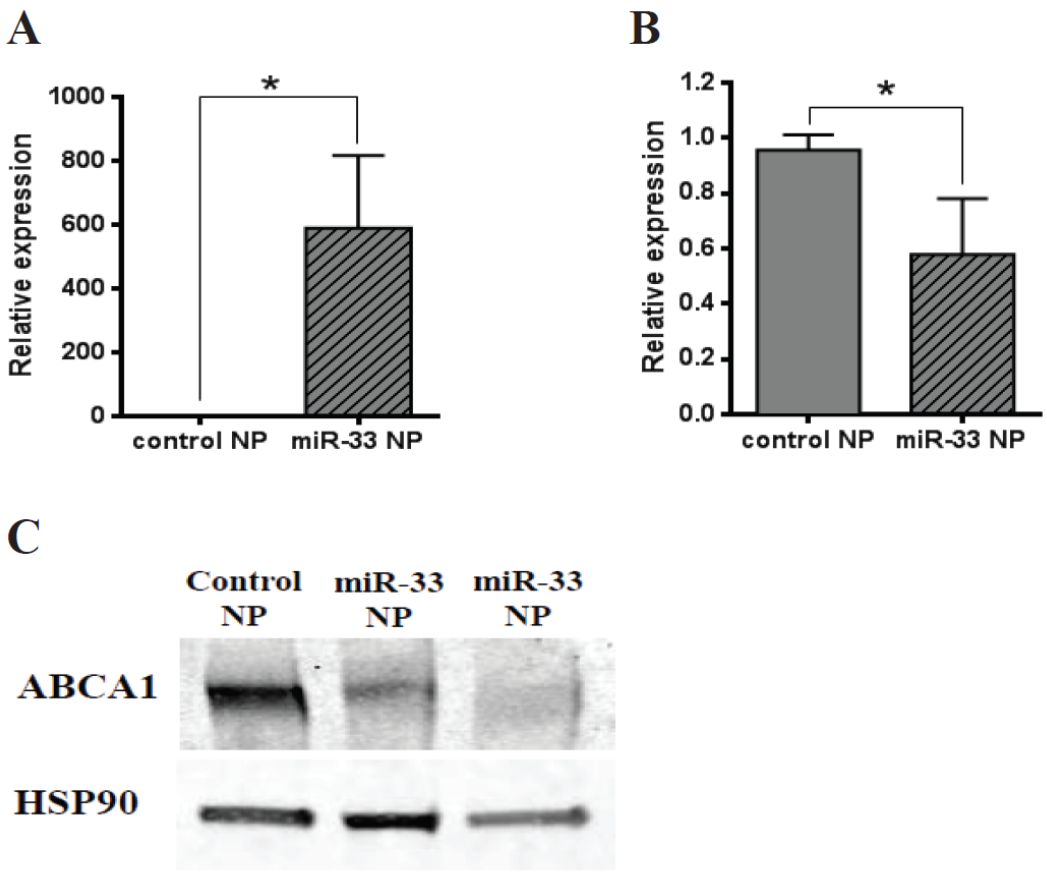

Figure 3.4. chNPs can transfer exogenous miR-33 to macrophages and regulate the expression of its target gene, ABCA1, in vivo. C57BL6 mice (n=4/group) were injected intraperitoneally with thioglycolate and 80h following thioglycolate injection, were treated with chNPs containing control mimic or miR-33 mimic for 60h. Peritoneal cells were collected and the expression of miR-33 as well as ABCA1 were analyzed by qPCR and Western blot. (**A**) miR-33 were efficiently delivered to peritoneal macrophages *in vivo.* (**B-C**) Treatment of mice with chNPs containing miR-33 mimic repressed macrophage ABCA1 expression at the mRNA (B) and protein (C) level. Graphs represent the means ± SD from n=4 mice per group, *$p<0.05$. Western blot is representative of pooled protein of n=4 mice per group.

3.5.4. Macrophage RCT is altered by chNPs containing miR-33 mimic

A critical step in excess cholesterol removal from tissues is the efflux of cholesterol into the periphery and out into the bile and feces through the RCT pathway. We therefore investigated whether miR33-chNPs might regulate cholesterol transport from peripheral cells for excretion using an *in vivo* RCT assay, which traces ^{3}H-cholesterol from macrophages loaded with cholesterol[13,49]. First, we loaded peritoneal macrophages with [^{3}H]cholesterol-labeled acetylated LDL and pre-treated with cont-miR-chNPs or miR33-chNPs. After for 48h, mice were injected subcutaneously with the [^{3}H]cholesterol-labeled chNP loaded macrophages (**Figure 3.5A**). ^{3}H-cholesterol delivery to the liver was reduced by 40% from miR33-chNPs macrophages compared with that of controls (**Figure 3.5B-C**). Analyses of fecal extracts collected at 24h and 48h indicated that treatment with miR33-chNPs significantly decreased the levels of fecal total ^{3}H-labeled sterols (35% for 24h samples and 42% for 48h samples) (**Figure 3.5D**). In contrast, we observed no significant reduction in plasma ^{3}H-labeled tracers at any of the indicated time points (**Supplemental Figure 3.2A**).

To confirm whether *in vivo* delivery of miR33-chNPs can modulate RCT, we performed a similar assay but this time chNPs were delivered directly *in vivo*. First, [^{3}H]cholesterol-labeled peritoneal macrophages were injected into mice as before, followed by subsequent subcutaneous delivery of either cont-chNP or miR33-chNP (**Figure 3.6A**). Mice treated with miR33-chNPs exhibited decreased levels of both ^{3}H-labeled tracer accumulated in the liver (47% decrease relative to control) (**Figure 3.6B-C**) and ^{3}H-labeled sterols excreted into feces (61% and 42% decrease at 24h and 48h, respectively) (**Figure 3.6D**). The levels of fecal total ^{3}H-labeled sterols normalized after 72h (**Figure 3.6D**). miR-33 NP treatment had no effect on plasma ^{3}H-labeled tracers, in consistent with previous results (**Supplemental Figure 3.2B**).

Together, these data confirm that our chNP platform can effectively delivery miRNAs *in vivo* and function to inhibit the RCT pathway by which excess cholesterol from peripheral is transported to the liver for excretion.

3.5.5. Delivery of efflux-promoting miRNAs enhances RCT *in vivo*

In order to reduce or regress atherosclerosis burden, it is critically important to promote lipid removal from foam cells through activation of cholesterol efflux *via* ABCA1/ABCG1[50]. Our data obtained from miR33-chNPs prompted us to search for microRNAs whose overexpression would serve to enhance ABCA1 expression, promote cholesterol efflux and be anti-atherogenic. Although the molecular mechanisms underlying the beneficial effects of these miRNAs are unclear, miR-206 and miR-223 have been shown to positively regulate ABCA1 expression and cholesterol efflux[51,52]. miR-223 was found to repress SP3 expression *via* directly targeting the 3'UTR of *SP3*, which acts as a negative regulator of ABCA1[53,54]. Therefore, miR-223 decreases SP3 expression and promotes ABCA1 expression in hepatocytes[51]. In contrast, overexpression of miR-206 was shown to enhance macrophage cholesterol efflux *via* controlling the expression of LXRα, a nuclear receptor that plays a crucial role in transcriptional regulation of lipid metabolism and inflammation[55], and its target genes[52]. We therefore selected miR-223 and miR-206 for further investigation. We treated naïve macrophages with chNPs containing control mimic, miR-223 mimic or miR-206 (miR223-chNP or miR206-chNP) and measured the expression level of ABCA1 following 72-hour exposure to chNPs, and found that both miRNAs increased the expression of ABCA1 at the protein level (**Figure 3.7A**).

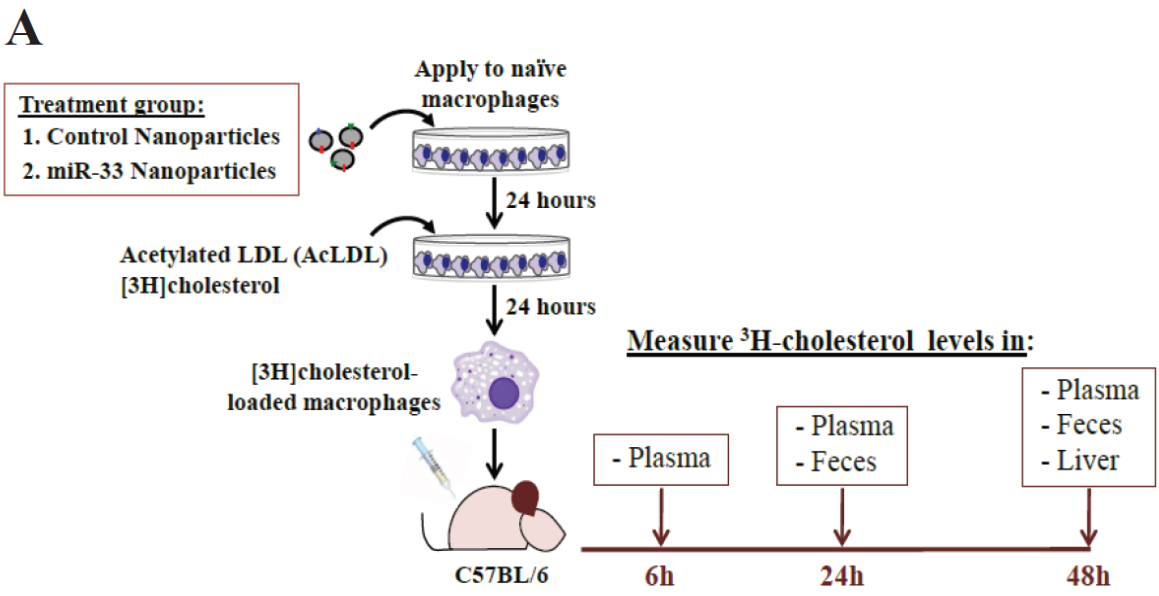
A
Treatment group:
1. Control Nanoparticles
2. miR-33 Nanoparticles
Apply to naïve macrophages
24 hours
Acetylated LDL (AcLDL)
[3H]cholesterol
24 hours
[3H]cholesterol-loaded macrophages
C57BL/6
Measure 3H-cholesterol levels in:
- Plasma
- Plasma
- Feces
- Plasma
- Feces
- Liver
6h
24h
48h

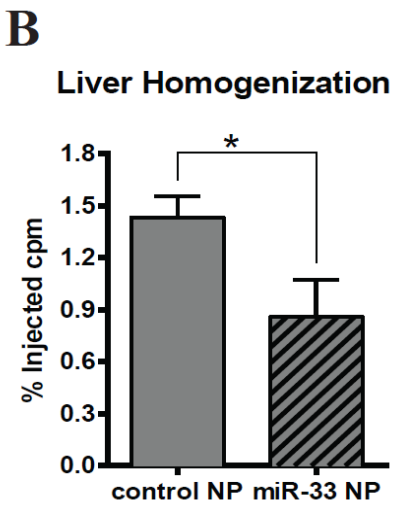
B
Liver Homogenization
% Injected cpm
1.8
1.5
1.2
0.9
0.6
0.3
0.0
*
control NP
miR-33 NP

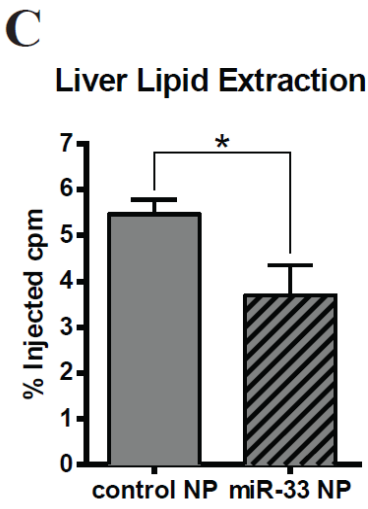
C
Liver Lipid Extraction
% Injected cpm
7
6
5
4
3
2
1
0
*
control NP
miR-33 NP

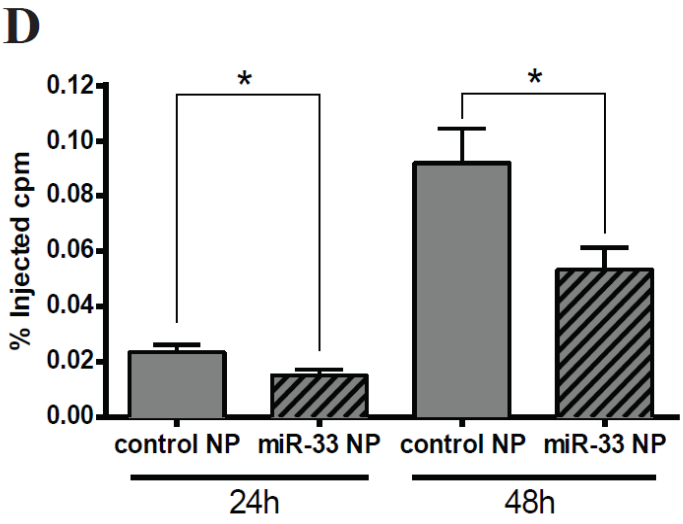
D
% Injected cpm
0.12
0.10
0.08
0.06
0.04
0.02
0.00
*
*
control NP
miR-33 NP
control NP
miR-33 NP
24h
48h

Figure 3.5. Ex vivo treatment with chNPs containing miR-33 inhibits RCT. **(A)** C57BL6 mice (n=5/group) were injected subcutaneously with acetylated LDL-loaded/[^{3}H]cholesterol-labeled peritoneal macrophages pre-treated with control/miR-33 NPs. **(B-C**) Hepatic ^{3}H-cholesterol tracer levels after 48h. (**D**) Fecal ^{3}H-cholesterol tracer levels. Feces were collected continuously from 0 to 48h after injection. Data are expressed as the percentage of the ^{3}H-cholesterol tracer relative to that of total cpm tracer injected ± SD. *$p<0.05$ by Student's t-test, compared with controls.

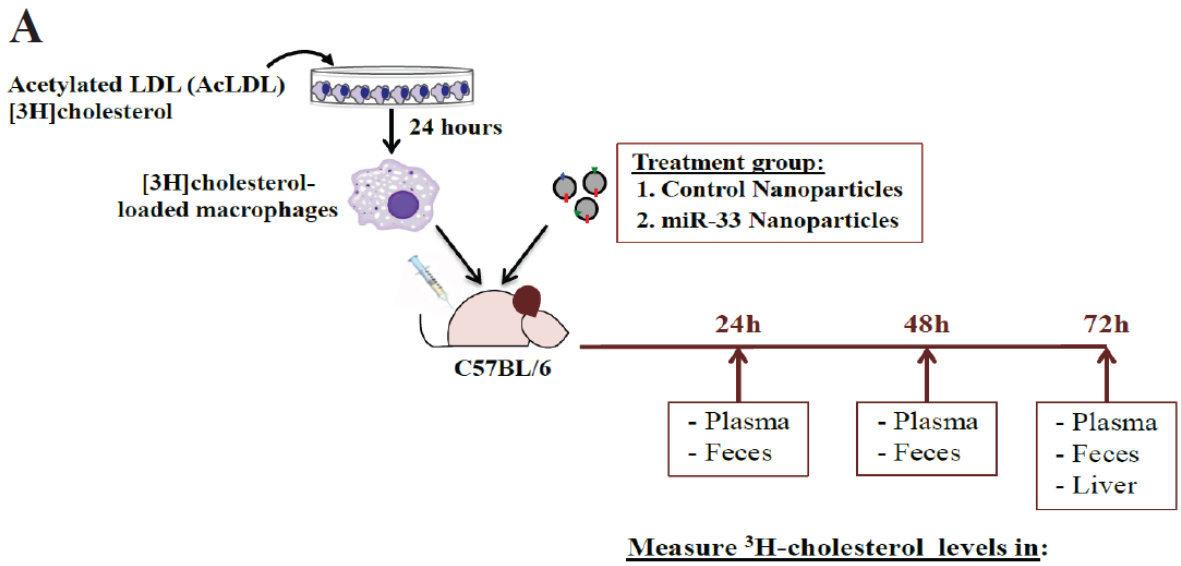
A
Acetylated LDL (AcLDL)
[3H]cholesterol
24 hours
[3H]cholesterol-
loaded macrophages
Treatment group:
1. Control Nanoparticles
2. miR-33 Nanoparticles
C57BL/6
24h
48h
72h
- Plasma
- Feces
- Plasma
- Feces
- Plasma
- Feces
- Liver
Measure 3H-cholesterol levels in:

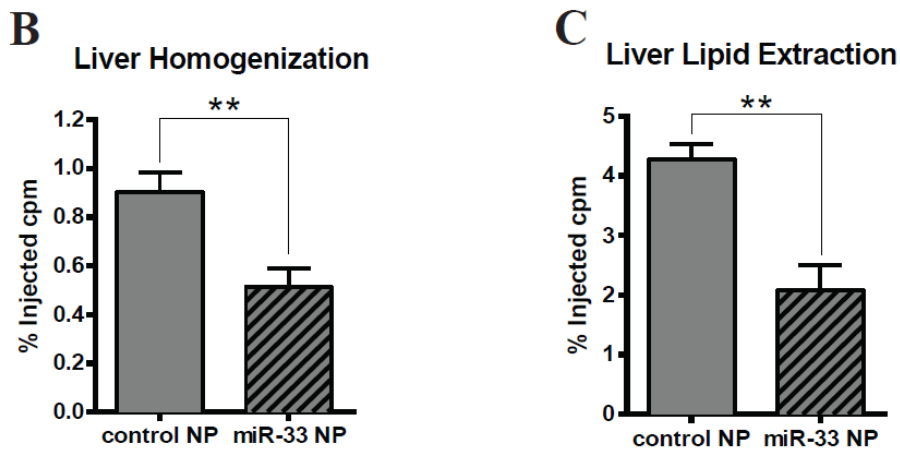
B
Liver Homogenization
% Injected cpm
1.2
1.0
0.8
0.6
0.4
0.2
0.0
**
control NP
miR-33 NP
C
Liver Lipid Extraction
% Injected cpm
5
4
3
2
1
0
**
control NP
miR-33 NP

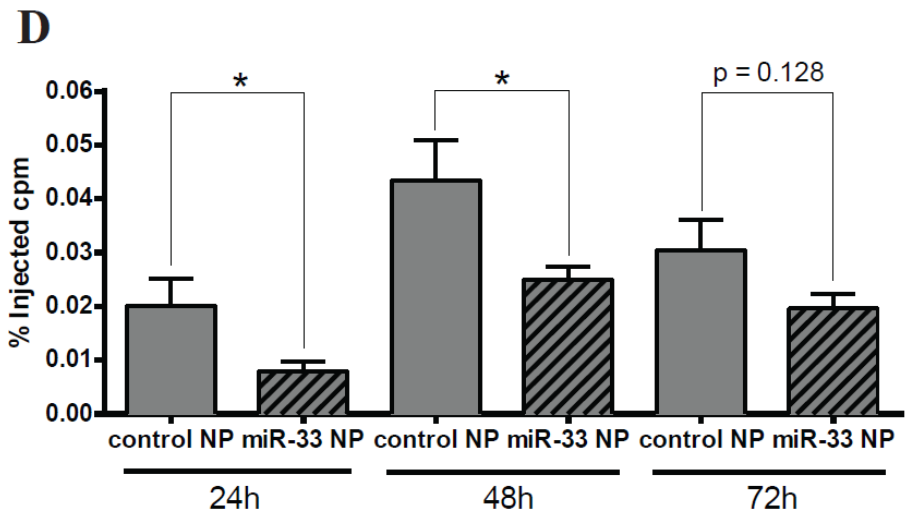
D
% Injected cpm
0.06
0.05
0.04
0.03
0.02
0.01
0.00
*
*
p = 0.128
control NP
miR-33 NP
control NP
miR-33 NP
control NP
miR-33 NP
24h
48h
72h

Figure 3.6. In vivo treatment with chNPs containing miR-33 inhibits RCT. (**A**) C57BL6 mice (n=5/group) were injected subcutaneously with acetylated LDL-loaded/[^{3}H]cholesterol-labeled peritoneal macrophages and chNPs containing either control or miR-33 mimics. (**B-C**) Hepatic ^{3}H-cholesterol tracer levels after 72h. (**D**) Fecal ^{3}H-cholesterol tracer levels. Feces were collected continuously from 0 to 72h after injection. Data are expressed as the percentage of the ^{3}H-cholesterol tracer relative to that of total cpm tracer injected ± SD. *$p<0.05$ ** $p<0.01$, by Student's t-test, compared with controls.

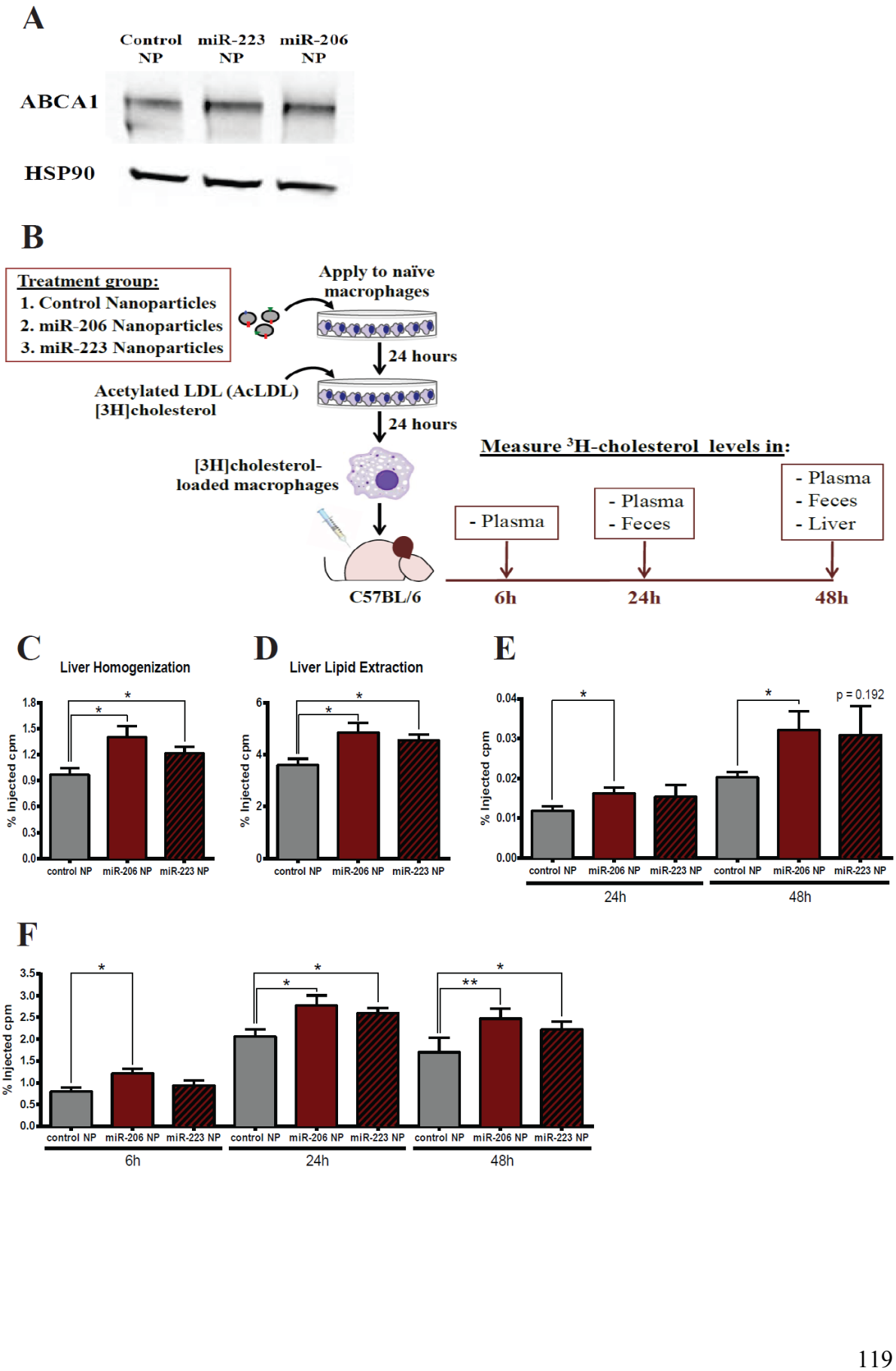
A
Control NP
miR-223 NP
miR-206 NP
ABCA1
HSP90
B
Treatment group:
1. Control Nanoparticles
2. miR-206 Nanoparticles
3. miR-223 Nanoparticles
Apply to naïve macrophages
24 hours
Acetylated LDL (AcLDL)
[3H]cholesterol
24 hours
[3H]cholesterol-loaded macrophages
C57BL/6
Measure 3H-cholesterol levels in:
- Plasma
- Plasma
- Feces
- Plasma
- Feces
- Liver
6h
24h
48h
C
Liver Homogenization
% Injected cpm
control NP
miR-206 NP
miR-223 NP
D
Liver Lipid Extraction
% Injected cpm
E
% Injected cpm
p = 0.192
24h
48h
F
% Injected cpm
6h
24h
48h

Figure 3.7. Treatment with chNPs containing miR-206/miR-223 enhances ABCA1 expression and promotes RCT. **(A)** Macrophages treated with miR-206/miR-223 containing chNPs showed increased ABCA1 expression. Western blot is representative of a single experiment done in triplicate (n=3). **(B)** C57BL6 mice (n=5/group) were injected subcutaneously with acetylated LDL-loaded/[^{3}H]cholesterol-labeled BMDMs pre-treated with control/miR-206/miR-223 NPs. **(C-D**) Hepatic ^{3}H-cholesterol tracer levels after 48h. (**E**) Fecal ^{3}H-cholesterol tracer levels. Feces were collected continuously from 0 to 48h after injection. (**F**) Time course of ^{3}H-cholesterol distribution in plasma. Data are expressed as the percentage of the ^{3}H-cholesterol tracer relative to that of total cpm tracer injected ± SD. *p<0.05 **p <0.01 by Student's t-test, compared with controls.

We next investigated whether delivery of miR223-chNP or miR206-chNP could regulate cholesterol transport from peripheral cells for excretion using the *in vivo* RCT experiment as described above (**Figure 3.7B**). Mice injected with miR223-chNPs or miR206-chNPs loaded macrophages showed significantly increased levels of plasma ^{3}H-cholesterol (27% and 31% for miR223-chNPs; 35% and 46% increase for miR206-chNPs over 24 or 48h, respectively) compared with control chNPs (**Figure 3.7F**). Furthermore, ^{3}H-cholesterol accumulation in the liver increased by 27% from miR223-chNPs and by 40% from miR206-chNPs loaded macrophages (**Figure 3.7C-D**). Treatment with miR206-chNPs also increased total fecal ^{3}H-sterol excretion by 45% and 60% at 24h and 48h, respectively (**Figure 3.7E**). Taken together, these data confirm that our chNP platform can be employed as a delivery modality for miRNA therapeutics to promote RCT.

3.6. Discussion

RNA-targeting therapies as a class of therapeutics have gained attention in recent years, with gene silencing being increasingly considered for treatment of cancers, metabolic disorders and genetic abnormalities[56]. These approaches have struggled with the challenge that double stranded RNA is immunogenic and susceptible to cleavage by serum endonucleases. As an alternative to siRNAs, ASOs were developed that are larger and contain a modified backbone to improve their tissue delivery, potency and toxicity[57]. While this may be an improvement for siRNA delivery, ASOs work best for abundant mRNA targets and only for tissues that are readily accessed by the ASOs (*i.e.* liver, kidney)[58,59]. Because both siRNAs and ASOs are designed to potently downregulate a single gene in a pathway, this can be problematic if the target gene is a multi-functional protein (such as a transcription factor) or if

there are compensatory mechanisms when a gene is inactivated. As such, miRNAs are increasingly being recognized for their potential as therapeutics modulators[60]. While their repressive capacity on any single target gene is small, usually less than 2-fold[61], because of their inherent ability to target multiple genes in the same biological pathway, miRNAs may offer a more potent effect on biological function than single-gene targeting siRNAs[62]. While single stranded anti-miRNAs to inhibit miRNA function have been developed that use similar chemistry to ASOs, the overexpression of functional microRNAs to tissues is a challenge and has hampered the development of miRNA-based therapeutics, particularly for diseases like atherosclerosis[63]. To overcome these challenges, we have demonstrated, to our knowledge, the first platform for effective delivery of miRNAs to modulate target gene expression *in vivo* to alter functional pathways in macrophages, which are central to the development of atherosclerosis.

To date, a variety of NP platforms have been developed for delivery of RNAi therapies. Similar to siRNA, double stranded mature miRNAs require the protection from extracellular endonucleases and modifications to improve their stability, which can prevent RNA duplex entry into the RISC complex and render the miRNA non-functional[27]. While some platforms have made significant advances towards the clinic, others have failed in different stages of clinical trials. For example, liposomal miR-34 was terminated in early stage trials due to immune related serious adverse effects[64–66]. This showcases the complexities in RNA delivery and the importance of biomaterials with lower toxicity and immunogenicity for successful therapeutic application. With this framework in mind, we sought to develop a chitosan-based miRNA NP platform. Chitosan polymers are naturally abundant, relatively non-toxic, are biodegradable, and are widely studied non-viral carriers for siRNAs and miRNAs[67,68].

Additionally, cationic charges on chitosan polymers can be controlled with conjugation and/or crosslinkers, to modulate the size of NPs and encapsulation of nucleic acids. Typically, chNPs are PEGylated *via* covalent and noncovalent methods to improve the stability and water solubility[69,70]. While covalent methods show successful PEGylation, they involve multi-step synthesis and might interfere with encapsulation of siRNAs/miRNAs, their cellular uptake, and their intracellular delivery[69,71]. To overcome these challenges, in this study we developed miR-chNPs using chitosan-PEG and TPP crosslinking *via* an ionic gelation method. We PEGylated chitosan polymer by reacting a minimum number of the amine groups with low molecular weight PEG in a simple one-step reaction, rendering remaining amine groups deacetylated, which may improve RNA cargo delivery[72]. While TPP strengthens the interaction between the miRNA mimic and chitosan, PEG stabilizes the NPs, prevents interparticle aggregation and improves their biodistribution[72,73]. Our results showed that PEGylation enhanced the solubility of polymer, did not affect the miRNA loading and delivery, and improved the stability of NPs in the biological conditions. The physicochemical properties of the miR-chNPs also indicate that particles have good hydrodynamic size, efficient at encapsulating miRNA mimics and protect them from serum nuclease degradation. Another barrier for nucleotide delivery is ensuring endosomal escape of NPs and the release of the cargo into the cytosol. Effective reduction of target gene expression in macrophages upon treatment with miR-chNPs confirm that NPs can escape the endolysosomal system and deliver miRNA mimics into cytosol and load efficiently into the RISC complex. Together these data indicate that miR-cNPs can be used effectively to delivery miRNA therapeutics to alter macrophage target gene expression *in vitro* and *in vivo*.

The retention of cholesterol-rich lipoproteins in the intima of the artery wall is the precipitating event in atherosclerosis, resulting in endothelial activation, the recruitment and transformation of monocytes into foam cells and the ensuing inflammation. In contrast, the regression and stabilization of plaques requires the removal of free cholesterol and other lipids through efflux by the transporters ABCA1 and ABCG1[6–8]. A number of miRNAs are known to regulate RCT, the most notable among them being miR-33, which blocks cholesterol mobilization through targeting sterol transporters (ABCA1, ABCG1, NPC1 and OSBPL6)[20,46,47,74–76], autophagy genes (ATG5, TFEB)[77], and bile acid transporters (CYP7A1, ABCB11, ATP8B1)[78,79]. We therefore used miR-33 as a prototype miRNA to test whether chNPs could deliver miRNAs to macrophages to regulate atherogenic processes. To date, only systemic anti-miR strategies have been used to promote RCT and plaque regression[21], while miRNA mimic delivery to macrophages has not been tested. Our data suggests that chNPs can be used as a delivery modality for miRNA overexpression that can successfully alter target gene expression and function in macrophages. This could offer an opportunity for the replacement of anti-atherogenic miRNAs whose expression is lost during disease or when global miRNA homeostasis is disturbed, for example due to loss of Dicer activity, which can promote atherosclerosis[80]. Delivery of anti-atherogenic miRNAs, particularly efflux-promoting miR-223 and miR-206 in this case, can promote cholesterol removal from macrophage-derived foam cells to the liver or intestine for excretion, thus bearing the potential to reduce vascular lipid accumulation and atherosclerosis. However, caution must be taken in considering miR-223 or miR-206 as atheroprotective therapeutic strategy, due to the fact that their contribution to the pathogenesis of atherosclerosis *in vivo* and the underlying mechanism by which they exert their favorable effects on macrophage function have not been well studied.

Thus, there is still an urgent need for a better understanding of the role of promising miRNAs in the development of atherosclerosis and for the identification of anti-atherogenic miRNAs that can be loaded into our chNP platform and delivered to the atherosclerotic plaque.

NPs containing anti-inflammatory proteins, lipids and siRNAs have been used successfully to reduce atherosclerosis in mice[81–85]. Although we did not use a targeting peptide in this study, macrophage-specific miRNA delivery could be improved by using external peptides like fibronectin, hyaluronan or integrin, which have been used to promote lesional NP delivery[86–88]. As more miRNAs are found to exert protective effects on atherosclerosis, our chNP platform could offer an effective and non-toxic way to alter gene expression and function in macrophages.

3.7. Conclusion

In summary, we developed and tested a strategy to deliver miRNA mimics to macrophages to alter cholesterol homeostasis. Our findings demonstrate that miRNAs can be efficiently delivered to macrophages *via* NPs where they escape endolysosmal degradation and can function to regulate ABCA1 expression and cholesterol efflux. Because our NPs functioned *in vivo* to alter reverse cholesterol transport from macrophages, this suggests that these same NPs can be used to target miRNAs to atherosclerotic lesions to alter lesion progression (**Figure 3.8**). In addition, our platforms are based on biocompatible and biodegradable chitosan derivatives that are useful for clinical use. Thus, our approach can easily be applied to other miRNA-based therapeutics, particularly in the setting of cardiovascular and inflammatory diseases, where macrophages dominate and promote pathology and may enable RNAi-based therapies for these diseases.

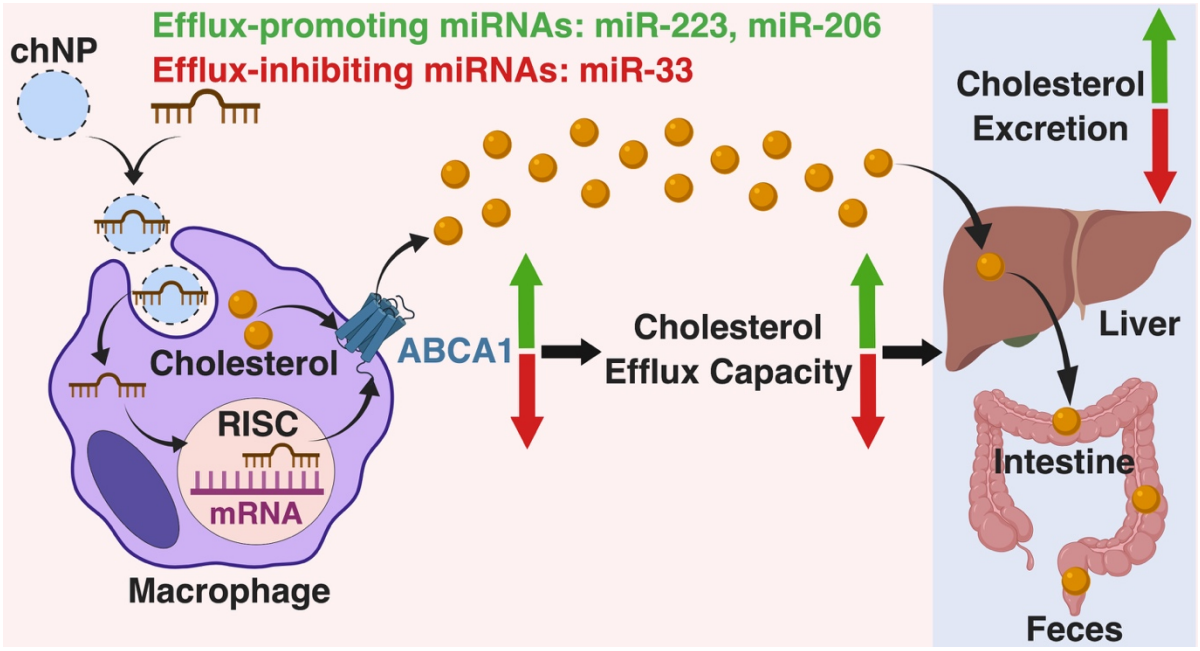

Figure 3.8. Schematic diagram illustrating the function of miR-chNPs in macrophages. miRNAs can be efficiently delivered to macrophages *via* chNPs where they can escape endolysosmal degradation and function to regulate ABCA1 expression as well as cholesterol efflux, altering cholesterol excretion from macrophages *in vivo*.

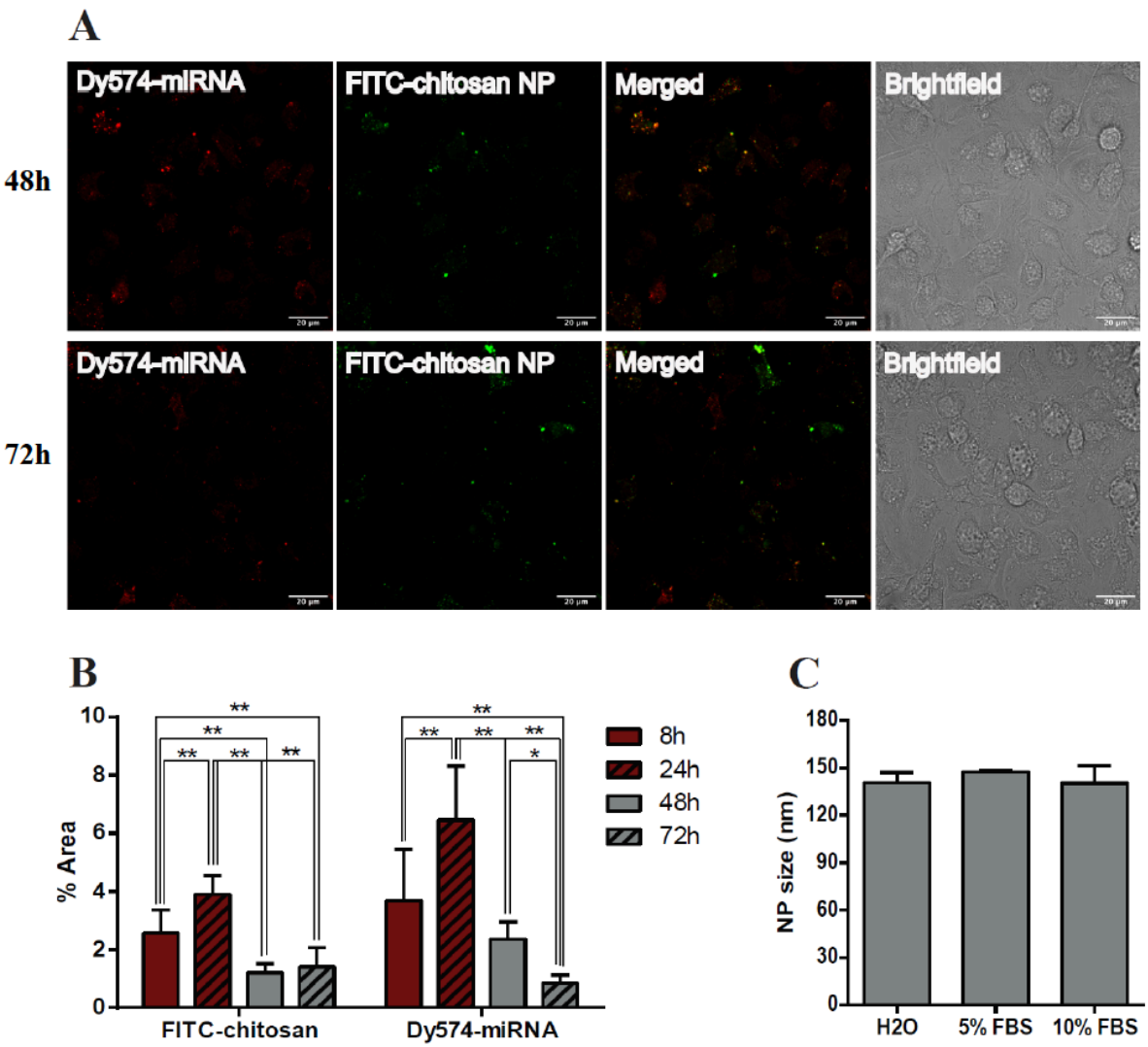

Supplemental Figure 3.1. chNPs containing miRNA mimics are taken up and deliver exogenous miRNAs to naïve macrophages. (**A**) FITC-labeled chNPs containing Dy547-labeled miRNA mimics were prepared and applied to peritoneal macrophages. Uptake of labeled NPs and miRNA mimics was visualized using confocal microscopy. Scale bars represent 20 µm. (**B**) The area of fluorescent signal from (A) was quantified using Image J software using 4 fields for each condition. Graph represents the mean ± SD from n=3 independent experiments. (**C**) ChNPs containing cel-miR-54 were incubated H2O, DMEM supplemented with 5% FBS, or DMEM supplemented with 10% FBS. The size of NPs was measured pre and 2h post incubation using Malvern Zetasizer.

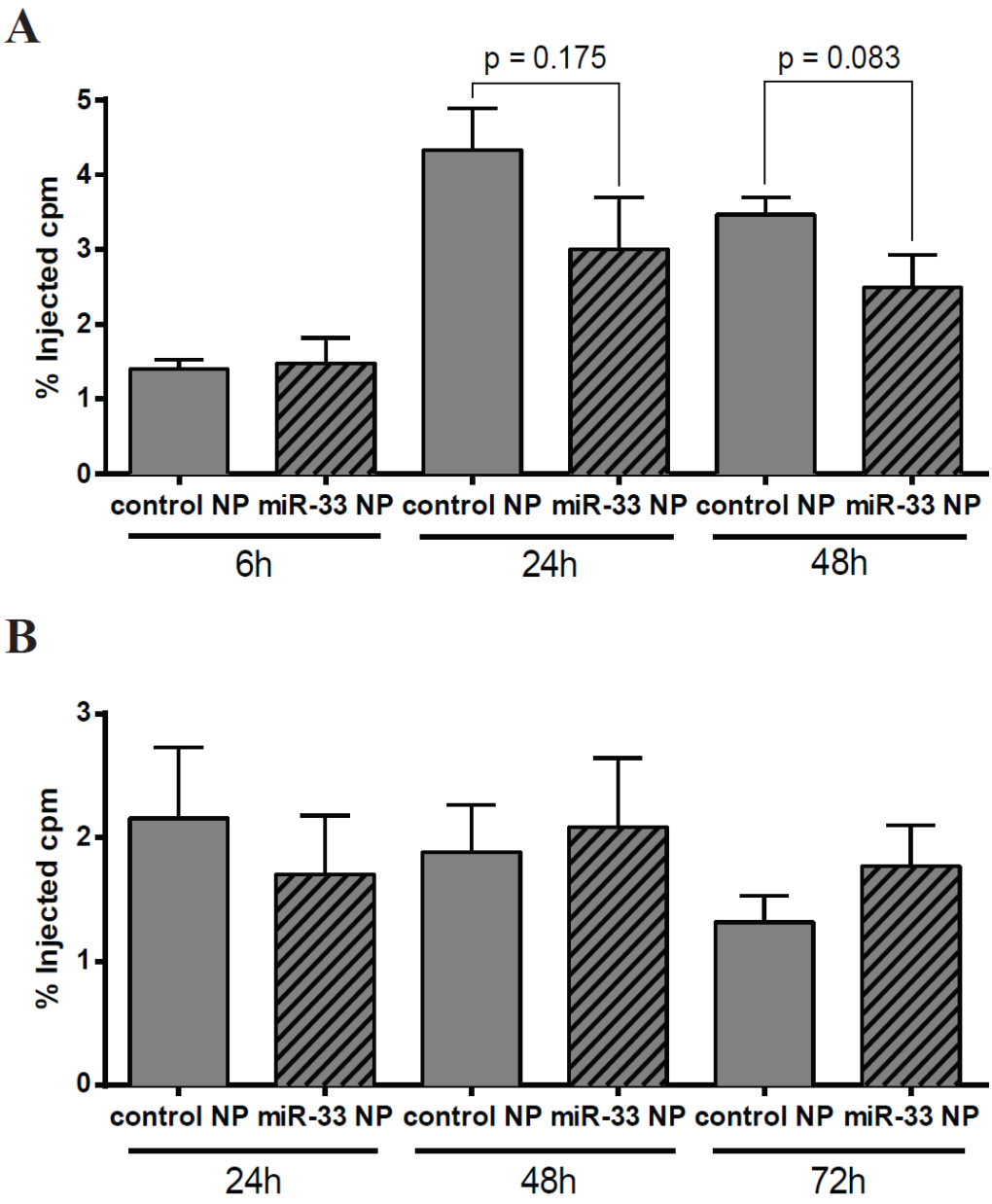

Supplemental Figure 3.2. Time course of 3H-cholesterol distribution in plasma. C57BL6 mice (n=5/group) were injected subcutaneously with (A) acetylated LDL-loaded/[3H]cholesterol-labeled peritoneal macrophages pre-treated with control/miR-33 NPs for 48h or (B) acetylated LDL-loaded/[3H]cholesterol-labeled peritoneal macrophages and chNPs containing control/miR-33 mimics. Data are expressed as the percentage of the 3H-cholesterol tracer relative to that of total cpm tracer injected ± SD.

3.8. Acknowledgements

The authors would like to thank Héloïse Ragelle for helpful discussions on this manuscript, and Dr. Mireille Ouimet for the graphical abstract.

3.9. References

1. Nabel, E. G. & Braunwald, E. A Tale of Coronary Artery Disease and Myocardial Infarction. *N. Engl. J. Med.* **366**, 54–63 (2012).
2. Golomb, B. A. & Evans, M. A. Statin adverse effects : a review of the literature and evidence for a mitochondrial mechanism. *Am. J. Cardiovasc. Drugs* **8**, 373–418 (2008).
3. Ecker, J. R. NEWS & VIEWS FORUM: Genomics Genome Feast. 6-9.
4. Chilton, R. J. Pathophysiology of coronary heart disease: a brief review. *J. Am. Osteopath. Assoc.* **104**, S5–S8 (2004).
5. Messier, C., Awad, N. & Gagnon, M. The relationships between atherosclerosis, heart disease, type 2 diabetes and dementia. *Neurol. Res.* **26**, 567–572 (2004).
6. Lusis, A. Atherosclerosis. *Nature* **407**, 233–241 (2000).
7. Moore, K. J. & Tabas, I. Macrophages in the pathogenesis of atherosclerosis. *Cell* **145**, 341–55 (2011).
8. Moore, K. J., Sheedy, F. J. & Fisher, E. a. Macrophages in atherosclerosis: a dynamic balance. *Nat. Rev. Immunol.* **13**, 709–21 (2013).
9. Tall, A. R., Yvan-Charvet, L., Terasaka, N., Pagler, T. & Wang, N. HDL, ABC Transporters, and Cholesterol Efflux: Implications for the Treatment of Atherosclerosis. *Cell Metab.* **7**, 365–375 (2008).
10. Yvan-Charvet, L., Wang, N. & Tall, A. R. Role of HDL, ABCA1, and ABCG1 transporters in cholesterol efflux and immune responses. *Arterioscler. Thromb. Vasc. Biol.* **30**, 139–143 (2010).
11. Cuchel, M. & Rader, D. J. Macrophage reverse cholesterol transport: Key to the regression of atherosclerosis? *Circulation* **113**, 2548–2555 (2006).
12. Van Eck, M. *et al.* Leukocyte ABCA1 controls susceptibility to atherosclerosis and macrophage recruitment into tissues. *Proc. Natl. Acad. Sci.* **99**, 6298–6303 (2002).
13. Wang, X. *et al.* Macrophage ABCA1 and ABCG1, but not SR-BI, promote macrophage reverse cholesterol transport in vivo. *J. Clin. Invest.* **117**, 2216–2224 (2007).
14. Brunham, L. R., Singaraja, R. R. & Hayden, M. R. Variations on a Gene: Rare and Common Variants in *ABCA1* and Their Impact on HDL Cholesterol Levels and Atherosclerosis. *Annu. Rev. Nutr.* **26**, 105–129 (2006).
15. Clee, S. M. *et al.* Common genetic variation in {ABCA1} is associated with altered lipoprotein levels and a modified risk for coronary artery disease. *Circulation* **103**, 1198–1205 (2001).
16. Westerterp, M. *et al.* Cholesterol Efflux Pathways Suppress Inflammasome Activation, NETosis, and Atherogenesis. *Circulation* **138**, 898–912 (2018).
17. Kim, V. N. MicroRNA biogenesis: coordinated cropping and dicing. *Nat. Rev. Mol. Cell Biol.* **6**, 376–385 (2005).

18. Filipowicz, W., Bhattacharyya, S. N. & Sonenberg, N. Mechanisms of post-transcriptional regulation by microRNAs: Are the answers in sight? *Nat. Rev. Genet.* **9**, 102–114 (2008).
19. Friedman, R. C., Farh, K. K. H., Burge, C. B. & Bartel, D. P. Most mammalian mRNAs are conserved targets of microRNAs. *Genome Res.* **19**, 92–105 (2009).
20. Rayner, K. J. *et al.* MiR-33 contributes to the regulation of cholesterol homeostasis. *Science* **328**, 1570–3 (2010).
21. Rayner, K. J. *et al.* Antagonism of miR-33 in mice promotes reverse cholesterol transport and regression of atherosclerosis. *J. Clin. Invest.* **121**, 2921–2931 (2011).
22. de Aguiar Vallim, T. Q. *et al.* MicroRNA-144 regulates hepatic ATP binding cassette transporter A1 and plasma high-density lipoprotein after activation of the nuclear receptor farnesoid X receptor. *Circ. Res.* **112**, 1602–12 (2013).
23. Ramírez, C. M. *et al.* Control of cholesterol metabolism and plasma high-density lipoprotein levels by microRNA-144. *Circ. Res.* **112**, 1592–601 (2013).
24. Goedeke, L. *et al.* MicroRNA-148a regulates LDL receptor and ABCA1 expression to control circulating lipoprotein levels. *Nat. Med.* **21**, 1280–1288 (2015).
25. Wagschal, A. *et al.* Genome-wide identification of microRNAs regulating cholesterol and triglyceride homeostasis. *Nat Med* **21**, 1290–1297 (2015).
26. Meiler, S., Baumer, Y., Toulmin, E., Seng, K. & Boisvert, W. A. MicroRNA 302a is a novel modulator of cholesterol homeostasis and atherosclerosis. *Arterioscler. Thromb. Vasc. Biol.* **35**, 323–331 (2015).
27. Condorelli, G., Latronico, M. V. G. & Cavarretta, E. microRNAs in cardiovascular diseases: current knowledge and the road ahead. *J. Am. Coll. Cardiol.* **63**, 2177–87 (2014).
28. Dahlman, J. E. *et al.* In vivo endothelial siRNA delivery using polymeric nanoparticles with low molecular weight. *Nat. Nanotechnol.* **9**, 648–655 (2014).
29. Yin, H. *et al.* Non-viral vectors for gene-based therapy. *Nat. Rev. Genet.* **15**, 541–55 (2014).
30. Khan, O. F. *et al.* Endothelial siRNA delivery in nonhuman primates using ionizable low–molecular weight polymeric nanoparticles. *Sci. Adv.* **4**, 1–11 (2018).
31. Guţoaia, A. *et al.* Fine-tuned PEGylation of chitosan to maintain optimal siRNA-nanoplex bioactivity. *Carbohydr. Polym.* **143**, 25–34 (2016).
32. Ragelle, H., Vanvarenberg, K., Vandermeulen, G. & Préat, V. Chitosan Nanoparticles for SiRNA Delivery In Vitro. *Methods Mol. Biol.* **1364**, 143–50 (2016).
33. Gadde, S. *et al.* Development of therapeutic polymeric nanoparticles for the resolution of inflammation. *Adv. Healthc. Mater.* **3**, 1448–1456 (2014).
34. Karunakaran, D. *et al.* Macrophage Mitochondrial Energy Status Regulates Cholesterol Efflux and Is Enhanced by Anti-miR33 in Atherosclerosis. *Circ. Res.* **117**, 266–278 (2015).
35. Nguyen, M. A. *et al.* Extracellular Vesicles Secreted by Atherogenic Macrophages Transfer MicroRNA to Inhibit Cell Migration. *Arterioscler. Thromb. Vasc. Biol.* **38**, 49–63 (2018).
36. Karunakaran, D. *et al.* Targeting macrophage necroptosis for therapeutic and diagnostic interventions in atherosclerosis. *Sci. Adv.* **2**, (2016).
37. Bhattarai, N., Ramay, H. R., Gunn, J., Matsen, F. A. & Zhang, M. PEG-grafted chitosan as an injectable thermosensitive hydrogel for sustained protein release. *J. Control.*

Release **103**, 609–624 (2005).
38. Chen, Y. *et al.* Evaluation of the PEG Density in the PEGylated Chitosan Nanoparticles as a Drug Carrier for Curcumin and Mitoxantrone. *Nanomaterials* **8**, 486 (2018).
39. Casettari, L. *et al.* Effect of PEGylation on the toxicity and permeability enhancement of chitosan. *Biomacromolecules* **11**, 2854–2865 (2010).
40. Malhotra, M., Lane, C., Tomaro-Duchesneau, C., Saha, S. & Prakash, S. A novel method for synthesizing PEGylated chitosan nanoparticles: strategy, preparation, and in vitro analysis. *Int. J. Nanomedicine* **6**, 485–494 (2011).
41. Zhang, Y., Satterlee, A. & Huang, L. In vivo gene delivery by nonviral vectors: Overcoming hurdles. *Mol. Ther.* **20**, 1298–1304 (2012).
42. Raja, M. A. G., Katas, H. & Wen, T. J. Stability, intracellular delivery, and release of siRNA from chitosan nanoparticles using different cross-linkers. *PLoS One* **10**, 1–19 (2015).
43. Vercauteren, D. *et al.* On the cellular processing of non-viral nanomedicines for nucleic acid delivery: Mechanisms and methods. *J. Control. Release* **161**, 566–581 (2012).
44. Zaki, N. M. & Tirelli, N. Gateways for the intracellular access of nanocarriers: a review of receptor-mediated endocytosis mechanisms and of strategies in receptor targeting. *Expert Opin. Drug Deliv.* **7**, 895–913 (2010).
45. Mindell, J. A. Lysosomal Acidification Mechanisms. *Annu. Rev. Physiol.* **74**, 69–86 (2012).
46. Gerin, I. *et al.* Expression of miR-33 from an SREBP2 intron inhibits cholesterol export and fatty acid oxidation. *J. Biol. Chem.* **285**, 33652–33661 (2010).
47. Najafi-Shoushtari, S. H. *et al.* MicroRNA-33 and the SREBP Host Genes Cooperate to Control Cholesterol Homeostasis. *Science* **328**, 1566–1569 (2010).
48. Young, M. P., Febbraio, M. & Silverstein, R. L. CD36 modulates migration of mouse and human macrophages in response to oxidized LDL and may contribute to macrophage trapping in the arterial intima. *J. Clin. Invest.* **119**, 136–145 (2009).
49. Zhang, Y. *et al.* Hepatic expression of scavenger receptor class B type I (SR-BI) is a positive regulator of macrophage reverse cholesterol transport in vivo. *J. Clin. Invest.* **115**, 2870–2874 (2005).
50. Feig, J. E. Regression of atherosclerosis: Insights from animal and clinical studies. *Ann. Glob. Heal.* **80**, 13–23 (2014).
51. Vickers, K. C. *et al.* MicroRNA-223 coordinates cholesterol homeostasis. *Proc. Natl. Acad. Sci.* **111**, 14518–14523 (2014).
52. Vinod, M. *et al.* miR-206 controls LXRα expression and promotes LXR-mediated cholesterol efflux in macrophages. *Biochim. Biophys. Acta* **1841**, 827–35 (2014).
53. Langmann, T. *et al.* Identification of sterol-independent regulatory elements in the human ATP-binding cassette transporter A1 promoter. Role of Sp1/3, E-box binding factors, and an oncostatin M-responsive element. *J. Biol. Chem.* **277**, 14443–14450 (2002).
54. Thymiakou, E., Zannis, V. I. & Kardassis, D. Physical and functional interactions between liver X receptor/retinoid X receptor and Sp1 modulate the transcriptional induction of the human ATP binding cassette transporter A1 gene by oxysterols and retinoids. *Biochemistry* **46**, 11473–11483 (2007).
55. Michael, D. R., Ashlin, T. G., Buckley, M. L. & Ramji, D. P. Liver X receptors, atherosclerosis and inflammation. *Curr. Atheroscler. Rep.* **14**, 284–293 (2012).

56. Crooke, S. T., Witztum, J. L., Bennett, C. F. & Baker, B. F. RNA-Targeted Therapeutics. *Cell Metab.* **27**, 714–739 (2018).
57. Vickers, T. A. & Crooke, S. T. Antisense oligonucleotides capable of promoting specific target mRNA reduction via competing RNase H1-dependent and independent mechanisms. *PLoS One* **9**, (2014).
58. Chery, J. RNA therapeutics: RNAi and antisense mechanisms and clinical applications. *Postdoc J.* **4**, 35–50 (2016).
59. Chi, X., Gatti, P. & Papoian, T. Safety of antisense oligonucleotide and siRNA-based therapeutics. *Drug Discov. Today* **22**, 823–833 (2017).
60. Rupaimoole, R. & Slack, F. J. MicroRNA therapeutics: Towards a new era for the management of cancer and other diseases. *Nat. Rev. Drug Discov.* **16**, 203–221 (2017).
61. Baek, D. *et al.* The impact of microRNAs on protein output. *Nature* **455**, 64–71 (2008).
62. He, L. & Hannon, G. J. MicroRNAs: small RNAs with a big role in gene regulation. *Nat. Rev. Genet.* **5**, 522–531 (2004).
63. van Rooij, E. & Olson, E. N. MicroRNA therapeutics for cardiovascular disease: opportunities and obstacles. *Nat. Rev. Drug Discov.* **11**, 860–72 (2012).
64. Liu, C. *et al.* The microRNA miR-34a inhibits prostate cancer stem cells and metastasis by directly repressing CD44. *Nat. Med.* **17**, 211 (2011).
65. Bader, A. G. MiR-34 - a microRNA replacement therapy is headed to the clinic. *Front. Genet.* **3**, 1–9 (2012).
66. Beg, M. S. *et al.* Phase I study of MRX34, a liposomal miR-34a mimic, administered twice weekly in patients with advanced solid tumors. *Invest. New Drugs* **35**, 180–188 (2017).
67. Garcia-Fuentes, M. & Alonso, M. J. Chitosan-based drug nanocarriers: Where do we stand? *J. Control. Release* **161**, 496–504 (2012).
68. Mao, S., Sun, W. & Kissel, T. Chitosan-based formulations for delivery of DNA and siRNA. *Adv. Drug Deliv. Rev.* **62**, 12–27 (2010).
69. Ragelle, H. *et al.* Chitosan nanoparticles for siRNA delivery: Optimizing formulation to increase stability and efficiency. *J. Control. Release* **176**, 54–63 (2014).
70. Corbet, C. *et al.* Delivery of siRNA targeting tumor metabolism using non-covalent PEGylated chitosan nanoparticles: Identification of an optimal combination of ligand structure, linker and grafting method. *J. Control. Release* **223**, 53–63 (2016).
71. Malhotra, M., Tomaro-Duchesneau, C., Saha, S., Kahouli, I. & Prakash, S. Development and characterization of chitosan-PEG-TAT nanoparticles for the intracellular delivery of siRNA. *Int. J. Nanomedicine* **8**, 2041–2052 (2013).
72. Alameh, M. *et al.* SiRNA Delivery with Chitosan: Influence of Chitosan Molecular Weight, Degree of Deacetylation, and Amine to Phosphate Ratio on in Vitro Silencing Efficiency, Hemocompatibility, Biodistribution, and in Vivo Efficacy. *Biomacromolecules* **19**, 112–131 (2018).
73. Bachir, Z. A. *et al.* Effects of PEG surface density and chain length on the pharmacokinetics and biodistribution of methotrexate-loaded chitosan nanoparticles. *Int. J. Nanomedicine* **13**, 5657–5671 (2018).
74. Horie, T. *et al.* MicroRNA-33 encoded by an intron of sterol regulatory element-binding protein 2 (Srebp2) regulates HDL in vivo. *Proc. Natl. Acad. Sci. U. S. A.* **107**, 17321–6 (2010).
75. Marquart, T. J., Allen, R. M., Ory, D. S. & Baldan, A. miR-33 links SREBP-2 induction

to repression of sterol transporters. *Proc. Natl. Acad. Sci.* **107**, 12228–12232 (2010).
76. Ouimet, M. *et al.* MiRNA targeting of oxysterol-binding protein-like 6 regulates cholesterol trafficking and efflux. *Arterioscler. Thromb. Vasc. Biol.* **36**, 942–951 (2016).
77. Ouimet, M. *et al.* Mycobacterium tuberculosis induces the MIR-33 locus to reprogram autophagy and host lipid metabolism. *Nat. Immunol.* **17**, 677–686 (2016).
78. Allen, R. M. *et al.* miR-33 controls the expression of biliary transporters, and mediates statin- and diet-induced hepatotoxicity. *EMBO Mol. Med.* **4**, 882–895 (2012).
79. Li, T., Francl, J. M., Boehme, S. & Chiang, J. Y. L. Regulation of cholesterol and bile acid homeostasis by the cholesterol 7α-hydroxylase/steroid response element-binding protein 2/microRNA-33a axis in mice. *Hepatology* **58**, 1111–1121 (2013).
80. Wei, Y. *et al.* Dicer in Macrophages Prevents Atherosclerosis by Promoting Mitochondrial Oxidative Metabolism. *Circulation* **138**, 2007–2020 (2018).
81. Yu, M. *et al.* Targeted Nanotherapeutics Encapsulating Liver X Receptor Agonist GW3965 Enhance Antiatherogenic Effects without Adverse Effects on Hepatic Lipid Metabolism in Ldlr−/−Mice. *Adv. Healthc. Mater.* **6**, 1–14 (2017).
82. Kamaly, N. *et al.* Targeted Interleukin-10 Nanotherapeutics Developed with a Microfluidic Chip Enhance Resolution of Inflammation in Advanced Atherosclerosis. *ACS Nano* **10**, 5280–5292 (2016).
83. Fredman, G. *et al.* Targeted nanoparticles containing the proresolving peptide Ac2-26 protect against advanced atherosclerosis in hypercholesterolemic mice. *Sci. Transl. Med.* **7**, (2015).
84. Pan, H. *et al.* Anti-JNK2 peptide-siRNA nanostructures improve plaque endothelium and reduce thrombotic risk in atherosclerotic mice. *Int. J. Nanomedicine* **13**, 5187–5205 (2018).
85. Majmudar, M. D. *et al.* Monocyte-directed RNAi targeting CCR2 improves infarct healing in atherosclerosis-prone mice. *Circulation* **127**, 2038–2046 (2013).
86. Yu, M. *et al.* Nanoparticles targeting extra domain B of fibronectin-specific to the atherosclerotic lesion types III, IV, and V-enhance plaque detection and cargo delivery. *Theranostics* **8**, 6008–6024 (2018).
87. Kheirolomoom, A. *et al.* Multifunctional Nanoparticles Facilitate Molecular Targeting and miRNA Delivery to Inhibit Atherosclerosis in ApoE$^{-/-}$ Mice. *ACS Nano* **9**, 8885–8897 (2015).
88. Beldman, T. J. *et al.* Hyaluronan Nanoparticles Selectively Target Plaque-Associated Macrophages and Improve Plaque Stability in Atherosclerosis. *ACS Nano* **11**, 5785–5799 (2017).

4. miR-223 Deficiency Accelerates Atherosclerosis *via* Regulating Cholesterol Efflux and Inflammatory Responses

Authors: My-Anh Nguyen, Huy-Dung Hoang, Adil Rasheed, Anne-Claire Duchez, Hailey Wyatt, Tommy Alain, Katey J. Rayner

Manuscript in Preparation and to be Submitted in October 2019.

4.1. Author contributions

The experiments were planned by Katey J. Rayner and me. As the first author, I conducted the majority of the experiments required for this study. Huy-Dung Hoang and Tommy Alain performed the ribosome profiling analysis. Adil Rasheed and Anne-Claire Duchez helped me perform the animal studies. Hailey Wyatt helped me perform the *in vitro* RNA analyses. I wrote the first draft of the manuscript and together, Katey J. Rayner and I edited the manuscript until the final version is acceptable.

4.2. Abstract

The prevention and treatment of CVD has largely focused on lowering circulating cholesterol, yet a significant burden of atherosclerotic disease still remains even in the setting of low plasma cholesterol. Recently, miRNAs have emerged as exciting therapeutic targets for CVD. miR-223 has been identified as a critical regulator of cholesterol metabolism and inflammation *via* targeting different components in cholesterol biosynthesis pathway (3-hydroxy-3-methylglutaryl-CoA synthase 1, HMGCS1 and methylsterol monooxygenase 1, SC4MOL) and NF-κB signalling pathway (IKKα). However, its

contribution to the pathogenesis of atherosclerosis *in vivo* and the mechanism underlying its effects has not been thoroughly characterized.

Objective: We aimed to define the role of miR-223 during the progression of atherogenesis and in macrophages in response to inflammatory and atherogenic stimuli.

Methods and Results: Irradiated *Ldlr*$^{-/-}$ mice were reconstituted with wild-type or miR-223$^{-/-}$ BM, and subsequently fed a Western diet for 12 weeks. Deficiency of miR-223 in BM-derived cells resulted in an increase in plaque size as well as lipid content and serum inflammatory cytokines (IL-1β, IL-2, IL-12(p70), IL-17A, GM-CSF). Mice receiving miR-223$^{-/-}$ BM also exhibited elevated levels of circulating pro-atherogenic cells (total monocytes and neutrophils) compared to control mice. Furthermore, the expression of miR-223 target gene (*Sp3*) and pro-inflammatory marker (*Il-6*) were enhanced whereas the expression of *Abca1* and anti-inflammatory marker (*Retnla*) were reduced in aortic arches from mice lacking miR-223 in BM-derived cells. Consistent with pro-atherogenic effects *in vivo,* loss of miR-223 in macrophages *in vitro* decreased ABCA1 gene and protein expression as well as cholesterol efflux to apoA1 and enhanced the pro-inflammatory responses. In contrast, overexpression of miR-223 promoted the ability of macrophages to effectively efflux intracellular cholesterol and macrophage polarization toward the anti-inflammatory M2 phenotype. These beneficial effects of miR-223 are dependent on the inhibition of its target gene, the transcription factor *Sp3*.

Conclusions: Our study demonstrates that miR-223 can protect against atherosclerosis by acting as a crucial modulator of macrophage cholesterol efflux and inflammation. To further understand the molecular mechanisms underlying the potential effects of miR-223 on the development of atherosclerosis *in vivo*, we are now characterizing global translation profile

of macrophages isolated from mice receiving wild-type or miR-223$^{-/-}$ BM using ribosome profiling.

4.3. Introduction

Atherosclerosis is a chronic inflammatory disease that is driven by the interplay of excess cholesterol accumulation in the vessel wall and a maladaptive immune response. It is characterized by retention of cholesterol-rich LPs in susceptible areas of the arterial vasculature, followed by chronic endothelial activation and recruitment of circulating monocytes into the vascular intima[1–3]. In the subendothelial space, the majority of recruited monocytes differentiate into macrophages, a process driven by M-CSF and other factors[4]. Monocyte-derived macrophages then scavenge retained modified LPs, which eventually transform them to cholesterol-laden foam cells. However, excessive cholesterol uptake, leading to excessive free cholesterol accumulation in macrophage-derived foam cells, triggers the activation of downstream cascades including NLRP3 inflammasome, TLR and NFκB signaling pathways, resulting in the secretion of pro-inflammatory mediators (cytokines, chemokines, and reactive oxygen and nitrogen species). These inflammatory signals exacerbate not only oxidative stress in the plaques but also the transmigration of additional inflammatory cells including monocytes into the intima, which further aggravate plaque inflammation[5–8]. Furthermore, free cholesterol accumulation impairs ER function and activates ER stress responses, which if prolonged and combined with other insults, leads to apoptotic cell death and the formation of a pro-thrombotic necrotic core formation[9]. Despite significant achievements in the diagnosis, prevention and treatment, atherosclerosis remains the leading cause of morbidity and mortality worldwide[10]. Traditionally, lipid lowering has

been the gold-standard therapy for atherosclerosis, yet a significant burden of atherosclerotic disease still remains even in the setting of low plasma cholesterol, likely as a result of residual inflammatory risk[11,12]. Thus, there is an urgent need to better understand the molecular mechanisms that govern atherogenesis particularly those that drive inflammation.

Over the past decade, miRNAs have emerged as key modulators and fine-tuners of multiple signaling pathways involved in atherosclerosis[13,14]. miRNAs are defined as highly conserved small RNA sequences of 20 to 23 nucleotides that contain complementary sequences for specific target mRNAs. *Via* binding to the 3' UTR, miRNAs post-transcriptionally regulate gene expression by degradation and/or translational inhibition of their bound targets. Notably, one miRNA can repress multiple target genes simultaneously through seed-based targeting and one functional gene network can be regulated by a group of miRNAs, providing a mechanism to coordinate complex programs of gene expression and thereby modulate many aspects of cellular homeostasis and physiology[15–17]. Indeed, accumulating evidence have highlighted the importance of miRNAs in regulating lipoprotein homeostasis, vascular inflammation, leukocyte recruitment/activation, and vascular smooth muscle function[18,19], thus controlling each stage of atherosclerosis from development, progression to disruption. One of the most well-characterized miRNAs in cardiovascular diseases is miR-223. miR-223 is the first miRNA to be experimentally validated to control cholesterol levels through directly repressing the expression of cholesterol biosynthesis enzymes including HMGCS1 and SC4MOL, thus inhibiting cholesterol biosynthesis. Furthermore, miR-223 can inhibit cholesterol uptake by targeting SR-BI in hepatocytes and coronary arterial endothelial cells[20]. In addition to cholesterol metabolism, a number of studies have confirmed that miR-223 plays an important role in controlling NFκB signaling

pathway. miR-223 has been shown to suppress TLR4-NFκB pathway, leading to a reduction lipid accumulation and pro-inflammatory cytokine production in LPS activated macrophages[21]. Not only in the canonical pathway, miR-223 has also been considered as a chief component in the noncanonical NFκB pathway. During monocyte-macrophage differentiation, a significant reduction of miR-223 expression, which was accompanied by a significant increase in IKKα protein that was a target of miR-223, induces a shift from the canonical to the noncanonical NFκB pathway. This aims to prevent macrophage from becoming overactivated while priming them for future NFκB signaling events[22]. Finally, genome-wide miRNA screens have identified miR-223 as a negative regulator of NLRP3 inflammasome activation by directly suppressing NLRP3 expression and reducing NLRP3-dependent induction of IL-1β in primary neutrophils[23,24]. Although the roles of miR-223 in cholesterol metabolism and inflammation has been clearly established, its contribution to the pathogenesis of atherosclerosis *in vivo* has not been evaluated.

Here, we investigated whether miR-223 deficiency in myeloid cells can alter atherosclerosis progression in mice deficient for the LDLR (*Ldlr*$^{-/-}$ mice). We find that deletion of miR-223 in BM-derived cells resulted in an increase in plaque size as well as lipid content, plasma inflammatory cytokines, and circulating pro-atherogenic cells. Furthermore, the expression of pro-inflammatory markers was enhanced whereas the expression of anti-inflammatory markers was reduced in aortic arches from mice lacking miR-223 in BM-derived cells. Consistent with pro-atherogenic effects *in vivo*, loss of miR-223 *in vitro* promoted the pro-inflammatory responses and dampened macrophage cholesterol efflux. These effects of miR-223 appear to be dependent on the inhibition of its target gene, the transcription factor *Sp3*. Thus, our study demonstrates that miR-223 can

protect against atherosclerosis by acting as a crucial modulator of macrophage cholesterol efflux and inflammation.

4.4. Materials and methods

4.4.1. Reagents

Acetylated human LDL (BT-906) and human apoA1 (BT-927) were purchased from Alfa Aesar (Thermo Fisher Scientific Inc.). Control mimic and miR-223 mimic (miRIDIAN microRNA mimic) were obtained from Dharmacon (Horizon Discovery Group). Lipofectamine RNAiMAX (DNase and protease-free) was purchased from Thermo Fisher Scientific Inc. Lipopolysaccharides (LPS) was obtained from Sigma-Aldrich. Recombinant mouse IFN-γ and IL-4 were purchased from R&D Systems. All of the antibodies and stains used in flow cytometry experiments were obtained from BD Biosciences.

4.4.2. Mice

C57BL6 wild-type mice were purchased from Charles River Laboratories. miR-223$^{-/-}$ mice (on a C57BL6 background) were kindly provided by Dr. Guo-Chang Fan, University of Cincinnati College of Medicine, United States. *Ldlr*$^{-/-}$ mice were first purchased from Jackson Laboratories and were bred in-house. All animal studies were permitted by the University of Ottawa Animal Care and Use Committee in accordance with the international standards established by the Canadian Council on Animal Care.

4.4.3. Macrophage isolation and polarization

BMDMs were harvested from femurs of wild-type mice or miR-223$^{-/-}$ mice and differentiated into macrophages using DMEM supplemented with 10% (v/v) FBS, 20% (v/v) L929 conditioned media and 1% (v/v) P-S for 7 days. To polarize macrophages to M1 or

M2, cells were treated with either 100 ng/ml LPS and 100 ng/ml IFN-γ or 10 ng/ml IL-4, respectively, for 24h.

4.4.4. Cell transfection with miRNA mimics

Macrophages were transfected with control mimic or miR-223 mimic (miRIDIAN microRNA mimic) at a concentration of 100nM using Lipofectamine RNAiMAX as previously described[25–27]. Briefly, transfection of macrophages was performed in OPTIMEM media overnight. The next day, same volume of DMEM containing 20% (v/v) FBS was added and transfected cells were harvested 72 hours after transfection. Similarly, macrophages were transfected with 25nM negative (non-silencing) control siRNA or *Sp3* siRNA (FlexiTube siRNA – QIAGEN) for 72 hours.

4.4.5. Cholesterol efflux

BMDMs were transfected with control mimic or miR-223 mimic for 48 hours and subsequently, were loaded with 37.5 μg/ml acetylated LDL and labeled with 1 μCi/ml [^{3}H] cholesterol (Perkin Elmer) for 24 hours. The next day, cells were washed extensively with PBS and equilibrated in 2% fatty acid-free BSA in DMEM media for 3 hours before being treated with 25 μg/ml apoA1 (Alfa Aesar) for 6 hours or 24 hours. Medium and cellular [^{3}H] were counted using liquid scintillation counting and expressed as a percentage of total cellular [^{3}H] cholesterol content.

4.4.6. miRNA and gene expression analysis

For miRNA expression analysis, total RNA was isolated using Trizol (Invitrogen) and the expression levels of miRNAs of interest was measured by qRT-PCR using miScript II Reverse Transcription kit, miScript Primer Assays and Quantitect SYBR Green (Qiagen), in which the expression of candidate miRNAs was normalized to RNA, U6 small nuclear 6,

pseudogene (QIAGEN). For gene expression analysis, total RNA was isolated using Trizol and reverse transcribed using iScript Reverse Transcription Supermix for qRT-PCR (Bio-Rad). qRT-PCR was performed using the SsoAdvanced Universal SYBR Green Supermix (Bio-Rad) and gene expression was normalized to *Hprt* and *18S*. The primers used are: *Abca1* (Forward: GCTTGTTGGCCTCAGTTAAGG; Reverse: GTAGCTCAGGCGTACAGAGAT), *Sp3* (Forward: AATCAAACCTTACTCGCCTCTG; Reverse: GCACATTAGCGACTACTTGAGTT), *Tnfα* (Forward: CCCTCACACTCAGATCATCT; Reverse: GCTACGACGTGGGCTACAG), *Nos2* (Forward: CGTTCTCAGCCCAACAATACAAGA; Reverse: GTGGACGGGTCGATGTCAC), *Il-1b* (Forward: GCAACTGTTCCTGAACTCAACT; Reverse: ATCTTTTGGGGTCCGTCAACT), *Il-6* (Forward: TAGTCCTTCCTACCCCAATTTCC; Reverse: TTGGTCCTTAGCCACTCCTTC), *Il-10* (Forward: GCTCTTACTGACTGGCATGAG; Reverse: CGCAGCTCTAGGAGCATGTG), *Arginase 1 (Arg1)* (Forward: GGTCCACCCTGACCTATGTGT; Reverse: ACGATGTCTTTGGCAGATATGC), *Retnla* (Forward: CTGGGTTCTCCACCTCTTCA; Reverse: TGCTGGGATGACTGCTACTG), *Pknox1* (Forward: GGTGGTCACGGAGTTAAAAACA; Reverse: TCGGCATCCATTGGGGTCT), *Rasa1* (Forward: TGTGGTGATTACTACATTGGTGG; Reverse: CGCCTTCTATCTTCTACTGGCTC), *Nfat5* (Forward: GTGACTATCCTTCCTAATGCCCT; Reverse: GGTCTCTGGGTTGTATGCCT)

4.4.7. Western blot analysis

Cells were washed in ice-cold PBS and lysed in ice-cold RIPA buffer supplemented with protease inhibitor cocktail (Roche). Proteins (50μg) were subjected to 4-20% SDS-

PAGE and transferred to PVDF membranes (Bio-Rad) for immunoblot analysis[26]. PVDF membranes were blocked with 5% (w/v) milk in TBST and incubated overnight with antibodies against ABCA1 (Novus Biologicals) and HSP90 (Santa Cruz Biotechnology). Goat anti-mouse or anti-rabbit IRDye® secondary antibodies were used for detection on a LI-COR Odyssey infrared imaging system (LI-COR Biosciences).

4.4.8. Atherosclerosis PCR pathway array analysis

The purity and integrity of RNA isolated from BMDMs isolated from wild-type mice or miR-223$^{-/-}$ was confirmed using the Agilent Bioanalyzer (Agilent Technologies) as per manufacturer's instructions. A total of 1 μg was reverse transcribed with the RT^2 First Strand kit (Qiagen) and used for the mouse atherosclerosis RT^2 Profiler PCR Array kit (Qiagen) as per manufacturer's instructions. Using the manufacturer's PCR Array Data Analysis software: https://www.qiagen.com/us/shop/genes-and-pathways/data-analysis-center-overview-page/, average data was normalized and used to determine the ΔΔCT. A full table of genes found on this PCR array can be found in Supplemental Table I as well as at https://b2b.qiagen.com/~/media/genetable/pa/mm/03/pamm-038za

4.4.9. Atherosclerosis studies

For BM transplantation study, 14-week-old recipient *Ldlr*$^{-/-}$ mice were subjected to whole-body irradiation (10 Gys) followed by injection of BM donor cells (1 x 10^6 cells) by retro-orbital injection, followed by recovery for 6 weeks. Mice were then fed an adjusted calories western diet (21% fat, 0.2% cholesterol; Harlan Teklad) for 12 weeks.

Enzymatic cholesterol assays: Plasma was collected from the saphenous vein or by cardiac puncture, and total cholesterol was assayed using the Cholesterol-E kit (Wako).

Flow cytometry: Peripheral blood was collected from the saphenous vein or by cardiac puncture to EDTA-coated microvettes (Sarstedt). For lysing red blood cells, 50ul of whole blood was mixed with 50ul of deionized water and incubated with 1ml of 1x PharmLyse (BD Biosciences) for 10 minutes of room temperature. The lysed cells were resuspended in 100ul of Brilliant Staining Buffer (BD Biosciences). To prevent non-specific antibody binding, the cells were incubated with Fc Block (1ug; BD Biosciences) for 5 minutes are room temperature. The cells were stained with the following antibodies at 4°C for 20 minutes: B220 BV786 (0.1875ug/test), Ly6C BV605 (0.75ug/test), CD8a BV510 (0.1875ug/test), CD11b BV421 (0.21875ug/test), CD4 PerCP-Cy5.5 (0.06ug/test), Ly6G PE-Cy7 (0.25ug/test), CD41 PE (0.09375ug/test), CD45 APC-Cy7 (0.045ug/test), and CD3e APC (1ug/test). Staining for dead cells was performed with Fixable Viability Stain 700 (1ul/test) at 4°C for 30 minutes. Cells were fixed using Cytofix (BD Biosciences) for 15 minutes at 4°C. The cells were resuspended in buffer and sample acquisition was performed on a FACS (fluorescence-activated cell sorting) Aria IIIu flow cytometer (BD Biosciences). The data was analysed using FlowJo (Tree Star). Neutrophils were identified as $CD11b^+$ $Ly6C^+$ $Ly6G^+$, monocytes as $CD11b^+$ $Ly6C^+$, B cells as $B220^+$, T cells as $CD3e^+$, T helper cells as $CD3e^+$ $CD4^+$ $CD8^-$, cytotoxic T cells as $CD3e^+$ $CD4^-$ $CD8^+$, and platelets as $CD41^+$.

Immunohistochemical analysis: Mice were perfused with saline, and aortic root, ascending as well as descending aorta, liver, and spleen were collected as previously described[27,28]. Briefly, the aortic sinus was embedded in optimum cutting temperature (OCT) compound medium, frozen, sectioned (10μm) and stained for hematoxylin & eosin for quantifications, where a minimum of 8-10 sections per animal were measured across the length of the entire

aortic root. For detection of neutral lipid, oil red O staining was performed as previously described[28].

Cytokine assays: Serum cytokines were analyzed using Bio-Plex Pro Mouse Cytokine 23-plex Assay (#M60009RDPD; Bio-Rad) as per manufacturer's instructions.

4.4.10. Gene expression analysis in mouse aorta

The aortic arch was excised from the heart, and tissue segments were homogenized in Trizol (Invitrogen) using microbeads along with the Bullet Blender. Total RNA was reverse transcribed using iScript Reverse Transcription Supermix for qRT-PCR (Bio-Rad). For droplet digital RT-PCR (ddRT-PCR), cDNA was mixed with QX200 ddPCR EvaGreen Supermix (Bio-Rad) according to the manufacturer's protocol and droplets were prepared using QX200 droplet generation oil on a QX200 Droplet Generator (Bio-Rad). Droplets were subjected to PCR using a C1000 thermocycler (Bio-Rad) using the cycling conditions: 95°C for 5 min, followed by 45 cycles of 95°C for 30 s at a ramp rate of 2°C/s and 60°C for 1 min at a ramp rate of 2°C/s. Positive/negative droplets were counted by a QX200 Droplet Reader (Bio-Rad), and gene expression was normalized to *B2m* and *Actb.*

4.4.11. Ribosome profiling

Ribosome profiling was performed as previously described on 2 biological replicates[29,30]. Briefly, polysomes in BMDM lysates were stabilized with cycloheximide and BMDM lysates were split into two parallel workflows. RNA-Seq on total RNA from one half of the lysate (see below) while RNase I footprinting was performed on the remaining half to capture RPFs. For RNA-Seq, 150 µg of total RNA was taken for RNA-Seq analysis and Poly-(A)+ mRNA was purified using magnetic oligo-dT DynaBeads (Thermo Fisher Scientific Inc.) according to the manufacturer's instructions. Purified RNA was eluted and

mixed with an equal volume of 2X alkaline fragmentation solution (2 mM EDTA, 10 mM Na_2CO_3, 90 mM $NaHCO_3$) and incubated for 20 min at 95ºC. Fragmentation reactions were mixed with stop/precipitation solution (300 mM NaOAc pH 5.5 and GlycoBlue), followed by isopropanol precipitation by standard methods. Fragmented mRNA samples were size-selected on a denaturing 10% urea-polyacrylamide gel. The area corresponding to 35-50 nucleotides was excised, eluted and precipitated with isopropanol. Isolated RPF RNA (corresponding to 28-32 nt fragments) and total RNA fragments were used to create cDNA libraries as previously described (*56*). Ribosomal RNA (rRNA) contamination was reduced by subtractive hybridization using biotinylated oligos that were reverse complements of abundant rRNAs. The mRNA and ribosome-footprint libraries were then amplified by PCR (10 cycles) using indexed primers and sequenced on the Illumina HiSeq 4000 platform with read length of 50 nucleotides at Fasteris SA, Switzerland.

4.4.12. Statistics

Data shown is either mean ± SD of at least 3 independent experiments or a single representative experiment that was performed in triplicate. Comparison between 2 groups was made using Student's t-test ($p \leq 0.05$) and comparison between groups was performed by one-way ANOVA ($p \leq 0.05$) using Prism GraphPad, as indicated in the Figure legends.

4.5. Results

4.5.1. Deletion of miR-223 in BM-derived cells promotes atherogenesis and enhances inflammatory signaling

To elucidate the role of miR-223 in BM-derived cells, we lethally irradiated *Ldlr*$^{-/-}$ mice and reconstituted them with wild-type or miR-223$^{-/-}$ BM (**Figure 4.1A**). BM-

transplanted mice were then fed a Western-type high cholesterol diet (HCD) for 12 weeks. Reconstitution of the hematopoietic compartment after transplantation of wild-type or miR-223$^{-/-}$ BM cells appeared to be normal as circulating levels of leukocytes and lymphocytes were similar between the two groups at 6 weeks after BM transplantation, prior to start of the HCD (**Supplemental Figure 4.1A**). Examination of aortic root lesions demonstrated male mice lacking miR-223 in BM-derived cells had a 51.3% increase in plaque size relative to control mice (n=6/group, P=0.0729), whereas plaque burden in the aortic root of female mice receiving miR-223$^{-/-}$ BM seemed to be unchanged (**Figure 4.1B**). Further, quantification of lipid accumulation in aortic sinus lesions by oil red O staining demonstrated a corresponding 20% increase in lipid plaque in mice receiving miR-223$^{-/-}$ BM compared with that of controls (**Figure 4.1C**). There was no significant in total plasma cholesterol and body weight before HCD administration, at early stages (*i.e.* 6-week HCD), or after 12 weeks of HCD (**Supplemental Figure 4.1B-C**).

The increase in lesion area as well as lipid accumulation in the aortic sinus was accompanied by signs of systemic inflammation. Using multiplex immunoassay, we detected higher levels of circulating pro-inflammatory cytokines IL-1β, IL-2, IL-9, IL-12(p70), IL-17A, and GM-CSF in mice receiving miR-223$^{-/-}$ BM after 12 weeks of HCD (**Figure 4.1D**), while other cytokines such as IL-1α, IL-4, Eotaxin, G-CSF, and MIP-1a remained unchanged (data not shown). Mice lacking miR-223 in BM-derived cells also had increased levels of circulating leukocytes including neutrophils, total monocytes, and Ly6C^{low} monocytes after 12 weeks of HCD (**Figure 4.1E**) whereas there were no differences in circulating levels of other leukocytes and lymphocytes (**Supplemental Figure 4.1D**).

Assessing circulating levels of leukocytes and lymphocytes at earlier stages (*i.e.* 6-week HCD) showed similar results (**Supplemental Figure 4.1E**).

To further evaluate the inflammatory profile of mice lacking hematopoietic miR-223, we analyzed gene expression in the aorta of mice receiving wild-type or miR-223$^{-/-}$ BM after 12 weeks of HCD. Interestingly, qRT-PCR analysis demonstrated that the expression of the transcription factor *Sp3,* a known miR-223 target gene[20], and pro-inflammatory marker (*Il-6*) were up-regulated whereas the expression of the cholesterol transporter *Abca1* and anti-inflammatory marker (*Retnla*) were down-regulated in aortic arches from mice lacking miR-223 in BM-derived cells (**Figure 4.1F**). On the other hand, other target genes of miR-223 including *Pknox1*[31], *Rasa1* and *Nfat5*[32] did not show significant changes or showed a reduction in mice receiving miR-223$^{-/-}$ BM (**Supplemental Figure 4.1F**).

To further characterize the pathways impacted by miR-223, we used a pathway-focused PCR array containing 84 genes related to atherosclerosis. We compared the expression of genes involved in the stress response, apoptosis, cell adhesion molecules, lipid transportation and metabolism, as well as cell growth and proliferation in Mo, M1 and M2 macrophages from wild-type and miR-223$^{-/-}$ mice. Results showed that lack of miR-223 significantly increased the expression of *Cd44*, *Fga*, *Mmp1a*, *Sod1* and *Tnfaip3*, and decreased the expression of *Bid*, *Csf2*, *Cxcl1*, *Eln*, *Hbegf*, *Icam1*, *Lif*, *Lpl*, *Plin2*, *Serpinb2*, *Tgfb2* and *Tnc* in all macrophage subtypes (**Supplemental Figure 4.2 and Table 4.1**). We

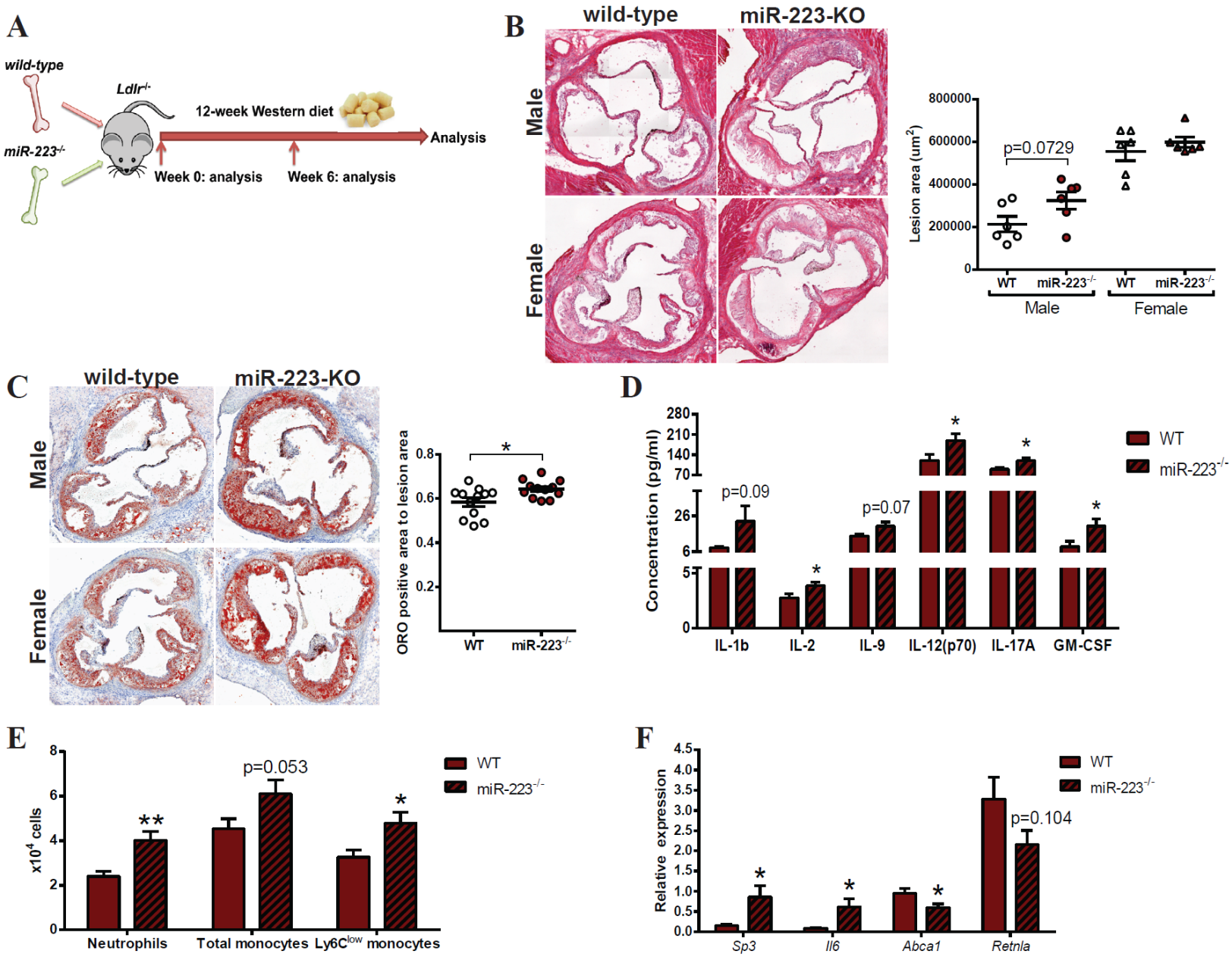
A
wild-type
miR-223-/-
Ldlr-/-
12-week Western diet
Analysis
Week 0: analysis
Week 6: analysis
B
wild-type
miR-223-KO
Male
Female
Lesion area (um2)
800000
600000
400000
200000
0
p=0.0729
WT
miR-223-/-
WT
miR-223-/-
Male
Female
C
wild-type
miR-223-KO
Male
Female
ORO positive area to lesion area
0.8
0.6
0.4
0.2
*
WT
miR-223-/-
D
Concentration (pg/ml)
280
210
140
70
26
6
5
0
p=0.09
p=0.07
*
IL-1b
IL-2
IL-9
IL-12(p70)
IL-17A
GM-CSF
WT
miR-223-/-
E
x10^4 cells
8
6
4
2
0
**
p=0.053
*
Neutrophils
Total monocytes
Ly6Clow monocytes
WT
miR-223-/-
F
Relative expression
4.5
4.0
3.5
3.0
2.5
2.0
1.5
1.0
0.5
0.0
*
*
*
p=0.104
Sp3
Il6
Abca1
Retnla
WT
miR-223-/-

Figure 4.1. Deletion of miR-223 in BM cells promotes atherogenesis and enhances inflammatory signaling. (**A**) *Ldlr*$^{-/-}$ mice (n=6 male and 6 female/group) were lethally irradiated and given BM transplantation from wild-type or miR-223$^{-/-}$ donors, followed by HCD for 12 weeks. miR-223 deficiency in BM cells increases atherosclerotic plaque (**B**) size and (**C**) lipid content. Aortic sinus lesion areas across the entire aortic root from H&E stained sections were quantified using ImageJ whereas lipid accumulation in aortic sinus lesions were measured by oil red O staining. Images show representative sections from *Ldlr*$^{-/-}$ mice with wild-type BM (left) and miR-223$^{-/-}$ BM (right). Data are the mean ± SEM, *p<0.05. (**D**) Circulating cytokine levels in mice receiving wild-type BM or miR-223$^{-/-}$ BM (n=9-12 mice per group) were determined by the Bio-Plex Pro Mouse Cytokine 23-plex assay at the end of the 12-week study. Data are the mean ± SEM. * p<0.05. (**E**) Circulating levels of leukocytes after 12 weeks of HCD were analyzed by FACS. Data are the mean levels from 9-12 mice per group ± SEM. *p<0.05; **p<0.01, compared with of mice receiving wild-type BM. (**F**) Gene expression in aortic arches from *Ldlr*$^{-/-}$ mice receiving wild-type BM or miR-223$^{-/-}$ BM. The aortic arch was homogenized using microbeads along with the Bullet Blender. Total RNA was isolated and the expression levels of *Sp3*, *Il6*, *Abca1*, and *Retnla* were measured by ddRT-PCR. Graphs represent means ± SEM from n=9-12 mice per group. *p<0.05, compared with of mice receiving wild-type BM.

Table 4.1. Most significantly different genes (up- or down-regulated) in miR-223-deficient macrophages. Atherosclerosis RT^2 Profiler PCR array was performed using RNA isolated from BMDMs of wild-type mice or miR-223$^{-/-}$ mice and normalized to housekeeping genes using the ΔΔCt method.

UP-Regulated (miR-223$^{-/-}$ vs. wild-type)	**DOWN-Regulated (miR-223$^{-/-}$ vs. wild-type)**
Cd44, Fga, Mmp1a, Sod1, Tnfaip3	*Bid, Csf2, Cxcl1, Eln, Hbegf, Icam1, Lif, Lpl, Plin2, Serpinb2, Tgfb2, Tnc*

then examined the presence of a miR-223 binding site in the 3'UTR of altered genes from the array using miRSystem[33], but none were identified. This suggests that miR-223 controls the expression of multiple pro-inflammatory genes indirectly and not *via* direct repression of the 3'UTR.

4.5.2. miR-223 positively regulates ABCA1 expression and promotes macrophage cholesterol efflux *in vitro*

ABCA1 plays a key role in stimulating the efflux of cholesterol from macrophages, thereby reducing foam cell formation and the development of atherosclerosis[34–36] miR-223 has been found to indirectly induce ABCA1 expression and cholesterol efflux in hepatocytes *via* targeting of SP3, which acts as a repressor of Abca1 expression[20,37,38]. We observed that deficiency of miR-223 in BM-derived cells resulted in an increase in *Sp3* expression, a decrease in *Abca1* expression, along with an increase in plaque lipid content *in vivo* (**Figure 4.1C and 1F**), suggesting that miR-223 regulates cholesterol efflux in a similar manner in macrophages. To test this, we first examined the expression of ABCA1 and SP3 in BMDMs transfected with miR-223 or isolated from miR-223$^{-/-}$ mice. As expected, over-expression of miR-223 suppressed and loss of miR-223 elevated *Sp3* expression (**Figure 4.2A**). In contrast, the expression of ABCA1 decreased or increased when miR-223 were knocked down or over-expressed, respectively (**Figure 4.2B**). We next investigated the effects of this miR-223 on macrophage cholesterol efflux and indicated that macrophages transfected with miR-223 exhibited enhanced cholesterol efflux to apoA1 relative to control (21.6 ± 2.5% for control mimic *versus* 35.2 ± 1.0% for miR-223; $P \leq 0.01$) (**Figure 4.2C**).

Atherosclerotic lesions have a highly heterogenous phenotype as indicated by the simultaneous co-existence of various macrophage subpopulations[39]. To determine whether

or not macrophage polarization to pro-inflammatory M1 or alternative M2 states can override the effect of miR-223 on cholesterol efflux, we also performed cholesterol efflux assays on various macrophage subtypes transfected with miR-223 or isolated from miR-223$^{-/-}$ mice. We confirmed that miR-223 over-expression increased apoA1-mediated cholesterol efflux from different macrophage subtypes including resting Mo macrophages, pro-inflammatory M1 macrophages and anti-inflammatory M2 macrophages. Conversely, Mo macrophages and M2 macrophages, but not M1 macrophages, from miR-223$^{-/-}$ mice showed decreased cholesterol efflux to apoA1 (**Figure 4.2D**). Supporting for the reduced cholesterol efflux capacity of different macrophage subtypes isolated from miR-223$^{-/-}$ mice was a reduction in *Abca1* expression at the mRNA level (**Supplemental Figure 4.3**). Taken together, these data confirm that miR-223 can indirectly enhance macrophage ABCA1 expression and cholesterol efflux through SP3.

4.5.3. miR-223 suppresses macrophage pro-inflammatory activation and promotes macrophage polarization toward the anti-inflammatory phenotype *in vitro*

Considering that miR-223 plays an important role in regulating NFκB signaling pathway[21,22] and mice lacking miR-233 in BM-derived cells showed signs of pro-inflammatory responses *in vivo*, we sought to determine if miR-223 may also instruct macrophage inflammatory polarization. Here, we treated BMDMs isolated from miR-223$^{-/-}$ mice with either LPS + IFN-γ (to induce M1) or IL-4 (to induce M2). qRT-PCR analysis showed that pro-inflammatory cytokines *Tnfα*, *Il-1b*, *Il-6,* and *Nos2* were significantly increased in miR-223$^{-/-}$ macrophages compared with wild-type cells. In contrast, overexpression of miR-223 in BMDMs repressed the expression of these M1 macrophage

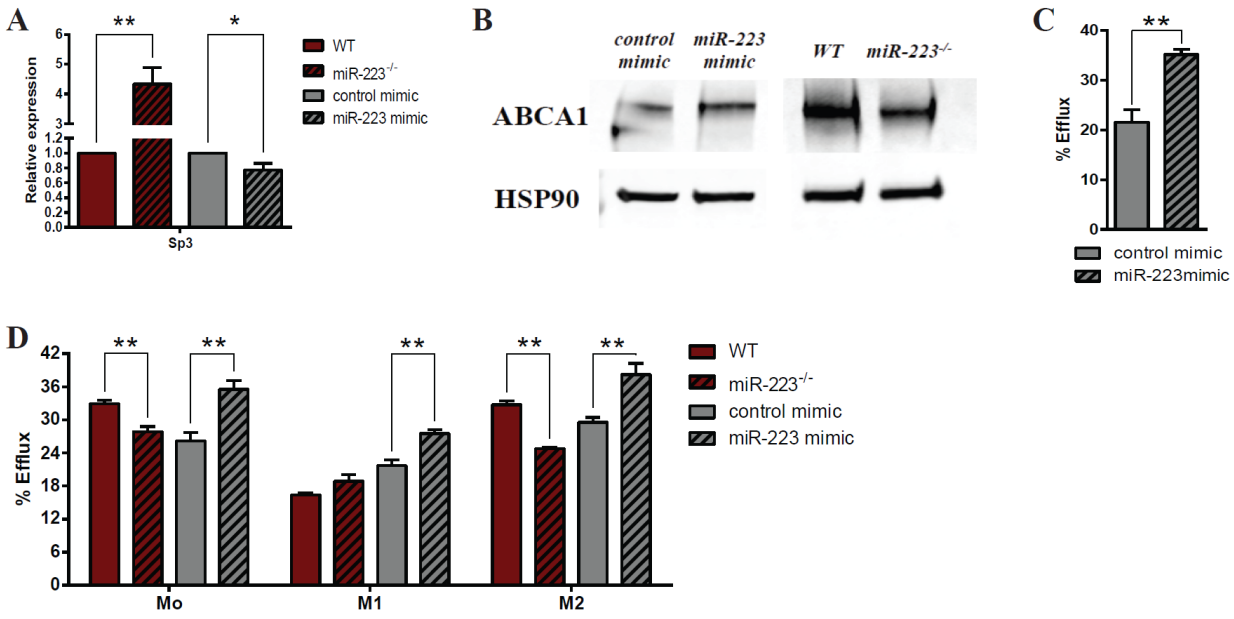

Figure 4.2. miR-223 positively regulates ABCA1 expression and promotes macrophage cholesterol efflux. BMDMs were transfected with control mimic/miR-223 mimic at a concentration of 100nM using Lipofectamine RNAiMAX or isolated from wild-type/miR-223$^{-/-}$ mice. The expression of (**A**) *Sp3* and (**B**) ABCA1 was examined. (**C**) Cholesterol efflux to apoA1 (25 ***μ***g/ml) was measured for 24h. (**D**) BMDMs were cholesterol-loaded and polarized into M1 macrophages or M2 macrophages by induction with LPS (100 ng/ml)/IFN-***γ*** (100 ng/ml) or IL-4 (10 ng/ml), respectively, for 24h. Cholesterol efflux to apoA1 (25 ***μ***g/ml) was measured for 24h. Graphs represent the means ± SD from n=3 independent experiments, *p<0.05, **p<0.01). Western blot is representative of a single experiment done in triplicate (n=3).

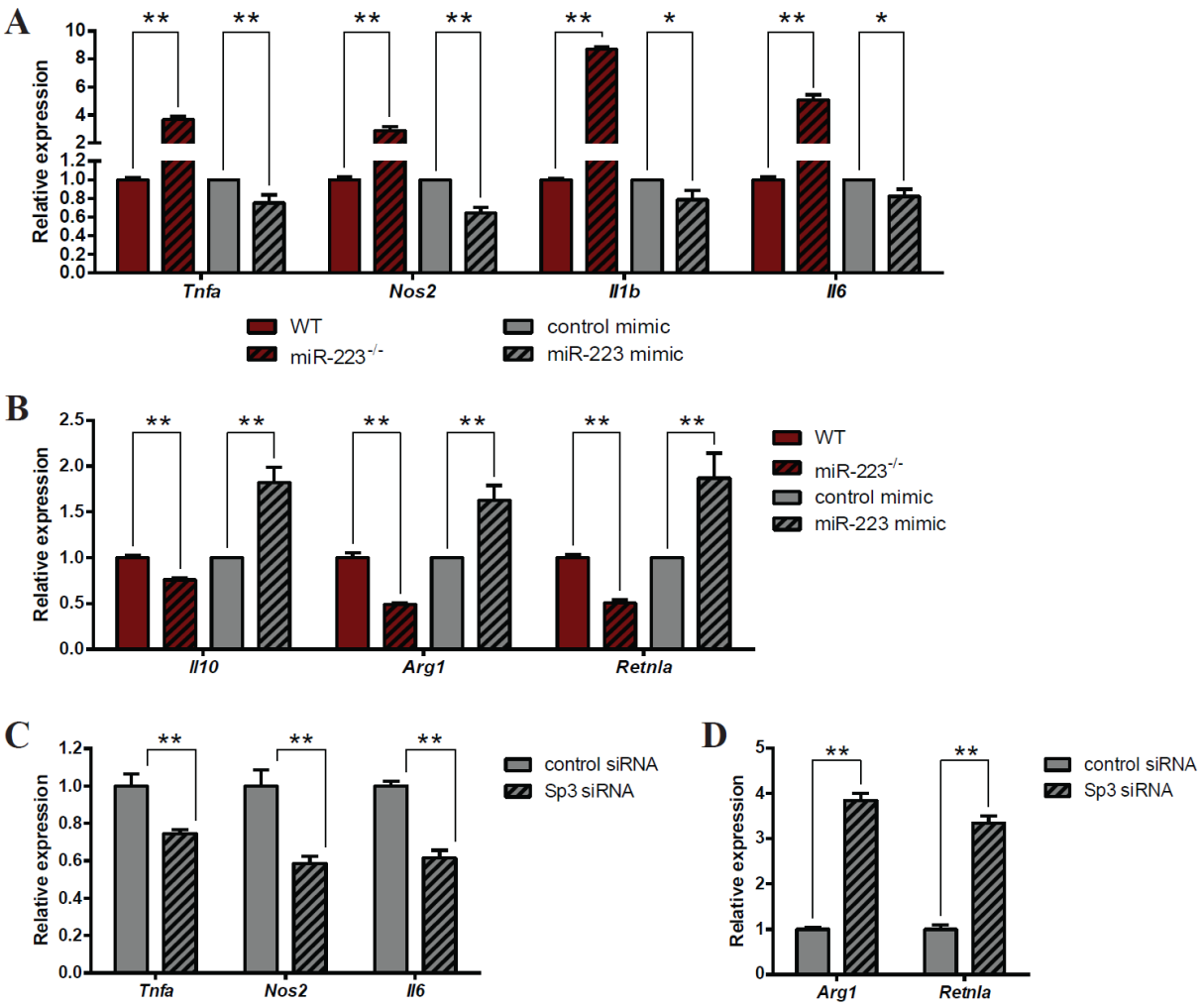

Figure 4.3. miR-223 suppresses macrophage pro-inflammatory activation and promotes macrophage polarization toward the anti-inflammatory phenotype. BMDMs transfected with control mimic/miR-223 mimic at a concentration of 100nM using Lipofectamine RNAiMAX or isolated from wild-type/miR-223$^{-/-}$ mice were polarized into either M1 macrophages by induction with LPS (100 ng/ml)/IFN-***γ*** (100 ng/ml) or M2 macrophages by induction with IL-4 (10 ng/ml) for 24h. Total RNA was isolated and the expression levels of (**A**) M1 markers (*Tnfa*, *Nos2*, *Il-1b*, *Il-6*) and (**B**) M2 markers (*Il-10*, *Arg1*, *Retnla*) were measured by qPCR. Graphs represent the means ± SD from n=3 independent experiments, *p<0.05, **p<0.01. (**C-D**) Inhibition of SP3 decreases the expression of M1 markers whereas increases the expression of M2 markers. BMDMs transfected with control siRNA or *Sp3* siRNA at a concentration of 25nM using Lipofectamine RNAiMAX. Total RNA was isolated and the expression levels of (**C**) M1 markers (*Tnfa*, *Nos2*, *Il-6*) and (**D**) M2 markers (*Arg1*, *Retnla*) were measured by qPCR. Graphs represent the means ± SD from n=3 independent experiments (**p<0.01).

markers (**Figure 4.3A**). Expression of M2-associated genes *Il-10*, *Arg1*, and *Retnla*, on the other hand, was decreased in miR-223-KO macrophages and elevated in macrophages transfected with miR-223 mimic, as compared to control cells (**Figure 4.3B**). Thus, miR-223 can suppress macrophage pro-inflammatory activation while promotes macrophage polarization toward the anti-inflammatory M2 phenotype *in vitro*.

We next sought to understand the mechanisms underlying the effects of miR-223 on macrophage activation. A recent study identified *Sp3*, the potent miR-223 target gene[20], as a critical regulator that can drive the production of inflammatory cytokines including TNFα in cancer cells through stimulating NFκB-mediated transcription activation[40]. Therefore, we postulated that SP3 might mediate the effects exerted by miR-223 on macrophage polarization. To address this, we measured the expression of M1 and M2 markers in macrophages where SP3 was knocked down by short interfering RNA (siRNA). Inhibition of SP3 resulted in a phenotype similar to that of miR-223 overexpression, with decreased expression levels of M1-associated genes such as *Nos2* and *Tnfα* (**Figure 4.3C**) and increased expression levels of M2-associated genes such as *Arg1* and *Retnla* (**Figure 4.3D**), suggesting that SP3 may mediate the effects of miR-223 on macrophage activation.

4.6. Discussion

Since their discovery in *C. elegans*, miRNAs have now shown to play important roles in modulating atherogenesis, with many miRNAs dysregulated in different disease states and alterations in miRNA expression associated with atherosclerosis progression[18,19]. Previous studies demonstrated that miR-223 is key to the regulation of the inflammatory response[21–24]. In addition, miR-223 serves as a critical regulatory hub controlling hepatic cholesterol

metabolism[20]. Nonetheless, the contribution of miR-223, particularly macrophage miR-223, to the development of atherosclerosis have not been well studied. In this study, we demonstrated that deficiency of miR-223 in BM-derived cells can accelerate the development of atherosclerosis lesions *in vivo* by increasing vascular lipid accumulation and exaggerating inflammatory response to HCD. *In vitro*, miR-223 indeed promotes macrophage cholesterol efflux and macrophage polarization toward the anti-inflammatory M2 phenotype; in contrast, loss of miR-223 attenuates cholesterol efflux and enhanced the pro-inflammatory responses. These beneficial effects of miR-223 appears to be dependent on the inhibition of its target gene, the transcription factor *Sp3*.

During atherogenesis, cholesterol accumulation in macrophage-derived foam cells results in inflammation activation, apoptosis cell death, and other adverse effects[5]. The efficacy of macrophages to efflux and remove intracellular cholesterol is crucial to attenuate lipid accumulation and atherosclerosis formation[35]. Thus, targeting ABCA1 and macrophage cholesterol efflux has been the major focus for the prevention and treatment of atherosclerosis. Multiple miRNAs such as miR-33[25,28], miR-144[41,42], miR-148a[43,44], and miR-302a[45] have been found to regulate cholesterol efflux. However, most of them supress ABCA1 expression and inhibit macrophage cholesterol efflux, thereby accelerating atherosclerosis progression. miR-223 is one of a few miRNAs whose overexpression can increase ABCA1 expression, promote cholesterol efflux and be anti-atherogenic. In hepatocytes, miR-223 was shown to positively regulate ABCA1 expression and cholesterol efflux[20]. Consistent with this study, we show that miR-223 can enhance the ability of macrophages to efflux intracellular cholesterol *via* up-regulating ABCA1. More importantly, miR-223 can promote macrophage ABCA1 and cholesterol efflux independently of the

activation state. *In vivo*, mice lacking miR-223 in BM-derived cells exhibited increased lipid accumulation in the aortic sinus and decreased *Abca1* gene expression in the aorta arch, further confirming the role of miR-223 in regulating macrophage cholesterol efflux. Interestingly, a recent work from our lab indicates that miR-223 delivered *via* nanoparticles can promote cholesterol removal from macrophage-derived foam cells to the liver or intestine for excretion[46], again highlighting the potential of this miRNA in reducing vascular lipid inflammation and atherosclerosis.

Our study also shows that deficiency of miR-223 in BM-derived cells exacerbate atherosclerosis progression in male mice, but not female mice, with a 51.3% increase in lesion size relative to control mice. Our data in male mice aligns with studies showing macrophage-specific deletion of ABCA1 resulted in an increase in atherosclerosis[47–49]. The reasons accountable for the difference between male and female mice lacking miR-223 in BM cells are not clear. Of note, the gene encoding for miR-223 is located within the q12 locus of the X chromosome[50], and this X-linked miRNA is less expressed in BM cells and BMDMs isolated from female mice (data not shown). In addition, sex hormones are known to affect endothelial and macrophage function during atherogenesis[51–53]. For example, due to a decline in circulating estrogen that have atheroprotective activity, the risk of atherosclerosis-related diseases increases in postmenopausal women and may even surpass that of men[54,55]. Further studies are needed to dissect the mechanism for these sex-specific differences in miR-223 in atherosclerosis.

Macrophages are central players in the development of atherosclerosis. Not only scavenger cells, macrophages also function as immune mediator cells and as sources of chemotactic molecules, cytokines, and chemokines. In response to specific environment

signals and molecules, macrophages exhibit remarkable plasticity that allows them to modulate their phenotype, fulfilling distinct functions in the regulation of the inflammatory response[56,57]. The phenotypic range of macrophages *in vivo* is complex, with several classes of macrophages have been described based on their markers, functions and secreted products. However, for purposes of simplicity, macrophages are mainly classified into two groups including classically activated M1 macrophages and alternatively activated M2 macrophages. Typically activated by TLR ligands such as LPS and IFN-γ, M1 macrophages produce high levels of pro-inflammatory cytokines (*i.e.* TNFα, IL-6, IL-1β, IL-12); whereas M2 macrophages is stimulated by IL-4 or IL-13, and secrete anti-inflammatory cytokines (*i.e.* IL-10 and TGF-β) as well as mediators of tissue repair (*i.e.* collagen)[6,39,58]. Even though both M1 and M2 macrophages are present in human and mouse atherosclerotic plaques, they localized to distinct areas[59]. Furthermore, studies of macrophage polarization *in vitro* and in mouse models of atherosclerosis have indicated that increasing macrophage activation toward the M1 phenotype or inhibiting macrophage activation toward M2 can promote plaque inflammation and potentiate atherosclerosis[60–65]. In contrast, driving plaque macrophages to M2-like cells by the administration of IL-13 can attenuate atherosclerosis progression[66]. Therefore, targeting macrophage polarization would be beneficial for the prevention of atherosclerosis. Our study shows that miR-223 can instruct macrophage polarization. Loss of miR-223 promotes macrophage activation toward the pro-inflammatory phenotype (M1) and suppress macrophage anti-inflammatory activation (M2) *in vitro* and *in vivo*, which is supported by an increase and a decrease in the expression of the M1 marker *Il-6* and the M2 marker *Retnla*, respectively. Our findings are consistent with the observation that ablation of miR-223 expression in mice fed a high-fat diet exacerbated obesity-

associated adipose tissue inflammation by enhancing classic proinflammatory responses[67]. It was shown that miR-223 regulates macrophage polarization *via* directly targeting *Pknox1*, *Rasa1*, and *Nfat5*[31,32]. However, we observed no difference the expression of *Pknox1*, *Rasa1*, and *Nfat5* in aortic arches from mice lacking miR-223 in BM-derived cells, suggesting that these genes may not mediate the effects of miR-223 on macrophage activation in our atherosclerosis model. On the other hand, the expression of *Sp3*, the other direct target of miR-223[20], was increased in aortic arches from mice receiving miR-223$^{-/-}$ BM. SP3 was shown to drive the production of inflammatory cytokines including TNFα in cancer cells by promoting NFκB-mediated transcription activation[40]. In addition, knockdown of SP3 using RNA interference resulted in a phenotype similar to that of miR-223 overexpression, with decreased expression levels of M1-associated genes and increased expression levels of M2-associated genes, suggesting that the effects of miR-223 on macrophage polarization may be dependent on the inhibition of SP3 in our model.

In addition to the increased expression of the M1 marker *Il-6* in the aorta arch, our study indicates higher levels of cytokines such as IL-1β[68,69], IL-2[70], IL-9[71,72], IL-12(p70)[73,74], IL-17A[75,76], and GM-CSF[77], which are known to exert pro-inflammatory and pro-atherogenic effects, and enhanced levels of circulating leukocytes (*i.e.* neutrophils, total monocytes) in the serum of mice receiving miR-223$^{-/-}$ BM, further confirming the pro-inflammatory profile of these mice. Several studies have shown that increased lipid raft formation and membrane cholesterol accumulation in ABCA1-deficient macrophages can account for the enhanced inflammatory responses in response to LPS or other TLR ligands[78–82]. Moreover, cholesterol accumulation in myeloid cells with genetic deficiency of ABCA1/G1 can activate the NLRP3 inflammasome[83], thereby indicating a role of ABCA1 in

modulating macrophage inflammatory response. Here, we cannot entirely determine whether miR-223 deficiency promotes the pro-inflammatory responses *in vitro* and *in vivo via* enhancing the expression of its target gene *Sp3* or *via* supressing the expression of *Abca1* or *via* both.

In conclusion, our study provides evidence that miR-223 can reduce susceptibility to atherosclerosis by acting as a crucial modulator of macrophage cholesterol efflux and inflammation. Systemic delivery or macrophage-specific delivery of miR-223 using viral-based vectors, nanoparticles, or extracellular vesicles could be a promising therapeutic strategy for atherosclerosis.

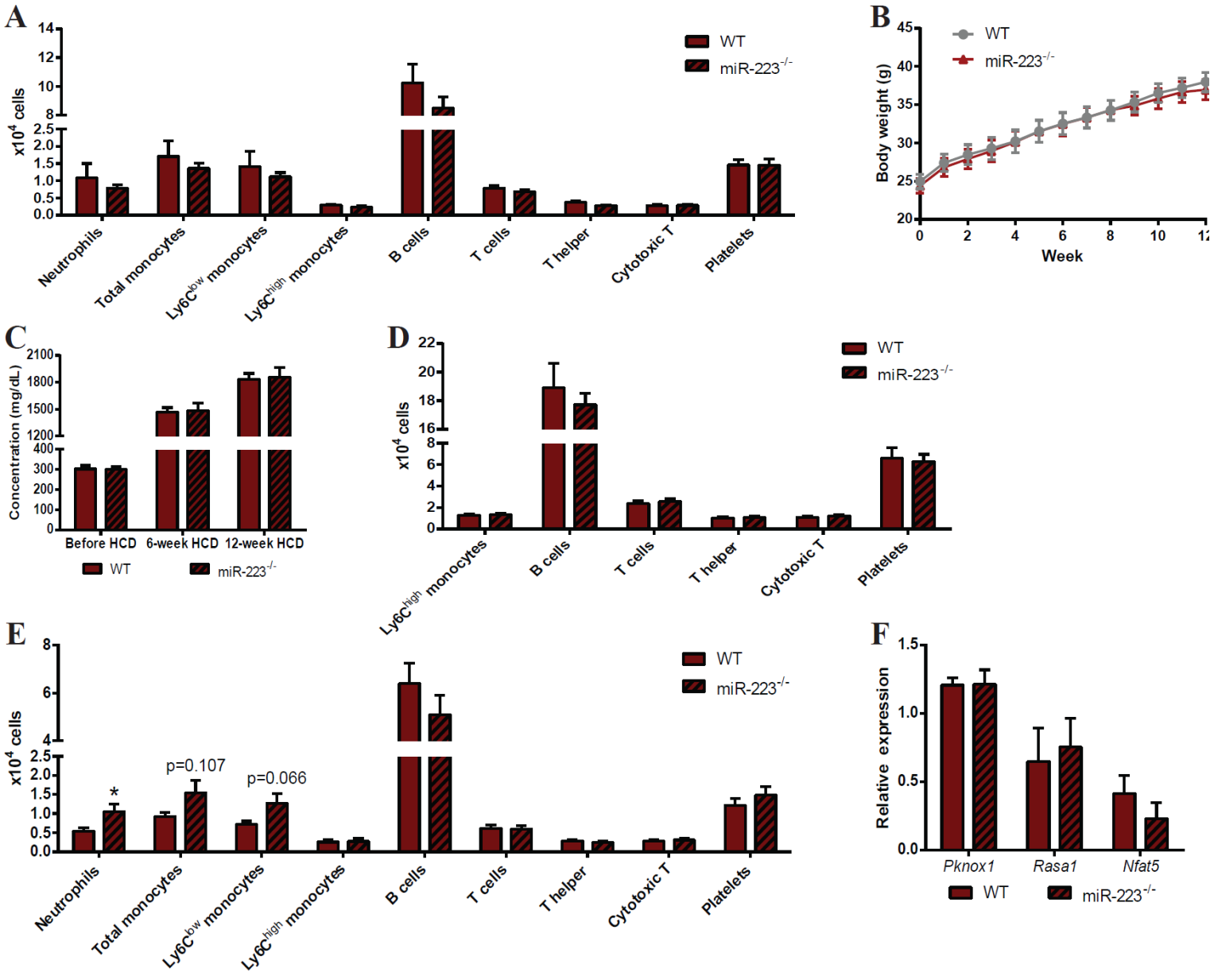
A
x10^4 cells
WT
miR-223-/-
Neutrophils
Total monocytes
Ly6C^low monocytes
Ly6C^high monocytes
B cells
T cells
T helper
Cytotoxic T
Platelets
B
Body weight (g)
Week
C
Concentration (mg/dL)
Before HCD
6-week HCD
12-week HCD
D
E
p=0.107
p=0.066
*
F
Relative expression
Pknox1
Rasa1
Nfat5

Supplemental Figure 4.1. Body weight, plasma cholesterol and circulating levels of most leukocytes and lymphocytes are unchanged in mice receiving miR-223 BM. (**A**) Circulating levels of leukocytes before HCD administration were analyzed by FACS. Data are the mean levels from 9-12 mice per group ± SEM. (**B-C**) No major difference in (**B**) body weight and (**C**) total plasma cholesterol were noted between mice receiving wild-type BM or miR-223$^{-/-}$ BM. (**D-E**) Circulating levels of leukocytes and lymphocytes after (**D**) 12 weeks of HCD and (**E**) 6 weeks of HCD were analyzed by FACS. Data are the mean levels from 9-12 mice per group ± SEM. (F) The expression of *Pknox1*, *Rasa1*, and *Nfat5* in aortic arches isolated from mice receiving wild-type BM or miR-223$^{-/-}$ BM. The aortic arch was homogenized using microbeads along with the Bullet Blender. Total RNA was isolated and gene expression levels were measured by ddRT-PCR. Graphs represent means ± SEM from n=9-12 mice per group.

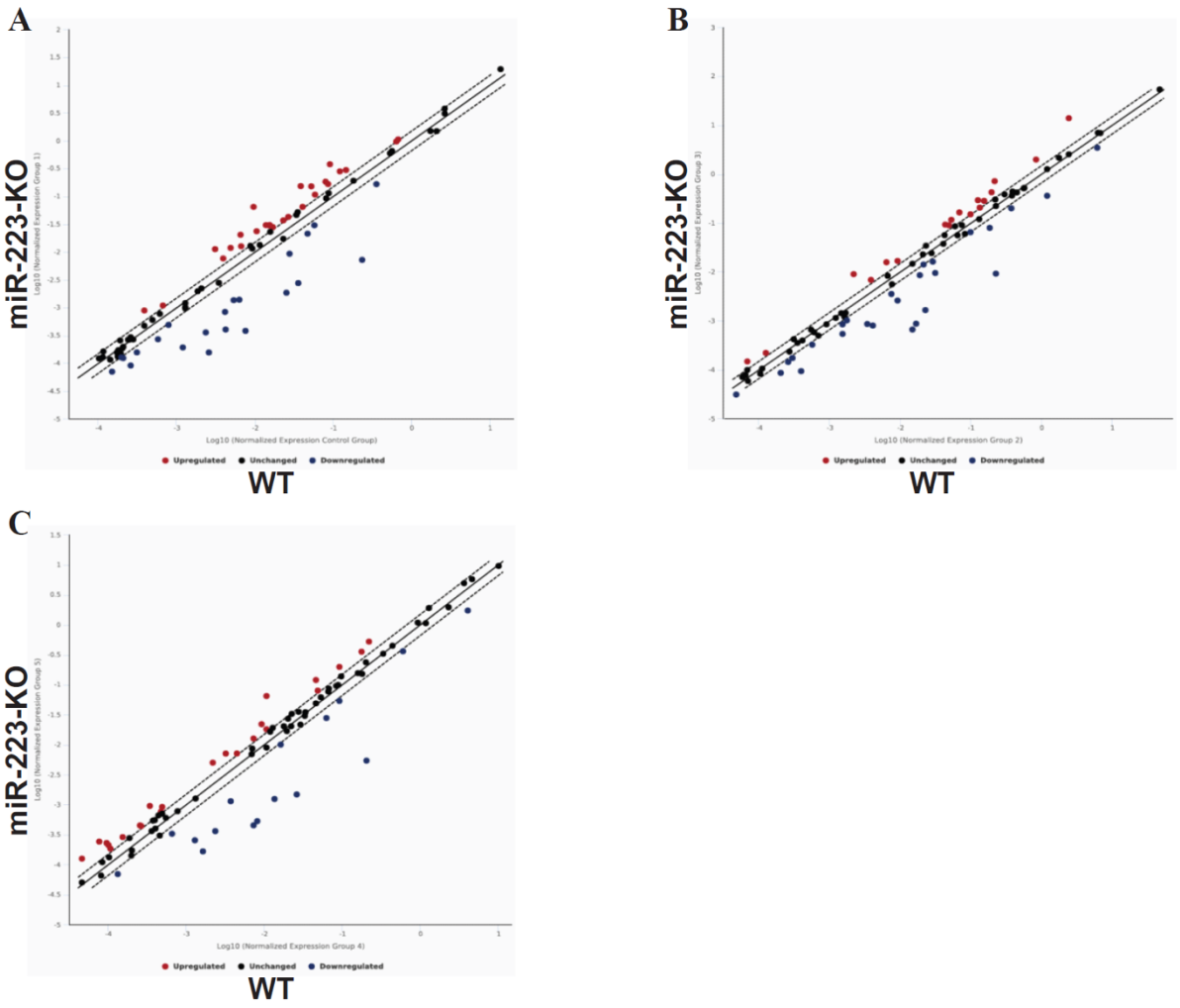

Supplemental Figure 4.2. Indirect regulation of atherosclerosis gene expression by miR-223. Atherosclerosis RT^2 Profiler PCR array was performed using RNA isolated from (**A**) resting Mo macrophages, (**B**) pro-inflammatory M1 macrophages and (**C**) anti-inflammatory M2 macrophages of wild-type mice or miR-223$^{-/-}$ mice and normalized to housekeeping genes using the ΔΔCt method. Graph depicts gene expression of wild-type (x-axis) *versus* miR-223$^{-/-}$ (y-axis). Red and blue symbols represent the up- and down-regulated genes (greater than 2-fold) in miR-223$^{-/-}$ compared to controls, respectively.

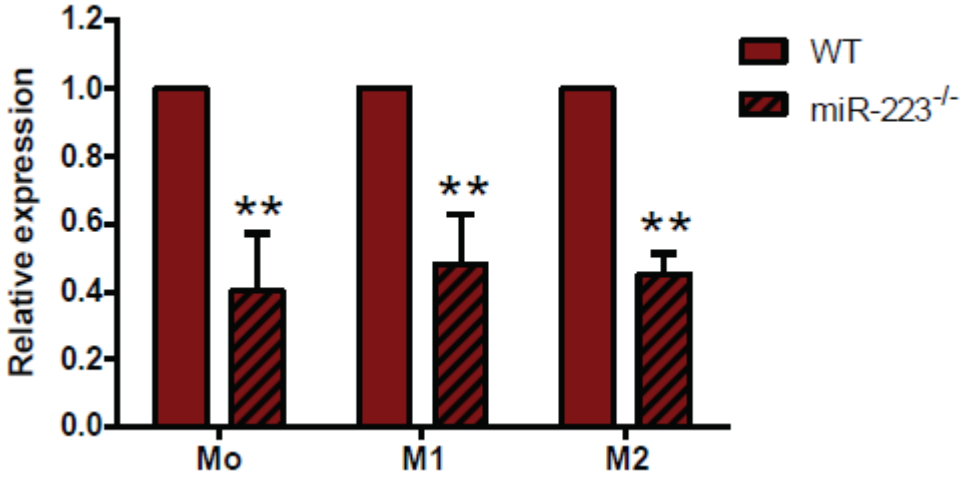

Supplemental Figure 4.3. Abca1 expression at the RNA level in different macrophage subtypes isolated from miR-223$^{-/-}$ mice. BMDMs isolated from wild-type/miR-223$^{-/-}$ mice were polarized into M1 macrophages or M2 macrophages by induction with LPS (100 ng/ml)/IFN-***γ*** (100 ng/ml) or IL-4 (10 ng/ml), respectively, for 24h. Total RNA was isolated and the expression levels of *Abca1* were measured by qPCR. Graphs represent the means ± SD from n=3 independent experiments, **p<0.01.

4.7. References

1. Lusis, A. Atherosclerosis. *Nature* **407**, 233–241 (2000).
2. Tabas, I., García-Cardeña, G. & Owens, G. K. Recent insights into the cellular biology of atherosclerosis. *J. Cell Biol.* **209**, 13–22 (2015).
3. Weber, C. & Noels, H. Atherosclerosis: Current pathogenesis and therapeutic options. *Nat. Med.* **17**, 1410–1422 (2011).
4. Di Gregoli, K. & Johnson, J. L. Role of colony-stimulating factors in atherosclerosis. *Curr. Opin. Lipidol.* **23**, 412–21 (2012).
5. Moore, K. J. & Tabas, I. Macrophages in the pathogenesis of atherosclerosis. *Cell* **145**, 341–55 (2011).
6. Moore, K. J., Sheedy, F. J. & Fisher, E. a. Macrophages in atherosclerosis: a dynamic balance. *Nat. Rev. Immunol.* **13**, 709–21 (2013).
7. Duewell, P. *et al.* NLRP3 inflammasomes are required for atherogenesis and activated by cholesterol crystals. *Nature* **464**, 1357–1361 (2010).
8. Maxfield, F. R. & Tabas, I. Role of cholesterol and lipid organization in disease. *Nature* **438**, 612–621 (2005).
9. Feng, B. *et al.* The endoplasmic reticulum is the site of cholesterol-induced cytotoxicity in macrophages. *Nat. Cell Biol.* **5**, 781–792 (2003).
10. Roth, G. A. *et al.* Global, regional, and national age-sex-specific mortality for 282 causes of death in 195 countries and territories, 1980–2017: a systematic analysis for the Global Burden of Disease Study 2017. *Lancet* **392**, 1736–1788 (2018).
11. Nabel, E. G. & Braunwald, E. A Tale of Coronary Artery Disease and Myocardial Infarction. *N. Engl. J. Med.* **366**, 54–63 (2012).
12. Yang, Q. *et al.* Assessing potential population impact of statin treatment for primary prevention of atherosclerotic cardiovascular diseases in the USA: Population-based modelling study. *BMJ Open* **7**, 1–11 (2017).
13. Madrigal-Matute, J., Rotllan, N., Aranda, J. F. & Fernández-Hernando, C. MicroRNAs and atherosclerosis. *Curr. Atheroscler. Rep.* **15**, 322 (2013).
14. Nguyen, M. A., Karunakaran, D. & Rayner, K. J. Unlocking the Door to New Therapies in Cardiovascular Disease: MicroRNAs Hold the Key. *Curr. Cardiol. Rep.* **16**, 1–12 (2014).
15. Kim, V. N. MicroRNA biogenesis: coordinated cropping and dicing. *Nat. Rev. Mol. Cell Biol.* **6**, 376–385 (2005).
16. Huntzinger, E. & Izaurralde, E. Gene silencing by microRNAs: contributions of translational repression and mRNA decay. *Nat. Rev. Genet.* **12**, 99–110 (2011).
17. He, L. & Hannon, G. J. MicroRNAs: small RNAs with a big role in gene regulation. *Nat. Rev. Genet.* **5**, 522–531 (2004).
18. Feinberg, M. W. & Moore, K. J. MicroRNA Regulation of Atherosclerosis. *Circ. Res.* **118**, 703–720 (2016).
19. Lu, Y., Thavarajah, T., Gu, W., Cai, J. & Xu, Q. Impact of miRNA in Atherosclerosis. *Arterioscler. Thromb. Vasc. Biol.* **38**, 159–170 (2018).
20. Vickers, K. C. *et al.* MicroRNA-223 coordinates cholesterol homeostasis. *Proc. Natl. Acad. Sci.* **111**, 14518–14523 (2014).
21. Wang, J. *et al.* miR-223 inhibits lipid deposition and inflammation by suppressing toll-like receptor 4 signaling in macrophages. *Int. J. Mol. Sci.* **16**, 24965–24982

(2015).
22. Li, T. *et al.* MicroRNAs modulate the noncanonical transcription factor NF-κB pathway by regulating expression of the kinase IKKα during macrophage differentiation. *Nat. Immunol.* **11**, 799–805 (2010).
23. Haneklaus, M. *et al.* Cutting edge: miR-223 and EBV miR-BART15 regulate the NLRP3 inflammasome and IL-1β production. *J. Immunol.* **189**, 3795–9 (2012).
24. Bauernfeind, F. *et al.* NLRP3 Inflammasome Activity Is Negatively Controlled by miR-223. *J. Immunol.* **189**, 4175–4181 (2012).
25. Rayner, K. J. *et al.* MiR-33 contributes to the regulation of cholesterol homeostasis. *Science* **328**, 1570–3 (2010).
26. Nguyen, M. A. *et al.* Extracellular Vesicles Secreted by Atherogenic Macrophages Transfer MicroRNA to Inhibit Cell Migration. *Arterioscler. Thromb. Vasc. Biol.* **38**, 49–63 (2018).
27. Karunakaran, D. *et al.* Macrophage Mitochondrial Energy Status Regulates Cholesterol Efflux and Is Enhanced by Anti-miR33 in Atherosclerosis. *Circ. Res.* **117**, 266–78 (2015).
28. Rayner, K. J. *et al.* Antagonism of miR-33 in mice promotes reverse cholesterol transport and regression of atherosclerosis. *J. Clin. Invest.* **121**, 2921–2931 (2011).
29. Alain, T. *et al.* Vesicular stomatitis virus oncolysis is potentiated by impairing mTORC1-dependent type I IFN production. *Proc. Natl. Acad. Sci. U. S. A.* **107**, 1576–1581 (2010).
30. Alain, T. *et al.* eIF4E/4E-BP ratio predicts the efficacy of mTOR targeted therapies. *Cancer Res.* **72**, 6468–6476 (2012).
31. Zhuang, G. *et al.* A novel regulator of macrophage activation: MiR-223 in obesity-associated adipose tissue inflammation. *Circulation* **125**, 2892–2903 (2012).
32. Ying, W. *et al.* MicroRNA-223 is a crucial mediator of PPARγ-regulated alternative macrophage activation. *J. Clin. Invest.* **125**, 4149–4159 (2015).
33. Lu, T.-P. *et al.* miRSystem: an integrated system for characterizing enriched functions and pathways of microRNA targets. *PLoS One* **7**, e42390 (2012).
34. Feig, J. E. Regression of atherosclerosis: Insights from animal and clinical studies. *Ann. Glob. Heal.* **80**, 13–23 (2014).
35. Tall, A. R., Yvan-Charvet, L., Terasaka, N., Pagler, T. & Wang, N. HDL, ABC Transporters, and Cholesterol Efflux: Implications for the Treatment of Atherosclerosis. *Cell Metab.* **7**, 365–375 (2008).
36. Yvan-Charvet, L., Wang, N. & Tall, A. R. Role of HDL, ABCA1, and ABCG1 transporters in cholesterol efflux and immune responses. *Arterioscler. Thromb. Vasc. Biol.* **30**, 139–143 (2010).
37. Langmann, T. *et al.* Identification of sterol-independent regulatory elements in the human ATP-binding cassette transporter A1 promoter. Role of Sp1/3, E-box binding factors, and an oncostatin M-responsive element. *J. Biol. Chem.* **277**, 14443–14450 (2002).
38. Thymiakou, E., Zannis, V. I. & Kardassis, D. Physical and functional interactions between liver X receptor/retinoid X receptor and Sp1 modulate the transcriptional induction of the human ATP binding cassette transporter A1 gene by oxysterols and retinoids. *Biochemistry* **46**, 11473–11483 (2007).
39. Chinetti-Gbaguidi, G., Colin, S. & Staels, B. Macrophage subsets in atherosclerosis.

Nat. Rev. Cardiol. **12**, 10–17 (2015).
40. Beug, S. T. *et al.* The transcription factor SP3 drives TNF- expression in response to Smac mimetics. *Sci. Signal.* **12**, (2019).
41. de Aguiar Vallim, T. Q. *et al.* MicroRNA-144 regulates hepatic ATP binding cassette transporter A1 and plasma high-density lipoprotein after activation of the nuclear receptor farnesoid X receptor. *Circ. Res.* **112**, 1602–12 (2013).
42. Ramírez, C. M. *et al.* Control of cholesterol metabolism and plasma high-density lipoprotein levels by microRNA-144. *Circ. Res.* **112**, 1592–601 (2013).
43. Goedeke, L. *et al.* MicroRNA-148a regulates LDL receptor and ABCA1 expression to control circulating lipoprotein levels. *Nat. Med.* **21**, 1280–1288 (2015).
44. Wagschal, A. *et al.* Genome-wide identification of microRNAs regulating cholesterol and triglyceride homeostasis. *Nat Med* **21**, 1290–1297 (2015).
45. Meiler, S., Baumer, Y., Toulmin, E., Seng, K. & Boisvert, W. A. MicroRNA 302a is a novel modulator of cholesterol homeostasis and atherosclerosis. *Arterioscler. Thromb. Vasc. Biol.* **35**, 323–331 (2015).
46. Nguyen, M. *et al.* Delivery of MicroRNAs by Chitosan Nanoparticles to Functionally Alter Macrophage Cholesterol Efflux in Vitro and in Vivo. *ACS Nano* **13**, 6491–6505 (2019).
47. Aiello, R. J. *et al.* Increased atherosclerosis in hyperlipidemic mice with inactivation of ABCA1 in macrophages. *Arterioscler. Thromb. Vasc. Biol.* **22**, 630–7 (2002).
48. Westerterp, M. *et al.* Deficiency of ATP-binding cassette transporters a1 and g1 in macrophages increases inflammation and accelerates atherosclerosis in mice. *Circ. Res.* **112**, 1456–1465 (2013).
49. Van Eck, M. *et al.* Leukocyte ABCA1 controls susceptibility to atherosclerosis and macrophage recruitment into tissues. *Proc. Natl. Acad. Sci.* **99**, 6298–6303 (2002).
50. Rodríguez, A. E. *et al.* Molecular Characterization of Chronic Lymphocytic Leukemia Patients with a High Number of Losses in 13q14. *PLoS One* **7**, (2012).
51. Huang, A. & Kaley, G. Gender-specific regulation of cardiovascular function: Estrogen as key player. *Microcirculation* **11**, 9–38 (2004).
52. Ng, M. K. C. *et al.* Androgens up-regulate atherosclerosis-related genes in macrophages from males but not females: Molecular insights into gender differences in atherosclerosis. *J. Am. Coll. Cardiol.* **42**, 1306–1313 (2003).
53. Ling, S. *et al.* Testosterone (T) Enhances Apoptosis-Related Damage in Human Vascular Endothelial Cells. *Endocrinology* **143**, 1119–1125 (2002).
54. Duvall, W. L. Cardiovascular disease in women. *Mt. Sinai J. Med.* **70**, 293–305 (2003).
55. Stolarz, A. J. & Rusch, N. J. Gender Differences in Cardiovascular Drugs. *Cardiovasc. Drugs Ther.* **29**, 403–410 (2015).
56. Gordon, S. & Taylor, P. R. Monocyte and macrophage heterogeneity. *Nat. Rev. Immunol.* **5**, 953–64 (2005).
57. Wynn, T. A., Chawla, A. & Pollard, J. W. Macrophage biology in development , homeostasis and disease. *Nature* **496**, 445–455 (2013).
58. Murray, P. J. & Wynn, T. A. Protective and pathogenic functions of macrophage subsets. *Nat. Rev. Immunol.* **11**, 723–737 (2011).
59. Chinetti-Gbaguidi, G. *et al.* Human Atherosclerotic Plaque Alternative Macrophages Display Low Cholesterol Handling but High Phagocytosis Because of Distinct

Activities of the PPARγ and LXRα Pathways. *Circ. Res.* **108**, 985–995 (2011).
60. Buono, C. *et al.* Influence of Interferon-γ on the Extent and Phenotype of Diet-Induced Atherosclerosis in the LDLR-Deficient Mouse. *Arterioscler. Thromb. Vasc. Biol.* **23**, 454–460 (2003).
61. Gupta, S. *et al.* IFN-gamma potentiates atherosclerosis in ApoE knock-out mice. *J. Clin. Invest.* **99**, 2752–2761 (1997).
62. Whitman, S. C., Ravisankar, P., Elam, H. & Daugherty, A. Exogenous interferon-gamma enhances atherosclerosis in apolipoprotein E-/- mice. *Am. J. Pathol.* **157**, 1819–24 (2000).
63. Hanna, R. N. *et al.* NR4A1 (Nur77) Deletion Polarizes Macrophages Toward an Inflammatory Phenotype and Increases Atherosclerosis. *Circ. Res.* **110**, 416–427 (2012).
64. Hamers, A. A. J. *et al.* Bone Marrow–Specific Deficiency of Nuclear Receptor Nur77 Enhances Atherosclerosis. *Circ. Res.* **110**, 428–438 (2012).
65. Liao, X. *et al.* Krüppel-like factor 4 regulates macrophage polarization. *J. Clin. Invest.* **121**, 2736–2749 (2011).
66. Cardilo-Reis, L. *et al.* Interleukin-13 protects from atherosclerosis and modulates plaque composition by skewing the macrophage phenotype. *EMBO Mol. Med.* **4**, 1072–1086 (2012).
67. Zhuang, G. *et al.* A novel regulator of macrophage activation: miR-223 in obesity-associated adipose tissue inflammation. *Circulation* **125**, 2892–903 (2012).
68. Bhaskar, V. *et al.* Monoclonal antibodies targeting IL-1 beta reduce biomarkers of atherosclerosis in vitro and inhibit atherosclerotic plaque formation in Apolipoprotein E-deficient mice. *Atherosclerosis* **216**, 313–320 (2011).
69. Kirii, H. *et al.* Lack of interleukin-1ß decreases the severity of atherosclerosis in apoE-deficient mice. *Arterioscler. Thromb. Vasc. Biol.* **23**, 656–660 (2003).
70. Upadhya, S., Mooteri, S., Peckham, N. & Pai, R. G. Atherogenic effect of interleukin-2 and antiatherogenic effect of interleukin-2 antibody in apo-E-deficient mice. *Angiology* **55**, 289–294 (2004).
71. Zhang, W. *et al.* IL-9 aggravates the development of atherosclerosis in ApoE-/-mice. *Cardiovasc. Res.* **106**, 453–464 (2015).
72. Li, Q. *et al.* Increased Th9 cells and IL-9 levels accelerate disease progression in experimental atherosclerosis. *Am. J. Transl. Res.* **9**, 1335–1343 (2017).
73. Hauer, A. D. *et al.* Blockade of interleukin-12 function by protein vaccination attenuates atherosclerosis. *Circulation* **112**, 1054–1062 (2005).
74. Lee, T. S., Yen, H. C., Pan, C. C. & Chau, L. Y. The role of interleukin 12 in the development of atherosclerosis in apoE-deficient mice. *Arterioscler. Thromb. Vasc. Biol.* **19**, 734–742 (1999).
75. Erbel, C. *et al.* Inhibition of IL-17A Attenuates Atherosclerotic Lesion Development in ApoE-Deficient Mice. *J. Immunol.* **183**, 8167–8175 (2009).
76. Smith, E. *et al.* Blockade of interleukin-17A results in reduced atherosclerosis in apolipoprotein E-deficient mice. *Circulation* **121**, 1746–1755 (2010).
77. Subramanian, M., Thorp, E. & Tabas, I. Identification of a non-growth factor role for GM-CSF in advanced atherosclerosis: Promotion of macrophage apoptosis and plaque necrosis through IL-23 signaling. *Circ. Res.* **116**, e13–e24 (2015).
78. Yvan-Charvet, L. *et al.* Increased inflammatory gene expression in ABC transporter-

deficient macrophages: Free cholesterol accumulation, increased signaling via toll-like receptors, and neutrophil infiltration of atherosclerotic lesions. *Circulation* **118**, 1837–1847 (2008).
79. Zhu, X. *et al.* Macrophage ABCA1 reduces MyD88-dependent Toll-like receptor trafficking to lipid rafts by reduction of lipid raft cholesterol. *J. Lipid Res.* **51**, 3196–3206 (2010).
80. Mogilenko, D. A. *et al.* Endogenous apolipoprotein A-I stabilizes ATP-binding cassette transporter A1 and modulates Toll-like receptor 4 signaling in human macrophages. *FASEB J.* **26**, 2019–2030 (2012).
81. Koseki, M. *et al.* Increased lipid rafts and accelerated lipopolysaccharide-induced tumor necrosis factor-α secretion in Abca1-deficient macrophages. *J. Lipid Res.* **48**, 299–306 (2007).
82. Zhu, X. *et al.* Increased cellular free cholesterol in macrophage-specific Abca1 knock-out mice enhances pro-inflammatory response of macrophages. *J. Biol. Chem.* **283**, 22930–22941 (2008).
83. Westerterp, M. *et al.* Cholesterol Efflux Pathways Suppress Inflammasome Activation, NETosis, and Atherogenesis. *Circulation* **138**, 898–912 (2018).

5. Discussion

Since the advent of statins as a first-line therapy for CVD, there have been only a few commercialized therapies that have made a significant impact on CVD burden[1]. Thus, the search for novel therapeutic targets that can be used individually or in combination with current therapies to reduce the morbidity and mortality associated with CVD is still in progress. The discovery that miRNAs are critical regulators of multiple signaling pathways involved in atherosclerosis has opened a new era not only for our understanding of the molecular mechanisms that govern atherogenesis but also for the treatment of CVD[2,3]. Consistent with numerous studies, this thesis highlights the importance of both endogenous and extracellular miRNAs in controlling different aspects of atherogenic response. In the first study, we find that EVs derived from cholesterol-loaded macrophages can inhibit macrophage migration *in vitro* and *in vivo*. This effect appears to be mediated by the transfer of several miRNAs, including miR-146a, to recipient macrophages where they repress the expression of specific pro-migratory target genes *Igf2bp1* and *HuR* (**Section 2**). Our work is the first demonstrating that EV-derived miRNAs secreted from atherogenic macrophages may accelerate the development of atherosclerosis lesions by decreasing cell migration and promoting macrophage entrapment in the vessel wall. These findings emphasize the concept that miRNAs are truly mediators of atherogenesis, which not only uncovers novel mechanisms that contribute to disease but ultimately identifies miRNAs (for example, miR-146a) that can be useful as clinical therapeutic targets to treat millions of Canadians that suffer from heart disease and its related complications. Furthermore, understanding macrophage communication *via* EV-mediated transfer of miRNAs during atherosclerosis provided the rationale for the design of NPs that mimic macrophage-derived EVs to deliver

beneficial miRNAs or other therapeutics directly to the atherosclerotic plaque. We explored this concept in the second study, where we have demonstrated, to our knowledge, the first platform for effective delivery of miRNAs to alter macrophage function *in vivo*. As a proof-of-concept, we show that our NPs made using a cross-linked chitosan polysaccharide polymer can protect as well as transfer exogenous miRNA to naïve macrophages and regulate the expression of its target gene (*Abca1*) as well as cholesterol efflux both *in vitro* and *in vivo* (**Section 3**). These findings suggested that our approach can be applied to other miRNA-based therapeutics, particularly in the setting of cardiovascular and inflammatory diseases, where macrophages dominate and promote pathology, and may open up new avenues for miRNA-based therapies for these diseases. Finally, almost all miRNAs that have been identified and characterized are considered as pro-atherogenic miRNAs or "bad" miRNAs. So, there remains a need to identify novel anti-atherogenic miRNAs or "good" miRNAs that can be loaded inside NPs and deliver to the plaque to treat atherosclerosis. We herein find that miR-223, whose expression is dependent on intracellular cholesterol levels[4], is indeed capable of suppressing plaque development *via* modulating cholesterol efflux and inflammatory responses, thus may serve as a potential therapeutic to reduce atherosclerosis (**Section 4**).

5.1. miR-223: A potential therapeutic agent for atherosclerosis

Atherosclerosis is a lipid-driven chronic inflammatory disease initiated by excess cholesterol accumulation in the vessel wall and maintained by a non-resolving immune response[5,6]. Thus, targeting dysregulation of cholesterol homeostasis and inflammation in atherosclerosis have attracted much attention as potential therapeutic approaches. During the

last ten years, miRNAs have emerged as critical regulators of cholesterol metabolism and inflammatory response[2,3]. For example, numerous miRNAs including miR-33[7,8], miR-144[9,10], miR-148a[11,12], and miR-302a[13] have been found to regulate cholesterol efflux *via* directly targeting the cholesterol transporter ABCA1. Modulating the expression of these above miRNAs can alter cholesterol clearance in macrophages and the development of atherosclerosis. Similarly, the inflammatory state of macrophage is controlled by multiple miRNAs such as miR-124[14], miR-33[15], miR-342-5p[16], miR-155[17,18], and miR-125a/b[19,20]. Here we identify a miRNA that can modulate both macrophage cholesterol efflux and macrophage activation state, miR-223. Different from most characterized miRNAs that negatively regulate ABCA1 expression and cholesterol efflux, overexpression of miR-223 enhance the ability of macrophages to efflux intracellular cholesterol through up-regulating ABCA1 whereas miR-223 deletion reduces ABCA1 expression and abolishes cholesterol efflux to apoA1 (**Figure 4.2**). Our data are consistent with a previous study reported that miR-223 can promote ABCA1 expression and cellular cholesterol efflux in hepatocytes[4]. In addition to cholesterol efflux, miR-223 is involved in fate of atherosclerotic macrophages as miR-223 overexpression can suppress macrophage pro-inflammatory activation (M1) while promote macrophage polarization toward the anti-inflammatory phenotype (M2) (**Figure 4.3**).

The most prominent characteristic of miRNA regulation perhaps is the ability of a single miRNA to coordinately regulate the expression of numerous genes across different signaling pathways to execute a particular phenotypic trait. Therefore, alterations in the expression of one specific miRNA involved in various aspects of atherogenesis can magnify its impact on the development of atherosclerosis. For instance, miR-148a inhibition in mice

improves the ratio of LDL cholesterol and HDL cholesterol, an important risk factor for CVD, by functioning as a key regulator of both hepatic LDL cholesterol clearance through direct modulation of LDLR expression and cholesterol efflux through direct modulation of ABCA1 expression[11,12]. Another example is miR-33. Antagonism of miR-33 in the hypercholesterolemic mouse model attenuates atherosclerosis progression not only by increasing RCT and circulating HDL levels but also by promoting inflammation-suppressing M2 macrophage polarization[8] and FOXP3^{+} Tregs induction[15]. Similarly, as miR-223 regulate both macrophage cholesterol efflux and macrophage polarization, deficiency of miR-223 in BM-derived cells can increase the severity of atherosclerosis *in vivo via* reducing vascular lipid removal as well as exaggerating inflammatory responses (**Figure 4.1**). Moreover, miR-223 have been shown to be critical in the maintenance of hepatic cholesterol homeostasis and miR-223$^{-/-}$ mice show symptoms of hypercholesterolemia, with significantly higher levels of plasma cholesterol, triacylglycerol and phospholipids[4]. It is postulated that miR-223 can further protect against atherosclerosis by acting as a key regulator of systemic cholesterol levels in addition to macrophage cholesterol efflux and inflammation. Future studies examining susceptibility to atherosclerosis of whole-body transgenic overexpression or whole-body deletion of miR-223 will help to address this hypothesis.

Results obtained in our studies indicate that the transcription factor Sp3 may mediate the effects of miR-223 on macrophage cholesterol efflux and macrophage polarization (**Figure 4.3**). However, we cannot entirely exclude the role of other target genes in miR-223-mediated regulation of macrophage cholesterol efflux and macrophage polarization. Indeed, bioinformatic analysis predicts that miR-223 target genes that have been shown to involve in cholesterol efflux and inflammation such as *Rhob* (Ras homolog family member B) and

Siah1 (seven in absentia homolog 1), respectively. For example, RhoB is a member of the Rho GTPase family that are subject to post-translational modification by geranylgeranylation and function as molecular switches controlling a wide variety of signal transduction pathways through their association with different effector molecules including kinases[21]. Negative regulation of the Rho-signaling pathway by using an inhibitor of geranylgeranyl transferase activity or an inhibitor of the Rho GTP-binding protein family increases peroxisome proliferator activated receptor γ (PPARγ) activity and the expression of PPARγ-responsive genes including *Lxra* and *Abca1*[22], thus promoting macrophage cholesterol efflux[23]. Moreover, miR-223 are predicted to target *Siah1* that encodes for a potent RING finger E3 ubiquitin ligase known to involve in several stress responses including hypoxia, oxidative stress and inflammation[24]. SIAH1 has been shown to potentiate TNF-α-mediated NF-κB activation[25], and conversely, inhibition of SIAH1 using siRNA decreases the expression of *Tnfα* and *Il-6* in murine macrophages after LPS stimulation[26]. In addition to predicted targets described above, a number of miR-223 validated targets are also identified genes involved in cholesterol efflux. It is known that IKKα is a bona fide target of miR-223[27]. Aside from its role in inducing NF-κB activation[28], IKKα can promote mTORC1 kinase activity through phosphorylating mTOR at serine 1415 in an AKT-dependent manner[29]. More importantly, inhibition of mTORC1 by rapamycin or Torin-1 increases cholesterol efflux to apoA1[30], suggesting that miR-223 can also positively regulate cholesterol efflux *via* supressing IKKα expression and mTORC1 activity. Therefore, miR-223 may employ different mechanisms to modulate macrophage cholesterol efflux and inflammatory response. Particularly, as one miRNA can repress multiple target genes simultaneously, we believe that the effects of miR-223 on cholesterol efflux and

inflammation should be a result of miR-223 functioning coordinately on multiple genes, rather than miR-223 exerting its effects on one specific target gene.

5.2. EVs, particularly their miRNA cargos, as important regulators of macrophage migration

EVs are known as important mediators of cell-to-cell communication in a diverse range of biological and pathological processes. Particularly, several recent studies found that vesicle-mediated transfer of miRNAs can mediate signals between cells in chronic inflammatory diseases including atherosclerosis[31]. EVs derived from KLF2-transduced or shear-stress-stimulated ECs were shown to contain high levels of miR-143/miR-145, which regulates SMC fate as well as plasticity and thus, attenuates atherosclerotic lesion development in *ApoE*$^{-/-}$ mice[32]. On the other hand, oxidized LDL-induced ECs release EVs enriched in miR-155 that is taken up by macrophages in which it promotes an anti-inflammatory M2- to pro-inflammatory M1- phenotype shift *in vitro* and *in vivo*[33]. Furthermore, monocyte-derived EVs deliver functional miR-150 to neighboring ECs where miR-150 represses the expression of its target gene *c-Myb*, leading to increased EC migration[34]. In agreement with these studies, we find that atherogenic macrophages secrete EVs containing a specific set of miRNAs including miR-146a, miR-128, miR-185, miR-365 and miR-503 (**Figure 2.2**), which can be taken up by naïve macrophages and mediate the transfer of miRNAs to naïve cells (**Figure 2.3**). Functionally, we show that EVs derived from atherogenic macrophages inhibit the migration of naïve cells *in vitro* and *in vivo* (**Figure 2.4**). Our data confirm that beside guidance cues and chemotactic proteins, EVs have emerged as important regulators of macrophage migration. Interestingly, EVs from

mycobacteria-infected macrophages has also been shown to induce cell migration[35,36], suggesting that EVs from atherogenic macrophages may target similar pathways but exert opposing effects. The effect of atherogenic EVs on macrophage migration may be attributable to the transfer of several miRNAs, in particular miR-146a, to recipient macrophages where they repress the expression of specific pro-migratory target genes *Igf2bp1* and *HuR* (**Figure 2.5 and 2.6**). However, not only miR-146a, the other miRNAs enriched in atherogenic EVs have been also shown to regulate cell migration. miR-185 suppresses the migration ability of hepatocellular carcinoma cells *via* directly targeting CDC42 (cell division cycle 42) and ROCK2 (Rho-associated coiled-coil containing protein kinase 2)[37,38]. Different from miR-185, miR-365 inhibits SMC migration through targeting ADAMTS1 (a disintegrin and metalloproteinase with thrombospondin motifs 1)[39] while miR-503 reduces LPS-induced EC migration by repressing the expression of CD40[40]. These data, when taken together, suggest that the other miRNAs enriched in atherogenic EVs, aside from miR-146a, may also contribute to the inhibitory effect of atherogenic EVs on macrophage migration. Thus, future studies are still needed to assess their individual contributions.

In addition to miRNAs, EVs contain other biological molecules such as lipids (*i.e.* free fatty acid, sphingolipids, saturated phospholipids), proteins (*i.e.* cytokines, enzymes, growth factors, transcription factors), and even functional organelles (i.e. proteasome, mitochondria)[41,42]. Particularly, comparative lipidomic and proteomic analyses of EVs derived from different cell types has identified more than 3,500 proteins and nearly 2,000 lipid species[43]. These components, more importantly, are likely to play a role in EV-mediated intercellular signaling. For example, lymphatic ECs secretes EVs carrying more

than 1,700 cargo proteins, the majority of which are motility-promoting proteins, and these EVs enhance directional migration of DCs[44]. Recently, Kriebel *et al.*[45] described an elegant system in which soil-dwelling amoeba *Dictyostelium discoideum*-derived EVs containing all the components necessary for cAMP (cyclic adenosine monophosphate) synthesis could function as the entire machinery for generating and releasing chemoattractants to promote chemotaxis of follower cells, highlighting the importance of cargo proteins in mediating EV function. Not only proteins, the lipid composition also contributes to the effects of EVs in recipient cells. EVs secreted from pancreatic ductal adenocarcinoma cell shows enrichment of ceramide-1-phosphate, which can promote the motility of pancreatic cancer stem cells[46]. As atherogenic EVs dramatically alter cell migration, we postulate that this will be a result of multiple components functioning simultaneously on multiple signaling pathways. Therefore, studies characterizing the protein and lipid profile of atherogenic EVs will help to further understand the mechanisms underlying the inhibitory effects of these EVs on macrophage migration.

The discovery that miRNAs can be released into extracellular fluids and function as paracrine molecules that regulate gene expression in recipient cells emphasizes not only the role of extracellular miRNAs in mediating pathophysiology but also the potential of extracellular miRNAs as therapeutic targets for CVD. For example, Chen *et al.* showed that delivery of cardiac progenitor-derived exosomes, which are enriched in miR-451, reduced cardiomyocyte apoptosis in a mouse myocardial ischemia/reperfusion model[47]. Moreover, injection of miR-146a-containing exosomes from DCs results in delivery of this miRNA to different mouse tissues (*i.e.* liver, spleen, BM), repression of its respective targets (*i.e.* IRAK1, TRAF6), and decreased inflammation response to endotoxin *in vivo*[48].

On the other hand, intra-tumor injection of marrow stromal cell-derived exosomes enriched in the other member of the miR-146 family, miR-146b, inhibits glioma xenograft growth in a rat model of primary brain tumor[49]. Due to the low yield of EVs isolated from atherogenic macrophages, here we cannot examine the effect of atherogenic EVs and their miRNA content on atherogenesis *in vivo.* Therefore, whether EVs from atherogenic macrophages have beneficial effects on the development of atherosclerosis still needs further investigation.

As EVs appear to be a natural way that cells transfer miRNAs, there is also growing interest in understanding in the therapeutic potential of EVs as delivery vehicles for specific miRNAs and their inhibitors. This concept has been supported by a recent study where donor cells were engineered to secrete exosomes expressing the GE11 peptide, which can bind specifically to EGFR (epidermal growth factor receptor), and these exosomes were loaded with tumor suppressive miRNA let-7a. Intravenous injection of modified exosomes specifically delivered let-7a to EGFR-expressing xenograft breast cancer tissue and inhibit tumor development in $RAG2^{-/-}$ mice[50]. To achieve neuron-specific targeting, another study engineered rabies virus glycoprotein (RVG) to the exosomal surface by fusing to exosomal protein lysosome-associated membrane glycoprotein 2b (Lamp2b) and loaded these exosomes with miR-124. Modified exosomes indeed could deliver miR-124 to the infarct site and protect against neuronal ischemic injury[51]. These findings, when taken together, have opened new doors for encapsulated miRNAs as therapeutics. However, in order to efficiently utilize EVs in a therapeutic context, many aspects of their fundamental biology including cargo selection and packaging, cell targeting, uptake mechanism, biodistribution profile, and clearance rate remains to be further elucidated.

5.3. Chitosan-based NPs for miRNA delivery

Despite their high potential, engineering EVs for specific human needs remains challenging due to problems associated with mass production and quality control. Moreover, understanding of EVs is still limited. The alternative way is designing nano-sized particles mimicking more or less closely the properties of natural EVs but retaining the desired function, which is the capacity to deliver bioactive miRNAs or other molecules. Among numerous biodegradable biopolymers that have been used as miRNA carriers for various therapeutic purposes, chitosan is a promising delivery vector because of its biocompatibility, biodegradability, low immunogenicity and ease of manufacturing[52]. For instance, Chen *et al.* used chitosan-based NPs as a carrier to deliver miR-199a-5p to mesenchymal stem cells both *in vitro* and *in vivo*, leading to improved bone generation[53]. Furthermore, chNP-mediated delivery of the tumor-suppressive miR-34 inhibited tumor growth and preserved bone integrity in a xenograft model representative of established prostate cancer bone metastasis[54]. However, the intracellular delivery of miRNAs to primary cells including macrophages is still troublesome due to their quiescent nature. Thus far, chNPs have only been utilized as a vehicle to successfully deliver siRNAs into macrophages[55,56]. Here we demonstrate the first chNP platform, to our knowledge, for effective delivery of miRNAs to modulate target gene expression and alter functional pathways in macrophages, which are central to the development of atherosclerosis. Our chNPs made using a cross-linked chitosan polysaccharide polymer can protect as well as transfer exogenous miR-33 to naïve macrophages and alter the expression of its target gene, *Abca1*, both *in vitro* and *in vivo* (**Figure 3.3 and 3.4**). Previous studies showed that although they are taken up by most target cells such as HEK293T (human embryonic kidney 293T), CHO (Chinese hamster ovary),

and COS-7 (CV-1 in origin with SV40 genes) *via* endocytosis[57], chNPs are susceptible to phagocytic capture by cells of the mononuclear phagocyte system including macrophages[58–60]. More importantly, miR33-chNPs can dampen cholesterol efflux to apoA1 *in vitro* (**Figure 3.3**) and inhibit reverse cholesterol transport *in vivo* (**Figure 3.5 and 3.6**). Together our data indicate that miR-chNPs can be used effectively to delivery miRNA therapeutics to alter target gene expression and macrophage function. This could offer an opportunity for the replacement of anti-atherogenic miRNAs whose expression is lost during disease or when global miRNA homeostasis is disturbed, for example due to loss of Dicer activity, which can promote atherosclerosis[61]. In fact, delivery of anti-atherogenic miRNAs, particularly efflux-promoting miR-223 and miR-206 in this case, can promote cholesterol removal from macrophage-derived foam cells to the liver or intestine for excretion, thus bearing the potential to reduce vascular lipid accumulation and atherosclerosis (**Figure 3.7**). Especially, miR-223 as discussed above can reduce susceptibility to atherosclerosis by acting as a crucial modulator of not only macrophage cholesterol efflux but also macrophage inflammation. Thus, systemic delivery or macrophage-specific delivery of miR-223 using our NP platform could be a promising therapeutic strategy for atherosclerosis.

Systemic delivery of NPs has been explored for CVD application; however, NPs in most cases tend to accumulate to a greater extent in non-targeted organs including liver and spleen than the target tissue such as atherosclerotic plaques[62]. Therefore, bioconjugation of affinity ligands to the NP surface is needed to increase their specificity and maximize their effects on tissue of interest. Although we did not use a targeting peptide in this study, the hydroxyl and amino groups of chitosan used in our NP platform can facilitate chemical conjugation of specific ligands tailored for targeted therapy. For instance, to achieve vascular

EC-specific delivery of miR-126, this miRNA was packaged into chNPs grafted with a short peptide REDV (Arg-Glu-Asp-Val). These NPs indeed were selectively taken up by ECs and promoted EC proliferation[63]. Macrophage-specific miRNA delivery, on the other hand, can be improved by using external peptides like fibronectin, hyaluronan, which have been used to promote lesional NP delivery[64,65], or folate, which can bind specifically to folate receptor highly expressed in activated macrophages[66]. Moreover, it is known that phosphatidylserine on the EV surface play a key role in mediating their macrophage-specific uptake. Phosphatidylserine-coated beads and phosphatidylserine-containing liposomes are targeted and taken up by macrophages *via* interacting with the phosphatidylserine receptors TIM1/4 (T-cell immunoglobulin mucin protein 1/4) on the surface of macrophages[67,68], suggesting that phosphatidylserine can be used as a ligand for macrophage targeting.

5.4. Challenges of miRNA-based therapies

Although the interest in miRNAs has constantly risen during the past few years and technologies to identify as well as characterize them has become more sophisticated, several limitations and challenges remain to be resolved before miRNAs can reach clinical applications.

The most prominent one is target specificity. As highlighted above, miRNAs have a unique capability to control complex physiologic functions, giving by the fact that a single miRNA can target multiple different mRNAs including genes involved in the same or similar pathways[69–71]. However, this same ability has raised concerns over potential unintended effects of miRNA-based therapeutic approaches. Indeed, modulating levels of a particular miRNA will alter the expression profiles of not only targets implicated in

cardiovascular diseases but also other targets that may or may not have beneficial effects. Of note, many miRNAs associated with cardiovascular pathology are also known as tumor suppressor *in vivo*. For instance, the let-7 family of miRNAs, which has emerged as a key regulators of glucose homeostasis and insulin sensitivity[72,73], has also been shown to be down-regulated in various cancer types and function to suppress tumor initiation[74]. Thus, the potential use of anti-let-7 as a therapy to treat diabetes should take into consideration the long-term risk of developing cancer. Another well-known example is miR-122. Despite exciting findings elucidating the critical role of miR-122 in regulating cholesterol metabolism, the increased prevalence of hepatosteatosis, hepatitis and hepatocellular carcinoma has dampened the enthusiasm for developing anti-miR-122 therapies to treat hypercholesterolemia in humans[75–77]. It is also important to consider that many validated targets of miR-122 has been shown to be involved in glucose and iron homeostasis[75,78].

Additionally, the pathological functions of miRNAs are highly context- and cell type-dependent, like the opposite effects of miR-206 in hepatic cells and macrophages. In the liver, miR-206 suppresses the expression of LXRα along with its targets including ABCA1, ABCG1, ABCG5, and SREBP-1c; conversely, miR-206 promotes LXRα abundance and cholesterol efflux in macrophages[79]. Similarly, whole-body loss of miR-33 in *Ldlr*$^{-/-}$ mice was found to result in increased body weight, which is exacerbated by a Western diet feeding, impaired insulin sensitivity, and a pro-atherogenic lipid profile (increased circulating levels of VLDL-C, LDL-C, and triglycerides (TAGs)), while selective loss of miR-33 in macrophages and other hematopoietic cells did impede the development of atherosclerotic plaques without any of the adverse effects mentioned above[80,81]. Thus, it is

necessary to define roles of individual miRNAs along with its important target in different settings based on cell types and pathological implication.

Finally, the translation of miRNA-based therapies into clinical applications should also take into account challenges such as dosage adjustment. For example, the efficacy of antisense technologies needs to be cautiously titrated against their toxicity because it has been demonstrated that off-target effects are likely to occur when doses are increased[82]. Thus, determining the right dosage of miRNA-based therapeutic approaches to strike a balance between therapeutic and side-effects is necessary. In addition, duration treatment is also important for further translational application of miRNA-based therapies. Acute miR-15 antagonism might confer benefits to cardiac repair and function following myocardial infraction by inducing myocyte proliferation, while prolonged anti-miR-15 therapy could potentially induce global cellular proliferation and promote neoplasia[83,84]. Similarly, 4-week treatment with anti-miR-33 raised circulating HDL-cholesterol, enhanced RCT, and accelerated atherosclerosis regression[8]; however, long-term treatment of anti-miR-33 therapy, on the other hand, resulted in hypertriglyceridemia along with hepatic steatosis and did not affect plasma HDL-cholesterol levels as well as plaque development[85–87].

5.5. Conclusion

miRNAs are without doubt important biological players in the development of atherosclerosis. By post-transcriptionally regulating the expression levels of multiple critical genes, miRNAs play a significant role in driving the dysregulation that affects EC, SMC, and macrophage function, thereby controlling every stage of atherosclerosis development. Interestingly, not only modulate intracellular signaling pathways, miRNAs can also function

as paracrine molecules to mediate the intercellular communication between different cell types involved in plaque formation. Thus, therapeutics to regulate miRNA activity are emerging as the next frontier in treatment options for atherosclerosis.

5.6. References

1. Chaudhary, R., Garg, J., Shah, N. & Sumner, A. PCSK9 inhibitors: A new era of lipid lowering therapy. *World J. Cardiol.* **9**, 76 (2017).
2. Madrigal-Matute, J., Rotllan, N., Aranda, J. F. & Fernández-Hernando, C. MicroRNAs and atherosclerosis. *Curr. Atheroscler. Rep.* **15**, 322 (2013).
3. Feinberg, M. W. & Moore, K. J. MicroRNA Regulation of Atherosclerosis. *Circ. Res.* **118**, 703–720 (2016).
4. Vickers, K. C. *et al.* MicroRNA-223 coordinates cholesterol homeostasis. *Proc. Natl. Acad. Sci.* **111**, 14518–14523 (2014).
5. Tabas, I., García-Cardeña, G. & Owens, G. K. Recent insights into the cellular biology of atherosclerosis. *J. Cell Biol.* **209**, 13–22 (2015).
6. Weber, C. & Noels, H. Atherosclerosis: Current pathogenesis and therapeutic options. *Nat. Med.* **17**, 1410–1422 (2011).
7. Rayner, K. J. *et al.* MiR-33 contributes to the regulation of cholesterol homeostasis. *Science* **328**, 1570–3 (2010).
8. Rayner, K. J. *et al.* Antagonism of miR-33 in mice promotes reverse cholesterol transport and regression of atherosclerosis. *J. Clin. Invest.* **121**, 2921–2931 (2011).
9. de Aguiar Vallim, T. Q. *et al.* MicroRNA-144 regulates hepatic ATP binding cassette transporter A1 and plasma high-density lipoprotein after activation of the nuclear receptor farnesoid X receptor. *Circ. Res.* **112**, 1602–12 (2013).
10. Ramírez, C. M. *et al.* Control of cholesterol metabolism and plasma high-density lipoprotein levels by microRNA-144. *Circ. Res.* **112**, 1592–601 (2013).
11. Goedeke, L. *et al.* MicroRNA-148a regulates LDL receptor and ABCA1 expression to control circulating lipoprotein levels. *Nat. Med.* **21**, 1280–1288 (2015).
12. Wagschal, A. *et al.* Genome-wide identification of microRNAs regulating cholesterol and triglyceride homeostasis. *Nat Med* **21**, 1290–1297 (2015).
13. Meiler, S., Baumer, Y., Toulmin, E., Seng, K. & Boisvert, W. A. MicroRNA 302a is a novel modulator of cholesterol homeostasis and atherosclerosis. *Arterioscler. Thromb. Vasc. Biol.* **35**, 323–331 (2015).
14. Ponomarev, E. D., Veremeyko, T., Barteneva, N., Krichevsky, A. M. & Weiner, H. L. MicroRNA-124 promotes microglia quiescence and suppresses EAE by deactivating macrophages via the C/EBP-α-PU.1 pathway. *Nat. Med.* **17**, 64–70 (2011).
15. Ouimet, M. *et al.* MicroRNA-33–dependent regulation of macrophage metabolism directs immune cell polarization in atherosclerosis. *J. Clin. Invest.* **125**, 4334–4348 (2015).
16. Wei, Y. *et al.* The microRNA-342-5p fosters inflammatory macrophage activation through an Akt1- and microRNA-155-dependent pathway during atherosclerosis.

Circulation **127**, 1609–19 (2013).
17. Cai, X. *et al.* Re-polarization of tumor-associated macrophages to pro-inflammatory M1 macrophages by microRNA-155. *J. Mol. Cell Biol.* **4**, 341–343 (2012).
18. Nazari-Jahantigh, M. *et al.* MicroRNA-155 promotes atherosclerosis by repressing Bcl6 in macrophages. *J. Clin. Invest.* **122**, 4190–4202 (2012).
19. Banerjee, S. *et al.* MiR-125a-5p regulates differential activation of macrophages and inflammation. *J. Biol. Chem.* **288**, 35428–35436 (2013).
20. Chaudhuri, A. A. *et al.* MicroRNA-125b Potentiates Macrophage Activation. *J. Immunol.* **187**, 5062–5068 (2011).
21. Etienne-Manneville, S. & Hall, A. Rho GTPases in cell biology. *Nature* **420**, 629–35 (2002).
22. Chinetti, G. *et al.* PPAR-α and PPAR-γ activators induce cholesterol removal from human macrophage foam cells through stimulation of the ABCA1 pathway. *Nat. Med.* **7**, 53–58 (2001).
23. Argmann, C. A. *et al.* Regulation of macrophage cholesterol efflux through hydroxymethylglutaryl- CoA reductase inhibition: A role for RhoA in ABCA1-mediated cholesterol efflux. *J. Biol. Chem.* **280**, 22212–22221 (2005).
24. House, C. M., Möller, A. & Bowtell, D. D. L. Siah proteins: Novel drug targets in the Ras and hypoxia pathways. *Cancer Res.* **69**, 8835–8838 (2009).
25. Polekhina, G. *et al.* Siah ubiquitin ligase is structurally related to traf and modulates tnf-α signaling. *Nat. Struct. Biol.* **9**, 68–75 (2002).
26. Alper, S. *et al.* Identification of innate immunity genes and pathways using a comparative genomics approach. *Proc. Natl. Acad. Sci.* **105**, 7016–7021 (2008).
27. Li, T. *et al.* MicroRNAs modulate the noncanonical transcription factor NF-κB pathway by regulating expression of the kinase IKKα during macrophage differentiation. *Nat. Immunol.* **11**, 799–805 (2010).
28. Hayden, M. S. & Ghosh, S. Shared Principles in NF-κB Signaling. *Cell* **132**, 344–362 (2008).
29. Dan, H. C. *et al.* Akt-dependent activation of mTORC1 complex involves phosphorylation of mTOR (mammalian target of rapamycin) by IκB kinase α (IKKα). *J. Biol. Chem.* **289**, 25227–25240 (2014).
30. Dong, F., Mo, Z., Eid, W., Courtney, K. C. & Zha, X. Akt inhibition promotes ABCA1-mediated cholesterol efflux to apoA-I through suppressing mTORC1. *PLoS One* **9**, 1–20 (2014).
31. Chistiakov, D. a., Orekhov, A. N. & Bobryshev, Y. V. Extracellular vesicles and atherosclerotic disease. *Cell. Mol. Life Sci.* **72**, 2697–2708 (2015).
32. Hergenreider, E. *et al.* Atheroprotective communication between endothelial cells and smooth muscle cells through miRNAs. *Nat. Cell Biol.* **14**, 249–56 (2012).
33. He, S. *et al.* Endothelial extracellular vesicles modulate the macrophage phenotype: Potential implications in atherosclerosis. *Scand. J. Immunol.* **87**, 1–16 (2018).
34. Zhang, Y. *et al.* Secreted monocytic miR-150 enhances targeted endothelial cell migration. *Mol. Cell* **39**, 133–44 (2010).
35. Singh, P. P., Smith, V. L., Karakousis, P. C. & Schorey, J. S. Exosomes Isolated from Mycobacteria-Infected Mice or Cultured Macrophages Can Recruit and Activate Immune Cells In Vitro and In Vivo. *J. Immunol.* **189**, 777–785 (2012).
36. Walters, S. B. *et al.* Microparticles from Mycobacteria-Infected Macrophages

Promote Inflammation and Cellular Migration. *J. Immunol.* **190**, 669–677 (2012).
37. Niu, Y. & Tang, G. Mir-185-5p targets rock2 and inhibits cell migration and invasion of hepatocellular carcinoma. *Oncol. Lett.* **17**, 5087–5093 (2019).
38. Zhang, Q., Chen, Y. & Liu, K. miR-185 inhibits cell migration and invasion of hepatocellular carcinoma through CDC42. *Oncol. Lett.* **16**, 3101–3107 (2018).
39. Qu, Y. & Zhang, N. miR-365b-3p inhibits the cell proliferation and migration of human coronary artery smooth muscle cells by directly targeting ADAMTS1 in coronary atherosclerosis. *Exp. Ther. Med.* **16**, 4239–4245 (2018).
40. Lee, A. *et al.* A PPARγ-dependent miR-424/503-CD40 axis regulates inflammation mediated angiogenesis. *Sci. Rep.* **7**, 1–13 (2017).
41. Kalra, H. *et al.* Vesiclepedia: A Compendium for Extracellular Vesicles with Continuous Community Annotation. *PLoS Biol.* **10**, 8–12 (2012).
42. Keerthikumar, S. *et al.* ExoCarta: A Web-Based Compendium of Exosomal Cargo. *J. Mol. Biol.* **428**, 688–692 (2016).
43. Haraszti, R. A. *et al.* High-resolution proteomic and lipidomic analysis of exosomes and microvesicles from different cell sources. *J. Extracell. Vesicles* **5**, 32570 (2016).
44. Brown, M. *et al.* Lymphatic exosomes promote dendritic cell migration along guidance cues. *J. Cell Biol.* **217**, 2205–2221 (2018).
45. Kriebel, P. W. *et al.* Extracellular vesicles direct migration by synthesizing and releasing chemotactic signals. *J. Cell Biol.* **217**, 2891–2910 (2018).
46. Kuc, N. *et al.* Pancreatic ductal adenocarcinoma cell secreted extracellular vesicles containing ceramide-1-phosphate promote pancreatic cancer stem cell motility. *Biochem. Pharmacol.* **156**, 458–466 (2018).
47. Chen, L. *et al.* Cardiac progenitor-derived exosomes protect ischemic myocardium from acute ischemia/reperfusion injury. *Biochem. Biophys. Res. Commun.* **431**, 566–71 (2013).
48. Alexander, M. *et al.* Exosome-delivered microRNAs modulate the inflammatory response to endotoxin. *Nat. Commun.* **6**, 7321 (2015).
49. Katakowski, M. *et al.* Exosomes from marrow stromal cells expressing miR-146b inhibit glioma growth. *Cancer Lett.* **335**, 201–204 (2013).
50. Ohno, S. I. *et al.* Systemically injected exosomes targeted to EGFR deliver antitumor microrna to breast cancer cells. *Mol. Ther.* **21**, 185–191 (2013).
51. Yang, J., Zhang, X., Chen, X., Wang, L. & Yang, G. Exosome Mediated Delivery of miR-124 Promotes Neurogenesis after Ischemia. *Mol. Ther. Nucleic Acids* **7**, 278–287 (2017).
52. Mokhtarzadeh, A. *et al.* Biodegradable nano-polymers as delivery vehicles for therapeutic small non-coding ribonucleic acids. *J. Control. Release* **245**, 116–126 (2017).
53. Chen, X. *et al.* Nanoparticle delivery of stable miR-199a-5p agomir improves the osteogenesis of human mesenchymal stem cells via the HIF1a pathway. *Biomaterials* **53**, 239–250 (2015).
54. Gaur, S. *et al.* Chitosan nanoparticle-mediated delivery of miRNA-34a decreases prostate tumor growth in the bone and its expression induces non-canonical autophagy. *Oncotarget* **6**, 29161–29177 (2015).
55. Howard, K. A. *et al.* Chitosan/siRNA nanoparticle-mediated TNF-α knockdown in peritoneal macrophages for anti-inflammatory treatment in a murine arthritis model.

Mol. Ther. **17**, 162–168 (2009).
56. Xiao, B., Ma, P., Viennois, E. & Merlin, D. Urocanic acid-modified chitosan nanoparticles can confer anti-inflammatory effect by delivering CD98 siRNA to macrophages. *Colloids Surfaces B Biointerfaces* **143**, 186–193 (2016).
57. Douglas, K. L., Piccirillo, C. A. & Tabrizian, M. Cell line-dependent internalization pathways and intracellular trafficking determine transfection efficiency of nanoparticle vectors. *Eur. J. Pharm. Biopharm.* **68**, 676–687 (2008).
58. Howard, K. A. *et al.* Influence of hydrophilicity of cationic polymers on the biophysical properties of polyelectrolyte complexes formed by self-assembly with DNA. *Biochim. Biophys. Acta* **1475**, 245–55 (2000).
59. Leroux, J. C. *et al.* Internalization of poly(D,L-lactic acid) nanoparticles by isolated human leukocytes and analysis of plasma proteins adsorbed onto the particles. *J. Biomed. Mater. Res.* **28**, 471–81 (1994).
60. Leroux, J.-C., De Jaeghere, F., Anner, B., Doelker, E. & Gurny, R. An investigation on the role of plasma and serum opsonins on the evternalization of biodegradable poly(D,L-lactic acid) nanoparticles by human monocytes. *Life Sci.* **57**, 695–703 (1995).
61. Wei, Y. *et al.* Dicer in Macrophages Prevents Atherosclerosis by Promoting Mitochondrial Oxidative Metabolism. *Circulation* **138**, 2007–2020 (2018).
62. Santel, A. *et al.* A novel siRNA-lipoplex technology for RNA interference in the mouse vascular endothelium. *Gene Ther.* **13**, 1222–1234 (2006).
63. Zhou, F. *et al.* Targeted delivery of microRNA-126 to vascular endothelial cells: Via REDV peptide modified PEG-trimethyl chitosan. *Biomater. Sci.* **4**, 849–856 (2016).
64. Yu, M. *et al.* Nanoparticles targeting extra domain B of fibronectin-specific to the atherosclerotic lesion types III, IV, and V-enhance plaque detection and cargo delivery. *Theranostics* **8**, 6008–6024 (2018).
65. Beldman, T. J. *et al.* Hyaluronan Nanoparticles Selectively Target Plaque-Associated Macrophages and Improve Plaque Stability in Atherosclerosis. *ACS Nano* **11**, 5785–5799 (2017).
66. Zhao, X., Li, H. & Lee, R. J. Targeted drug delivery via folate receptors. *Expert Opin. Drug Deliv.* **5**, 309–319 (2008).
67. Matsumoto, A. *et al.* Role of Phosphatidylserine-Derived Negative Surface Charges in the Recognition and Uptake of Intravenously Injected B16BL6-Derived Exosomes by Macrophages. *J. Pharm. Sci.* **106**, 168–175 (2017).
68. Flannagan, R. S., Canton, J., Furuya, W., Glogauer, M. & Grinstein, S. The phosphatidylserine receptor TIM4 utilizes integrins as coreceptors to effect phagocytosis. *Mol. Biol. Cell* **25**, 1511–1522 (2014).
69. Kim, V. N. MicroRNA biogenesis: coordinated cropping and dicing. *Nat. Rev. Mol. Cell Biol.* **6**, 376–385 (2005).
70. Huntzinger, E. & Izaurralde, E. Gene silencing by microRNAs: contributions of translational repression and mRNA decay. *Nat. Rev. Genet.* **12**, 99–110 (2011).
71. He, L. & Hannon, G. J. MicroRNAs: small RNAs with a big role in gene regulation. *Nat. Rev. Genet.* **5**, 522–531 (2004).
72. Frost, R. J. A. & Olson, E. N. Control of glucose homeostasis and insulin sensitivity by the Let-7 family of microRNAs. *Proc. Natl. Acad. Sci.* **108**, 21075–21080 (2011).
73. Zhu, H. *et al.* The Lin28/let-7 axis regulates glucose metabolism. *Cell* **147**, 81–94

(2011).
74. Balzeau, J., Menezes, M. R., Cao, S. & Hagan, J. P. The LIN28/let-7 pathway in cancer. *Front. Genet.* **8**, 1–16 (2017).
75. Esau, C. *et al.* miR-122 regulation of lipid metabolism revealed by in vivo antisense targeting. *Cell Metab.* **3**, 87–98 (2006).
76. Tsai, W. C. *et al.* MicroRNA-122 plays a critical role in liver homeostasis and hepatocarcinogenesis. *J. Clin. Invest.* **122**, 2884–2897 (2012).
77. Hsu, S. *et al.* Essential metabolic, anti-inflammatory, and anti-tumorigenic functions of miR-122 in liver. *J. Clin. Invest.* **122**, 2871–83 (2012).
78. Castoldi, M. *et al.* The liver-specific microRNA miR-122 controls systemic iron homeostasis in mice. *J. Clin. Invest.* **121**, 1386–1396 (2011).
79. Vinod, M. *et al.* miR-206 controls LXRα expression and promotes LXR-mediated cholesterol efflux in macrophages. *Biochim. Biophys. Acta* **1841**, 827–35 (2014).
80. Horie, T. *et al.* MicroRNA-33 regulates sterol regulatory element-binding protein 1 expression in mice. *Nat. Commun.* **4**, 1–12 (2013).
81. Price, N. L. *et al.* Genetic Dissection of the Impact of miR-33a and miR-33b during the Progression of Atherosclerosis. *Cell Rep.* **21**, 1317–1330 (2017).
82. van Rooij, E. & Olson, E. N. MicroRNA therapeutics for cardiovascular disease: opportunities and obstacles. *Nat. Rev. Drug Discov.* **11**, 860–72 (2012).
83. Porrello, E. R. *et al.* MiR-15 family regulates postnatal mitotic arrest of cardiomyocytes. *Circ. Res.* **109**, 670–679 (2011).
84. Hullinger, T. G. *et al.* Inhibition of miR-15 protects against cardiac ischemic injury. *Circ. Res.* **110**, 71–81 (2012).
85. Marquart, T. J., Wu, J., Lusis, A. J. & Baldán, Á. Anti-miR-33 therapy does not alter the progression of atherosclerosis in low-density lipoprotein receptor-deficient mice. *Arterioscler. Thromb. Vasc. Biol.* **33**, 455–458 (2013).
86. Goedeke, L. *et al.* Long-term therapeutic silencing of miR-33 increases circulating triglyceride levels and hepatic lipid accumulation in mice. *EMBO Mol. Med.* **6**, 1133–1141 (2014).
87. Allen, R. M., Marquart, T. J., Jesse, J. J. & Baldán, Á. Control of very low-density lipoprotein secretion by N-ethylmaleimide- sensitive factor and miR-33. *Circ. Res.* **115**, 10–22 (2014).

6. Curriculum Vitae

SUMMARY OF QUALIFICATIONS

- M.Sc. and Ph.D. candidate, studying Biochemistry at the University of Ottawa.
- Strong problem-solving, critical-thinking and analytical skills developed through ten years of experience in laboratory research, specializing in molecular biology, cell biology, and biochemistry.
- Significant experience in cell culture including primary cells (macrophages) and cell lines (macrophages, smooth muscle cells, hepatocytes, fibroblasts) as well as animal studies.
- Extensive experience in handling radioisotopes such as 125-Iodine and Tritium.
- Excellent communication (both written and verbal), organizational and management skills honed through five years of Teaching Assistant at the University of Ottawa, three years of serving as a Trainee Committee member (Position: Communication Officer) at the University of Ottawa Heart Institute, and three years of volunteering in the "Let's Talk Science" program.
- Proven ability to work both independently and as part of a team as well as supervise students and junior staffs.
- Very good technical skills in Microsoft Word, Excel, PowerPoint, GraphPad PRISM and online research tools.
- Fluent in English and Vietnamese.

EDUCATION

Doctor of Philosophy 2013-present
Major in Biochemistry – University of Ottawa, Ottawa, Canada
Projects: Targeting macrophage microRNAs as potential therapeutics for the treatment of atherosclerosis (Supervisor: Dr. Katey Rayner).

Master of Science 2011-2013
Major in Biochemistry – University of Ottawa, Ottawa, Canada
Project: Investigating underlying mechanisms that lead to dissimilar responses of different cell types to PCSK9-mediated LDL receptor degradation (Supervisor: Dr. Thomas Lagace).

Honours Bachelor of Science 2005-2009
Major in Biotechnology - University of Science, Vietnam National University in Ho Chi Minh City, Ho Chi Minh City, Vietnam

SCHOLARSHIPS AND ACHIEVEMENTS

Canadian Institutes of Health Research (CIHR) Travel Award 06/2018
Canadian Institutes of Health Research

2018 Ottawa Region's Cardiovascular Research Trainee of the Year 05/2018
University of Ottawa and University of Ottawa Heart Institute

Basic Science Oral Presentation Honorable Mention (2nd place) 05/2017
University of Ottawa Heart Institute

Best Poster Presentation Award 03/2017
The 5th International Ottawa Heart Conference

University of Ottawa Cardiac Research Graduate Awards 2016-2018

University of Ottawa Heart Institute

Institute Community Support (ICS) Travel Award 08/2016
Canadian Institutes of Health Research

Basic Science Oral Presentation Honorable Mention (2nd place) 05/2016
University of Ottawa Heart Institute

Award of Excellence in Graduate Studies for the Ph.D. in Biochemistry program 12/2015
Faculty of Medicine – University of Ottawa

Graduate Student Poster Presentation Award 10/2015
Canadian Lipoprotein Conference

Institute Community Support (ICS) Travel Award 07/2015
Canadian Institutes of Health Research

Ontario Graduate Scholarship 2015-2016
University of Ottawa

Excellence Scholarship 2015-2016
Tuition Scholarship – University of Ottawa

ATVB Travel Award for Young Investigators 04/2015
Rewarding accepted abstracts that are ranked in the top 5 percentile – ATVB (Arteriosclerosis, Thrombosis and Vascular Biology) Council

Faculty Scholarship for Excellence Student 2005-2009
Tuition Scholarship – University of Science, Vietnam National University in Ho Chi Minh City

Ajinomoto Scholarship 2008-2009
Ajinomoto Vietnam, Inc.

Encouraging Scholarship 2006
HSBC Bank, Vietnam

Encouraging Scholarship 2005
United Airlines, Vietnam

"Mendel's nursery garden" - 3rd prize 2008
The annual biology contest at the University of Science, Vietnam National University in Ho Chi Minh City

PUBLICATIONS

Journal Articles

- **Nguyen, MA.**, Hoang, HD., Rasheed, A., Duchez, AC., Wyatt, H., Alain, T., Rayner, KJ. miR-223 Deficiency Accelerates Atherosclerosis via Regulating Cholesterol Efflux and Inflammatory Responses. Manuscript in preparation.
- Rasheed, A., Robichaud, S., **Nguyen, MA.**, Geoffrion, M., Cottee, ML., Dennison, T., Pietrangelo, A., Lee, R., Ouimet, M., Rayner, KJ. Loss of MLKL Decreases Necrotic Core but Increases Macrophage Lipid Accumulation in Atherosclerosis. Published online at *BioRxiv* and Submitted to *Arterioscler Thromb Vasc Biol.* **Impact Factor 6.6**
- **Nguyen, MA.**, Rayner, KJ. Non-coding RNAs in the Development of Atherosclerosis: Current Understanding and Future Opportunities. Minor revision at *Biochemistry and Cell Biology.*
- Karunakaran, D., Turner, AW., Duchez, AC., Soubeyrand, S., Rasheed, A., Smyth, D., Cook, DP., Kandiah, JW., Pan, C., Geoffrion, M., Nikpay, M., Lee, R., Boytard, L., Wyatt, H., **Nguyen, MA.**, Lau, P., Laakso, M., Ramkhelawon, B., Alvarez, M.,

Pietilainen, KH., Pajukanta, P., Vanderhyden, BC., Liu, P., Berger, SB., Gough, PJ., Beal, AM., Bertin, J., Harper, ME., Lusis, AJ., McPherson, R., Rayner, KJ. RIPK1 Directs Immunometabolism in Humans and can be Therapeutically Silenced to Improve Metabolic Dysfunction in Diet-Induced Obesity. Under revision at *Nature Medicine.* **Impact Factor 30.6**

- Karunakaran, D., **Nguyen, MA.**, Geoffrion, M., Lister, Z., Cheng, HS., Wyatt, H., Kandiah, JW., Jung, R., Alenghat, FJ., Mompeon, A., Lee, R., Pan, C., Lusis, AJ., Liu, P., Matic, LP., Hedin, U., Fish, JE., Guo, L., Kolodgie, F., Virmani, R., Rayner, KJ. (2018). Therapeutic Knockdown of RIPK1 Gene Expression Reduces NF-κB Inflammation in Macrophages and Prevents Atherosclerotic Lesion Development. Under revision at *Circulation.* **Impact Factor 23.0**
- **Nguyen, MA.**, Wyatt, H., Susser, L., Geoffrion, M., Rasheed, A., Duchez, AC., Cottee, ML., Afolayan, E., Farah, E., Kahiel, Z., Cote, M., Gadde, S., Rayner, KJ. (2018). Delivery of microRNAs by Chitosan Nanoparticles to Functionally Alter Macrophage Cholesterol Efflux in vitro and in vivo. *ACS Nano* 13(6), 6491-6505. **Impact Factor 13.9**
- **Nguyen, MA.**, Karunakaran, D., Geoffrion, M., Cheng, HS., Tandoc, K., Perisic Matic, L., Hedin, U., Maegdefessel, L., Fish, JE., Rayner, KJ. (2018). Extracellular Vesicles Secreted by Atherogenic Macrophages Transfer MicroRNA to Inhibit Cell Migration. *Arterioscler Thromb Vasc Biol* 38(1), 49-63. (This paper selected for editorial highlights on the same issue: http://atvb.ahajournals.org/content/38/1/2.short, and to receive the **2019 Daniel Steinberg Early Career Investigator Award in Atherosclerosis/Lipoproteins**). **Impact Factor 6.6**
- Cheng, HS., Besla, R., Li, A., Chen, Z., Shikatani, EA., Nazari-Jahantigh, M., Hammoutene, A., **Nguyen, MA.**, Geoffrion, M., Cai, L., Khyzha, N., Li, T., MacParland, SA., Husain, M., Cybulsky, MI., Boulanger, CM., Temel, RE., Schober, A., Rayner, KJ., Robbins, CS., Fish, JE. (2017). Paradoxical Suppression of Atherosclerosis in the Absence of microRNA-146a. *Circ Res* 121(4), 354-367. **Impact Factor 15.8**
- Singaravelu, R., O'Hara, S., Jones, DM., Chen, R., Taylor, NG., Srinivasan, P., Quan, C., Roy, DG., Steenbergen, RH., Kumar, A., Lyn, RK., Özcelik, D., Rouleau, Y., **Nguyen, MA.**, Rayner, KJ., Hobman, TC., Tyrrell, DL., Russell, RS and Pezacki, JP. (2015). "MicroRNAs Regulate the Immunometabolic Response to Viral Infection in the Liver". *Nat Chem Biol* 11(12): 988-993. **Impact Factor 12.1**
- Karunakaran, D., Thrush, AB., **Nguyen, MA.**, Richards, L., Geoffrion, M., Singaravelu, R., Ramphos, E., Shangari, P., Ouimet, M., Pezacki, JP., Moore, KJ., Perisic, L., Maegdefessel, L., Hedin, U., Harper, ME., Rayner, KJ. (2015). "Macrophage Mitochondrial Energy Status Regulates Cholesterol Efflux and Is Enhanced by Anti-MiR33 in Atherosclerosis". *Circ Res* 117(3), 266-278. **Impact Factor 15.8**
- **Nguyen, MA.**, Karunakaran, D., Rayner, KJ. (2014). "Unlocking the Door to New Therapies in Cardiovascular Disease: MicroRNAs Hold the Key". *Curr Cardiol Rep* 16(11), 539.
- **Nguyen, MA.**, Kosenko, T., Lagace, TA. (2014). "Internalized PCSK9 Dissociates from Recycling LDL Receptors in PCSK9-resistant SV-589 Fibroblasts". *J Lipid Res* 55(2), 266-275. **Impact Factor 4.7**

7. Copyrights

SPRINGER NATURE LICENSE TERMS AND CONDITIONS	
Jul 11, 2019	
This Agreement between Ms. My-Anh Nguyen ("You") and Springer Nature ("Springer Nature") consists of your license details and the terms and conditions provided by Springer Nature and Copyright Clearance Center.	
License Number	4626010571691
License date	Jul 11, 2019
Licensed Content Publisher	Springer Nature
Licensed Content Publication	Current Cardiology Reports
Licensed Content Title	Unlocking the Door to New Therapies in Cardiovascular Disease: MicroRNAs Hold the Key
Licensed Content Author	My-Anh Nguyen, Denuja Karunakaran, Katey J Rayner
Licensed Content Date	Jan 1, 2014
Licensed Content Volume	16
Licensed Content Issue	11
Type of Use	Thesis/Dissertation
Requestor type	academic/university or research institute
Format	print and electronic
Portion	full article/chapter
Will you be translating?	no
Circulation/distribution	<501
Author of this Springer Nature content	yes
Title	Mechanistic and Therapeutic Insights of Macrophage microRNAs in Atherosclerosis
Institution name	University of Ottawa